Key Functions for Id4 in Gliogenesis and Id2 in Spermatogenesis Discovered by the Analysis of Knockout Mice

A thesis submitted to University College London for the degree of Doctor of Philosophy in Molecular Genetics

2002

Lynn Bedford

Department of Medicine

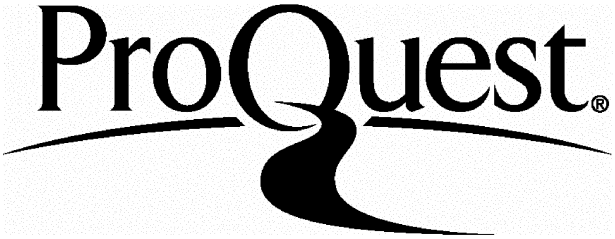

Acknowledgements

First I would like to thank Fred for his supervision throughout this work and infinite patience. Thanks also go to my fellow lab members, who have kept me sane when things weren't going too well.

Huge thanks also go to my family: Dad, Mum, David and Karen, and also to Andy, for just being there for me and making me smile.

I would also like to acknowledge our collaborator Dr Toru Kondo at The Department of Cell Fate Modulation, Kumamoto University, Japan who kindly provided figures 3.20-3.24 presented in this thesis.

Abstract

Id proteins belong to the family of helix-loop-helix (HLH) transcription factors, and are well known as positive regulators of cell growth and negative regulators of cell differentiation. The mammalian Id subfamily currently has four members, Id1-Id4, and the Id proteins are key intracellular factors in numerous developmental processes. The results presented here demonstrate novel functions for Id4 and Id2 in nervous system and germ cell development respectively.

Here we describe the generation of Id4 knockout mice, and present evidence that Id4 is necessary for normal development of mice. Id4 knockout mice exhibited reduced viability, and mice surviving to adulthood had drastically altered brain morphology, with an overall reduction in size, indicating fewer neuronal and glial cells, but larger ventricles. Analysis of neural-specific markers revealed a disproportional reduction in the number of glia, but not neurons, in the adult $Id4^{-/-}$ brain. *In vitro*, we show that adult neural stem cells (NSCs) lacking Id4 have a significantly reduced proliferation capacity and prematurely differentiate into glia. Neuronal differentiation *in vitro* was independent of Id4. Together, the results indicate that Id4 is a crucial intracellular factor that functions to positively regulate NSC proliferation and negatively regulate glial cell differentiation.

We also show that male Id2 knockout mice (Yokota *et al.*, 1999) have reduced fertility, which correlates with defective spermatogenesis. Although testis weight of homozygous Id2 mutant mice was not significantly affected, approximately 60% of the $Id2^{-/-}$ seminiferous tubules were undergoing defective spermatogenesis. We

present data that suggests Id2 is not involved in Sertoli cell proliferation, but suggest that Id2 is involved in regulating Sertoli cell differentiated functions. Id2 may also function in meiotic and post-meiotic germ cells. Together, the results show that the presence of a functional Id2 protein in the testis, be it in the Sertoli cell and/or germ cell development, is crucial for normal spermatogenesis.

Table of Contents

List of Figures

Chapter 1

Chapter 2

Chapter 3

Chapter 4

Chapter 5

Chapter 6

List of Tables

Chapter 1

Chapter 2

Chapter 3

Chapter 4

Chapter 1

Introduction

1.1 Id Helix-Loop-Helix Proteins

Id proteins are a subfamily of the helix-loop-helix (HLH) family of transcription factors. The mammalian prototype of the Id HLH subfamily was identified in 1990 in the laboratory of Harold Weintraub (Benezra *et al.*, 1990), and was named Id for its functional properties as an inhibitor of DNA binding and an inhibitor of cell differentiation. Today, the Id proteins are implicated in other cellular processes important for normal development besides cell differentiation, including cell proliferation and apoptosis.

There are four main HLH protein subfamilies, basic HLH (bHLH) leucine zipper, bHLH-PAS, bHLH and Id HLH, based on the presence or absence of additional functional domains (figure 1.1). The conserved HLH domain consists of two amphipathic α helices, each 15-20 amino acid residues long, joined by a shorter loop of more variable length and sequence, and mediates homo- or hetero-dimerisation, which is a functional prerequisite. HLH proteins typically contain a region of highly basic amino acid residues immediately N-terminal to the HLH domain (figure 1.1), which, following dimerisation, is responsible for DNA-binding to a hexanucleotide sequence known as the 'E box' (CANNTG) in the regulatory regions of their target genes (Murre *et al.*, 1989). The Id HLH proteins do not contain this basic DNA-binding region (figure 1.1). Therefore, Id proteins form heterodimers with transcriptional regulators, such as the bHLH proteins, through their HLH motif, but

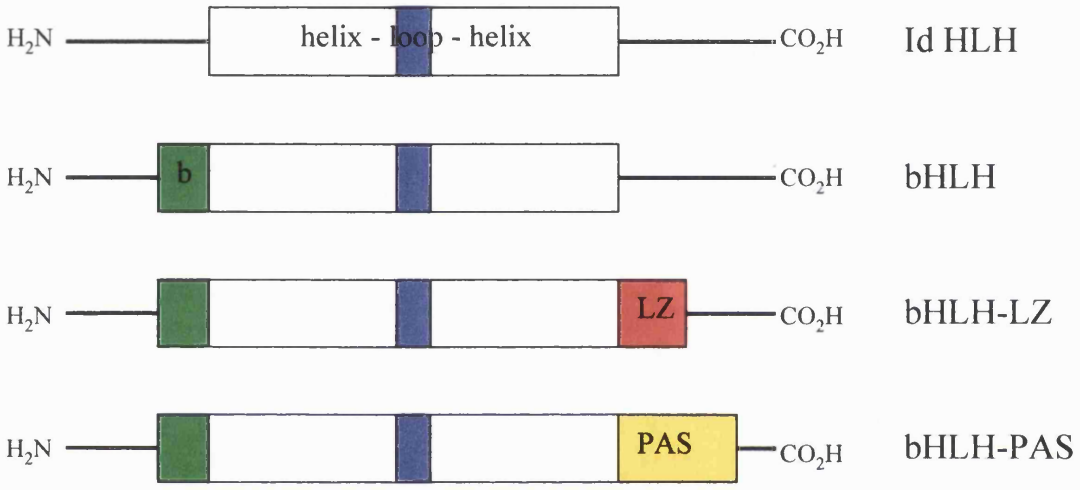

Figure 1.1 Schematic structure of the four main subfamilies of HLH proteins. b, basic DNA-binding domain; LZ, leucine zipper region; PAS, Per/Arnt/Sim region. Figure modified from Norton (2001).

the Id-bHLH heterodimers are unable to bind to DNA. As the Id proteins primarily function through dimerisation with bHLH proteins, Id proteins are said to function as dominant negative regulators of bHLH transcription factors. (Benezra *et al.*, 1990; Ellis *et al.*, 1990; Garrell and Mondolell, 1990; Sun *et al.*, 1991). There are two main classes of bHLH proteins, the ubiquitously expressed Class A bHLH proteins and the tissue-specific Class B bHLH proteins, and bHLH proteins typically bind to DNA as a heterodimer between a Class A and Class B protein (figure 1.2A). Id proteins preferentially dimerise with the ubiquitously expressed Class A bHLH proteins, such as E12 and E47, which prevents their interaction with the Class B proteins and binding to DNA (figure 1.2B). Therefore, Id proteins regulate the activity of the Class B bHLH proteins by sequestering their Class A protein partners (Norton *et al.*, 1998; Massari and Murre, 2000).

Work in the Id field has shown that Id proteins can also modulate the functions of non-bHLH proteins. Id proteins have been shown to interact with the retinoblastoma proteins (pRB and related pocket proteins p107 and p130; Iavarone *et al.*, 1994; Lasorella *et al.*, 1996), ETS-domain transcription factors (Yates *et al.*, 1999), mouse Id-associated protein 1 (MIDA1; Shoji *et al.*, 1995; Inoue *et al.*, 1999, 2000), paired homeobox transcription factors (PAX-2/PAX-5/PAX-8; Roberts *et al.*, 2001) and the adipocyte determination and differentiation factor 1 (ADD1; Moldes *et al.*, 1999). Similar to their interaction with the bHLH proteins, Id proteins interact with the non-bHLH proteins via their HLH domain. The evidence of such interactions between Id and non-bHLH proteins suggests that the HLH domain can associate with diverse structural motifs. With the exception of MIDA1, the interaction with Id protein antagonised the activity of the DNA-binding protein, as with the Id-bHLH protein interactions. Notably, the interactions between Id and non-bHLH proteins have been

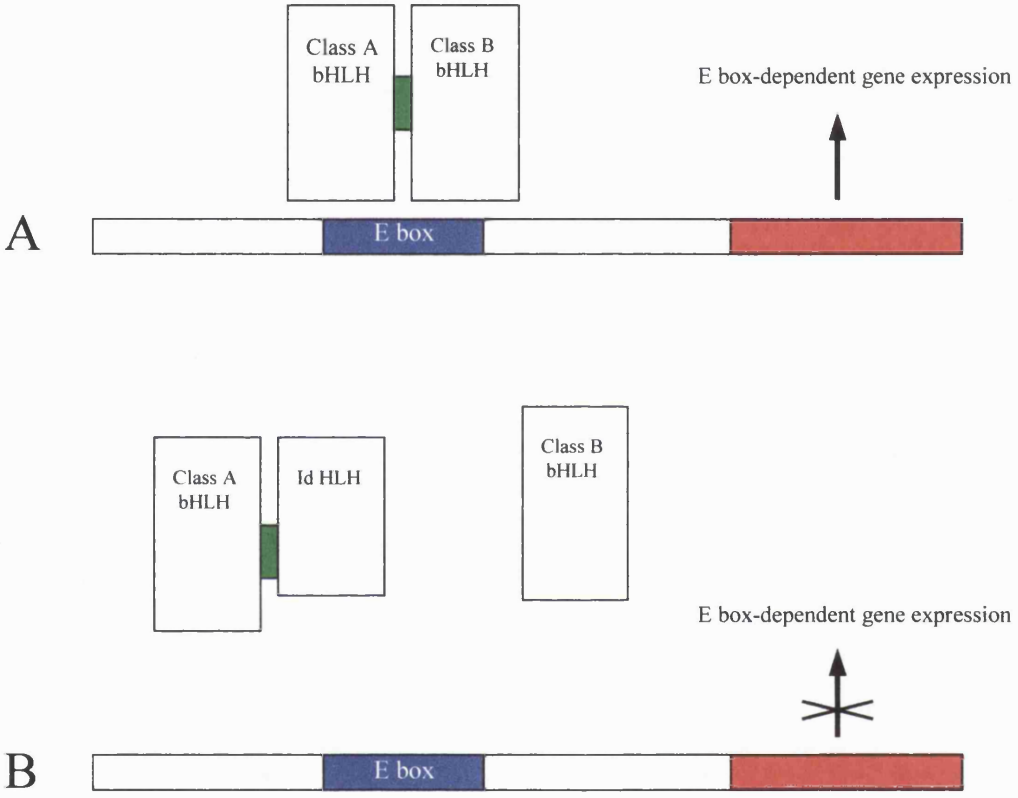

Figure 1.2 Id proteins function as dominant negative regulators of bHLH transcription factors. bHLH proteins bind to E box sequences in DNA as a heterodimer between a ubiquitously expressed Class A and tissue-specific Class B bHLH protein (A). Id proteins preferentially dimerise with the Class A bHLH proteins, preventing their interaction with the Class B bHLH proteins and binding to DNA (B). Thereby, Id proteins inhibit E box-dependent gene expression. Figure modified from Norton *et al.* (1998).

shown mostly only *in vitro*. Lasorella *et al.* (2000) showed an association between Id2 and pRb *in vivo* by intercrossing Id2 and pRb mutant mice. They found that the embryonic lethality of pRb knockout mice was rescued by inactivation of Id2.

Genes encoding Id HLH proteins have been identified in diverse species, including mammals (Benezra *et al.*, 1990; Christy *et al.*, 1991; Sun *et al.*, 1991; Biggs *et al.*, 1992; Riechmann *et al.*, 1994), *Drosophila* (Garrell and Mondolell, 1990; Ellis *et al.*, 1990) and *Xenopus laevis* (Wilson and Mohun, 1995; Zhang *et al.*, 1995). In the mouse, the Id HLH subfamily has four members to date, Id1 (Benezra *et al.*, 1990), Id2 (Sun *et al.*, 1991; Biggs *et al.*, 1992), Id3 (Christy *et al.*, 1991) and Id4 (Riechmann *et al.*, 1994), each encoded by an individual gene. The murine Id1, Id2, Id3 and Id4 genes are located on chromosomes 2 (Sun *et al.*, 1991), 12 (Sun *et al.*, 1991; Mantani *et al.*, 1998), 4 (Christy *et al.*, 1991) and 13 (Mantani *et al.*, 1998; van Crüchten *et al.*, 1998) respectively. Despite the unlinked chromosomal locations of the different Id genes, the genomic organisation within their coding regions is similar, suggesting that they evolved from a common ancestral Id gene (Sun *et al.*, 1991; Deed *et al.*, 1994; Mantani *et al.*, 1998; van Crüchten *et al.*, 1998). The Id proteins' amino acid sequences outside of the conserved HLH motif are mostly divergent, and the functions of the N- and C-terminal regions of Id proteins are largely unknown.

1.1.1 Functions of Id Helix-Loop-Helix Proteins

The functions of Id proteins are the subject of extensive research in diverse biological fields, including cell cycle research and developmental biology. Id proteins are considered to be key players in cellular processes that are fundamental in

development, including cell determination, differentiation, proliferation and apoptosis.

1.1.1.1 Id Proteins are Negative Regulators of Cell Differentiation

The most established function of Id proteins is as negative regulators of cell differentiation. Id proteins typically inhibit differentiation by antagonising bHLH proteins that are involved in cell lineage commitment and differentiation (figure 1.3). Numerous *in vitro* studies involving diverse cell lineages have shown that overexpression of Id genes inhibits cell differentiation, including in muscle cells (Jen *et al.*, 1992; Atherton *et al.*, 1996; Melnikova and Christy; 1996), myeloid cells (Kreider *et al.*, 1992), erythroid cells (Shoji *et al.*, 1994; Lister *et al.*, 1995), mammary epithelial cells (Desprez *et al.*, 1995) and adipose cells (Moldes *et al.*, 1997). This was associated with inhibition of bHLH-dependent gene expression in most studies. *In vitro* studies have also shown that Id gene expression is downregulated as cells exit from the cell cycle. Studies in *Drosophila* provided genetic evidence for the function of Id proteins as negative regulators of cell differentiation. The *Drosophila extramacrochaetae* (*emc*) locus encodes a protein that is structurally and biochemically similar to the Id protein, and gain- and loss-of-function studies have shown that the *emc* protein antagonises the *achaete-scute* complex and *Daughterless* bHLH proteins, which are important in neural fate and sex determination (Ellis *et al.*, 1990; Garrell and Modolell, 1990). Genetic studies in mice also support the role of Id proteins as negative regulators of differentiation. Constitutive overexpression of Id1 in the B cell lineage of mice lead to severe defects in early B lymphocyte development, suggesting that downregulation of Id1 is required for B cell differentiation (Sun, 1994). The phenotype of these transgenic mice resembles that of E2A knockout mice (Dorshkind, 1994). Furthermore,

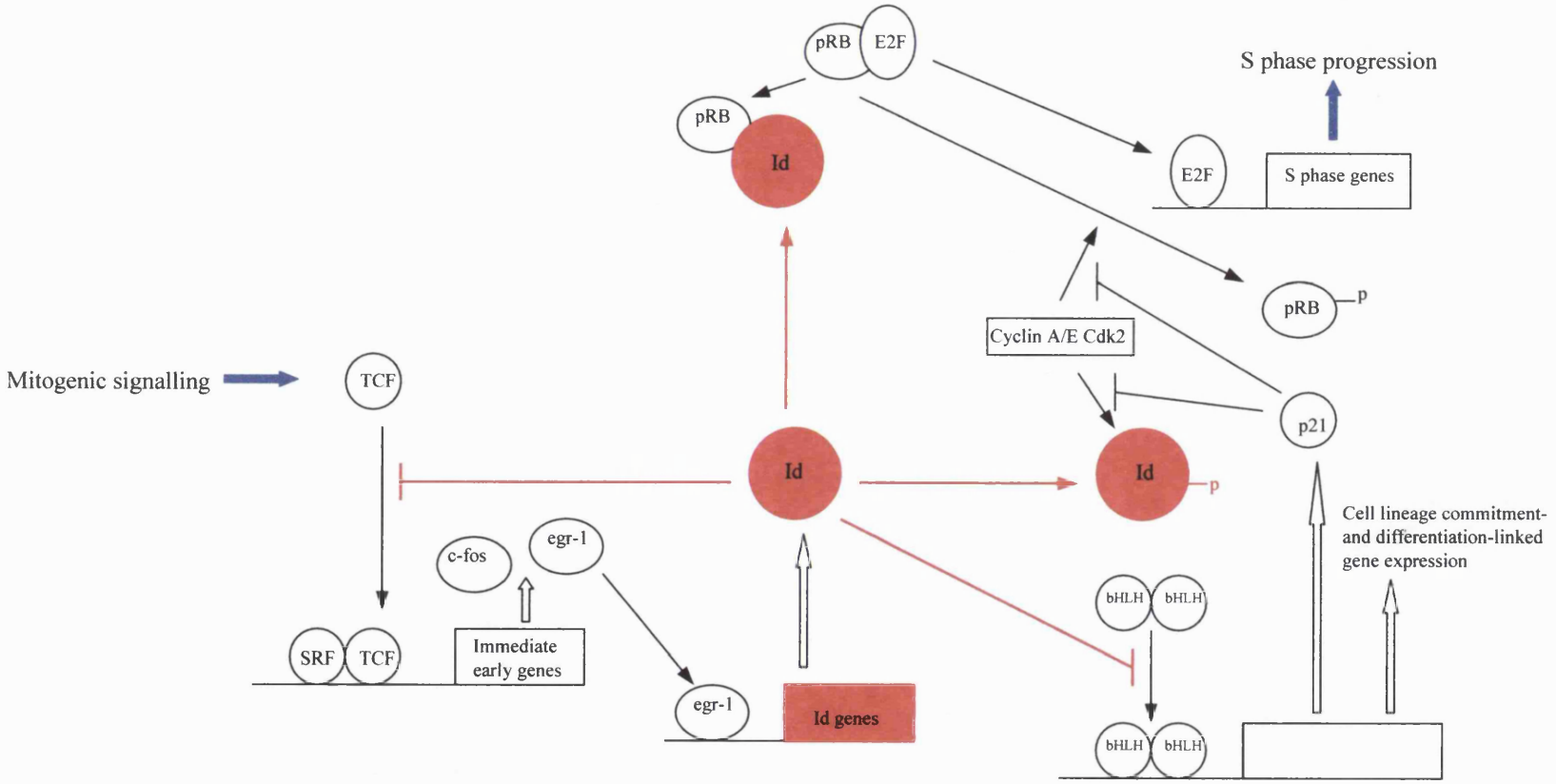

Figure 1.3 Model showing how Id proteins (red) may function as negative regulators of cell differentiation and positive regulators of cell growth. Refer to sections 1.1.1.1 and 1.1.1.2 for details. Figure modified from Norton (2001).

inactivation of the Id1 gene partly rescued the neonatal lethality of E2A knockout mice, which implicates Id1 in E2A-mediated regulatory pathways (Yan *et al.*, 1997). More recent work highlighted the function of Id proteins in cell fate determination. For example, ectopic expression of Id2 in chick-embryo surface ectoderm directed ectodermal precursor cells to neural crest and neurogenic fates at the expense of epidermal lineages (Martinsen and Bonner-Fraser, 1998).

1.1.1.2 Id Proteins Promote Cell Cycle Progression

The ability of Id proteins to function as positive regulators of cell growth is also well characterised. In addition to inhibiting differentiation, ectopic expression of Id genes in mammalian cell line models enhanced proliferation of a number of cell types, including muscle cells (Atherton *et al.*, 1996), erythroid cells (Lister *et al.*, 1995), mammary epithelial cells (Deprez *et al.*, 1995) and osteosarcoma cells (Iavarone *et al.*, 1994). In general, Id genes are highly expressed in proliferating cells and are downregulated upon induction of differentiation. Id gene expression is rapidly upregulated as part of the early transcriptional response to mitogenic stimulation of quiescent cells *in vitro*, in which Id gene expression is low/absent. Expression then declines, but is sustained during G_1, and a second peak of Id gene expression occurs as cells enter S phase of the cell cycle (Christy *et al.*, 1991; Deed *et al.*, 1993; Barone *et al.*, 1994; Hara *et al.*, 1994). Furthermore, Id expression has been shown to be required for the G_0 to S phase transition. Inhibition of Id protein expression/function by antisense oligonucleotides to Id1-3 mRNAs delayed re-entry of growth-arrested cells into the cell cycle in response to mitogenic stimulation (Barone *et al.*, 1994; Hara *et al.*, 1994). Several pathways have been identified through which Id proteins may function as positive regulators of cell growth (figure 1.3). Interestingly, their

function in cell cycle control involves Id HLH-mediated interactions, similar to their mechanism for negative regulation of cell differentiation.

Mitogenic stimulation activates a cascade of gene expression. Ternary complex factors (TCFs), which are a subfamily of the ETS-domain transcription factors, play an important role in immediate-early gene expression stimulated by mitogens. TCFs form ternary complexes with the serum response factor (SRF) and serum response elements (SREs) found in the regulatory regions of immediate-early genes, such as *c-fos* and *egr-1* (Cahill *et al.*, 1996). Yates *et al.* (1999) showed that Id proteins interact with the ETS DNA-binding domain of TCFs, and that this interaction antagonises ternary complex formation between TCFs and SRF on the *c-fos* SRE *in vitro* (figure 1.3). The authors also demonstrated that overexpression of Id proteins reduced TCF-mediated transcriptional activation in transfected cells. Therefore, Id proteins may downregulate immediate-early gene expression following mitogenic signalling. Notably, EGR-1 upregulates the expression of Id1, and likely Id3 (Tournay and Benezra, 1996; Deed *et al.*, 1994), which may be part of a negative feedback loop in cell cycle control.

Id2 and Id4 proteins bind to proteins of the retinoblastoma (Rb) family (Iavarone *et al.*, 1994; Lasorella *et al.*, 1996; J. Newton, R. Deed, J. Norton and F. Sablitzky, unpublished). This is not true for Id1 and Id3. In the context of cell cycle control, it is thought that this association with Id proteins is important to alleviate pRb suppression of E2F-DP1 transcriptional complexes during mid-late G_1 (figure 1.3). E2F-DP1 heterodimers activate the expression of genes required for S phase progression. Therefore, Id proteins would promote G_1 to S phase transition of the cell cycle. An independent mechanism by which Id proteins may attenuate pRb

suppression of E2F-DP1 transcriptional complexes has been described for Id1. Id1 protein could antagonise E2A bHLH-activated expression of the cyclin-dependent kinase (Cdk) inhibitor $p21^{Cip1/Waf1}$ (figure 1.3; Prabhu *et al.*, 1997). Downregulation of $p21^{Cip1/Waf1}$ expression would relieve its inhibition of cyclin-A/E-Cdk2 activity, allowing cyclin-A/E-Cdk2 to phosphorylate pRb. This causes pRb to dissociate from E2F-DP1 transcriptional complexes, which then promote G_1 to S phase transition of the cell cycle. As all the Id proteins function primarily through the antagonism of bHLH proteins, this pathway is likely to be used by other members of the Id family.

Id activity at the G_1 to S phase transition of the cell cycle may be regulated by post-translational modifications, such as phosphorylation. Id2, Id3 and Id4 proteins share a conserved consensus cyclin-A/E-Cdk2 phosphorylation site at serine 5 in their N-terminal region, and cyclin-A/E-Cdk2-dependent phosphorylation of this site during late G1/early S phase of the cell cycle has been shown for Id2 and Id3 (Deed *et al.*, 1997; Hara *et al.*, 1997). This cell cycle-linked phosphorylation of Id2 and Id3 proteins modulates their bHLH binding specificities, and therefore, may be a mechanism for influencing Id-bHLH functions in cell cycle control. Cdk2-dependent phosphorylation also abrogated their function as positive regulators of cell growth. However, phosphorylation of Id2 and Id3 proteins appears to be necessary for cell cycle progression, as ectopic expression of Id2 and Id3 proteins lacking the Cdk2 phosphorylation site caused S phase arrest and cell death (Deed *et al.*, 1997). The functions of the phosphorylated Id proteins during the cell cycle are not known.

It has been reported that Id1 protein interacts with the mouse Id-associated 1 (MIDA1) protein, which positively regulates cell growth in erythroleukaemia cells (Shoji *et al.*, 1995). The interaction with Id1 stimulated DNA-binding of the MIDA1

protein to a canonical 7 bp motif, which is found in the regulatory regions of several growth factor and cytokine genes (Inoue *et al.*, 1999, 2000). The findings suggest that the growth-promoting function of Id1, and possibly that of the other Id proteins, may also be mediated, at least in part, by MIDA1.

1.1.1.3 Id Proteins in Apoptosis

Several studies have now shown a pro-apoptotic function of Id proteins. Enforced overexpression of Id1, Id2 or Id3 in primary rat embryo fibroblasts (REF) induced apoptosis under serum-free conditions (Norton and Atherton, 1998). This was mostly associated with cells in S phase, reflecting the ability of Id proteins to promote transition of cells into S phase (Deed *et al.*, 1997). No significant apoptosis was observed in the presence of serum. In cells of the nervous system, overexpression of Id4 in U373 astrocytes, which is an astrocyte-derived cell line that retains properties of primary astrocytes, induced cell death by apoptosis (Andres-Barquin *et al.*, 1999). Overexpression of Id2 in interleukin-3 (IL-3)-dependent 32D.3 mouse myeloid progenitor cells promoted apoptotic cell death following survival factor withdrawal (Florio *et al.*, 1998). Interestingly, the apoptotic activity of Id2 was independent of HLH-mediated interactions, through which the Id proteins are known to function in cell proliferation and differentiation. Instead, this function of Id2 required its N-terminal domain and was linked with expression of the pro-apoptotic molecule Bax. *In vivo* evidence for pro-apoptotic functions of Id proteins comes from transgenic mice overexpressing Id1 in thymocytes. These mice exhibit differentiation arrest, T cell lymphomagenesis and widespread apoptosis (Kim *et al.*, 1999).

1.1.2 Id Gene-Targeting Studies

Id function *in vivo* has been mostly studied in *Drosophila* and mice. To date, single- and double-knockout mice of Id1-Id3 genes have been reported. Id4 knockout mice have not been described. Id1- and Id3-deficient mice are viable and display no obvious phenotypic anomalies (Yan *et al.*, 1997a; Pan *et al.*, 1999). However, Pan *et al.* (1999) found that the Id3-deficient mice had subtle abnormalities during humoral immune responses. *In vitro* studies of Id3-deficient lymphocytes showed defects in B-cell proliferation in response to B-cell receptor cross-linking, and in IFN-γ cytokine expression by T cells. Id2 knockout mice show no embryonic lethality, but exhibit neonatal death and retarded growth following birth (Yokota *et al.*, 1999). Yokota *et al.* (1999) found that Id2-deficient mice lacked lymph nodes and Peyer's patches, which was due to a greatly reduced population of lymphotoxin-producing $CD4^+CD3^-IL\text{-}7R\alpha^+$ cells. The family of lymphotoxins are necessary for the formation of secondary lymphoid organs during development (De Togni *et al.*, 1994; Koni *et al.*, 1997; Chaplin and Fu, 1998; Fütterer *et al.*, 1998; Rennert *et al.*, 1998). Id2-deficient mice also displayed defective natural killer (NK) cell production, which was due to a cell-intrinsic defect in NK cell precursors, and resulted in significantly decreased numbers of NK cells (Yokota *et al.*, 1999). Female Id2 null mice had a lactation defect (Mori *et al.*, 2000). Mori *et al.* (2000) found that mammary gland development during pregnancy was impaired in Id2 deficient mice, due to intrinsic defects in mammary epithelial cells. The lack of a more severe phenotype in single-knockout mice is likely due to the overlapping expression of the Id genes (section 1.1.3) and their functional redundancy. In contrast to single-knockout mice of Id1-Id3 genes, double knockout mice of these Id genes are inviable and die in utero (Lyden *et al.*, 1999; Norton 2000). Only the Id1/Id3 double-knockout phenotype has

been reported to date (Lyden *et al.*, 1999). Id1/Id3 double-knockout mice exhibit defective angiogenesis and neurogenesis, and do not survive beyond 13.5 dpc. Aberrant angiogenesis was the result of defects in vascular endothelial cells in the brain, and defective neurogenesis was associated with premature exit of neuroblasts from the cell cycle and precocious neuronal differentiation. Id1 and Id3 function in neurogenesis is described in section 1.2.3.4.2.

1.1.3 Id Gene Expression in the Mouse

1.1.3.1 Pattern of Id Gene Expression During Mouse Embryogenesis

Each of the Id genes displays a distinct spatiotemporal pattern of expression during mouse embryonic development (Duncan *et al.*, 1992; Evans and O'Brien, 1993; Riechmann and Sablitzky, 1995; Jen *et al.*, 1996, 1997). Only Id1-Id3 are expressed during gastrulation, where Id1 and Id3 are expressed in inner cell mass-derived tissues and Id2 in tissues originating from trophoblasts (Jen *et al.*, 1997). During post-gastrulational development, Id1-Id3 genes are expressed in multiple tissues and their expression patterns show considerable overlap (Jen *et al.*, 1997). For example, Id1-Id3 are expressed in the mandibular arch, heart, somites and the mesenchyme surrounding the dorsal portion of the developing stomach. The expression of Id1-Id3 is often associated with regions undergoing active morphogenesis. The expression of Id4 is upregulated during post-gastrulational mouse development and is primarily restricted to the nervous system (Riechmann and Sablitzky, 1995; Jen *et al.*, 1997). Id4 expression also occurs in the ventral epithelial cells of the developing stomach during early development, and in several other tissues during later development, associated with more differentiated regions. The pattern of Id gene expression during mouse nervous system development is described in section 1.2.3.1.

1.1.3.2 Pattern of Id Gene Expression in Adult Mouse Organs

Each Id gene has a unique pattern of expression in adult mouse organs (table 1.1). All four Id genes are expressed in brain, kidney, liver, spleen and testis. Id1 is the only Id gene to exhibit high expression in the heart, and Id4 in the testis. Expression of Id2 in the liver is high compared to that of Id1, Id3 and Id4 genes. Id4 expression is low in the spleen and barely detectable in the liver, and Id1 exhibits the opposite in these two organs.

	Id1	Id2	Id3	Id4
Brain	+++	+++	+++	++++
Heart	++++	+	+	-
Kidney	++++	++++	+	++++
Liver	++	++++	++	+
Spleen	+	+++	+++	++
Testis	+	+	+	++++

Table 1.1 Expression of the Id genes in adult mouse organs. ++++ high expression → + low expression, - no expression. Data based on results from Christy *et al.* (1991), Hernandez *et al.* (1996), van Crüchten (1997) and van Crüchten *et al.* (1998).

1.2 Nervous System Development

The development of the nervous system is a complex process that results in the ordered generation of neurons and glia. All cell types of the central nervous system (CNS) arise from neural stem cells (NSCs), self-renewing multipotent progenitor cells that gradually become restricted in their potential to lineage-restricted progenitor cells for neurons or glia, and then cell type-restricted precursor cells to neurons or glia (figure 1.4; Gage, 2000; Anderson, 2001). NSCs in the CNS generate

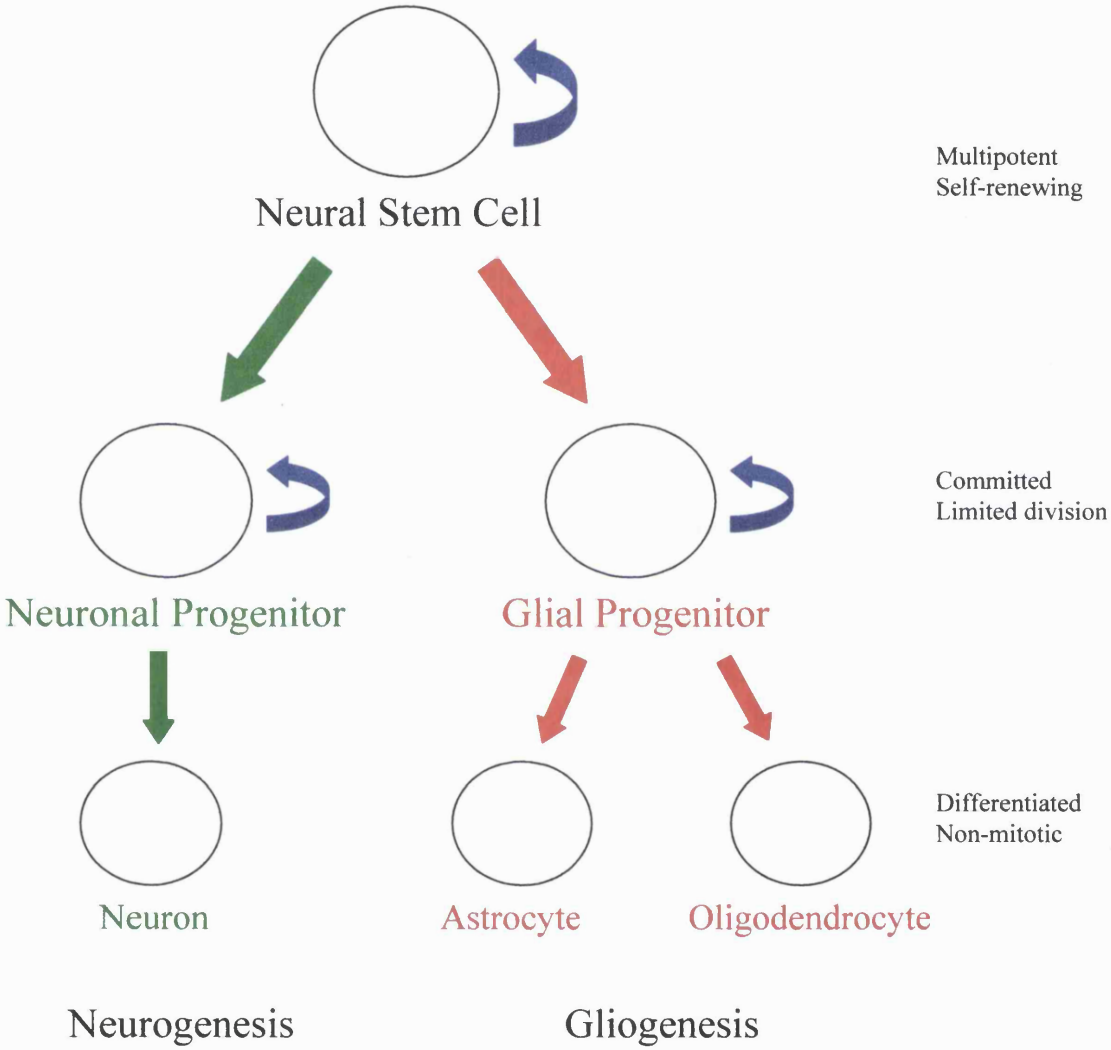

Figure 1.4 An illustration of the development of neural cell types in the mammalian central nervous system. The fate restrictions at each step are also shown. Notably, neurogenesis largely precedes gliogenesis during nervous system development.

neurons and glia, which include astrocytes and oligodendrocytes. In the peripheral nervous system (PNS), neural crest stem cells (NCSCs) generate neurons, Schwann cells, and other non-neural derivatives. During mammalian nervous system development, neurogenesis largely precedes gliogenesis. Neurons are generated primarily in the embryonic period, whilst most glia are generated after birth (Bayer and Altman, 1991; Jacobson, 1991; Qian *et al.*, 2000). The mechanisms involved in the spatial and temporal regulation of neurogenesis and gliogenesis in the nervous system are the subject of much interest, and are particularly intriguing knowing that neurons and glia arise from multipotent progenitor cells.

1.2.1 Control of Neural Stem Cell Self-Renewal

A stem cell has the ability to self-renew (Morrison *et al.*, 1997), and cell-extrinsic and cell-intrinsic factors have been shown to influence multipotent stem cell self-renewal. Stem cell mitogens, such as fibroblast growth factor 2 (FGF2), promote the proliferation of CNS-NSCs *in vitro* (Kilpatrick and Bartlett, 1993, 1995; Palmer *et al.*, 1995; Gritti *et al.*, 1996). In a recent study, Taupin *et al.* (2000) found that a glycosylated form of the cysteine protease inhibitor cystatin C produced by adult hippocampal progenitors (AHPs) cooperated with FGF2 to promote the growth of these cells. This suggests that mitogens and autocrine factors may cooperate to promote self-renewal. It has been suggested that Notch signalling can maintain the multipotency of neuroepithelial progenitors without influencing cell division (Artavanis-Tsakonas *et al.*, 1999). However, several recent studies suggest that Notch signalling promotes glial differentiation rather than self-renewal (Furukawa *et al.*, 2000; Gaiano *et al.*, 2000; Morrison *et al.*, 2000; Tanigaki *et al.*, 2001). Intrinsic control of stem cell self-renewal is still elusive. Individual stem cells may self-renew

via asymmetric divisions. However, asymmetric division patterns to generate lineage-restricted progenitors could be a property of stem cell populations, in which all divisions are symmetric, but half are self-renewing and half are differentiative (Morrison *et al.*, 1997; Fuchs and Segre, 2000). CNS and PNS stem cells have been shown to undergo symmetric self-renewing divisions *in vitro* (Stemple and Anderson, 1992; Davis and Temple, 1994). In more recent time-lapse studies, individual multipotent cortical progenitor cells were shown to divide asymmetrically, both *in vitro* (Qian *et al.*, 1998, 2000) and *in vivo* (Noctor *et al.*, 2001), but it was not certain if the asymmetric divisions were self-renewing.

1.2.2 Control of Neural Stem Cell Fate

The decision of stem cells to acquire a neuronal or glial fate is influenced by the action of both cell-extrinsic signals and cell-intrinsic programs. The molecular mechanisms that orchestrate the stereotyped sequence of differentiation during development, whereby neurons are generated first, followed by glial cells, are beginning to be elucidated. Extrinsic signals, such as platelet-derived growth factor (PDGF) (Johe *et al.*, 1996; Williams *et al.*, 1997), bone morphogenetic proteins (BMPs) (Gross *et al.*, 1996; Shah *et al.*, 1996; Li *et al.*, 1998; Rajan and McKay, 1998) and ciliary neurotrophic factor (CNTF) (Johe *et al.*, 1996), have been shown to influence stem cell fate, and many appear to act instructively, promoting one fate at the expense of others. Intrinsic programs in the control of stem cell fate were made evident in clonal cell culture. Individual cortical stem cells underwent a stereotyped pattern of cell type production, neurons first and glia later, altering their neurogenic and gliogenic capacities over time (Park *et al.*, 1999; Qian *et al.*, 1998, 2000). The

intrinsic mechanisms likely modulate the ability of a cell to respond to extrinsic signals in a complex milieu and select a neuronal or a glial fate.

1.2.2.1 Neuronal Cell Fate Decision

Multiple extrinsic signals, such as PDGF (Johe *et al.*, 1996; Williams *et al.*, 1997), BMPs (Shah *et al.*, 1996; Li *et al.*, 1998) and neurotrophin-3 (NT-3) (Ghosh and Greenberg, 1995), have been shown to promote the decision of stem cells to acquire a neuronal fate. Shah *et al.* (1996) found that BMP2 promoted autonomic neurogenesis by NCSCs, and a role for BMPs in neurogenesis was supported by the work of Li *et al.* (1998) in CNS-NSCs. Li *et al.* (1998) provided evidence that BMPs are present within the VZ and they promote neuronal differentiation of neocortical VZ precursors.

Although the signalling mechanisms by which neuronal cell fate is specified have yet to be defined, a subset of bHLH transcription factors have long been recognised as mediators of neuronal differentiation due to their ability to positively regulate the neuronal cell fate decision (Kageyama *et al.*, 1997; Lee, 1997). Vertebrate neuronal bHLH genes were identified by obtaining homologues of the *Drosophila* proneural bHLH genes, such as the *achaete-scute* complex (*as-c*) and *atonal* (*ato*) genes, which had been shown to positively regulate the neuronal fate decision in *Drosophila* (Jan and Jan, 1993). The *as-c*-homologue Mash1 and the *ato*-homologues neurogenin1, neurogenin2 (Ngn1, Ngn2) and NeuroD, have been shown to promote neuronal differentiation by overexpression studies in Xenopus embryos and knockout studies in mice (Guillemot *et al.*, 1993; Lee *et al.*, 1995; Sommer et al., 1995; Ma *et al.*, 1996). In particular, Mash1, Ngn1 and Ngn2 have similar determination functions in

distinct lineages of the developing central and peripheral nervous system (Cau *et al.*, 1997; Lo *et al.*, 1997; Fode *et al.*, 1998, 2000; Casarosa *et al.*, 1999; Ma *et al.*, 1999).

Mice lacking Mash1 function showed defects in the specification of progenitors in the olfactory epithelium, ventral forebrain and autonomic ganglia (Guillemot *et al.*, 1993; Sommer *et al.*, 1995; Cau *et al.*, 1997; Casarosa *et al.*, 1999). The most severe defects were apparent in the olfactory epithelium and ventral forebrain, where neuronal progenitor populations were absent (Cau *et al.*, 1997; Casarosa *et al.*, 1999). A less severe phenotype was observed in sympathetic ganglia, where neuronal precursor cells were generated and began to differentiate, but arrested in their terminal differentiation (Sommer *et al.*, 1995). Sommer *et al.* (1995) suggested that the lack of a determination function of Mash1 in sympathetic neurogenesis could be due to another related bHLH protein compensating for the loss of Mash1 in neural crest precursors.

In early studies in Xenopus embryos, overexpression of NeuroD (XneuroD) or Ngn1 (X-ngnr-1) generated ectopic neurons (Lee *et al.*, 1995; Ma *et al.*, 1996). However, XneuroD is expressed after the neural lineage has been determined *in vivo*, whereas X-ngnr-1 is expressed before overt neuronal differentiation. Ma *et al.* (1996) showed that overexpression of X-ngnr-1 induced ectopic neurogenesis and ectopic expression of endogenous XneuroD, suggesting that it is a neuronal determination factor that directs XneuroD-dependent neuronal differentiation. Thus, XneuroD likely promotes only differentiation of neuronal lineage cells. Ngn and NeuroD are also sequentially expressed in the mammalian nervous system, suggesting that the Ngn-NeuroD bHLH gene cascade may be conserved in mammals (Ma *et al.*, 1996). In support of this early work, Ngn1 and Ngn2 knockout mice showed defects in the specification of

progenitors in the dorsal root and cranial ganglia, and in the dorsal telencephalon (Fode *et al.*, 1998; Ma *et al.*, 1999), supporting neuronal determination functions for these genes.

Johnson *et al.* (1992) showed that Mash1 formed a heterodimer with E2A, bound to the E-box and activated transcription *in vitro*. Thus, bHLH proteins may positively regulate neuronal differentiation by their classical mechanism. Target genes for the neuronal bHLH transcription factors *in vivo* are beginning to be identified. PHD1 may be a target gene for Mash1 (Saito *et al.*, 1996). PHD1 is a paired homeodomain gene related to *C. elegans unc-4* that is required for the specification of a subset of neurons (Saito *et al.*, 1996). PHD1 is expressed following Mash1 expression and is absent in the olfactory epithelium of Mash1 knockout mice. The relationship between Mash1 and PHD1 remains to be determined.

1.2.2.2 Glial Cell Fate Decision

1.2.2.2.1 Astrocyte Cell Fate Decision

Instructive extracellular signals for the astrocyte cell fate have been identified in the CNS and PNS. Ciliary neurotrophic factor (CNTF) (Johe *et al.*, 1996) and BMPs (Gross *et al.*, 1996; Rajan and McKay, 1998) promote astrocyte differentiation by CNS-NSCs *in vitro*. In the PNS, neuregulin-1 (Nrg1)/glial growth factor-2 (GGF2) promotes Schwann cell differentiation by NCSCs (Shah *et al.*, 1994; Morrison *et al.*, 1999). These instructive glial differentiation cues are thought to be secreted proteins that can act at long range. More recent work has identified Notch activation as a glial-inducing signal, which is a contact-mediated signalling system. Evidence *in vitro* and *in vivo* supports a role for Notch signalling in glial fate specification in the

CNS and PNS (Furukawa *et al.*, 2000; Gaiano *et al.*, 2000; Morrison *et al.*, 2000; Tanigaki *et al.*, 2001). Previous studies have shown that Notch signalling can inhibit the generation of both neurons (Nye *et al.*, 1994; Dorsky *et al.*, 1995; Bao and Cepko, 1997; Morrison *et al.*, 2000) and oligodendrocytes (Wang *et al.*, 1998), but astrocyte differentiation did not appear to be affected (Nye *et al.*, 1994).

Long-Range Signals

The cytokines CNTF and leukaemia inhibitory factor (LIF) promote astrocyte differentiation mainly via the JaK/STAT signalling pathway (Bonni *et al.*, 1997; Rajan and McKay, 1998). Binding of CNTF or LIF to its receptor activates a receptor-associated tyrosine kinase, Janus kinase (JaK1; Stahl and Yancopoulos, 1994). Activated JaK1 phosphorylates signal transducers and activators of transcription 1 and 3 (STAT1 and STAT3) in the cytoplasm, resulting in STAT dimerisation and translocation into the nucleus. STAT proteins associate with the transcriptional coactivator CBP/p300 in the nucleus and activate astrocyte-specific programs of gene expression. BMP-induced astrocyte differentiation is mediated by the Smad proteins (Nakashima *et al.*, 1999). Binding of BMP to its serine/threonine kinase receptor results in direct phosphorylation of Smad1. Phosphorylated Smad1 dimerises with Smad4 and then translocates into the nucleus. Smad proteins bind to CBP/p300 in the nucleus and cooperate with the STATs to activate astrocyte-specific gene expression (Nakshima *et al.*, 1999). The STAT and Smad proteins bind to different domains of CBP/p300, and the complex acting at STAT binding elements in the promoters of astrocyte-specific genes, such as the glial fibrillary acidic protein (GFAP), has been shown to promote astrocyte differentiation by NSCs (Nakshima *et al.*, 1999).

Short-Range Signals

Morrison *et al.* (2000) found that Notch activation instructively promoted glial differentiation by NCSCs *in vitro*. A soluble form of the Notch ligand Delta-1 inhibited neuronal differentiation by NCSCs, and this was dominant to the neurogenic signal BMP2. In fact, even transient Notch activation triggered an irreversible loss of neurogenic capacity in NCSCs. The authors showed that Notch signalling increased the extent and rate of glial differentiation, suggesting that Notch promotes gliogenesis. Taken together, the findings suggest that Notch activation instructs an irreversible and cell-heritable switch from neurogenesis to gliogenesis in NCSCs.

Gaiano *et al.* (2000) and Furukawa *et al.* (2000) focused on the effects of Notch activation within the developing nervous system *in vivo*. Gaiano *et al.* (2000) showed that Notch activation promoted radial glial identity by mouse forebrain progenitors. In general, neurogenesis precedes gliogenesis during nervous system development. However, radial glia appear before, or concurrent with, the first cortical neurons (Choi and Lapham, 1978; Levitt *et al.*, 1983). This specialised glial cell type serves as a scaffold along which newborn neurons migrate into the developing cerebral cortex. Gaiano *et al.* (2000) injected retroviral vectors encoding either a control or a constitutively active form of Notch into telencephalic progenitors of 9.5 dpc mouse embryos, thereby activating Notch signalling in progenitor cells before the onset of neurogenesis. As expected, control cells were found dispersed throughout the brain at later stages of development. However, Notch-infected cells were found in clusters along the ventricular surface, and had the morphological and molecular characteristics of radial glia. Notch activation also reduced the numbers of neurons and oligodendrocytes generated by cortical stem cells during nervous system

development. Notch signalling was also found to promote gliogenesis in the vertebrate retina (Furukawa *et al.*, 2000). Furukawa *et al.* (2000) reported that more than 90 % of retinal stem cells expressing a constitutively active form of the Notch receptor generated Muller glial cells, compared to 8 % of control cells. The number of bipolar cells and rods formed in the retina was decreased, indicating that the increase in glial generation was at the expense of other cell types.

Since members of the Notch gene family are expressed in the VZ of the developing brain (Lindsell *et al.*, 1996), it is likely that Notch signalling plays a role in vertebrate nervous system development *in vivo*. The most likely explanation is that neuroblasts and newly generated neurons, which express Notch ligands, activate Notch receptors on neighbouring uncommitted NSCs in the VZ, thereby triggering a switch to gliogenesis in these cells. This feedback signal mediated by Notch ligands could partly explain why glia are generated after neurons in the developing nervous system, and may help to explain how multipotent stem cells are able to generate neurons and glia in the face of conflicting instructive signals *in vivo*. For example, Notch activation in NCSCs overrides the instructive neurogenic signal BMP2 and promotes gliogenesis (Morrison *et al.*, 2000).

In the mammalian Notch signalling pathway, the transcription factor RBP-J interacts with the intracellular region of Notch, RAM23 (Tamura *et al.*, 1995). Activation of Notch by its ligand leads to proteolytic cleavage of its intracellular domain (Schroeter *et al.*, 1998; Struhl and Greenwald, 1999; Ye *et al.*, 1999), and the complex consisting of the intracellular region of Notch and RBP-J translocates into the nucleus. In the nucleus, this complex upregulates the expression of Hes bHLH transcription factors, such as Hes1 and Hes5. These bHLH proteins have a proline

residue in their basic domain, which results in these proteins binding to a DNA sequence known as the N box, rather than binding to the E box (Sasai *et al.*, 1992; Tietze *et al.*, 1992). The Hes proteins act as transcriptional repressors, via binding to the N box and actively repressing transcription of their target genes, and via antagonism of bHLH proteins that act as E box-dependent transcriptional activators (Sasai *et al.*, 1992; Ohsako *et al.*, 1994; Van Doren *et al.*, 1994). Notch signalling acts instructively to inhibit neurogenesis. Hes1 binds to the promoter region of Mash1 and represses Mash1 transcription, and also antagonises Mash1 activity in a dominant negative manner (Sasai *et al.*, 1992; Ishibashi *et al.*, 1995; Chen *et al.*, 1997). Notch signalling may promote gliogenesis by a similar mechanism to that which inhibits neurogenesis. Notch signalling, via either RBP-J or Hes proteins, may promote gliogenesis by upregulating transcription factors that induce glial differentiation, and/or by inhibiting inhibitors of glial-specific gene expression, such as Ngn1, which was recently shown to directly inhibit the transcription of GFAP, independent of its ability to promote neurogenesis (Sun *et al.*, 2001). It is unlikely that gliogenesis is a default fate due to loss of neurogenic capacity induced by Notch signalling because Notch activation promoted radial glial identity, which is one of the first cell types present in the forebrain. Also, NCSCs have three possible fates: neuronal, glial or smooth muscle, so inhibiting neurogenesis cannot simply lead to glial differentiation by default. Together, the findings suggest that Notch activation is a positive glial differentiation signal. Another idea is that Notch signalling may promote gliogenesis by enabling or prolonging the responsiveness of the stem cell to instructive signals. Wang and Sternberg (1999) found that the ability of certain cells to respond to the EGF family homologue LIN-3 was regulated by Notch signalling. Interestingly, TGFα and Nrg1/GGF2, which are instructive signals that have been implicated in Muller glia, radial glia and Schwann cell differentiation, are also EGF

family homologues. In a recent study, Hes5 expression was induced by BMP2 as part of its antineurogenic effect in telencephalic neuroepithelial cells, which suggests the existence of cross-talk between Notch and BMP signalling (Nakashima *et al.*, 2001).

The qualitative outcome of Notch signalling will no doubt be influenced by the presence of other extracellular signals, such as CNTF or Nrg1/GGF2, as well as intrinsic mechanisms. Seemly, multipotent neural crest progenitors are found in tissues where Notch ligands are expressed, such as dorsal root ganglia (Hagedorn *et al.*, 1999). It is possible that these cells are not in direct contact with neuroblasts expressing Notch ligands. Alternatively, intracellular inhibitors of Notch signalling, such as Numb, may be differentially expressed among progenitor cells (Zhong *et al.*, 1997; Verdi *et al.*, 1999; Wakamatsu *et al.*, 1999). Whatever the reason, both extrinsic and intrinsic signals likely cooperate to regulate gliogenesis in the nervous system *in vivo*.

1.2.2.2.2 Oligodendrocyte Cell Fate Decision

Extracellular signals have been identified that promote oligodendrocyte differentiation by stem cells, including thyroid hormone (TH; Barres *et al.*, 1994; Johe *et al.*, 1996) and Sonic Hedgehog (Shh; Orentas *et al.*, 1999; Lu *et al.*, 2000). Early studies found that Shh could induce oligodendrocyte development in explant cultures and at ectopic locations in the chick embryonic spinal cord (Poncet *et al.*, 1996; Pringle *et al.*, 1996). A more recent study demonstrated that Shh was required for oligodendrocyte precursor cell specification in the chick embryo spinal cord (Orentas *et al.*, 1999). The intracellular mediators and molecular mechanisms that control oligodendrocyte development are still elusive. Transcription factors linked to the formation of glia have been described in *Drosophila*, such as *glial cells missing*

(*gcm/glide*) and *pointed* (Klaes *et al.*, 1994; Hosoya *et al.*, 1995), but whether their vertebrate homologues play a role in gliogenesis is uncertain at the present time (Kim *et al.*, 1998). Two related Class B bHLH proteins have been linked to the formation of oligodendrocytes by multipotent neural progenitors in the vertebrate CNS, Olig1 and Olig2 (Lu *et al.*, 2000; Takebayashi *et al.*, 2000; Zhou *et al.*, 2000). The Olig genes were expressed in the restricted region of the ventral spinal cord VZ where oligodendrocyte precursors arise, and their expression was in migrating oligodendrocyte precursors and in mature oligodendrocytes. In addition, ectopic expression of Olig1 in multipotent cortical progenitors *in vitro* significantly increased the number of cells expressing NG2, a marker of oligodendrocyte precursors, compared to controls (Lu *et al.*, 2000), and ectopic expression of Olig2 in chick mesoderm *in vivo* induced ectopic expression of Sox10, another oligodendrocyte precursor marker (Zhou *et al.*, 2000). Together, the findings suggested that Olig proteins may function in oligodendrocyte fate determination. The region of the neuroepithelium where the Olig genes are expressed also generates motor neurons earlier in spinal cord development (Sun *et al.*, 1998; Richardson *et al.*, 2000; Xu *et al.*, 2000). Olig2 is expressed in the ventral spinal cord well before the appearance of oligodendrocyte precursors, during the period of motor neuron generation (Lu *et al.*, 2000; Takebayashi *et al.*, 2000; Zhou *et al.*, 2000), and recent data has demonstrated that Olig2 also has a role in motor neuron fate determination (Mizuguchi *et al.*, 2001; Novitch *et al.*, 2001). Therefore, the studies suggest that Olig2 functions in both motor neuron and oligodendrocyte fate determination in the spinal cord.

Different domains of the ventral spinal cord VZ generate different neuronal subtypes, such as motor neurons or interneurons. The subtype-specific domains are defined by

sets of homeodomain (HD) transcription factors, and the pattern of expression of the HD proteins along the ventral-dorsal axis of the spinal cord is the result of graded Shh signalling from the notochord and floor plate (Briscoe *et al.*, 2000; Jessell, 2000; Briscoe and Ericson, 2001). There are two main groups of HD proteins based on their regulation by Shh, class I and class II proteins, which are repressed and induced by Shh signalling respectively. Crossrepressive interactions between class I and class II proteins maintain the boundaries of the subtype-specific domains (Briscoe and Ericson, 2001; Muhr *et al.*, 2001). The progenitors of the motor neuron domain in the chick express HD proteins Pax6, Nkx6.1 and Nkx6.2 (Briscoe *et al.*, 2000; Cai *et al.* 2000; Vallstedt *et al.*, 2001). Evidence from misexpression experiments in chick embryos and knockout studies in mice demonstrates that HD proteins regulate the pattern of Olig2 expression in the spinal cord. Novitch *et al.* (2001) found that expression of Olig2 was promoted by Nkx6.1, and that the HD protein Nkx2.2, which is involved in defining the neuronal subtype domain that is ventral to the motor neuron domain, repressed Olig2 expression, fixing the ventral boundary of Olig2 expression. In addition, crossrepression between Olig2 and the HD protein Irx3 appears to maintain the dorsal boundary of the motor neuron domain (Mizuguchi *et al.*, 2001; Novitch *et al.*, 2001), similar to the crossrepressive interactions between Pax6 and Nk2.2, which set the ventral boundary of the motor neuron domain (Ericson *et al.*, 1997). Together, the findings suggest that the function of Olig2 in motor neuron fate specification involves interactions with HD proteins. Olig2 also has a role in directing pan-neuronal features of motor neuron differentiation, which is associated with expression of Ngn2 (Mizuguchi *et al.*, 2001; Novitch *et al.*, 2001). Mizuguchi *et al.* (2001) and Novitch *et al.* (2001) provide evidence that Olig2 may induce Ngn2 expression.

As spinal cord development progresses, progenitors in the motor neuron-specific domain cease generating motor neurons and generate oligodendrocytes, and the Olig genes are implicated in oligodendrocyte fate determination in the spinal cord (Lu *et al.*, 2000; Takebayashi *et al.*, 2000; Zhou *et al.*, 2000). Zhou *et al.* (2001) focused on how Olig2 could play a sequential role in motor neuron then oligodendrocyte fate specification in the ventral spinal cord, and report that the dual function of Olig2 was possible due to spatial and temporal alterations in the patterns of expression of transcription factors within the ventral VZ with which Olig2 interacts. Just before the generation of oligodendrocytes in the ventral spinal cord, Ngn expression was downregulated in the Olig2 expressing domain, and then the mutually exclusive expression domains of Olig2 and Nkx2.2 became overlapping in the ventral VZ. In addition, $Olig2^{+}Nkx2.2^{+}$ cells migrated from the neuroepithelium in a pattern that reflected that of oligodendrocyte precursors. Zhou *et al.* (2001) showed that comisexpression of Olig2 and Nkx2.2 in chick embryo spinal cord induced ectopic and premature oligodendrocyte differentiation, which was not observed by misexpression of either gene alone, and this effect was suppressed by comisexpression of Ngn1 with Olig2 and Nkx2.2, indicating that the changes in gene expression in the ventral VZ are important in specification of oligodendrocyte fate. Together, the studies of Olig2 indicate that Olig2 functions in motor neuron and oligodendrocyte specification in the spinal cord, through interactions with different HD proteins at different development stages, and suggest that the Olig genes are potential candidates to play a role in oligodendrocyte cell fate decision by multipotent progenitor cells in the CNS.

1.2.2.3 The Neuronal Versus Glial Fate Decision

Many factors have been identified that are involved in the neuronal or the glial cell fate decision. Another important issue is how the specification of one cell fate is linked to the suppression of alternative lineages, and the neuronal versus glial fate decision is currently the subject of much interest. Several recent papers have implicated bHLH proteins in the regulatory mechanisms that orchestrate the timing of neurogenesis and gliogenesis during development, and demonstrate how neurogenic bHLH factors may delay the onset of gliogenesis.

Sun *et al.* (2001) reported that Ngn1 promoted neurogenesis and inhibited gliogenesis via independent molecular mechanisms in multipotent cortical progenitors *in vitro*. As they expected, overexpression of Ngn1 induced neurogenesis, accordant with the established function for Ngn1 in promoting neuronal cell fate by NSCs, but they also found Ngn1 inhibited astrocyte differentiation. While Ngn1 induces neuronal differentiation by forming heterodimers with ubiquitous bHLH proteins and functioning as a transcriptional activator at E box DNA sequences, Sun *et al.* (2001) showed that astrocytogenesis was repressed via a DNA binding-independent mechanism. Ngn1 inhibited glial-specific gene expression by interfering with the CNTF and BMP signalling pathways, which specify astrocytic cell fate. Sun *et al.* (2001) found that Ngn1 binds to the transcriptional coactivator complex CBP/p300-Smad1, preventing its interaction with the STAT factors at astrocyte-specific genes. Ngn1 also inhibited phosphorylation and therefore activation of the STAT proteins, which are important in the signalling mechanisms by which astrocytic fate is specified. The functions of Ngn1 may help to explain the sequential generation of cortical neurons and glia in the presence of conflicting environmental cues during development *in vivo*. Ngn1

expression is high during the period of cortical neurogenesis and is then downregulated, which would allow progenitors to respond to gliogenic factors following neurogenesis. Therefore, the temporal control of neurogenesis and gliogenesis in the cortex may be regulated, at least in part, by the actions of bHLH proteins, such as Ngn1.

Recent genetic studies have also implicated bHLH factors in the neuronal versus glial fate decision *in vivo* (Tomita *et al.*, 2000; Nieto *et al.*, 2001). Ngn2 and Mash1 are both expressed in the germinal layers of the developing cortex during the period of neurogenesis, at high levels (Gradwohl *et al.*, 1996; Fode *et al.*, 2000) and low levels (Guillemot *et al.*, 1993; Fode *et al.*, 2000) respectively. Interestingly, no overt defects in neuronal or glial differentiation were apparent during early corticogenesis in either Ngn2 or Mash1 single-mutant mice. Fode *et al.* (2000) found that Mash1 was upregulated, and compensated for Ngn2, in Ngn2 mutant cortical progenitor cells. Studies on Ngn2/Mash1 double-mutant embryos found severe defects in cortical development. Fode *et al.* (2000) showed that neurogenesis was significantly decreased in the cortex of Ngn2/Mash1 double-mutant embryos, accordant with the role for these factors in neurogenesis, and in a subsequent study, Nieto *et al.* (2001) showed precocious astrocyte differentiation in the double-mutant cortex. Nieto *et al.* (2001) also found that cortical progenitor cells were heterogeneous for Ngn2 expression. To further study the roles of Ngn2 and Mash1 in cortical development, wild-type and mutant cortical progenitor populations were analysed in clonal cultures. Cortical progenitors expressing Ngn2 ($Ngn2^+$) could be sorted from those that do not express Ngn2 ($Ngn2^-$) by expression of a lacZ reporter, which replaced the Ngn2 allele. Mash1 function was required for normal development of $Ngn2^-$ cortical progenitors, as shown by the increased number of astrocytic clones in the

Ngn2$^-$ subpopulation of Mash1 mutant progenitors at the expense of neuronal and neuronal/astrocytic (mixed) clones (Nieto *et al.*, 2001). The number of neuronal clones was decreased in cultures of Ngn2$^+$ progenitors from double-homozygous Ngn2/Mash1 mutant embryos compared to in control cortical cultures, and this was accompanied by an increase in the number of mixed clones, which were larger in size compared to wild-type and were mostly astrocytes, with only a few neurons (Nieto *et al.*, 2001). Taken together, the studies indicate that Ngn2 and Mash1 are involved in the fate decision of distinct populations of cortical progenitor cells, functioning to promote the neuronal fate and inhibit the astrocytic fate. Math3 has also been implicated in the neuronal versus glial fate decision in the CNS (Tomita *et al.*, 2000). Tomita *et al.* (2000) found decreased neurogenesis and concomitant astrocytogenesis in the tectum, hindbrain and retina of Mash1/Math3 double-mutant mice, which are regions of the CNS where Mash1 and Math3 are coexpressed. Therefore, this study supports a role for Mash1, and indicates a role for Math3, in the inhibition of glial fate as well as in the determination of neuronal fate. It seems likely that the lack of an apparent phenotype in single-mutant mice for neuronal bHLH genes is due to genetic redundancy between these genes in regions of the nervous system. A role for neurogenic bHLH factors in inhibiting the astrocytic fate is supported by the recent work of Sun *et al.* (2001), which demonstrated that Ngn1 actively suppressed astrocyte differentiation in cultured cortical progenitors.

While increased numbers of astrocytic precursors were found in the cortex of Ngn2/Mash1 and in the tectum of Mash1/Math3 double-mutant mice, mature astrocytes were not evident, indicating that complete astrocyte differentiation did not occur (Tomita *et al.*, 2000; Nieto *et al.*, 2001). Also, neuronal progenitors were detected in double-mutant animals, albeit at reduced numbers. These studies argue

that other factors are present that may be sufficient to specify neuronal cell fate and/or preclude complete astrocyte differentiation. The progenitors in these regions of the CNS may express additional bHLH proteins, which function to promote neuronal fate and/or inhibit astrocyte differentiation, such as Ngn1 (Sun *et al.*, 2001). Alternatively, astrocyte-promoting signals that are expressed by neuroblasts and newly generated neurons, such as Notch ligands, may be lacking in double-mutant mice since neurogenesis is decreased, and this may preclude complete astrocyte differentiation. A misexpression study in the murine cerebral cortex also argues that signals in addition to bHLH factors are involved in the neuronal versus glial fate choice (Cai *et al.*, 2000a). Cai *et al.* (2000a) used retroviral vectors to infect cortical progenitors *in vivo* with bHLH factors. They found that overexpression of Ngn1, Ngn2 or Mash1 in postnatal cortical progenitors resulted in only a modest switch of progenitors to the neuronal fate at the expense of the astrocytic fate. The results of this study and the studies in knockout mice suggest that expression of bHLH factors is not by itself sufficient to promote neuronal development and/or inhibit astrocyte differentiation. Recent studies *in vitro* and *in vivo* have implicated Notch signalling in instructing the glial fate during nervous system development (Furukawa *et al.*, 2000; Gaiano *et al.*, 2000; Morrison *et al.*, 2000; Tanigaki *et al.*, 2001). Furthermore, Tanigaki *et al.* (2001) showed that Notch activation in AHPs *in vitro* promoted astrocyte differentiation in a manner independent of the CNTF signalling pathway, which is blocked by bHLH factor Ngn1 (Sun *et al.*, 2001). Further studies are required to understand the relative importance of each signal in the neuronal versus glial fate decision during nervous system development.

1.2.3 Ids in Nervous System Development

1.2.3.1 Patterns of Id Gene Expression During Mouse Nervous System Development

All four of the Id genes are expressed in the developing nervous system (Duncan *et al.*, 1992; Ellmeier *et al.*, 1992; Wang *et al.*, 1992; Evans and O'Brien, 1993, Neuman *et al.*, 1993; Nagata and Todokoro, 1994, Riechmann and Sablitzky, 1995; Jen *et al.*, 1996, 1997). Although each Id exhibits a unique overall spatial and/or temporal expression pattern during nervous system development, their expression is overlapping. The spatial and temporal expression of Id1 and Id3 overlap considerably during embryonic neurogenesis. For example, during early spinal cord development (9.5-13.5 dpc), both Id1 and Id3 are highly expressed in the roof plate and in the ventral portion of the ventricular zone (VZ), which is composed of mitotically active neural precursor cells. However, their expression is not completely overlapping because Id3 is also expressed in the floor plate. The expression of Id1 and Id3 decreases in later stages of nervous system development (14.5 dpc), when most of the cells in the VZ exit from the cell cycle. Moderate levels of Id2 are also expressed in the roof plate and VZ during early neurogenesis, overlapping with the expression of Id1 and Id3. A small domain of the ventral VZ also expresses Id4. Id2 and Id4 expression is also in distinct presumptive post-mitotic neurons that are undergoing maturation. Id2 is expressed in a subset of motor neurons or/and interneurons in the putative dorsal end of the motor neuron column, whereas Id4 expression is in the majority of the motor neuron column during early neurogenesis. The expression of Id2 and Id4 is not overlapping. In later stages, Id2 expression in the motor neuron column diminishes, but Id2 is expressed in the pars ventralis and the pars dorsalis (intermediate gray) of the spinal cord. Id4 expression occurs in the

future substantia gelatinosa, a region where sensory neurons reside, and in the motor neuron column (Jen *et al.*, 1997).

The overall expression pattern of the Ids in the developing brain is similar to that in the spinal cord. All of the Id genes are expressed in the mitotically active ventricular zone of the developing brain, where their expression along the dorsal-ventral axis is analogous to that which has just been described for the spinal cord. For example, Id1, Id2 and Id3 are expressed in the dorsal-most region of the developing brain, and only Id3 is expressed in the ventral-most region, which are the equivalent regions to the roof plate and floor plate of the spinal cord. The expression of Id1 and Id3 in the brain diminishes as cells in the VZ cease dividing during later stages of neurogenesis. Id4 is expressed in presumptive motor neurons in the metencephalon during early development, as in the spinal cord, and the expression of Id2 or Id4 is found in many post-mitotic nuclei of the developing brain at 14.5 and 16.5 dpc (Jen *et al.*, 1997). The expression patterns of the Id genes are somewhat different in the developing telencephalon to the rest of the nervous system. During early telencephalic development (10-11.5 dpc), Id1, Id2 and Id3 are expressed only in the VZ in the region from which the future hippocampus is derived, and Id4 is expressed in the VZ throughout the rest of the telencephalic vesicles (Jen *et al.*, 1997). Id2 is expressed in the entire vesicles by 12.5 dpc, but the expression of Id1/Id3 and Id4 is still mutually exclusive. In later development (14.5 dpc), only Id1 and Id3 are expressed in the hippocampus (Jen *et al.*, 1997). As the multi-laminar cerebral cortex is formed, Id4 is still expressed in the VZ, Id2 is in the intermediate zone, and both Id2 and Id4 are expressed throughout the cortical plate (Jen *et al.*, 1997). The sharp boundaries between Id1/Id3 and Id4 expression in the VZ of the telencephalic vesicles may reflect the different developmental fates of the neural precursors.

In general terms, the expression data on the Id genes indicates that Id1 and Id3 expression is localised to most mitotically active neural precursor cells in the VZ, and hence, their expression decreases in later stages of neurogenesis when many cells in the VZ cease dividing. Id2 and Id4 are expressed in some dividing neural precursors in the VZ, but expression of Id2 and Id4 is also in specific presumptive post-mitotic neurons.

1.2.3.2 Id Gene Expression During Neuronal and Astrocyte Differentiation *In Vitro*

Regulation of Id gene expression during neuronal and astrocyte differentiation has been studied in cell culture models. Upon nerve growth factor (NGF)-induced neuronal differentiation of rat pheochromocytoma PC12 cells, Id1-Id3 gene expression, which are detectable in undifferentiated cells, rapidly and transiently increased several fold, and then decreased (Nagata and Todokoro, 1994; Einarson and Chao, 1995). Einarson and Chao (1995) reported that active bHLH protein complexes existed throughout PC12 neuronal differentiation, and that these complexes could be disrupted by the presence of Id1. Together these studies suggest that HLH protein interactions may be involved in the regulation of neuronal differentiation. The NGF-mediated downregulation of Id1-3 gene expression during PC12 neuronal differentiation was blocked by DNA methyltransferase inhibitor 5-azacytidine (Persengiev and Kilpatrick, 1997). Moreover, this effect was coincident with the block of NGF-induced neuronal differentiation mediated by 5-azacytidine, implying that the decrease of Id gene expression is associated with neuronal differentiation. Downregulation of Id2 mRNA levels was also observed during neuronal differentiation of SMS-KCNR neuroblastoma cells and neuroblastoma-glioma hybrid NG108 cells (Biggs *et al.*, 1992; Neuman *et al.*, 1993). However, Id2

gene expression was upregulated during neuronal differentiation of neuroblastoma N18 cells and was unaltered during neuronal differentiation of tetracarcinoma PCC7 cells (Neuman *et al.*, 1993). The divergent regulation of Id2 gene expression in different neuronal cell lines suggests that Id2 is not simply an inhibitor of differentiation, and that Id2, and most likely other members of the Id family, has different functions in different cell types.

Several *in vitro* models have been used to analyse the regulation of Id gene expression during astrocyte differentiation. All four Id genes were expressed in the mouse astrocyte precursor cell line NSEHip2-28, which can differentiate along the astroglial lineage (Andres-Barquin *et al.*, 1997). Upon induction of astrocyte differentiation, the expression of all four Id genes initially increased significantly, coincident with the time that GFAP expression became detectable, and subsequently decreased. This study suggests that the Id genes may be involved in the regulatory mechanisms that modulate astrocyte differentiation. In a following study, Andres-Barquin *et al.* (1999) found that Id1-Id4 were expressed in primary cultures of mouse forebrain astrocytes. Biochemical and morphological differentiation of astrocytes in culture is known to be promoted by activation of the cAMP-dependent signal transduction pathway (Couchie *et al.*, 1985; Pollenz and McCarthy, 1986; Le Prince *et al.*, 1991; Huneycutt and Benveniste, 1995). In the absence of serum, the expression of Id1-Id4 genes in primary cultures of forebrain astrocytes was decreased following activation of the cAMP-dependent signalling pathway, which was accompanied by astrocyte differentiation (Andres-Barquin *et al.*, 1999). Interestingly, upon induction of astrocyte differentiation in the presence of serum, only Id4 gene expression was downregulated. Id4 mRNA levels transiently increased and then progressively decreased during astrocyte differentiation, similar to the

pattern of expression observed during astrocytic differentiation of NSEHip2-28 cells (Andres-Barquin *et al.*, 1997). The expression of Id1-Id3 genes has been shown to be responsive to serum (Benezra *et al.*, 1990; Christy *et al.*, 1991; Barone *et al.*, 1994; Tzeng and de Vellis, 1997), which may explain the decrease in the expression of these genes in astroglial primary cultures in the absence of serum. Id4 mRNA levels did not decrease in astroglial primary cultures under serum-free conditions in the absence of cAMP (Andres-Barquin *et al.*, 1999). The findings suggest that the cAMP signalling pathway is an inhibitor of Id4 gene expression in astrocytes, and that Id4 is involved in the molecular mechanisms regulating the astrocyte differentiation programme. Notably, Andres-Barquin *et al.* (1999) also found that overexpression of Id4 in U373 astrocytes, which is an astrocyte-derived cell line that retains properties of primary astrocytes, induced cell death by apoptosis. Taken together the studies suggest that Id4 may be an important factor in the regulation of both astrocyte differentiation and apoptosis.

1.2.3.3 Id Proteins in Neural Cell Fate Determination

Id2 has been shown to take part in the regulation of neural crest specification in the chick (Martinsen and Bronner-Fraser, 1998). Ectopic expression of Id2 in chick-embryo surface ectoderm indicated that Id2 directs ectodermal precursor cells to neural crest and neurogenic fates at the expense of epidermal lineages. This suggests that a bHLH protein may exist that promotes epidermalisation, and that its functional regulation by Id2 is involved in cell fate determination.

1.2.3.4 Id Proteins Mediate the Anti-Neurogenic Effect of BMP2

A recent *in vitro* study showed that BMP2 induces a switch in the fate of telencephalic neural progenitor cells from neurogenesis to astrocytogenesis, and the Id factors were proposed as part of the mechanism by which BMP2 signalling interacts with the neurogenic bHLH transcription factors to induce this effect (Nakashima *et al.*, 2001). Nakashima *et al.* (2001) found that BMP2 signalling via the Smad proteins upregulated the expression of Id1, Id3 and Hes-5, which inhibit the transcriptional activity of Mash1 and neurogenin to suppress neurogenesis. Adenovirus-mediated ectopic expression of Id1 or Id3 was sufficient to inhibit the neurogenic fate, but did not induce the formation of mature astrocytes. It is possible that activation of Smads by BMP2 is required for astrocyte differentiation. In addition, BMP-induced only a transient expression of Id1 and Id3 in telencephalic neuroepithelial cells (Nakashima *et al.*, 2001). Notably, the expression of Id1 and Id3 is not found in the brain at a late stage of development, when mature astrocytes are detected (Duncan *et al.*, 1992; Jen *et al.*, 1997). In an earlier *in vivo* study, Cai *et al.* (2000a) found that retrovirus-mediated expression of Id1 in the cerebral cortex of embryonic or postnatal mouse inhibited neurogenesis and induced gliogenesis, as judged by cellular morphology. Although the expression of glial marker proteins was not analysed, it is quite possible that extrinsic signals *in vivo* cooperate with Id1 to promote gliogenesis. In the developing brain, expression of Id1 and Id3 is restricted to proliferating neural precursor cells in the ventricular zone (Duncan *et al.*, 1992; Jen *et al.*, 1997). BMP receptors are also expressed on cells in the ventricular zone at a time when Id1 and Id3 genes are expressed (Zhang *et al.*, 1998). Therefore, the mechanism by which BMP2 exerts its anti-neurogenic effect may occur under physiological conditions. It is conceivable that, in addition to Mash1 and neurogenin,

other proneural bHLH transcription factors are also targets of Id proteins and may be involved in the anti-neurogenic effect of BMP2.

1.2.3.5 Id Knockout Mice

No phenotype was apparent in the nervous system of Id1 or Id3 single knockout mice (Yan *et al.*, 1997a; Pan *et al.*, 1999; Lyden *et al.*, 1999). In Id2 knockout mice, the olfactory bulb was small and the frontal cortex slightly narrow (Yokota and Mori, 2002), although the mechanisms for these effects have not been described. The subtle effects of targeted disruption of individual Id genes may be because of compensation by other members of the Id family, due to the functional redundancy among Id proteins and their overlapping patterns of expression. In support of this, mice lacking Id1 and Id3 were inviable (Lyden *et al.*, 1999). Id1/Id3 double knockout mice died in utero due to a defect in angiogenesis, and had small brains. No significant increase in apoptosis was observed in the $Id1^{-/-}Id3^{-/-}$ embryonic brain. However, Lyden *et al.* (1999) found fewer proliferating cells in the neuroepithelium of the telencephalon and rhombencephalon in E11.5 mutants compared to wild-type, indicating premature withdrawal of neuroblasts from the cell cycle. This was accompanied by increased expression of cyclin-dependent kinase inhibitors, p16 and p27. In addition, the expression of post-mitotic neuronal differentiation markers, microtubule-associated protein 2 (MAP2) and unique β-tubulin (TUJ1), was detected more widely in $Id1^{-/-}$ $Id3^{-/-}$ than in control embryos. Premature and ectopic expression of both determination- and differentiation-related neurogenic bHLH genes, MATH1, MATH3 and NeuroD1, MATH2 respectively, was detected in the E11.5 mutant embryonic brain. Given the hierarchy of activities within the neural bHLH family, where the determination proteins activate the expression of the differentiation

effectors, this study suggests premature activation of the cascade of neurogenic bHLH factors in the absence of Id1 and Id3. Therefore, the premature neuronal differentiation in $Id1^{-/-}Id3^{-/-}$ mice indicates that Id1 or Id3 is required to block the precocious functioning of neurogenic bHLH factors, and thereby maintain the timing of neuronal differentiation during mammalian development.

1.2.3.6 Id Proteins in Oligodendrocyte Development

Oligodendrocytes differentiate from proliferating oligodendrocyte precursor cells (OPCs; figure 1.4; Rogister *et al.*, 1999). The normal timing of oligodendrocyte development can be reconstituted *in vitro*, in cultures of dissociated perinatal rodent optic nerve cells under the appropriate conditions (Raff *et al.*, 1985, 1988; Miller *et al.*, 1985; Barres and Raff, 1994). In general, OPCs are stimulated to proliferate by PDGF, and oligodendrocyte differentiation can be induced by either PDGF withdrawal or TH addition (in the presence of PDGF). Studies indicate that both an intracellular timer and extracellular signals are important in determining when OPCs stop dividing and initiate differentiation (Temple and Raff 1986; Barres *et al.*, 1994; Gao *et al.*, 1998; Durand and Raff, 2000).

Recent studies found that rat OPCs express all four Id HLH proteins *in vitro* (Kondo and Raff, 2000; Wang *et al.*, 2001). Id2 and Id4 proteins were localised to the nucleus, whereas Id1 and Id3 proteins were diffuse in proliferating OPCs. Kondo and Raff (2000) showed that only the expression of Id4 decreased over time as OPCs proliferated *in vitro* and *in vivo*, with a time course expected if Id4 were part of the cell-intrinsic timer in oligodendrocyte development. The expression of Id1, Id2 and Id3 did not change *in vitro*. The rate at which Id4 decreased was accelerated when OPCs were induced to differentiate prematurely. The authors also showed that

overexpression of Id4 in OPCs blocked OPC differentiation into oligodendrocytes and stimulated cell proliferation, similar to the overexpression of Id proteins in other cell types. The results of Kondo and Raff (2000) suggest that Id4 negatively regulates oligodendrocyte differentiation, and the progressive fall in Id4 expression in proliferating OPCs may play a part in regulating the timing of oligodendrocyte differentiation. Two studies have found that overexpression of Id2 in OPCs blocked their differentiation into oligodendrocytes (Sdrulla *et al.*, 1999; Wang *et al.*, 2001), suggesting that Id2 also plays a part in the control of oligodendrocyte differentiation. However, Id2 expression does not decrease over time in proliferating OPCs *in vitro* (Kondo and Raff, 2000; Wang *et al.*, 2001). Wang *et al.* (2001) demonstrated that in OPCs stimulated to differentiate in culture, Id2 protein translocated out of the nucleus prior to the onset of differentiation. As anticipated, overexpression of Id2 stimulated cell proliferation in response to PDGF. Id2 is not essential for the generation of oligodendrocyte lineage cells because OPCs were isolated from Id2 knockout mice. $Id2^{-/-}$ OPCs showed a decreased proliferation rate compared to $Id2^{+/+}$ OPCs in the presence of PDGF, and differentiated prematurely in response to TH. The findings suggest that Id2 is part of the intrinsic mechanism that controls oligodendrocyte differentiation. Taken together, the studies indicate that Id2 and Id4 are components of the intracellular programme that times when OPCs withdraw from the cell cycle and differentiate, and function to enhance the rate of proliferation and to slow the rate of differentiation of OPCs. Multiple intracellular proteins are thought to contribute to the timer, and it is possible that the functions of Id2 and Id4 in these cells are at least partially redundant. Hence, OPCs lacking a single component, such as $Id2^{-/-}$ OPCs, may not show a dramatic defect in oligodendrocyte development.

Id proteins function mainly as dominant-negative regulators of bHLH proteins, therefore these reports point to the existence of a positively acting bHLH protein in oligodendrocyte development. Although oligodendrocyte-specific bHLH transcription factors, Olig1 and Olig2, have recently been identified (Lu *et al.*, 2000; Takebayashi *et al.*, 2000; Zhou *et al.*, 2000), it is not clear whether Id proteins are acting to inhibit their functions or that of other, as yet unidentified, bHLH factors.

1.2.3.7 Summary: Ids in Nervous System Development

Evidently, Id proteins may be involved in the regulation of various developmental programs during mammalian nervous system development. Each Id gene displays a unique spatial and temporal pattern of expression during development of the nervous system, and *in vivo* studies in mice and studies in neural cells in culture have implicated Id proteins in cell determination, differentiation, proliferation and apoptosis of the nervous system. Together the data suggests that Ids may have distinct and/or overlapping functional roles during mammalian nervous system development.

1.3 Germ Cell Development

During embryonic development of the mouse, the gonads begin to form at approximately 10.5 dpc. Germ cells of the mouse testis originate from the allantois (Ginsburg *et al.*, 1990; Gomperts *et al.*, 1994) and somatic Sertoli cells from the coelomic epithelium (Karl and Capel, 1998).

1.3.1 Spermatogenesis

Spermatogenesis is the process by which diploid spermatogonia form mature haploid spermatozoa. This process is highly spatially and temporally organised within the seminiferous tubule compartment of the testis. Spatially, the developing germ cells move from the basal lamina, which is the periphery of the testicular tubule, to the tubule lumen in the centre (figure 1.5). Spermatogenesis can be divided into three main phases: 1) mitotic proliferation and differentiation of spermatogonia, 2) meiotic division of spermatocytes, and 3) spermiogenesis, in which spermatids are transformed into spermatozoa (figure 1.6).

1.3.1.1 Mitotic Proliferation

Spermatogenic capability resides in the stem cell spermatogonia, which are a reservoir of self-regenerating germ cells in the basal compartment of the seminiferous tubule. Spermatogenesis begins when stem cell spermatogonia (Type $A_{isolated}$, A_{is}; Huckins, 1971) enter a phase of mitotic proliferation as follows ($\rightarrow$ indicates cell division):

$$A_{is} \rightarrow A_{pr} \rightarrow A_{al} \rightarrow A_{al} \rightarrow A_{al} \qquad A_1 \rightarrow A_2 \rightarrow A_3 \rightarrow A_4 \rightarrow In \rightarrow B$$

Where Type A_{paired} (A_{pr}) and Type $A_{aligned}$ (A_{al}) are named 'proliferative' spermatogonia, and Type $A_{1\text{-}4}$, Intermediate (In) and Type B (B) are 'differentiating' spermatogonia. A_{al} spermatogonia become A_1 spermatogonia at a set time, without cell division. The A_{al} spermatogonia are thought to renew themselves, and the number of divisions contributing to the A_1 spermatogonial pool may vary. This proliferative phase of spermatogenesis takes place within the basal intratubular

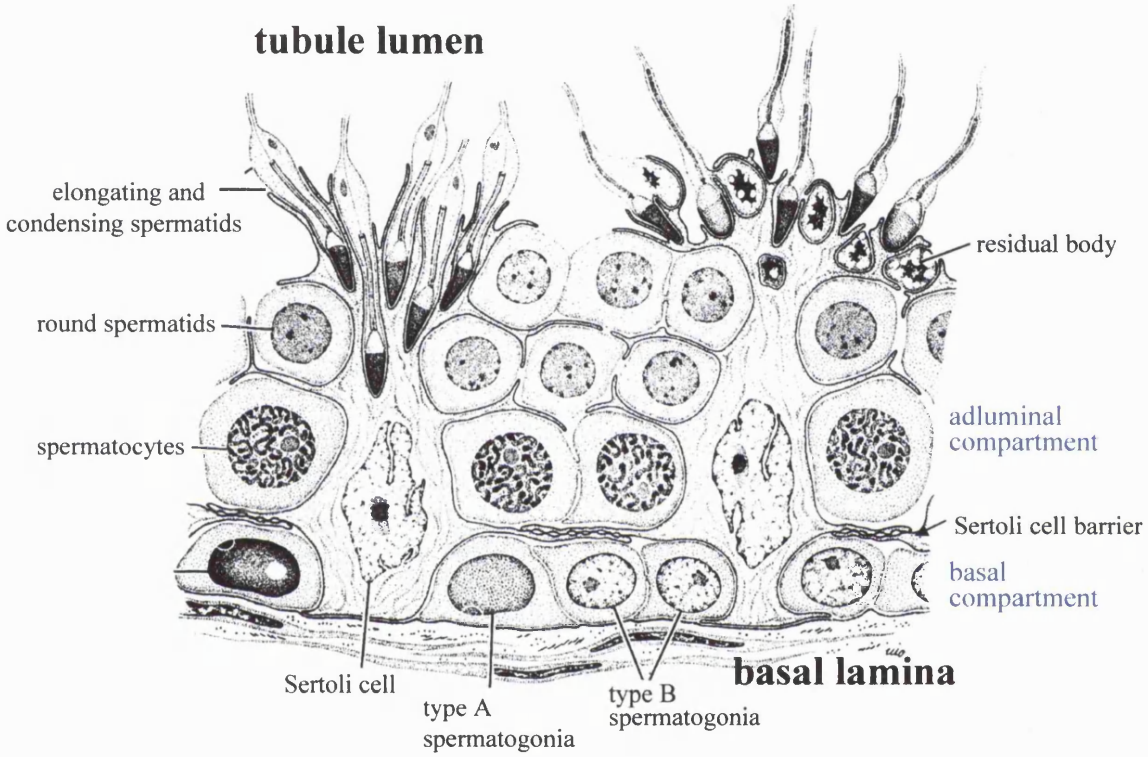

Figure 1.5 A representation of a portion of the seminiferous tubule wall showing the organisation of cells within the tubule epithelium. Spermatogonia, spermatocytes and round spermatids are organised in successive layers towards the tubule lumen. Elongating and condensing spermatids are often in deep recesses of the Sertoli cell. The Sertoli cells extend from the base of the tubule to the tubule lumen and contact all the developing germ cells. Release of mature sperm is accompanied by elimination of the residual cytoplasm (residual body). The Sertoli cell barrier separates the seminiferous epithelium into basal and adluminal compartments.

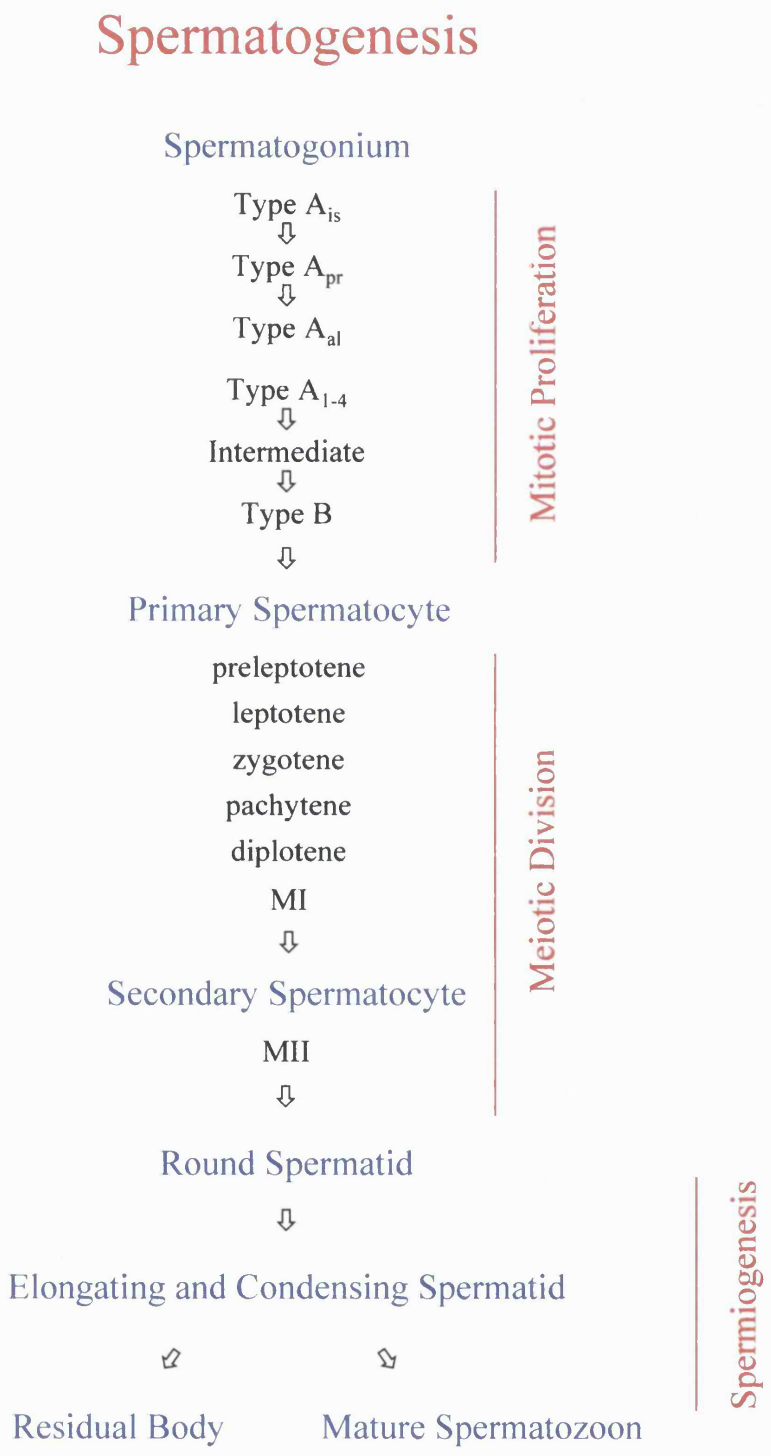

Figure 1.6 Overview of Spermatogenesis.

compartment of the testis (figure 1.5). Whilst the dividing spermatogonia undergo complete karyokinesis, cytokinesis is incomplete, and the developing germ cells remain connected by areas of open cytoplasmic continuity, known as intercellular bridges (Fawcett *et al.*, 1959; Weber and Russell, 1987). The intercellular bridges persist throughout the further development of sperm, and promote the synchronous development of germ cell clones (Huckins, 1978). The Type A spermatogonial cells show only minor structural differences. However, Type A as a class, Intermediate and Type B spermatogonia display clear structural differences and can be identified based on morphological criteria. The sequence of spermatogonial divisions during early sperm development builds a large population of cells that will subsequently form sperm.

1.3.1.2 Meiotic Division

The Type B spermatogonia undergo a final mitotic division to form preleptotene (resting) primary spermatocytes, thereby entering the meiotic phase (figure 1.6). Preleptotene cells are the last germ cell type to go through S-phase of the cell cycle. Following DNA synthesis, they move via the intermediate compartment into the adluminal intratubular compartment of the seminiferous tubule (figure 1.5), and then enter leptotene, the first stage in the prolonged meiotic prophase. All further germ cell development occurs on the adluminal side of the Sertoli cell barrier (Dym and Caviccia, 1977). The stages in meiotic prophase are as follows:

preleptotene → leptotene → zygotene → pachytene → diplotene

Primary spermatocytes at different stages in prophase may be identified by their characteristic nuclear morphologies. Genetic recombination (crossing over) occurs

during pachytene, resulting in germ cell chromosomes that are genetically distinct from the somatic cell chromosomes of the animal. Following prophase, metaphase, anaphase and telophase of the cell division process are brief, to form secondary spermatocytes, and these phases are referred to as the first meiotic division (MI). All phases of the second meiotic division (MII) are rapid, producing spermatids.

1.3.1.3 Spermiogenesis

Spermiogenesis occurs without cell division, and is a series of cell transformations that converts round spermatids into spermatozoa. This process occurs in three main phases, round, elongating and condensing spermatids. In the mouse, post-meiotic sperm development can be further subdivided into sixteen steps (Oakberg, 1956). Several events occur simultaneously during this phase of sperm development, including the development of a flagellum, the development of an acrosome and the nuclear reshaping and condensation of spermatids. The release of sperm is accompanied by the elimination of cytoplasm, known as a residual body, which is phagocytosed by the Sertoli cell (figure 1.5; Kerr and de Kretser, 1974).

Spermatogenesis is complete with the formation of mature spermatozoa. The intercellular bridges that linked clones of developing sperm during spermatogenesis rupture and individual sperm are released into the lumen of the seminiferous tubule. Spermatogenesis is initiated regularly and in mice, the entire spermatogenic process takes 35 days.

In cross-sectioned seminiferous tubules, germ cell types at specific developmental stages are always found in association with each other. Each cell association has a defined germ cell composition and this aids morphological identification of germ cell

types. The complete developmental sequence of cell associations that occurs in a given segment of the seminiferous epithelium over time is called the cycle of the seminiferous epithelium (Le Blond and Clermont, 1952).

1.3.2 The Sertoli Cell

The testicular Sertoli cells support spermatogenesis. Sertoli cells are somatic cells within the seminiferous tubules, which extend from the base of the tubule to the lumen (figure 1.5), providing a microenvironment and cytoarchitectural support to the developing germ cells (Fawcett, 1975). Sertoli cell proliferation occurs only during a period of development in foetal and neonatal life (Steinberger and Steinberger, 1971; Orth, 1982; Johnson *et al.*, 1984; Kluin *et al.*, 1984; Bortolussi *et al.*, 1990; Hochereau-de Reviers *et al.*, 1995; Baker and O'Shaughnessy, 2001). Proliferation is maximal during late foetal life and declines steadily after parturition. After 2-3 weeks of life, Sertoli cell proliferation ceases. Hence, the number of Sertoli cells in the adult testis is fixed by the time of puberty. Each Sertoli cell can only support a finite number of developing germ cells, therefore the total Sertoli cell number within the testis sets the upper limit for sperm production (Orth *et al.*, 1988; Cook *et al.*, 1991; Simorangkir *et al.*, 1995). The number of germ cells supported by each Sertoli cell varies between species. In rodents, Sertoli cells support 10-12 elongated spermatids, whereas in man, the number is only 4 (Sharpe, 1994).

The main phase of Sertoli cell differentiation occurs during pubertal development, when Sertoli cell differentiated functions, such as transferrin expression, increase to reach optimal levels in the adult to maintain testicular function (Griswold, 1988; Skinner *et al.*, 1989; Jegou, 1992). The iron-binding protein transferrin is a major

secretory product expressed by differentiated Sertoli cells (Skinner and Griswold, 1980, 1982; Skinner *et al.*, 1989), and transports iron to developing germ cells that are within the Sertoli cell barrier. In the adult testis, Sertoli cells are a post-mitotic, terminally differentiated cell population (Jegou, 1992). The cessation of proliferation and onset of Sertoli cell differentiation is also associated with the formation of the Sertoli cell barrier (Griswold, 1998). Numerous tight junctions between Sertoli cells at their basolateral surfaces form a barrier that divides the seminiferous tubule into basal and adluminal intratubular compartments (figure 1.5; Dym and Fawcett, 1970). This was originally named the blood-testis barrier, but is also aptly known as the Sertoli cell barrier (Setchell and Waites, 1975; Weber *et al.*, 1988). Germ cells move from the basal to adluminal compartment via an intermediate compartment formed by the consecutive breakdown and formation of tight junctions (Russell, 1977, 1978). Therefore, the integrity of the Sertoli cell barrier is maintained. The basal and adluminal environments differ. Basal compartment cells have access to substances from the lymphatic and vascular systems, which diffuse into the lymph that surrounds the seminiferous tubule. The Sertoli cell regulates the environment of the adluminal compartment, although the Sertoli cell barrier allows substances to enter the adluminal compartment at low levels.

Many functions for the Sertoli cell have been suggested (Fawcett, 1975; Dym 1977), in addition to the Sertoli cell barrier. The attachments formed between Sertoli cells, and to other cells and acellular elements, maintain the integrity of the seminiferous epithelium (Russell, 1980; Russell and Peterson, 1985). The Sertoli cell secretes fluid, which forms the tubular lumen and transports mature spermatozoa within the male tract (Setchell and Waites 1975). It also phagocytoses degenerating germ cells and eliminated cytoplasm during normal spermatogenesis (Kerr and de Kretser,

1974; Russell and Clermont, 1977), and actively participates in spermiation (Fawcett and Phillips, 1969; Russell, 1984).

1.3.3 Endocrine Control of Spermatogenesis

It is well known that the gonadotropins, follicle-stimulating hormone (FSH) and leutinizing hormone (LH), are the main hormones regulating spermatogenesis. FSH acts on seminiferous tubules directly, whereas LH stimulates the Leydig cells of the testis to produce androgens, such as testosterone, which affect the tubules in a paracrine manner. Leydig cells are found within the interstitial compartment of the testis between the seminiferous tubules, and are the main source of testicular testosterone. Since male germ cells do not possess receptors for either FSH or androgens, the actions of FSH and testosterone are mediated by Sertoli cells, which have FSH and androgen receptors (Verhoeven, 1992; Sharpe, 1994). Androgen receptors are also found on peritubular myoid cells that surround the seminiferous tubule. In response to androgens, myoid cells produce PmodS, a paracrine factor that modulates Sertoli cell function (Skinner and Fitz, 1985; Skinner *et al.*, 1988). FSH receptors are only found on Sertoli cells of the testis.

The roles and contributions of FSH and androgens in the control of spermatogenesis have been the subject of extensive research. Several studies using rats have shown that after hypophysectomy (Clermont and Harvey, 1965; Cunningham and Huckins, 1979; Santulli *et al.*, 1990), or removal of gonadotropic support using gonadotropin releasing hormone (GnRH) antagonists (Rea *et al.*, 1996) or antisera to GnRH (McLachlan *et al.*, 1994, 1994a), spermatogenesis could be maintained by administration of testosterone alone. However, spermatogenesis was at a reduced

rate. The administration of high doses of exogenous testosterone could initiate and maintain spermatogenesis in hypogonadal mice, which lack circulating gonadotropins, but the testes of these mice were reduced in size and spermatid numbers decreased compared to normal (Singh *et al.*, 1995). These studies show that testosterone has a key role in spermatogenesis, but also indicate that FSH is important in the process of germ cell development. This is supported by a recent study showing that immunoneutralisation of FSH in rats using specific antibodies impairs spermatogonial development (Meachem *et al.*, 1999).

The importance of both FSH and LH in human male gonadal function has been highlighted by several case reports published over the last 20 years. Spermatogenesis was partly restored in gonadotropin-suppressed men by administration of FSH (Matsumoto *et al.*, 1983), and precocious maturation of the testis has been observed in boys bearing a constitutively activating mutation of the LH receptor (Shenker *et al.*, 1993). Males with an inactivating mutation of the FSH receptor or LH deficiency (fertile eunuch syndrome) were found to be fertile, indicating that the presence of either androgens or FSH is sufficient for fertility (Vaskivuo *et al.*, 1998; Weinbauer and Nieschlag, 1998). The importance of FSH in gonadal function was illustrated by a case report on a hypophysectomised patient with an activating mutation of the FSH receptor (Gromoll *et al.*, 1996). Although the patient had undetectable serum gonadotropin levels, testis size and sperm number were normal, and the patient was fertile upon testosterone substitution. The available clinical and experimental evidence indicates that FSH or testosterone alone may maintain spermatogenesis qualitatively, but only a combination of both supports a qualitatively and quantitatively normal spermatogenesis.

Although FSH and LH are established as the hormonal regulators of spermatogenesis, the mechanisms by which they ultimately affect spermatogenesis are only partly understood. FSH has been shown to regulate many Sertoli cell differentiated functions *in vitro*, including stimulation of transferrin, androgen binding protein (ABP) and androgen receptor expression (Fakunding *et al.*, 1976; Verhoeven and Caillaeu, 1988; Lincoln *et al.*, 1989; Skinner *et al.*, 1989). The role of FSH in maintaining Sertoli cell differentiated functions has been substantiated *in vivo* in knockout mice (Wreford *et al.*, 2001). The actions of FSH or the activins, which are a group of proteins with the capacity to stimulate FSH secretion, were disrupted by targeted inactivation of the FSH β-subunit or activin type II receptor respectively. These mice exhibited a decreased Sertoli cell complement, which was consistent with loss of FSH stimulation of Sertoli cell proliferation during perinatal life, resulting in decreased numbers of germ cells in both models. However, the analysis also revealed that spermatogenesis was impaired in addition to the reduction in Sertoli cell number, shown by a decrease in round spermatid to Sertoli cell ratio. Hence, FSH has a role in Sertoli cell function *in vivo*. Testosterone stimulation of Sertoli cell differentiated functions, including transferrin synthesis, has been shown to be indirectly mediated via the paracrine factor PmodS *in vitro* (Skinner and Griswold, 1980; Skinner and Fitz, 1985; Skinner *et al.*, 1988; Norton and Skinner, 1989).

At the cellular level, FSH regulates Sertoli cell functions primarily through the cAMP-dependent protein kinase A (PKA) pathway (Fakunding *et al.*, 1976; Skinner *et al.*, 1989; Walker *et al.*, 1995; Whaley *et al.*, 1995). Other signalling pathways, including protein kinase C (PKC), may also be involved in FSH actions (Jia *et al.*, 1996). The actions of PmodS on Sertoli cells do not involve PKA or PKC signal

transduction pathways (Norton and Skinner, 1989; Norton *et al.*, 1994; Whaley *et al.*, 1995), but appear to be in part via activation of tyrosine kinases (Norton *et al.*, 1994). These signal transduction pathways activate a number of transcription factors, including immediate-early gene *c-fos* and the cAMP response-element binding protein (CREB), which either directly or indirectly, via intermediate transcription factors, activate Sertoli cell-specific gene expression (Norton and Skinner, 1992; Walker *et al.*, 1995; Whaley *et al.*, 1995).

The effect of FSH on the Sertoli cell is age-specific, since FSH has a key role in promoting Sertoli cell proliferation during perinatal development of the testis (Orth, 1984; Thomas *et al.*, 1994; Baker and O'Shaughnessy, 2001). Orth (1984) showed that there was a dramatic reduction in the number of dividing Sertoli cells on day 19 of gestation in the testes of rats which were either decapitated *in utero* or treated with anti-FSH on day 18. In hypogonadal mice, the number of Sertoli cells was normal up to day 18 of foetal life, but was reduced by about 30 % on day 1 after birth, indicating an important requirement for gonadotropins in late foetal life (Baker and O'Shaughnessy, 2001). Thereafter, Sertoli cells proliferated at a slower rate, but proliferation continued beyond day 20, when proliferation ceases in the normal testes, and in the adult, the number of Sertoli cells was 65 % of normal. Further evidence supporting FSH in the expansion of the Sertoli cell population is provided by FSH β-subunit and activin type II receptor knockout mice (Wreford *et al.*, 2001). Both of these mice have a decreased Sertoli cell complement. Androgens are not involved in the regulation of Sertoli cell proliferation. Testosterone concentrations are normal in the testes of hypogonadal mice in the foetal period (O'Shaughnessy *et al.*, 1998), and although testosterone is very low after birth (O'Shaughnessy and Sheffield, 1990; O'Shaughnessy *et al.*, 1998), neonatal treatment of the mice with

testosterone does not alter subsequent numbers of Sertoli cells in the adult mice (Singh and Handelsman, 1996).

1.3.4 Id Proteins in Spermatogenesis

Sablitzky *et al.* (1998) described the expression pattern for each Id protein within the seminiferous tubule of the adult mouse testis. The *in situ* immunohistology analysis revealed the expression of Id proteins in developing germ cells and supporting Sertoli cells. Whereas Id1 and Id4 were restricted to germ cells, Id2 was expressed in both germ cells and Sertoli cells, and Id3 expression was restricted to Sertoli cells.

Id1 and Id4 were expressed in the cytoplasm of spermatogonia. Id1 protein was expressed at low levels throughout spermatogonial cell development, however the clear expression of Id4 was restricted to the cytoplasm of early, Type A spermatogonia. Id2 protein was not detectable in spermatogonia. Following early proliferative spermatogenesis, Id1, Id2 and Id4 proteins were differentially expressed during meiosis. Id1 was expressed at low levels in the cytoplasm of primary spermatocytes, but was abundant in MI/MII spermatocytes, where the subcellular distribution of the protein was dependent on the phase of cell division. Id2 was clearly expressed in both the nucleus and cytoplasm of pachytene and diplotene spermatocytes, and the cytoplasm of zygotene spermatocytes also showed weak Id2 expression. Id4 protein was restricted to late pachytene and diplotene nuclei, where a high, focal expression was localised to a juxta- or perinucleolar region. In contrast to Id1, Id2 and Id4 were not expressed in cells undergoing meiotic division. During spermatid maturation, Id1 was detectable at low levels in the cytoplasm of round spermatids. In early, elongating spermatids, Id1 protein became abundant in both the

cytoplasm and nucleus, but in later stages Id1 was again restricted to the cytoplasm. Similar to Id1, Id2 was detectable in the cytoplasm of spermatids. The cytoplasmic expression of Id2 protein increased throughout post-meiotic sperm development. A more focal Id2 expression was also detectable in round spermatids, associated with the developing acrosome. Id4 protein was not detectable in the cytoplasm during spermatid maturation. Id4 was highly expressed in a focus within the nucleus of round spermatids, suggesting association with a juxta- or perinucleolar compartment again. In elongating and condensing spermatids, Id4 protein was detectable in two distinct lines extending behind the nucleus, suggesting that the protein is associated with the manchette, a transient microtubular organelle. Id proteins were not expressed in mature spermatozoa released from the seminiferous epithelium. Id1 and Id2 were detectable in residual bodies, indicating that they were eliminated with the residual cytoplasm. Id4 protein was not expressed in the stages just prior to sperm release and was undetectable in residual bodies, suggesting that the Id4 protein is specifically degraded before the release of testicular spermatozoa. In Sertoli cells, Id2 and Id3 proteins were expressed, where Id2 was abundant in the nuclei and Id3 expression was restricted to the cytoplasm.

Each Id protein displayed a unique stage- and subcellular-specific expression pattern in germ cells and supporting Sertoli cells of the mouse testis. The observed stage-specific expression of Id1, Id2 and Id4 during meiosis suggests that these proteins have a regulatory role in meiotic, as well as mitotic cell divisions. In addition to this, the unique spatial and temporal expression pattern of Id1, Id2 and Id4 during spermatid maturation implies distinct functional roles in non-dividing post-meiotic cells. The mutually exclusive expression of Id2 and Id3 in post-proliferative mature

Sertoli cells suggests distinct roles for these members of the Id family in Sertoli cell differentiated function.

Although no further studies have documented the functions of Id proteins in the development of sperm, several studies have focused on HLH proteins in the post-mitotic Sertoli cell. A large number of genes associated with Sertoli cell differentiated functions have putative E box response elements within their promoter region, which are potential targets for bHLH proteins (Chaudhary *et al.*, 1997; Chaudhary and Skinner, 1999). This suggests that the bHLH proteins are involved in Sertoli cell differentiated function. Further evidence to support this is furnished by the observation that overexpression of Id1 in Sertoli cells inhibits transferrin promoter activation (Chaudhary *et al.*, 1997). The promoters of SF-1 and FSH receptor also contain functional E box elements (Daggett *et al.*, 2000; Goetz *et al.*, 1996). Recent reports have shown that Sertoli cells express the class A bHLH proteins E47 (Chaudhary and Skinner, 1999a) and REBα (rat homolog of human HEB; Chaudhary *et al.*, 1999). Sertoli cell-specific class B bHLH proteins have yet to be identified. Taken together, these studies imply that bHLH proteins are important in Sertoli cell differentiated functions. The functions of bHLH proteins are modulated by the Id proteins, which sequester bHLH proteins in non-functional heterodimers. Since Id2 and Id3 are expressed in the Sertoli cell *in vivo* (Sablitzky *et al.*, 1998), Id proteins may play a key role in the regulation of Sertoli cell function, possibly by regulating the activity of bHLH proteins.

The methods described in chapter 2 are adapted from protocols found in Wood *et al.* (1993) and Hogan *et al.* (1994) for ES cell-morula aggregation and cell culture, Joyner (2000) for X-gal staining, Maniatis *et al.* (1982) for molecular biology, and/or are modified from methods advocating the use of (or supplied with) the reagents.

Although the majority of the functions of Id proteins involve the Id HLH domain, an apoptotic activity of Id2 has been described that requires the N-terminal region of Id2 and is independent of HLH-mediated interactions (Florio *et al.*, 1998). Therefore, it is important to note that, although the Id4 HLH domain has been deleted, the N-terminal region of the Id4 gene is still intact in Id4 knockout mice and may have functional activity. This activity has not been investigated to date.

Chapter 2

Materials and Methods

The composition of buffers/solutions can be found at the end of this chapter in section 2.7. All steps were carried out at room temperature unless otherwise stated.

2.1 Id4 Knockout Mice

In order to analyse the function(s) of Id4 in a mammalian system, Id4 knockout mice were generated. Id4 knockout mice were generated by embryonic stem (ES) cell-morula aggregation.

2.1.1 Id4 Knockout Targeting Construct

The Id4 knockout targeting construct (figure 2.1) was generated by Dr Inge van Crüchten in our laboratory. An 8.3 kb ClaI fragment containing the Id4 gene was isolated as described in van Crüchten *et al.* (1998). A 215 bp PstI-SacII fragment containing the HLH encoding domain was replaced with a lacZ/neomycin reporter gene cassette. The lacZ gene was inserted in-frame of the Id4 coding sequence to allow expression of an Id4/lacZ fusion protein. The neomycin resistance gene was inserted to allow selection of ES cells containing the targeting construct following electroporation.

2.1.2 Production of Targeted Embryonic Stem Cells

Dr Inge van Crüchten made the Id4 knockout targeted ES cells in our laboratory. The Id4 knockout targeting vector DNA was electroporated into pluripotent E14.1 ES

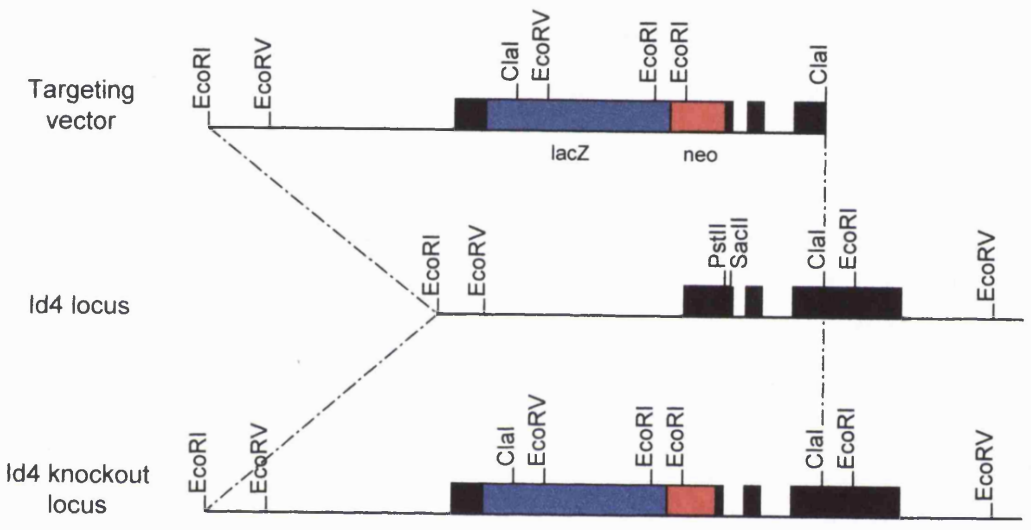

Figure 2.1 Gene inactivation of Id4. A 215 bp PstI-SacII fragment of the Id4 gene containing the HLH encoding domain was replaced with a lacZ/neomycin (neo) reporter gene cassette for the targeting vector. The resulting Id4 knockout locus following specific homologous recombination at the Id4 locus in E14.1 ES cells is shown.

cells. The E14.1 clone of ES cells was originally derived from the mouse 129 substrain 129/OlaHsd, and has the A^W coat colour gene. Following electroporation, geneticin (G418; Gibco BRL, #066-1811) was used to select ES cell clones containing the targeting vector DNA. Southern blot analysis was then used to screen DNA from the ES cell clones for specific homologous recombination at the Id4 locus. In this strategy a single Id4 allele was targeted. Three Id4 knockout ES cell clones were produced, numbered 58, 62 and 65. Each Id4 knockout ES cell clone was used to produce ES cell-morula aggregation chimeras.

2.1.3 Generation of Chimeric Mice

All solutions in the mouse work were either those used in the culture of ES cells or embryo-tested solutions. Care was taken to avoid exposing the embryos to any toxic materials that might harm them.

2.1.3.1 Production of Embryos for Aggregation

The embryo donors were superovulated to increase the number of embryos produced by each female mouse. 4 week old CD1 female mice were injected intraperitoneally with 5 IU of pregnant mare's serum (Intervet UK Ltd., #856 563) at 4pm. Two days later, the same CD1 female mice were injected intraperitoneally with 5 IU of human chorionic gonadotrophin (hCG; Intervet UK Ltd., #804 745) at 1pm. Care was taken to adhere to the injection times as deviation resulted in lower yields of embryos. After the hCG injection, each female was mated with a CD1 male. The next day mice were checked for vaginal plugs. The day of the plug was day 0.5 or 0.5 days postcoitum (0.5 dpc).

2.1.3.2 Collection of Embryos for Aggregation

Superovulated mice were sacrificed in the morning on day 2.5 to obtain non-compacted 8-cell embryos. Uteri and oviducts were dissected out and placed in M2 medium (Sigma, #M-7167). Using a dissecting microscope, a bevelled needle attached to a 1 ml syringe containing M2 was inserted into the infundibulum of the oviduct, and M2 was flushed through the oviduct and uterus. 8-cell embryos (morulae) were flushed from the oviduct and uterus in the M2. Embryos were collected using a mouth pipette attached to a hard glass capillary tube (BDH, #321242C). The glass capillary tube was pulled to a point just wider than the diameter of a morula. Embryos were washed through a series of drops of M2. After the embryos were separated from any debris, they were stored in drops of pre-equilibrated M16 medium (Sigma, #M-7292) overlaid with mineral oil (Sigma, #M-8410), and incubated in a humidified atmosphere at 37 °C, 5 % CO_2 in air.

2.1.3.3 Preparation of the Aggregation Plate

Six drops of pre-equilibrated M16 were placed in a circle in a 10 cm tissue culture dish, and the dish was flooded with mineral oil. Six conical depressions were made in a circle in each drop of M16 using an aggregation needle (BLS, #DN-09), which was pressed into the tissue culture dish in a circular movement. The conical depressions are called aggregation wells. The plate was returned to the incubator at 37 °C and 5 % CO_2 in air, whilst the embryos were prepared.

2.1.3.4 Preparation of Embryos for Aggregation

Before aggregation of the morula with ES cells, the zona pellucida is removed from the 2.5 dpc morula by treatment with acidified Tyrode's solution (Irvine Scientific,

#9282). In the lid of a tissue culture dish, one drop of M2, three drops of acidified Tyrode's solution (pH 2.5), two drops of M2 and one drop of M16 were set up in a line. Up to five morulae were taken and placed in the first drop of M2. The next stages were observed using a microscope, and when the embryos were to be transferred from one drop to the next, the capillary used for the transfer was first flushed with the solution in the next drop. The morulae were transferred to the first drop of acidified Tyrode's solution, left for 10 seconds, moved to the second drop for 10 seconds and then transferred to the third drop. The morulae were closely observed, and when the zona pellucida began to dissolve the embryos were quickly transferred to a drop of M2. The morulae were transferred through the remaining M2 and M16 drops, and then a single morula was placed in each aggregation well in the aggregation plate. This was repeated for all morulae, and then the aggregation plate was returned to the incubator at 37 °C, 5 % CO_2 in air.

2.1.3.5 Preparation of Embryonic Stem Cells for Aggregation

Two days prior to the day of aggregation, a subconfluent plate of ES cells was passaged onto gelatin-treated tissue culture dishes without feeder cells. ES cells were passaged at 1:20 dilution to ensure small ES cell colonies on the day of aggregation. On the day of aggregation, ES cells were washed with PBS (pH 7.4) and trypsinised until clumps of loosely connected cells 'lifted off' the surface of the dish (section 2.3.3). ES cell medium was added to the dish to inactivate the trypsin, and the ES cell suspension was gently pipetted up and down. This produced clumps of 10-15 ES cells. The ES cell suspension was used to assemble aggregates within 1-2 hours.

2.1.3.6 Embryonic Stem Cell-Morula Aggregation

The aggregation plate was taken from the incubator, and the ES cell-morula aggregations were set up using a dissecting microscope. Using a mouth pipette attached to a glass capillary tube, a clump of 10-15 ES cells was placed next to the morula in each aggregation well, ensuring that the ES cells and the morula were in contact. The aggregation plate was then left in the incubator overnight at 37 °C and 5 % CO_2, to allow aggregation to occur. The next day, ES cell-morula aggregations that had expanded into blastocysts were transferred to 2.5 dpc pseudopregnant female mice.

2.1.3.7 Production of Pseudopregnant Female Mice

Aggregated embryos were transferred to pseudopregnant CD1 female mice. 7-8 week old (20-25 g) CD1 female mice in estrus were mated with sterile male mice (T145). The following day, the female mice were checked for vaginal plugs (0.5 dpc). Females 2.5 dpc were used for embryo transfers.

2.1.3.8 Embryo Transfer

Aggregated embryos (blastocysts) were loaded into a transfer capillary. Transfer capillaries were hard glass capillary tubes pulled to a long tapered end, with a diameter just wider than a blastocyst. Each transfer capillary was half-filled with mineral oil, followed by an air bubble, 0.5 cm M2, an air bubble, 0.5 cm M2 containing the blastocysts, an air bubble and then a small amount of M2. A maximum of 8-10 embryos were loaded per transfer capillary. The pseudopregnant female recipient was weighed and then anaesthetised using the general anaesthetic avertin (section 2.7). 15 µl/g mouse body weight was administered intraperitoneally.

The middle back of the mouse was swabbed with 70 % ethanol and a small incision was made in the skin at the approximate height of the ovaries. The left ovary was located and a small incision was made in the peritoneal wall above the ovary, taking care to avoid cutting any blood vessels. The left ovarian fat pad was located and the ovary, oviduct and uterus were gently taken out of the body cavity in the direction of the midline. These were laid across the back of the mouse and the ovary was secured outside the peritoneum by clamping the fat pad with a Serrefine clip. Holding the fat pad gently, a small hole was made in the top of the uterus with a bevelled needle. The end of the transfer capillary was inserted into the hole in the uterus wall and the embryos were gently blown into the uterus. The air bubbles loaded into the transfer capillaries were used as markers, when the last bubble in the capillary was reached, no more material was transferred and the transfer capillary was removed. The uterus, oviduct, ovary and fat pad were returned to the body cavity. This process was repeated with the right uterine horn. The incision in the back of the mouse was stapled shut using a body stapler. Care was taken to only staple the skin together. The mouse was returned to its cage and monitored until it was conscious.

2.1.3.9 Detection and Quantification of Chimerism

Pups were born approximately 18 days after a successful transfer. Coat colour alleles were used as genetic markers of chimerism. The 129/OlaHsd ES cells and CD1 embryo donor cells have different coat colour alleles. The ES cells have the dominant A^W allele at the agouti locus. A^W produces hair with a yellow subapical band. The CD1 cell contribution produces white hair. Therefore, when hair colour was detectable at 1 week old, it was easy to identify the chimeric mice. Coat colour chimerism also allowed a simple visual appreciation of the degree of tissue contribution of each component, by the proportion of the coat expressing each allele.

Chimeric mice were crossed with CD1 mice to ascertain the ES cell contribution to the germline, and to generate mice derived from the targeted ES cells. The Id4 knockout mice were then maintained in a mixed genetic background.

2.2 Id2 Knockout Mice

The Id2 knockout mice were generated by Yoshifumi Yokota at Kyoto University in Japan (Yokota *et al.*, 1999). Yoshifumi Yokota sent two pairs of heterozygous Id2 mutant mice from Japan to enable us to establish a colony of Id2 knockout mice in our animal facility. The Id2 mutant mice were of 129/Sv genetic background.

2.3 Cell Culture Techniques

2.3.1 Cell Growth Media

For embryonic stem (ES) cell and primary murine embryonic fibroblast (EMFI) cell growth media, Dulbecco's modified eagle medium (DMEM; Gibco BRL, #41965-039) was supplemented with ES cell qualified foetal calf serum (FCS; Gibco BRL, #10120-160), penicillin/streptomycin (Gibco BRL, #15140-122), glutamine (Gibco BRL, #25030-024), sodium pyruvate (Gibco BRL, #11360-039), 2-mercaptoethanol (Gibco BRL, #31350-010), non-essential amino acids (MEM; Gibco BRL, #11140-035) and leukaemia inhibitory factor (LIF) as shown in table 2.1. Cells were incubated in a humidified atmosphere at 37 °C, 5 % CO_2 in air.

EMFI	ES
DMEM	DMEM
10 % (v/v) ES qualified FCS	15 % (v/v) ES qualified FCS
100 units/ml penicillin 100 μg/ml streptomycin	100 units/ml penicillin 100 μg/ml streptomycin
2 mM glutamine	2 mM glutamine
1 mM sodium pyruvate	1 mM sodium pyruvate
0.1 mM 2-mercaptoethanol	0.1 mM 2-mercaptoethanol
1X MEM	1X MEM
	LIF

Table 2.1 The composition of growth media for embryonic stem (ES) cells and primary murine embryonic fibroblast (EMFI) cells.

2.3.2 Defrosting Cell Lines

The vial of cryogenically frozen cells was placed in a 37 °C water bath. As soon as the cells thawed, they were quickly transferred to 50 ml of pre-warmed growth media and gently inverted to remove the cryoprotectant from the cells. The cells were pelleted by centrifugation at 3000 rpm for 3 minutes. The media was aspirated to leave the cell pellet, which was resuspended by gentle pipetting up and down in a small volume of growth media. The cells were then transferred to a tissue culture flask (EMFI) or feeder plate (ES) containing the appropriate volume of growth media. The growth media was replaced after 24 hours to remove any cells that had not become attached to the growing surface.

2.3.3 Passaging of Cell Lines

Cells were passaged when they approached confluency (80-90 % confluent). Following aspiration of the growth media, the cells were washed with PBS (pH 7.4) and then trypsinised. Sufficient 1X trypsin-EDTA (Gibco BRL, #35400-027) was added to cover the layer of cells and the flask/dish was incubated at 37 °C for 2-5 minutes. This resulted in cells 'lifting off' the flask/dish surface. A similar volume of growth media was then added to the flask/dish to inactivate the trypsin, and the cells were pelleted by centrifugation at 3000 rpm for 3 minutes. The media was aspirated to leave the cell pellet, which was resuspended by gentle pipetting up and down in a small volume of media. The cells were counted using a haematocytometer and then seeded at the appropriate density into a flask for EMFI cells or onto a feeder plate for ES cells.

ES cells were cultured on monolayers of mitotically inactivated EMFI cells (feeder cells) for routine culture, to ensure that the pluripotency of the ES cells was maintained. ES cells were passaged onto gelatin-coated dishes before they were used for aggregation. This limits the number of feeder cells in the ES cell culture.

2.3.4 Preparation of Feeder Plates for Embryonic Stem Cell Culture

Feeder plates were prepared from confluent flasks of EMFI cells. The EMFI growth media was supplemented with mitomycin C (Sigma, #M-0503) to a final concentration of 10 μg/ml, and the cells incubated for 3 hours in a humidified atmosphere at 37 °C, 5% CO_2 in air. After 3 hours, the media was aspirated and the EMFI cells were washed three times with PBS (pH 7.4). The EMFI cells were then trypsinised as described in section 2.3.3 and seeded onto gelatin-coated dishes. The

cells were seeded at 1.2 X 10^6 cells/60 mm gelatin-coated dish, and were left for at least 2 hours to adhere to the dish. Gelatin-coated dishes were prepared by adding sufficient 0.1 % (w/v) gelatin solution to cover the surface of a dish, and after 15 minutes at room temperature, the gelatin solution was aspirated and the dish left to dry for 15 minutes. Feeder plates for ES cells were used within one week of preparation.

2.3.5 Cryopreservation of Cell Lines

A confluent flask or dish of cells was used. Following aspiration of the growth media, the cells were washed with PBS (pH 7.4). The cells were trypsinised and counted as described in section 2.3.3, and then the cells were pelleted by centrifugation at 3000 rpm for 3 minutes. The cells were resuspended in the appropriate cryopreservation media (table 2.2) at 1 X 10^7 cells/ml, and 1 ml of cells was transferred to cryogenic vials (Nalgene, #5000-0020). Cryogenic vials were quickly transferred to a pre-cooled styrofoam rack at –70 °C. After 1 week, the vials were transferred on dry ice to liquid nitrogen for long-term storage.

EMFI	ES
EMFI growth media	ES growth media
10 % (v/v) DMSO	10 % (v/v) DMSO

Table 2.2 The composition of cryopreservation media for embryonic stem (ES) cells and primary murine embryonic fibroblast (EMFI) cells. DMSO, dimethyl sulphoxide (Sigma, #D-2650).

2.4 Histology

2.4.1 Preparation of Tissue for Histology

2.4.1.1 Fixation of Tissues

The tissue was dissected from the mouse, washed in PBS (pH 7.4) and placed into 4 % (w/v) paraformaldehyde (Sigma, #P-6148) in PBS (pH 7.4). At least 10 volumes of fixative to the volume of tissue were used. The tissue was left in 4 % paraformaldehyde at 4 °C overnight or for 12-24 hours. After fixation, the tissue was washed in PBS (pH 7.4) and processed for sectioning. The tissue was either embedded in paraffin wax or cryoprotected and frozen.

2.4.1.2 Preparation of Paraffin Wax-Embedded Tissue

After fixation, the tissue was dehydrated at room temperature. The tissue was dehydrated through 50 % ethanol (BDH, #10107) for 3 hours, 70 % ethanol for 5 hours, 90 % ethanol for 12 hours and three times in absolute ethanol for 3 hours each. Following dehydration, the tissue was incubated in clearing solution (section 2.7) for 12-24 hours or until the tissue was clear in appearance. The tissue was removed from the clearing solution and placed in liquid paraffin wax (> 55 °C) for 3 hours, this was repeated twice using fresh liquid paraffin wax, then the tissue was left overnight in liquid paraffin wax. The tissue was then placed in a mould filled with liquid paraffin wax and was left to solidify on a cold surface. 5-10 micron sections were cut using a Lecia microtome. The sections were floated in a 37 °C water bath for 5 minutes and then were collected on aminoalkylsilane coated slides (Sigma, #S-4651). The sections were left to dry at 37 °C overnight and were stored in a dry, dust free rack at room temperature until use.

2.4.1.3 Cryoprotection and Freezing of Tissue

Following fixation, the tissue was allowed to sink through 25 ml of 30 % (w/v) sucrose (BDH, #102744B) in PBS (pH 7.4) containing 2 mM Mg^{2+} at 4 °C. The cryoprotected tissue was placed on paper towels to absorb any excess sucrose and then onto crushed dry ice, and frozen rapidly by application of dry ice directly onto the tissue. The tissue was left in the dry ice for 2 minutes, and then placed in a foil envelope and stored at –70 °C until use. Immediately prior to sectioning, the tissue was mounted in ornithine carbamyl transferase (OCT; Sigma, #0-2501). 10 micron sections were cut using a Leica cryostat and mounted on poly-lysine coated microscope slides (Sigma, #P-0425). The sections were stored in a slide box at –70 °C until use. Just prior to use, the sections were dried overnight at 45 °C.

2.4.2 Histochemistry

Microscopic analysis was performed using an Axioskop 2 MOT microscope (Carl Zeiss). Images were taken using an AxioCam CCD camera and supporting AxioVision 2.05 software (Carl Zeiss).

2.4.2.1 Hematoxylin and Eosin Staining of Paraffin-Embedded Sections

Sections were de-waxed in low sulphur xylene (BDH, #360716Y) for 5 minutes and rehydrated through 100 % ethanol, 90 % ethanol, 70 % ethanol and distilled water for 5 minutes each. The sections were immersed in Gills haematoxylin (Sigma, #GHS-3-32) for 5 minutes, rinsed twice in distilled water for 30 seconds each, and dipped in 2 % (w/v) sodium bicarbonate (Sigma, #S-6297) until blue in appearance. Sections were then incubated in eosin Y (Sigma, #HT110-3-32) for 5 minutes, and washed in two changes of distilled water for 30 seconds each. The sections were

dehydrated through 70 % ethanol for 10 seconds, 90 % ethanol for 10 seconds and 100 % ethanol for 30 seconds, cleared in low sulphur xylene for 30 seconds and then mounted in DPX (BDH, #360294H).

2.4.2.2 Cresyl Violet Staining for Cell Bodies

Paraffin wax-embedded tissue sections were de-waxed and rehydrated as described in section 2.4.2.1. The sections were stained in cresyl violet solution (section 2.7) for 15 minutes, rinsed in water for 2 minutes, and then immersed in 95 % ethanol until the desired staining intensity was reached. Sections were dipped in 100 % ethanol, cleared in low sulphur xylene for 30 seconds and then mounted in DPX.

2.4.2.3 X-gal Staining of Cryosections

Cryosections were taken from –70 °C and dried at 45 °C overnight. The sections were washed in three changes of distilled water for 10 minutes each and then immersed in X-gal staining buffer (section 2.7) for 1 hour. Sections were then incubated in X-gal staining solution (section 2.7) at 37 °C overnight or until X-gal staining became visible. After incubation, the sections were washed three times in distilled water for 5 minutes each and counterstained with either eosin Y (Sigma, #HT110-3-32) or cresyl violet solution (section 2.7) for 3-5 or 15-30 minutes respectively. The sections were then rinsed in two changes of distilled water for 1 minute each and dehydrated through 70 % ethanol for 10 seconds, 90 % ethanol for 10 seconds and absolute ethanol for 30 seconds. Sections were cleared in low sulphur xylene for 30 seconds and then mounted in DPX.

2.4.2.4 X-gal Staining of Embryos

The embryos were dissected from the mouse, washed in PBS (pH 7.4) and fixed in solution A (section 2.7) for 15 minutes. Embryos were washed three times in solution B (section 2.7) for 15 minutes each wash and then stained in solution C (section 2.7) at 37 °C for 2-6 hours. After staining, the embryos were fixed in 4 % (w/v) paraformaldehyde in PBS (pH 7.4) for 1 hour (embryos up to 12.5 dpc) or 2 hours (embryos 12.5-14.5 dpc). Following fixation, embryos up to 12.5 dpc were dehydrated through 70 % ethanol, 90 % ethanol and absolute ethanol for 1 hour each. 12.5-14.5 dpc embryos were dehydrated through 70 % ethanol for 2 hours, 90 % ethanol for 4 hours and absolute ethanol for 4 hours. The embryos were then placed in clearing solution (section 2.7) until the embryos were clear in appearance. Microscopic analysis of whole embryos was performed following clearing. After this, the embryos were embedded in paraffin wax for sectioning.

2.4.2.5 Detection of Apoptosis in Paraffin-Embedded Sections

The Apoptosis Detection System, Fluorescein, from Promega (#G3250) was used to detect apoptotic cells in paraformaldehyde-fixed paraffin-embedded sections. The procedure, which uses the principle of TUNEL, was carried out according to the assay protocol in the technical literature provided by Promega.

2.4.3 Immunohistochemistry

Indirect immunoperoxidase or immunofluorescent techniques were used to detect mouse antigens in paraformaldehyde-fixed paraffin-embedded sections.

2.4.3.1 Indirect Immunoperoxidase Staining of Antigens

Paraffin wax-embedded tissue sections were de-waxed and rehydrated as described in section 2.4.2.1. Tissue fixation can interfere with, or mask, antigens in the tissue, therefore target retrieval was carried out on the tissue sections. The sections were placed in alternate spaces in a glass rack, immersed in 1 litre of 0.01 M sodium citrate (pH 6) (Sigma, #S-4641) and microwaved at 800 W for 25 minutes. Sections were left to stand in the hot solution for 15 minutes, and then were cooled in running tap water for 5 minutes. After target retrieval, the sections were immersed in TBS (section 2.7) for 5 minutes and then in a blocking solution of 5 % marvel (Premier Beverages UK) in TBS for 10 minutes. The sections were then incubated in the appropriate primary antibody in TBS overnight at 4 °C. Anti-GATA-1 rat monoclonal antibody (Santa Cruz, #sc-265) was applied at 4 μg/ml in TBS. The sections were washed in two changes of TBS for 5 minutes each and then incubated in the appropriate secondary antibody in TBS for 1 hour at room temperature. For GATA-1 staining, a biotinylated rabbit anti-rat antibody (DAKO, #E0468) was used at 1:200 dilution. The sections were washed twice in TBS for 5 minutes each, and then were immersed in 0.3 % hydrogen peroxide (BDH, #101284N) plus 0.1 % sodium azide (Sigma, #S-8032) in TBS for 10 minutes, to block endogenous peroxidase. Sections were washed in water and in TBS for 5 minutes each, and then were incubated in 1:500 streptavidin-horseradish peroxidase (DAKO, #P0397) for 30 minutes. Sections were rinsed in TBS for 5 minutes and then incubated in 0.5 mg/ml diaminobenzidine-4-HCl (Sigma, #D-5637) plus 0.03 % hydrogen peroxide in TBS until staining was visible. The sections were washed in distilled water for 2 minutes and then were counterstained with Gills haematoxylin (Sigma, #GHS-3-32). Sections were washed in distilled water and then dehydrated through 70 % ethanol, 90 %

ethanol and 100 % ethanol for 10 seconds each, cleared in low sulphur xylene and mounted in DPX.

2.4.3.2 Indirect Immunofluorescent Staining of Antigens

Astrocytes, oligodendrocytes and neurons were detected using anti-glial fibrillary acidic protein (GFAP; Sigma, #G-3893), anti-2',3'-cyclic nucleotide 3'-phosphodiesterase (CNPase; Sigma, #C-5922) and anti-neurofilament 200 (N200; Sigma, #N-0142) mouse antibodies respectively. Paraffin wax-embedded tissue sections were de-waxed and rehydrated as described in section 2.4.2.1. The sections were washed in TBS for 5 minutes and immersed in 0.1 % triton X-100 (BDH, #437002A) in TBS for 20 minutes. The sections were then incubated in 50 % normal goat serum (DAKO, #X0907) for 10 minutes. Sections were rinsed in TBS for 5 minutes and then incubated in 1% sodium borohydride (Sigma, #S-9125) for 30 minutes. The sections were washed in distilled water and TBS for 5 minutes each and then incubated in the appropriate anti-mouse primary antibody in TBS for 1 hour at room temperature. The anti-GFAP, anti-CNPase and anti-N200 antibodies were applied at 1:300, 1:400 and 1:400 dilutions respectively. The sections were washed in TBS for 5 minutes and then twice in 0.1% triton X-100 in TBS for 10 minutes each. Sections were incubated in Alexa 546 goat anti-mouse secondary antibody (Molecular Probes, #A-11003) at 5 μg/ml for 1 hour protected from light. The sections were washed three times in TBS for 5 minutes each and then mounted in aqueous mounting medium (Molecular probes, #S-7461).

2.5 Molecular Biology

2.5.1 Extraction of RNA from Tissues and Cells

The RNeasy kit from Qiagen (#74104) was used to isolate total RNA from mouse tissues and cultured cells, according to the protocols given by the manufacturer. The total RNA was treated with RNase-free DNase I (Roche, #776 785) at a final concentration of 1-2 U/μg total RNA for 1 hour at 37 °C, and then the DNase I was inactivated by incubation at 70 °C for 15 minutes. The concentration of total RNA in a sample was determined by gel electrophoresis.

2.5.2 Extraction of Genomic DNA from Mouse Tail

Approximately 0.3 cm of tail was taken from the mouse under investigation. The tail was agitated in 700 μl of tail lysis buffer (section 2.7) at 55 °C overnight. RNase A (Sigma, #R-4875) was then added to the tail lysate to a final concentration of 0.35 μg/ml, and the lysate was incubated at 37 °C for 1 hour. The tail lysate was centrifuged at 10 000 rpm for 10 minutes to pellet the tail debris, and the supernatant was removed to a clean microcentrifuge tube. An equal volume of propan-2-ol (BDH, #102244J) was added to the supernatant and the tube was inverted for 1 minute to precipitate the DNA. The DNA was pelleted by centrifugation at 10 000 rpm for 10 minutes, and the supernatant was removed to leave the DNA pellet. The DNA pellet was washed with 70% ethanol. Following centrifugation at 10 000 rpm for 10 minutes, the 70% ethanol was removed and the genomic DNA pellet allowed to dry. The pellet was dissolved in 50-100 μl of sterile distilled water.

2.5.3 Extraction of DNA from Yolk Sac

Yolk sac was incubated in 100 µl of yolk sac lysis buffer (section 2.7) at 55 °C overnight. RNase A (Sigma, #R-4875) was then added to the lysate to a final concentration of 0.35 µg/ml, and the lysate was incubated at 37 °C for 1 hour. An equal volume of phenol (equilibrated with Tris pH 8) (Fisons, #T/P633/05) was added to the yolk sac lysate. The microcentrifuge tubes were then shaken vigorously for 3 minutes and centrifuged for 3 minutes at 10 000 rpm. The upper aqueous phase was transferred to a clean microcentrifuge tube and an equal volume of phenol:chloroform (1:1) (BDH, #1007763) was added. Tubes were shaken vigorously for 2 minutes and then centrifuged at 10 000 rpm for 2 minutes. The upper aqueous phase was transferred to a clean tube and an equal volume of chloroform:isoamyl alchohol (24:1) (BDH, #100776B, #100383L) was added. The tubes were then shaken vigorously for 2 minutes and centrifuged at 10 000 rpm for 2 minutes. The upper aqueous phase was transferred to a clean microcentrifuge tube and 0.1 volumes of 3 M sodium acetate (pH 6) plus 2.5 volumes of 100 % ethanol were added, and the tubes shaken well to precipitate the DNA. The DNA was pelleted by centrifugation at 10 000 rpm for 10 minutes, and the supernatant removed. The pellet was washed with 70 % ethanol, centrifuged and the wash removed. The DNA pellet was left to air dry and then was resuspended in 20-40 µl of sterile distilled water.

2.5.4 Reverse Transcription

First-strand cDNA was synthesised from total RNA according to the Superscript^{TM} II RNase H$^-$ Reverse Transcription protocol (Gibco BRL, #18064-014). 1-5 µg of total RNA, 1 µl of 500 µg/ml oligo$(dT)_{18}$, 1 µl of 10 mM dNTP mix [10 mM each dATP,

dCTP, dGTP and dTTP (Boehringer Mannheim, #1051 440, #1051 458, #1051 446 and #1051 482)] and diethyl pyrocarbonate (DEPC; BDH, 441703D)-treated water to a final volume of 12 µl were added to a microcentrifuge tube and mixed gently. The tube was heated at 65 °C for 5 minutes, chilled on ice for 1 minute and then the contents were collected by brief centrifugation. 4 µl of 5X first-stand buffer (Gibco BRL, #Y00146) and 2 µl of 0.1 M dithiothreitol (Gibco BRL, #Y00147) were added to the tube. The contents of the tube were mixed gently and then the tube was incubated at 42 °C for 2 minutes. 1 µl (200 U) of Superscript II™ (Gibco BRL, #18064-014) was added and the contents of the microcentrifuge tube mixed by gentle pipetting up and down. The tube was incubated at 42 °C for 1 hour and then the reaction was inactivated by heating at 70 °C for 15 minutes. 1 µl (1 U) of ribonuclease H (Boehringer Mannheim, #786 349) was added and the tube was incubated at 37 °C for 30 minutes, to remove any RNA complementary to the cDNA in the reaction mixture. The cDNA was then used as a template for amplification in polymerase chain reaction (PCR).

2.5.5 Polymerase Chain Reaction

PCR is a rapid *in vitro* method for amplifying a defined region of a target DNA sequence. The composition of the PCR reaction mixture varied depending on the DNA sequence to be amplified. PCR amplifications were carried out in a total reaction volume of 20 µl. Each reaction contained 2 µl of cDNA or 50-100 ng of genomic DNA, 1X PCR buffer (+ Mg^{2+}) (Boehringer Mannheim, #1 271 318), 0.2 mM of dATP, dCTP, dGTP and dTTP, 0.2 µM of each primer, 1mg/ml of bovine serum albumin (Sigma, #A-4503) and 1 U of Taq DNA polymerase (Boehringer Mannheim, #1 146 173). For amplification of Id2 and Id4 sequences, the reaction

also contained 0.1 % tween-20 (Sigma, #P 1379), and for Id4, 1.8 µl of DMSO. PCR amplification was performed in an MWG-BIOTECH thermal cycler. A standard PCR programme was as follows:

Initial Denaturation	94 °C for 5 minutes	
Denaturation	94 °C for 1 minute	⎤
Primer Annealing	XX °C for 1 minute	⎥ Y
DNA	72 °C for 1 minute	⎦
Final Extension	72 °C for 5 minutes	

The primer annealing temperature (XX) and the number of cycles of amplification (Y) were optimised for each PCR product. The primer sequences, annealing temperatures, number of cycles of amplification and expected product size are given in table 2.3.

Target sequence	Primer sequences (5'-3'): sense antisense	Annealing temperature (XX) (°C)	Number of cycles (Y)	Product size (bp): genomic DNA cDNA
β-actin	TGGAATCCTGTGGCATCCATGAAAC TAAAACGCAGCTCAGTAACAGTCCG	61	23	472 348
Id4	GCGATATGAAACGACTGCTAC TCACCCTGCTTGTTCACGGC	59	29	600 270
LacZ	CGTCGTGACTGGGAAAACCC CGCGTAAAAATGCGCTCAGG	62	35	500 500
Id2	GGTGGATCCACCATGGCAATTCAGGGATGC GGCGGATCCTTATTTAGCCACAGAGTA	59	33	870 -
Id2KO	TCGTGCTTTACGGTATCGCCGCTC TTTTAACCTTTTCGCTCCCCATGG	59	27	700 -

Table 2.3 Primer sequences, annealing temperatures, number of cycles of amplification and product sizes for amplification of target DNA sequences.

2.5.6 Agarose Gel Electrophoresis

Agarose gel electrophoresis was used to examine products of PCR amplification and to check the quality and quantity of DNA samples. Different percentages of agarose gels were used depending on the size of the DNA under investigation. A 1 % agarose gel was made by melting 1 g of agarose (Roche, #1 388 991) in 100 ml of 1X TBE (section 2.7). Ethidium bromide was added to a final concentration of 0.5 μg/ml. DNA loading dye was added to the samples before loading onto the gel. Smart ladder (Eurogentec, #MW-1700-10) was run along side samples for size and approximate quantification. DNA was visualised by UV illumination and gels were documented using AlphaImager software.

2.6 Neural Stem Cells

The materials and methods described in this section were prepared in collaboration with Dr Toru Kondo at The Department of Cell Fate Modulation, Kumamoto University, Japan.

2.6.1 Culture of Neural Stem Cells

Ventricular and subventricular zone were prepared from the brains of 2 month old mice, cut into small pieces, cultured in MEM medium (Gibco BRL) containing 2 mg/ml papain (Worthington, NJ) plus 0.4 mg/ml l-cysteine for 30 minutes at 37 °C, and then dissociated mechanically with a pipette. The cells were resuspended in serum-free DMEM/F12 medium (Life Technologies) containing 10 μg/ml bovine insulin, 100 μg/ml human transferrin, 100 μg/ml BSA, 60 ng/ml progesterone, 16 μg/ml putrescine, 40 ng/ml sodium selenite, 60 μg/ml N-acetylcysteine, 5 μM forskolin, 20 ng/ml bFGF, 20 ng/ml EGF, penicillin and streptomycin (Gibco BRL).

To expand NSCs from Id4 knockout mice ($Id4^{-/-}$ NSCs), culture supernatant of wild-type NSCs was added to 20 % in the $Id4^{-/-}$ culture medium. After 6 days for wild-type NSCs or 12 days for $Id4^{-/-}$ NSCs, the neurospheres were collected by centrifugation, resuspended in fresh culture medium and mechanically dissociated with a pipette. This procedure results in a second generation of spheres. To examine the proliferation of NSCs, the cells were grown in poly-D-lysine (M.W. 300000)-coated slide flasks (Nunc). After 3 days, 20 mM BrdU was added and the cells incubated for 6 hours, and then NSC cultures were fixed and stained for BrdU (section 2.6.3). To generate astrocytes from NSCs, NSCs were cultured in 10 ng/ml BMP2 or 10 ng/ml CNTF. To generate oligodendrocytes from NSCs, NSCs were cultured in BS medium containing either 30 ng/ml tri-idothyronine (T3), 50 ng/ml sonic hedgehog N (ShhN) or a combination of both. Neuronal differentiation was induced by culturing NSCs in 10 ng/ml PDGFAA. Chemicals were purchased from Sigma unless otherwise indicated. Recombinant human bFGF, EGF, PDGFAA and CNTF were purchased from Peprotech.

2.6.2 Recombinant Id4 Retrovirus Vector

A recombinant retroviral vector, pBabeG, was made based on the pBabe retroviral vector of Morgenstern and Land (1990), where the coding sequence of interest is driven by the Moloney murine leukemia virus (MMLV) long terminal repeat (LTR) promoter, but also contained the coding sequence for green fluorescent protein (GFP) driven by the SV40 early promoter. Wild-type and Id4 knockout NSCs were infected with the empty control vector that encoded GFP or a recombinant retroviral vector that encoded Id4 as well as GFP and grown overnight in culture medium. NSCs were washed and then grown in the same culture medium for a further two days. Efficiency of viral infection was about 40 %.

2.6.3 Immunohistochemistry

NSCs were fixed in 2 % paraformaldehyde for 10 minutes at room temperature, treated with 50 % normal goat serum for surface antigens or 50 % normal goat serum and 0.1 % triton X-100 for intracellular filaments, and then stained for NSC, neuronal or glial markers. To detect NSCs, fixed cells were stained for nestin (PharMingen, diluted 1:100) or MAP2a,b,c (HM-2), followed by Texas Red-conjugated goat anti-mouse IgG (Amersham). The cells were immunolabelled for middle-size neurofilament (NFM) to detect neurons (Sigma, diluted 1:100), glial fibrillary acidic protein (GFAP) to detect astrocytes (Sigma, diluted 1:100) and galactocerebroside (GC) to detect oligodendrocytes (supernatant diluted 1:3; Johe *et al.*, 1996). These monoclonal antibodies were detected with conjugated goat anti-mouse IgM or IgG (Jackson ImmunoResearch, diluted 1:100). Finally, the cells were counterstained with 1 mg/ml Hoechst 33324. For BrdU staining, the cells were fixed with 2 % paraformaldehyde for 10 minutes at room temperature, postfixed in 100 % methanol for 10 minutes at –20 °C, incubated in 2 M HCl for 30 minutes to denature the DNA, followed by 0.1 M sodium borate (pH 8.5) for 10 minutes. The cells were incubated in 50 % normal goat serum and 0.1 % triton X-100, and then were stained with a monoclonal BrdU antibody (culture supernatant diluted 1:5; Magaud *et al.*, 1988), followed by Texas Red-conjugated goat anti-mouse IgG (Amersham, diluted 1:100). Stained slides were mounted in mounting medium (CitiFluor, UK), sealed with nail varnish, and the intensity of fluorescence was quantified in a Bio-Rad MRC 1000 confocal laser-scanning fluorescence microscope.

2.7 Composition of Buffers/Solutions

Avertin:	Dissolve 10 g of 2,2,2-tribromoethanol (Fluka, #90710) in 10 ml 2-methyl-2-butanol (Fluka, #66000). Dilute 1:40 before use. Store at 4 °C protected from light. Use within 1 month.
Clearing Solution:	1 volume benzyl alcohol (Sigma, #B-1042) : 2 volumes benzyl benzoate (Sigma, #B-6630).
Cresyl Violet Solution:	Dissolve 1 g of cresyl violet acetate (Sigma, #C-5042) in 100 ml of distilled water and add 0.25 ml of acetic acid (Fisher, #A/0040/PB17).
Phosphate-Buffered Saline (PBS):	Dissolve 8 g of NaCl (Fisher, #S/3160/63), 0.2 g of KCl (BDH, #101984L), 1.44 g of Na_2HPO_4 (Fisher, #S/4400/53) and 0.24 g of KH_2PO_4 (Sigma, #P-5655) in 800 ml of distilled H_20. Adjust pH to 7.4 with HCl. Add H_20 to 1 litre. Sterilise by autoclaving.
X-gal Staining Solutions (for sections)	
X-gal Staining Buffer:	0.1 M Na_2HPO_4 (Fisher, #S/4400/53), 2 mM $MgCl_2$ (BDH, #101494V), 0.01 % deoxycholic acid (Sigma, #D-5670), 0.02 % IGEPAL CA-630 (Sigma, #I-3021), 5 mM $K_3Fe(CN)_6$ (Sigma, #P-3667), 5 mM $K_4Fe(CN)_6$ (Sigma, #P-3289).
X-gal Staining Solution:	X-gal staining buffer containing 1 mg/ml X-gal (Eurogentec, #OP-0020-10).

X-gal Staining Solutions (for embryos)

Solution A (fix):	0.2 % gluteraldehyde (Sigma, #G-6257), 5 mM EGTA (BDH, #437013D) and 2 mM $MgCl_2$ (BDH, #101494V) in 100 mM KH_2PO_4 (Sigma, #P-5655).
Solution B (wash):	0.01 % deoxycholic acid (Sigma, #D-5670), 0.02 % IGEPAL CA-630 (Sigma, #I-3021), 5 mM EGTA (BDH, #437013D) and 2 mM $MgCl_2$ (BDH, #101494V) in 100 mM KH_2PO_4 (Sigma, #P 5655).
Solution C (stain):	0.5 mg/ml X-gal (Eurogentec, #OP-0020-10), 10 mM $K_3Fe(CN)_6$ (Sigma, #P-3667) and 10 mM $K_4Fe(CN)_6$ (Sigma, #P-3289) in solution B.
Tail Lysis Buffer:	0.1 M Tris-HCl (pH 8.5) (Gibco BRL, #15504-020), 5 mM EDTA (BDH, #100935V), 0.2 % SDS (Fisher, #S/P530/53), 0.2 M NaCl (Fisher, #S/3160/63). Add proteinase K (Sigma, #P-6556) to a final concentration of 0.5 mg/ml just before use.
Tris-Borate (TBE):	10.8 g of Tris (Gibco BRL, #15504-020), 5.5 g of boric acid (Fisher, #B/3800/53) and 4 ml of 0.5 M EDTA (pH 8) in 1 litre of distilled H_20. Sterilise by autoclaving.
Tris-Buffered Saline (TBS):	0.05 M Tris-HCl (pH 7.6) (Gibco BRL, #15504-020), 0.15 M NaCl (Fisher, #S/3160/63).
Yolk Sac Lysis Buffer:	50 mM Tris-HCl (pH 8) (Gibco BRL, #15504-020), 100 mM EDTA (BDH,

#100935V), 0.5 % SDS (Fisher, #S/P530/53). Add proteinase K (Sigma, #P-6556) to a final concentration of 0.5 mg/ml just before use.

Chapter 3

Results

Defective Neural Stem Cell Proliferation and Glial Cell Development in Mice Lacking Helix-Loop-Helix Protein Id4

Knockout mice for Id1, Id2 and Id3 family members of the Id genes have been described (Yan *et al.*, 1997a; Lyden *et al.*, 1999; Pan *et al.*, 1999; Yokota *et al.*, 1999), but Id4 single knockout mice have not been reported. Therefore, a strain of mice that carried a targeted disruption in the Id4 gene was generated and analysed.

3.1 Generation of Id4 Knockout Mice

The Id4 knockout targeting construct and the targeted ES cells were generated by Dr Inge van Crüchten in our laboratory (sections 2.1.1 and 2.1.2). The Id4 gene (Riechmann *et al.*, 1994; van Crüchten *et al.*, 1998) was inactivated in E14.1 ES cells by replacement of a 215 bp PstI-SacII fragment containing the HLH encoding domain with a lacZ/neomycin reporter gene cassette via homologous recombination (figure 2.1). The lacZ gene was inserted in-frame of the Id4 coding sequence to allow expression of an Id4/lacZ fusion protein. Southern blot analysis identified three homologous recombinant Id4 knockout ES cell clones, numbered 58, 62 and 65 (data not shown). All subsequent work involved in the generation of Id4 knockout mice was carried out by myself. Chimeric mice were generated by ES cell-morula

aggregation, which is described in detail in section 2.1.3. Id4 knockout ES cell clone 65 produced a germline chimera that became the founder of the Id4 knockout mice.

As can be seen in figure 3.1, RT-PCR analysis of total RNA isolated from brain and testis of homozygous Id4 mutant ($Id4^{-/-}$), heterozygous Id4 mutant ($Id4^{+/-}$) and wild-type ($Id4^{+/+}$) mice confirmed that no mRNA encoding the HLH domain of Id4 was present in the tissues of homozygous Id4 mutant mice. Therefore, the Id4 gene had been inactivated. $Id4^{-/-}$ and $Id4^{+/-}$ mice exhibited expression of the Id4/lacZ fusion gene by amplification of lacZ (figure 3.1).

3.2 Decreased Viability of Id4 Knockout Mice

To analyse the viability of homozygous Id4 mutant mice, heterozygous Id4 mutant mice were intercrossed and the offspring were genotyped at weaning. In a total of 308 male and female mice, the ratio of $Id4^{+/+}$: $Id4^{+/-}$: $Id4^{-/-}$ mice was 1 : 1.84 : 0.51 (table 3.1). This indicated that approximately 50 % of homozygous Id4 mutant mice die, either in utero or during the postnatal period.

	Total number of mice			Ratio of mice		
	$Id4^{+/+}$	$Id4^{+/-}$	$Id4^{-/-}$	$Id4^{+/+}$	$Id4^{+/-}$	$Id4^{-/-}$
Male	50	90	25	1	1.80	0.50
Female	42	79	22	1	1.88	0.52
Both	92	169	47	1	1.84	0.51

Table 3.1 The total number of wild-type ($Id4^{+/+}$), heterozygous ($Id4^{+/-}$) and homozygous ($Id4^{-/-}$) Id4 mutant mice at weaning from $Id4^{+/-}$ intercrosses, and the ratio of $Id4^{+/+}$: $Id4^{+/-}$: $Id4^{-/-}$ mice. Note that 50 % of $Id4^{-/-}$ mice die before weaning.

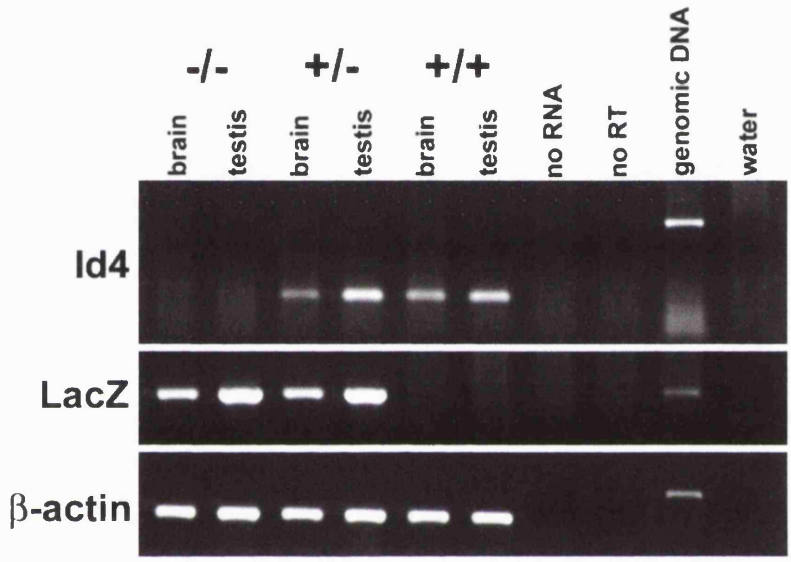

Figure 3.1 Generation of Id4 knockout mice. Results of RT-PCR analysis of total RNA from brain and testis of $Id4^{-/-}$ (-/-), $Id4^{+/-}$ (+/-) and $Id4^{+/+}$ (+/+) mice, showing Id4, lacZ and β-actin amplification. Lack of amplification of Id4 in $Id4^{-/-}$ mice confirmed inactivation of the Id4 gene. Amplification of β-actin was performed as a control.

3.3 Retarded Growth and Death of Id4 Knockout Mice

To compare the growth of the $Id4^{+/+}$, $Id4^{+/-}$ and $Id4^{-/-}$ mice, six litters from five different $Id4^{+/-}$ intercrosses were weighed from weaning (2 or 3 weeks old) into adulthood (12 weeks old). The ratio of $Id4^{+/+}$: $Id4^{+/-}$: $Id4^{-/-}$ genotypes represented by this group was 1 : 1.43 : 0.52, were the total number of mice was 62 (data not shown). Figure 3.2A is a graph showing the average weight of $Id4^{+/+}$, $Id4^{+/-}$ and $Id4^{-/-}$ mice against age. As shown in figure 3.2A, there was no significant difference between the growth of wild-type and heterozygous Id4 mutant mice over the analysed time period. Whereas, homozygous Id4 mutant mice exhibited retarded growth compared to wild-type and heterozygous Id4 mutant mice (figure 3.2A). These results were the same when male and female mice were considered separately (data not shown). Also, it was possible to identify $Id4^{-/-}$ mice in a litter by their smaller size compared to $Id4^{+/+}$ and $Id4^{+/-}$ littermates (data not shown).

During the period of this growth study, six of the eleven homozygous Id4 mutant mice died. Mice were found dead at three, eight, nine, ten and twelve weeks of age. A further $Id4^{-/-}$ mouse died at fourteen weeks of age (data not shown). No $Id4^{+/+}$ or $Id4^{+/-}$ mice died during this growth analysis. The growth pattern of each $Id4^{-/-}$ mutant mouse that was weighed in this study is shown in figure 3.2B. The mice that died exhibited a similar significant weight loss over approximately three weeks before death (figure 3.2B, asterisk). Therefore, in addition to the death observed in early development, $Id4^{-/-}$ mice also die during their development following weaning and in adulthood, which is considered to be 8 weeks of age in mice. The results indicate that there is not a particular age at which the homozygous Id4 mutant mice die. The $Id4^{-/-}$

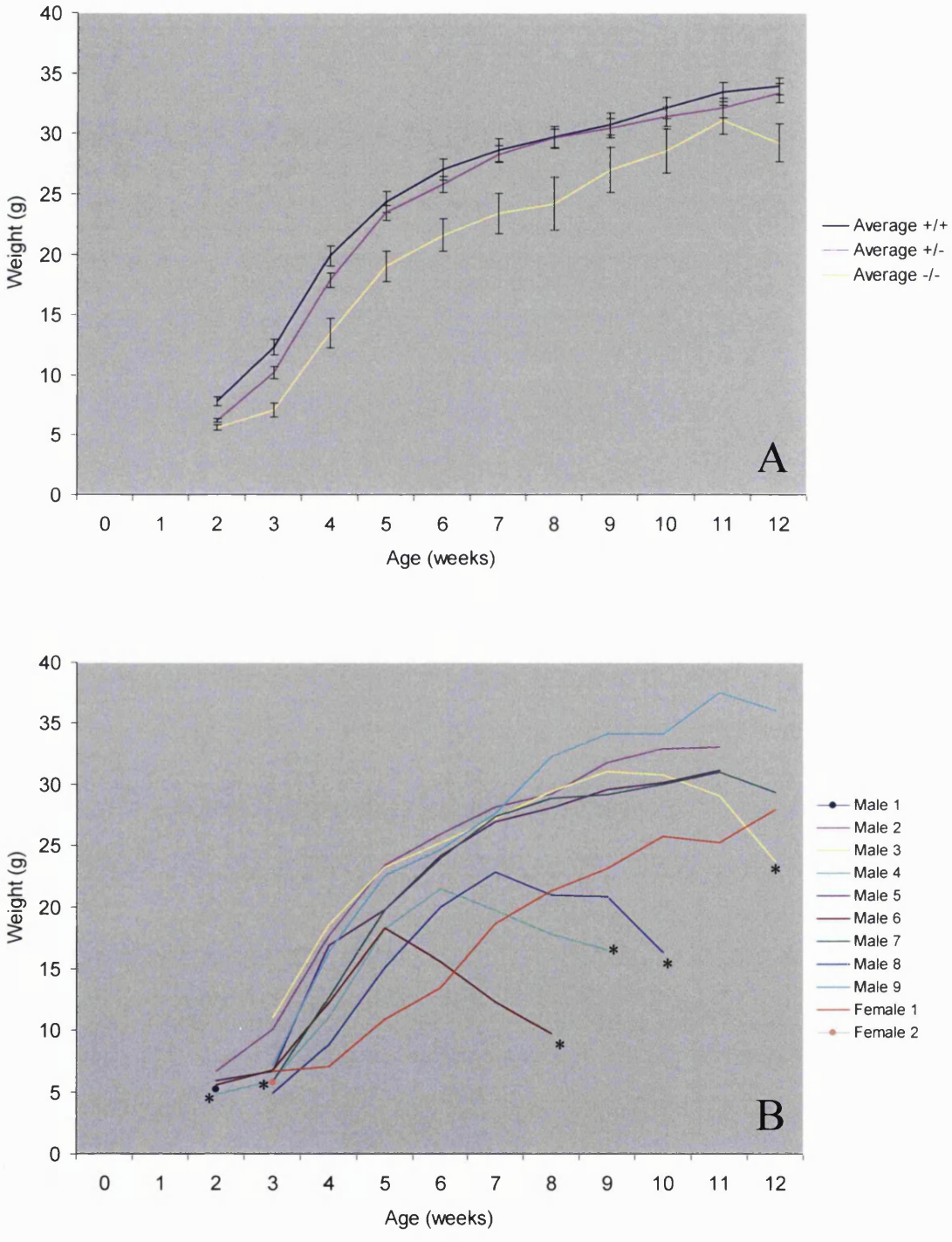

Figure 3.2 Retarded growth and death of Id4 knockout mice. (A) Average growth rate of wild-type (+/+), heterozygous (+/-) and homozygous (-/-) Id4 mutant mice from weaning into adulthood, showing the retarded growth of homozygous Id4 mutant mice. (B) Growth pattern of each homozygous Id4 mutant mouse involved in the growth study. Six of the eleven Id4 null mice died (*). Male 7 died at 14 weeks of age.

mice that survive are smaller than their $Id4^{+/+}$ and $Id4^{+/-}$ littermates, but appear to be normal and healthy.

3.4 Embryonic Development of Id4 Knockout Mice

3.4.1 Id4/lacZ Fusion Protein Expression is Mostly Restricted to the Nervous System During Embryogenesis

During mouse embryogenesis, Id4 mRNA expression is first detected at 9.5 dpc and is mainly restricted to specific regions of the developing nervous system (Riechmann and Sablitzky, 1995; Jen *et al.*, 1996, 1997). Although the expression patterns of the Id genes during mouse embryonic development have been described, this data is based on mRNA analysis, which may not be indicative of the presence of the protein. To document the expression pattern of the Id4 protein during mouse embryogenesis, the expression of the Id4/lacZ fusion protein was analysed by X-gal staining of embryos that were generated by intercrossing $Id4^{+/-}$ mice. In general, there were no apparent morphological differences between $Id4^{+/+}$, $Id4^{+/-}$ and $Id4^{-/-}$ embryos at any of the embryonic stages analysed (8.5-14.5 dpc).

3.4.1.1 Id4/lacZ Fusion Protein Expression in 8.5 dpc and 9.5 dpc Mouse Embryos

The Id4/lacZ fusion protein was observed at 8.5 dpc, where it appeared to be in the paired dorsal aortae of the mouse embryo (data not shown). At 9.5 dpc, the Id4/lacZ fusion protein was expressed in the prosencephalon and the rhombencephalon, which are the developing forebrain and hindbrain regions respectively (figure 3.3). The prosencephalon is subdivided into the telencephalon that overlays the telencephalic vesicles, and the diencephalon that surrounds the third ventricle of the brain. The

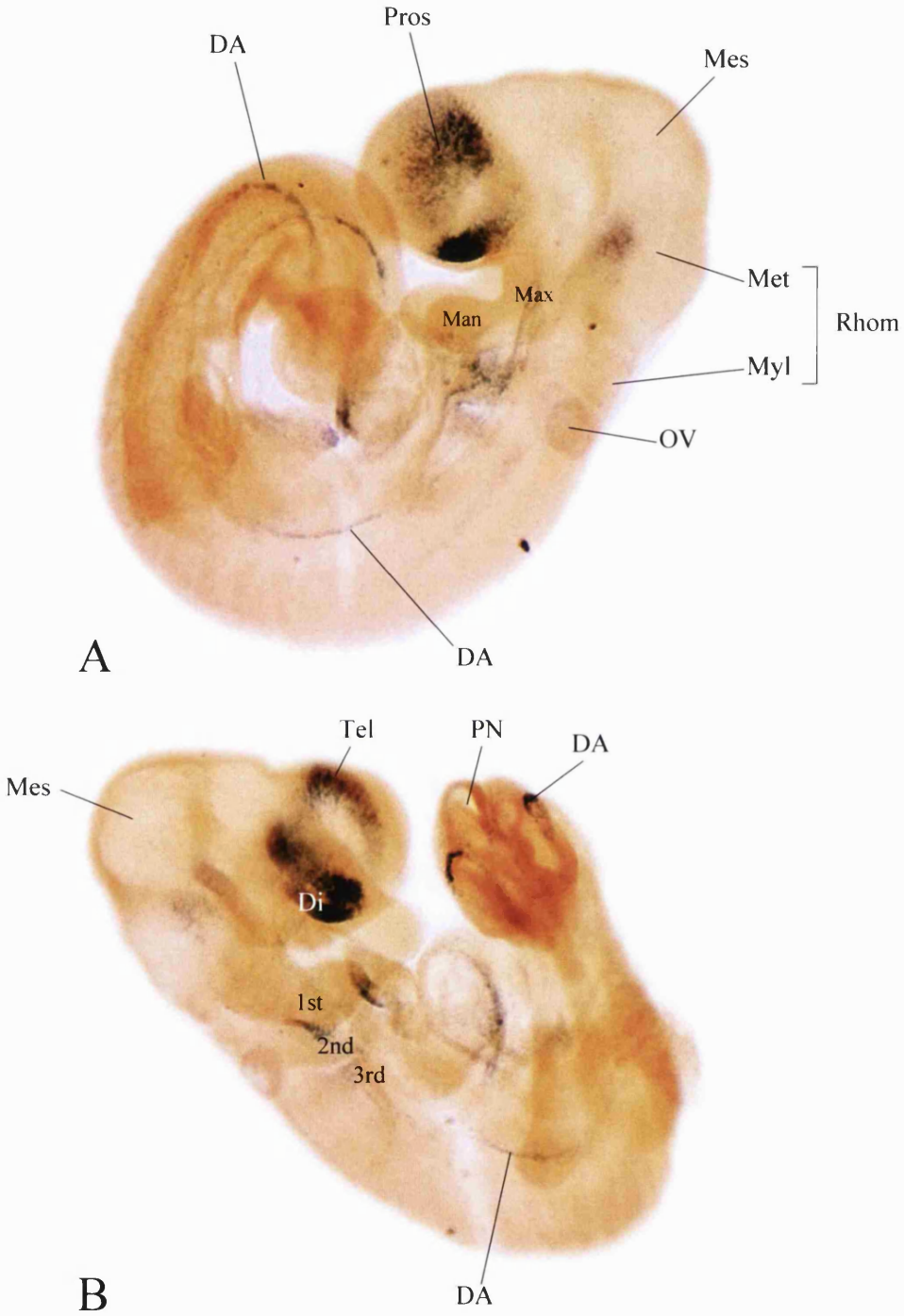

Figure 3.3 Id4/lacZ fusion protein expression is in the developing nervous system and paired dorsal aortae at 9.5 dpc. 9.5 dpc whole mouse embryos were stained with X-gal to establish the expression pattern of the Id4/lacZ fusion protein (dark blue). X-gal staining is evident in the telencephalon, diencephalon and metencephalon of the developing brain, the first, second and third branchial arches, and the dorsal aorta. 1st, first branchial arch; 2nd, second branchial arch; 3rd, third branchial arch; DA, dorsal aorta; Di, diencephalon; Max, maxillary component of first branchial arch; Man, mandibular component of first branchial arch; Mes, mesencephalon; Met, metencephalon; Myl, mylencephalon; OV, otic vesicle; PN, posterior neuropore; Pros, prosencephalon; Rhom, rhombencephalon; Tel, telencephalon.

rhombencephalon is subdivided into the metencephalon and the mylencephalon that, together with the thin layer of cells at the dorsal-most aspect of this region, surround the fourth ventricle of the brain. In addition, the first, second and third branchial arches, and the dorsal aorta showed Id4/lacZ expression at 9.5 dpc (figure 3.3).

3.4.1.2 Id4/lacZ Fusion Protein Expression in the 10.5 dpc Mouse Embryo

In the 10.5 dpc embryo, strong X-gal staining was observed in both the central and peripheral nervous system (figure 3.4), indicating that Id4/lacZ protein expression was significantly upregulated in the nervous system between 9.5 and 10.5 dpc of mouse embryogenesis. As can be seen in figure 3.4, X-gal staining was evident in the telencephalon, diencephalon, mesencephalon, metencephalon and mylencephalon. In the developing forebrain region, the tissue of the telencephalon will form the cerebral hemispheres and hippocampus, and that of the diencephalon will form the thalamus and hypothalamus. The tissue of the mesencephalon is not subdivided and becomes the midbrain. The cerebellum and pons develop from the metencephalon, which is the rostral extremity of the primitive hindbrain, and the medulla oblongata forms from the mylencephalon, which is the caudal part of the primitive hindbrain. In the spinal cord of the 10.5 dpc embryo, high expression of the Id4/lacZ fusion protein was evident in the ventral (basal) portion, which forms the motor area (figure 3.4). In addition, X-gal staining was observed in the roof plate of the spinal cord (figure 3.4C). In the PNS, strong X-gal staining was evident in the sensory ganglia of the trigeminal (V), acoustic (VIII), facial (VII), glossopharyngeal (IX) and vagal (X) cranial nerves (figure 3.5A and data not shown). Figure 3.5A shows Id4/lacZ expression in the sensory ganglia of the acoustic (VIII), facial (VII),

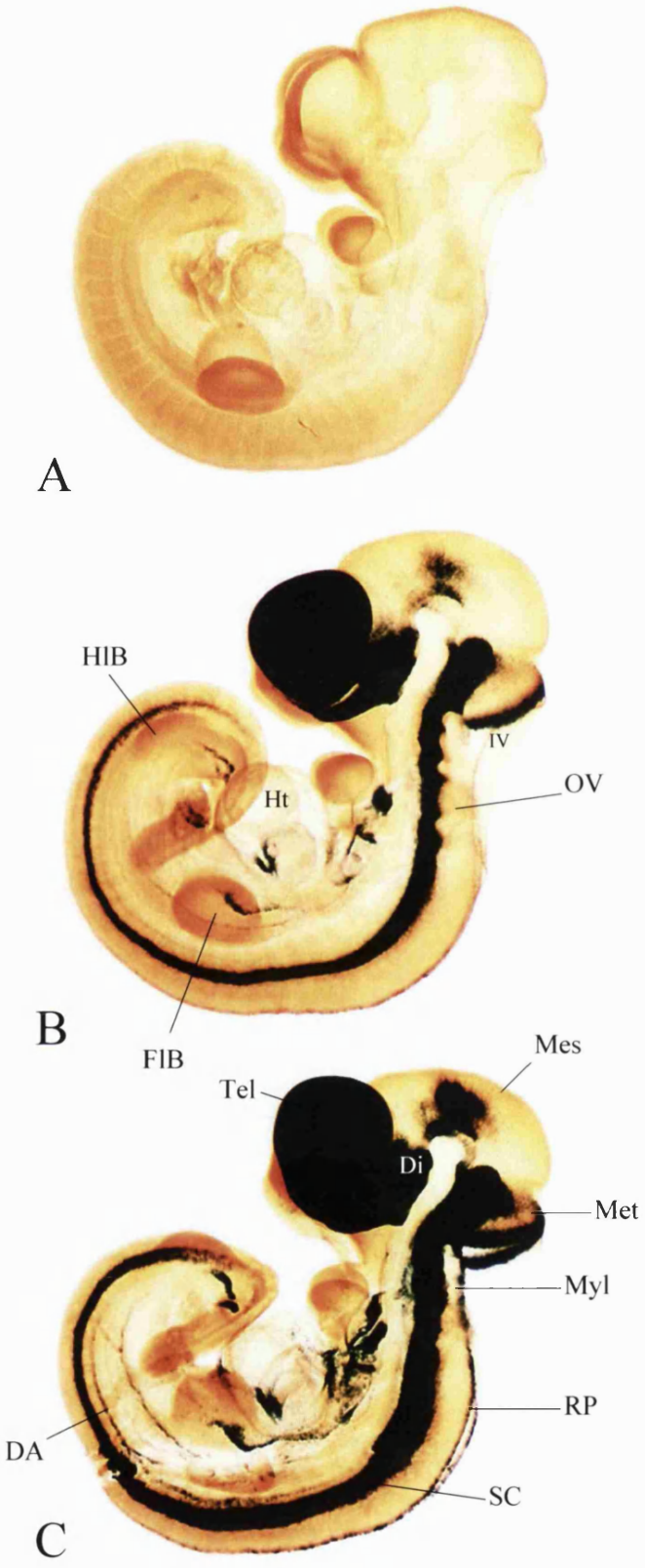

Figure 3.4 Id4/lacZ fusion protein expression is mostly in the developing central and peripheral nervous system at 10.5 dpc. 10.5 dpc $Id4^{+/+}$ (A), $Id4^{+/-}$ (B) and $Id4^{-/-}$ (C) mouse embryos were stained with X-gal to establish the expression pattern of the Id4/lacZ fusion protein (dark blue). The wild-type embryos served as a control for the X-gal staining. DA, dorsal aorta; Di, diencephalon; FlB, forelimb bud; HlB, hindlimb bud; Ht, heart; IV, fourth ventricle; Mes, mesencephalon; Met, metencephalon; Myl, mylencephalon; OV, otic vesicle; RP, roof plate of spinal cord; SC, spinal cord; Tel, telencephalon.

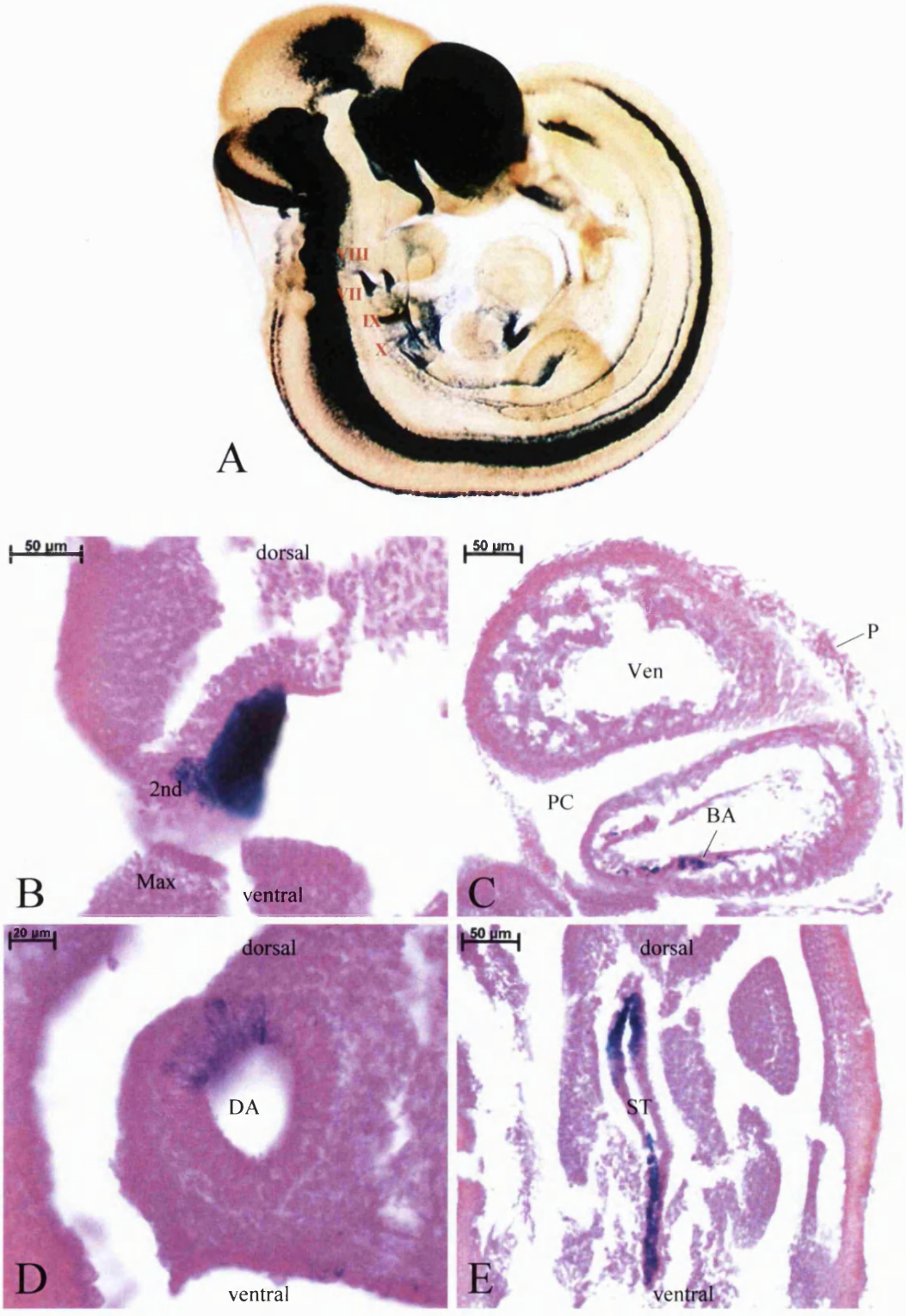

Figure 3.5 Id4/lacZ fusion protein expression in a 10.5 dpc Id4$^{-/-}$ mouse embryo (A) and in transverse sections of the same embryo (B-E). (A) shows X-gal staining (dark blue) in the sensory ganglia of the acoustic (VIII), facial (VII), glossopharyngeal (IX) and vagal (X) nerves. (B-E) show Id4/lacZ expression in the second branchial arch, bulbus arteriosus of the heart, dorsal aorta and future stomach region, respectively. The dorsal-ventral orientation of the section is indicated. 2nd, second branchial arch; BA, bulbus arteriosus; DA, dorsal aorta; Max, maxillary component of the first branchial arch; P, pericardium; PC, pericardial cavity; ST, gastric dilatation of the foregut (future stomach region); Ven, ventricle.

glossopharyngeal (IX) and vagal (X) nerves. These sensory ganglia are derived from neural crest cells, which migrate into the branchial arches from different axial levels along the dorsal aspect of the neural tube, and cells of the epibranchial placodes, which are specialised regions of surface ectoderm that invaginate to contribute to the formation of the ganglia (Webb and Noden, 1993). The remaining craniofacial ganglia are derived from only neural crest cells.

Although many internal structures can be discerned in the cleared whole embryos, additional regions of Id4/lacZ expression were evident in X-gal stained embryos that were difficult to identify, particularly in the regions of the developing heart and stomach. In order to identify these, and to analyse in more detail the regions that express the Id4/lacZ fusion protein, serial transverse sections of the X-gal stained embryos were made. Figures 3.5C-E show X-gal staining in the bulbus arteriosus of the heart, in the dorsal aspect of the dorsal aorta and in the future stomach region of the 10.5 dpc embryo respectively. In addition, the embryo sections confirmed the domains of Id4/lacZ expression in the developing CNS and PNS that were evident in the whole embryo (figure 3.5B and data not shown). For example, figure 3.5B shows intense X-gal staining in the second branchial arch, which contains the facial (VII) neural crest tissue. The expression pattern of the Id4/lacZ fusion protein in the $Id4^{+/-}$ compared to the $Id4^{-/-}$ embryo will be described later in this section.

3.4.1.3 Id4/lacZ Fusion Protein Expression in the 12.5 dpc Mouse Embryo

A similar pattern of Id4/lacZ fusion protein expression was observed at 12.5 dpc to at 10.5 dpc (figures 3.4 and 3.6). In the 12.5 dpc embryo, strong X-gal staining was

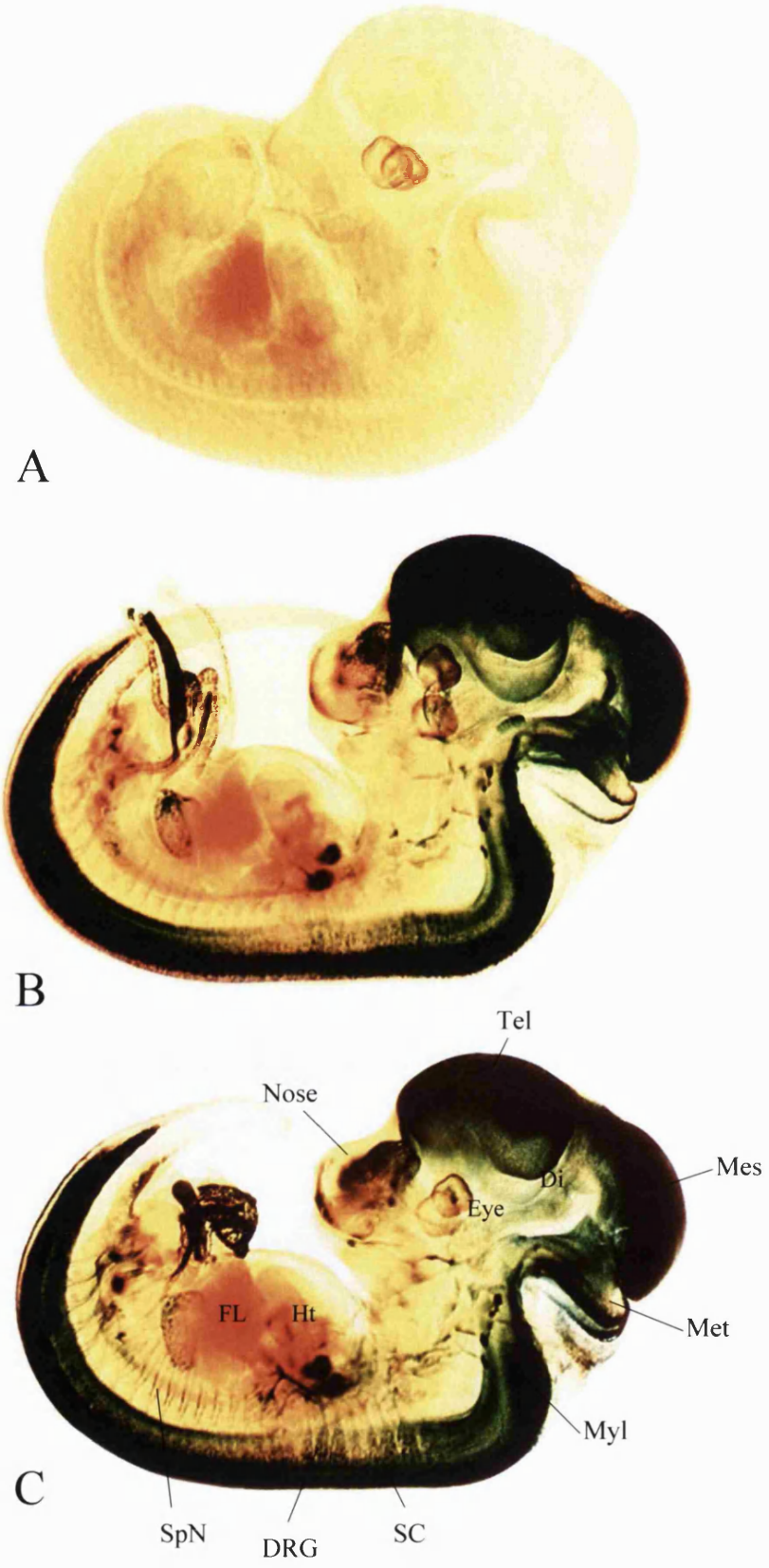

Figure 3.6 Expression of the Id4/lacZ fusion protein is mostly in the developing CNS and PNS at 12.5 dpc. 12.5 dpc $Id4^{+/+}$ (A), $Id4^{+/-}$ (B) and $Id4^{-/-}$ (C) mouse embryos were stained with X-gal to establish the expression pattern of the Id4/lacZ fusion protein (dark blue). The wild-type embryos served as a control for the X-gal staining. Di, diencephalon; DRG, dorsal root ganglion; FL, fetal liver; Ht, heart; Mes, mesencephalon; Met, metencephalon; Myl, mylencephalon; SC, spinal cord; SpN, spinal nerve; Tel, telencephalon.

Figure 3.7 Id4/lacZ fusion protein expression in the cephalic region of a $Id4^{-/-}$ 12.5 dpc mouse embryo. Id4/lacZ expression is in the eye, nose and vibrissae of the developing face, and in the V, VIII and VII craniofacial ganglia.

evident in the telencephalon, mesencephalon, metencephalon and mylencephalon of the developing brain. X-gal staining in the 12.5 dpc diencephalon appeared to be less intense than that observed in the 10.5 dpc embryo, suggesting a downregulation of Id4/lacZ protein expression in this region of the brain. It is possible that the expanding telencephalon and telencephalic vesicles, which partly overlay the developing diencephalon and third ventricle at this stage of development, block the observation of any staining in this region in the whole embryo. Also in the cephalic region of the embryo at 12.5 dpc, the Id4/lacZ fusion protein was expressed in the developing eye, nose and hair follicles (vibrissae; figure 3.7). In the nose, the X-gal staining appears to be in the olfactory (I) nerves that pass to the telencephalon. Sensory cranial ganglia and their branches clearly expressed the Id4/lacZ fusion protein at 12.5 dpc, and are shown in figure 3.7. In contrast to the staining pattern at 10.5 dpc, X-gal staining was observed in both the dorsal (alar) and ventral (basal) portions of the spinal cord at 12.5 dpc, where X-gal staining was stronger in the dorsal part of the spinal cord (figure 3.6). In addition, dorsal root (spinal) ganglia and spinal nerves exhibited Id4/lacZ expression (figures 3.6C and 3.7).

3.4.1.4 Id4/lacZ Fusion Protein Expression in the 14.5 dpc Mouse Embryo

At 14.5 dpc, X-gal staining was still mainly restricted to specific regions of the developing central and peripheral nervous system (figure 3.8). Similar to earlier stages of embryonic development, the Id4/lacZ fusion protein was highly expressed in the cerebral hemispheres (telencephalon), midbrain (mesencephalon) and medulla oblongata (mylencephalon), which tapers into the spinal cord of the brain. However, X-gal staining in the cerebellum and pons (subdivisions of the metencephalon) was

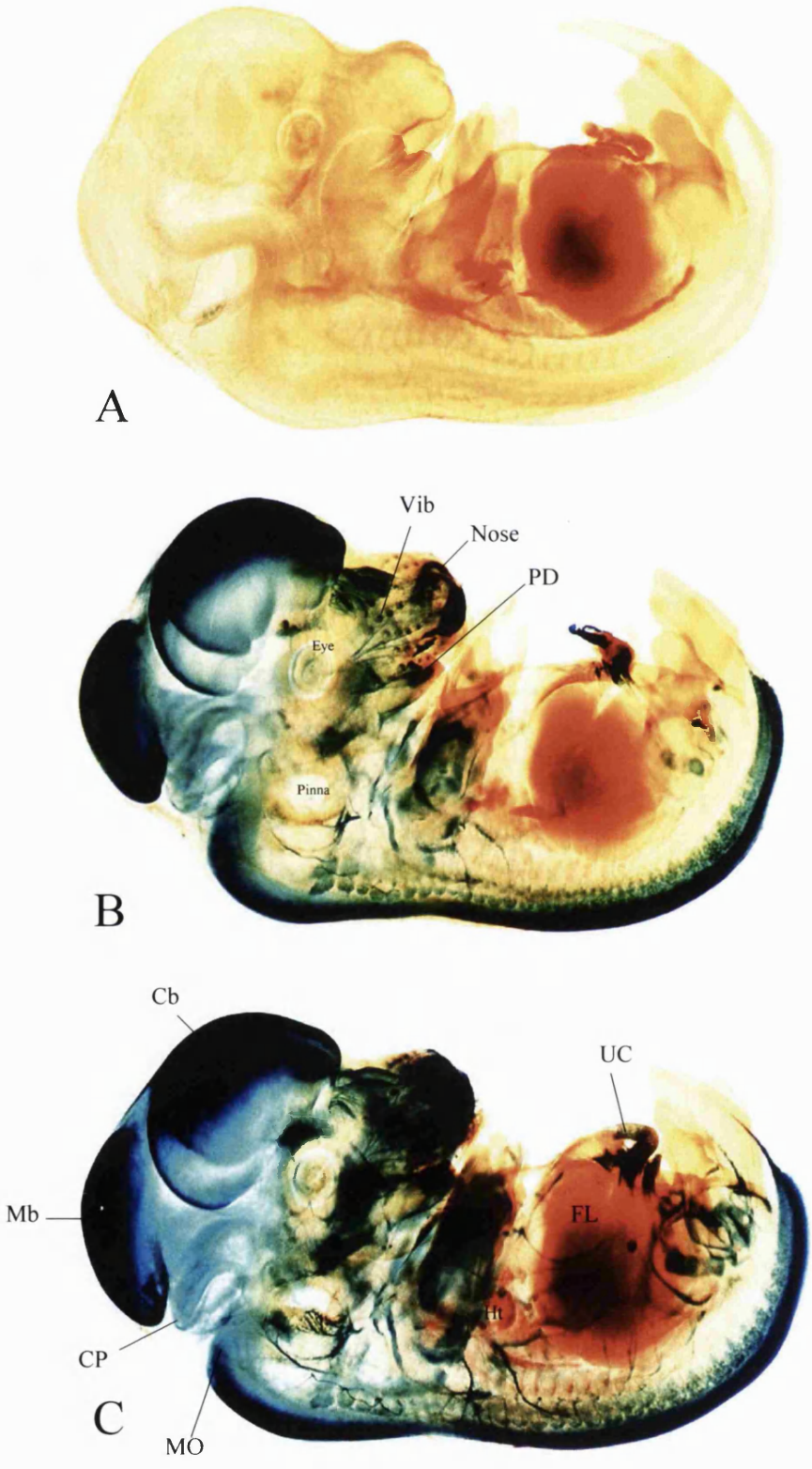

Figure 3.8 Id4/lacZ fusion protein expression at 14.5 dpc is in the developing nervous system and sensory organs of the mouse embryo. 14.5 dpc $Id4^{+/+}$ (A), $Id4^{+/-}$ (B) and $Id4^{-/-}$ (C) whole mouse embryos were stained with X-gal to establish the expression pattern of the Id4/lacZ fusion protein (dark blue). The wild-type embryos served as a control for the X-gal staining. Cb, cerebral hemispheres; CP, cerebellar primordium; FL, fetal liver; Ht, heart; Mb, mibrain; MO, medulla oblongata; PD, primordia of the dentition; UC, umbilical cord; Vib, vibrissae.

greatly reduced in comparison to that which was observed at 10.5 dpc and at 12.5 dpc (figures 3.4, 3.6 and 3.8), suggesting a downregulation of Id4 protein expression in these regions of the brain between 12.5 dpc and 14.5 dpc. In the spinal cord, strong X-gal staining was restricted to just the dorsal portion by 14.5 dpc (figure 3.8), which is the future substantia gelatinosa region. The crainofacial ganglia and their branches still exhibited Id4/lacZ fusion protein expression at 14.5 dpc. Id4/lacZ expression was observed in the dorsal root ganglia (figures 3.9A-C), in the dorsal root sensory nerves (figure 3.9A) and in the spinal nerves (figures 3.9A-C). The spinal nerves contain both sensory fibres from the dorsal root ganglia and motor axons that extend from neurons in the basal plate in the ventral root of the spinal cord. X-gal staining was evident in both anterior and posterior ramifications of the spinal nerves (figures 3.9B and C). Anterior nerves supply the muscles and skin of the limbs and over the anterolateral body wall, and posterior nerves pass around the vertebral column to supply the muscles and skin of the back. X-gal staining was evident in various regions of the developing face at 14.5 dpc. The numerous sensory olfactory (I) nerves that convey sensory information from the olfactory epithelium to the olfactory lobes of the brain were intensely stained (figure 3.9D). In addition, sections of 14.5 dpc embryos showed X-gal staining in the olfactory epithelium (figure 3.10D). The primordia of the dentition (figure 3.8B) and the five parallel rows of vibrissae (figures 3.8, 3.9D and 3.9F) clearly expressed the Id4/lacZ fusion protein at this stage of embryonic development. As can be seen in figure 3.9E, the eye and the optic (II) nerve exhibited X-gal staining. In the eye, the staining is likely to be nerve fibres that pass from ganglion cells of the neural retina to the region of the future optic disc, which then pass centrally along the optic nerve. In addition, this figure shows Id4/lacZ fusion protein expression in the ophthalmic branch of the

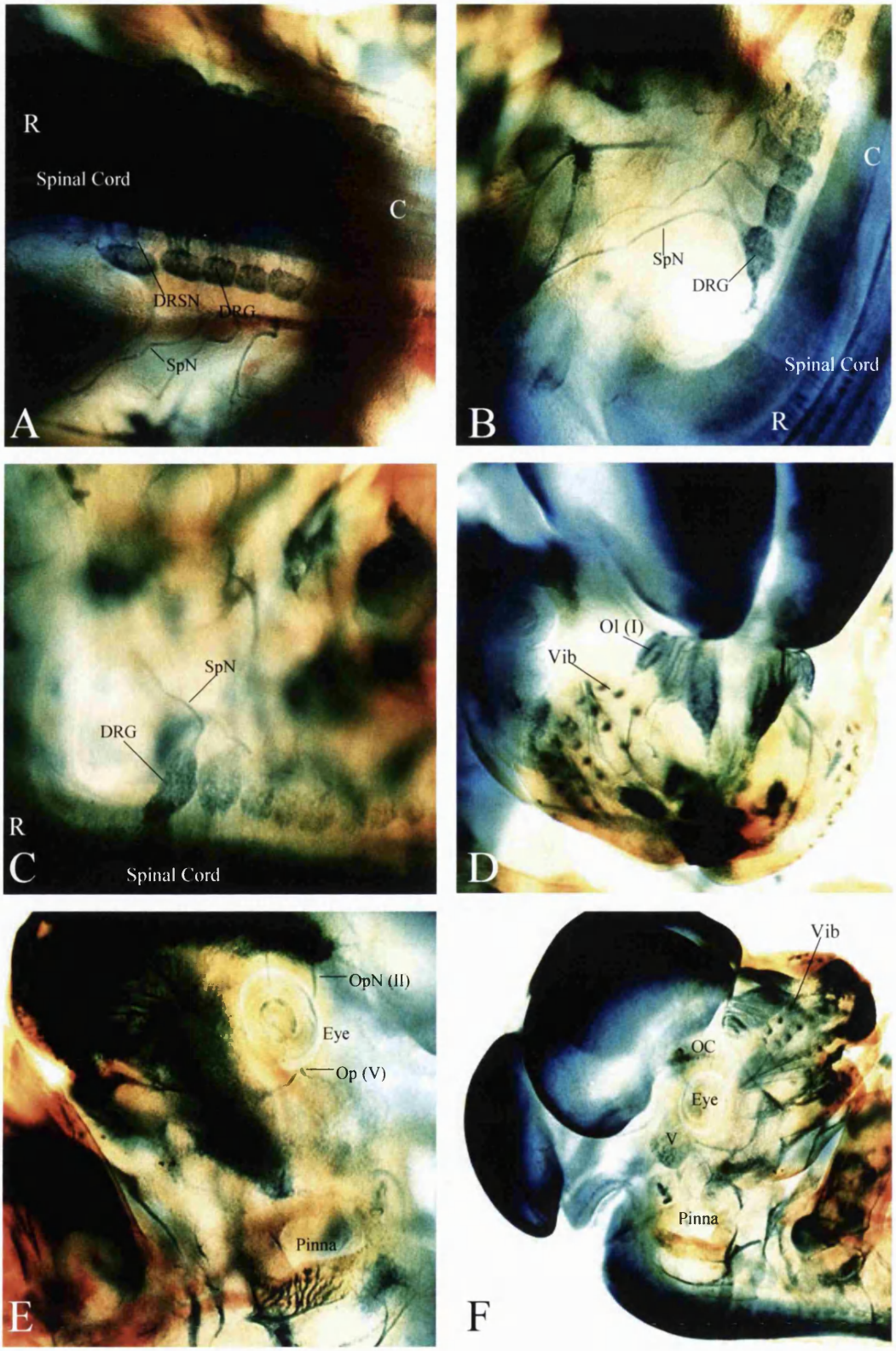

Figure 3.9 Pattern of expression of the Id4/lacZ fusion protein (dark blue) in various regions of the 14.5 dpc mouse embryo. The rostral (R) to caudal (C) direction of the spinal cord is indicated in A-C. DRG, dorsal root ganglion; DRSN, dorsal root sensory nerve; OC, optic chiasm; Ol (I), olfactory (I) sensory nerves; OpN (II), optic (II) nerve; Op (V), ophthalmic branch of the trigeminal (V) ganglion; SpN, spinal nerve; V, trigeminal (V) ganglion; Vib, vibrissae.

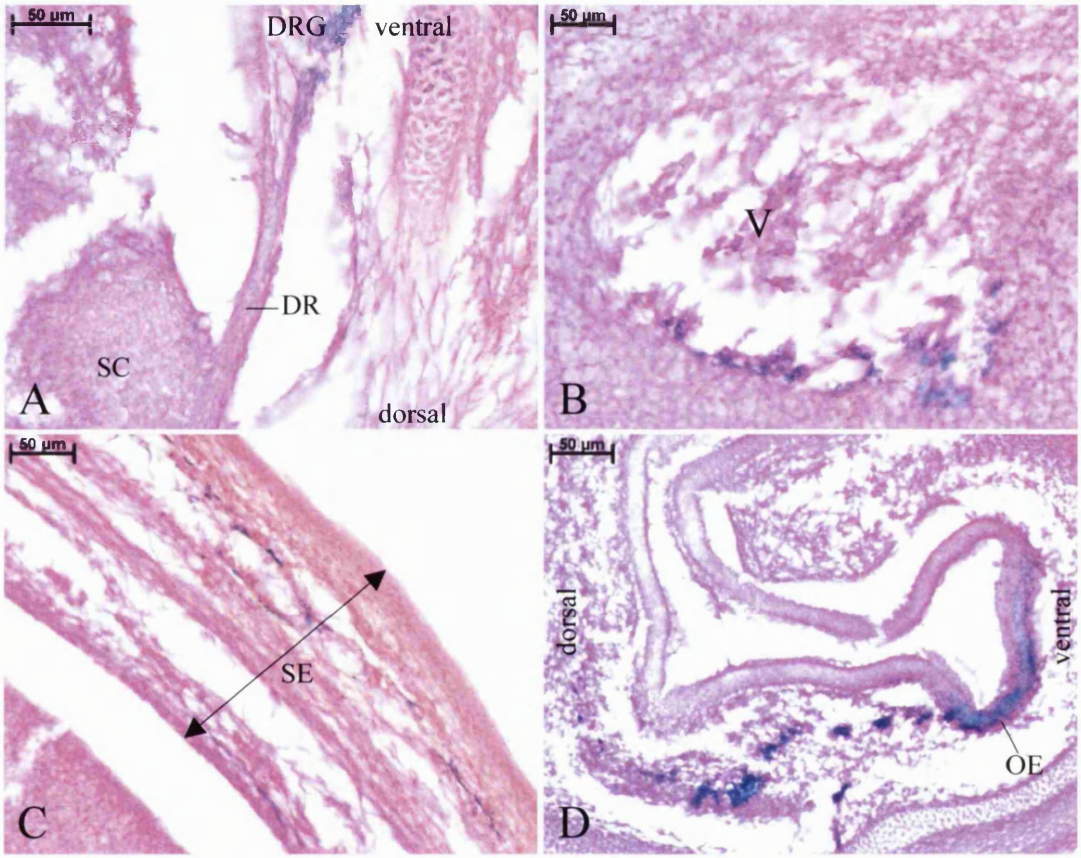

Figure 3.10 Transverse sections of an X-gal stained 14.5 dpc mouse embryo. Sections were eosin Y counterstained (pink). Figures A-D show Id4/lacZ fusion protein expression in the dorsal root ganglion (DRG) and dorsal root (DR) sensory nerve, the trigeminal (V) ganglion, the skin and the olfactory epithelium (OE) respectively. The dorsal-ventral orientation of the section is indicated in A and D. SE, surface ectoderm; SC, spinal cord.

trigeminal (V) nerve. X-gal staining was also evident in the optic chiasm (figure 3.9F).

Transverse sections of 14.5 dpc embryos confirmed the expression pattern of the Id4/lacZ fusion protein at this stage of mouse embryogenesis. Figures 3.10A and 3.10B show X-gal staining in the dorsal root ganglion and dorsal root sensory fibres, and in the trigeminal (V) ganglion, respectively. In addition, the sections revealed Id4/lacZ expression in cells of the surface ectoderm (figure 3.10C).

3.4.2 Comparison of Id4/lacZ Fusion Protein Expression between $Id4^{+/-}$ and $Id4^{-/-}$ Embryos

To compare the morphology between $Id4^{+/+}$, $Id4^{+/-}$ and $Id4^{-/-}$ embryos, and the X-gal staining pattern within the domains of Id4/lacZ expression between $Id4^{+/-}$ and $Id4^{-/-}$ embryos, transverse sections of X-gal stained 10.5 dpc and 14.5 dpc embryos were made.

3.4.2.1 Cerebral Cortex Development

In early development, the nervous system is a single layer of proliferating neuroepithelial cells, which are the progenitors for neurons and glia. This layer is called the ventricular zone (VZ; figure 3.11). The VZ that is the roof of the telencephalic vesicles (future lateral ventricles) develops into the multi-laminar cerebral cortex. The earliest post-mitotic neurons to exit the VZ form the preplate (PP) layer (figure 3.11). The axons of PP neurons and the axons of neurons growing into the cortex from the thalamus form the intermediate zone (IZ), which separates the VZ from the PP (figure 3.11). As well as containing the axons that are the

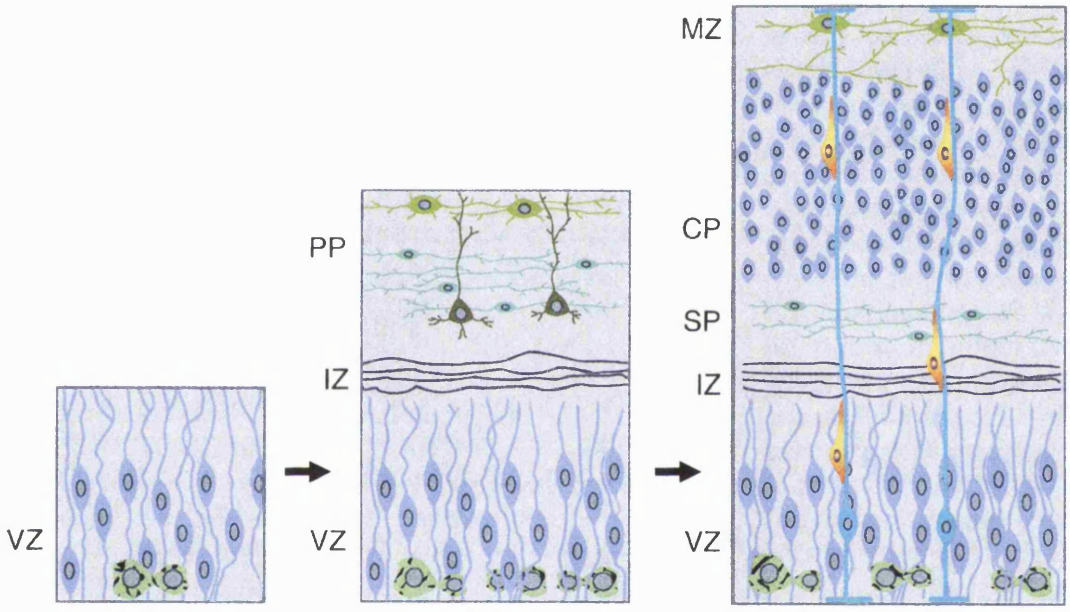

Figure 3.11 Cerebral cortex development. The ventricular zone (VZ) contains mitotically active cells that are the progenitors for neurons and glia. The first post-mitotic neurons to exit the VZ form the preplate (PP), and their axons, together with axons growing into the cortex, form the intermediate zone (IZ). As development continues, the IZ also contains post-mitotic migrating neurons, which are destined for different layers of the cortex, and form the cortical plate (future cortical layers II-VI). This splits the PP into the marginal zone (MZ; future layer 1) and transitory subplate (SP). Figure modified from Zigmond *et al.* (1999).

connections between the cortex and the thalamus, the IZ contains migrating post-mitotic neural cells. Subsequently, as the migrating cells form the cortical plate (CP), which will generate layers II-VI of the adult cerebral cortex, the PP is split into the marginal zone (MZ), which is the future layer I, and the subplate (SP), which is a transient population of neurons (figure 3.11). Cajal-Retzius cells within the cell-sparse MZ provide signals that are important for the migration of neurons in the patterning of the cortical laminae. In mid- to late-stages of neurogenesis, a subventricular zone (SVZ) forms between the ventricular and intermediate zones, which is a second zone of mitotically active cells.

3.4.2.2 Id4/lacZ Fusion Protein Expression Differs between $Id4^{+/-}$ and $Id4^{-/-}$ 10.5 dpc Mouse Embryos

In a comparison of equivalent transverse sections from $Id4^{+/+}$, $Id4^{+/-}$ and $Id4^{-/-}$ 10.5 dpc embryos, there were no gross morphological abnormalities evident in the mutant embryos (figures 3.12A-C and data not shown). In the 10.5 dpc $Id4^{-/-}$ embryo, there was widespread expression of the Id4/lacZ fusion protein in the developing brain (figure 3.12C). Strong X-gal staining was evident in the walls of the telencephalon and diencephalon, whereas the lamina terminalis and infundibular recess of the diencephalon were devoid of any staining. In the hindbrain, the Id4/lacZ fusion protein was expressed in the majority of the ventral portion, as well as in a small domain in the dorsal portion of the metencephalon. Interestingly, comparison of the X-gal staining between $Id4^{+/-}$ and $Id4^{-/-}$ embryos revealed significant differences in the size of the Id4/lacZ expression domains in the early developing brain (figures 3.12B and C). This was particularly evident in the ventral part of metencephalon, where X-gal staining was extensive in the $Id4^{-/-}$ embryo, but restricted to a small band in the $Id4^{+/-}$ embryo (figures 3.12B-E). The Id4/lacZ expression domain in the

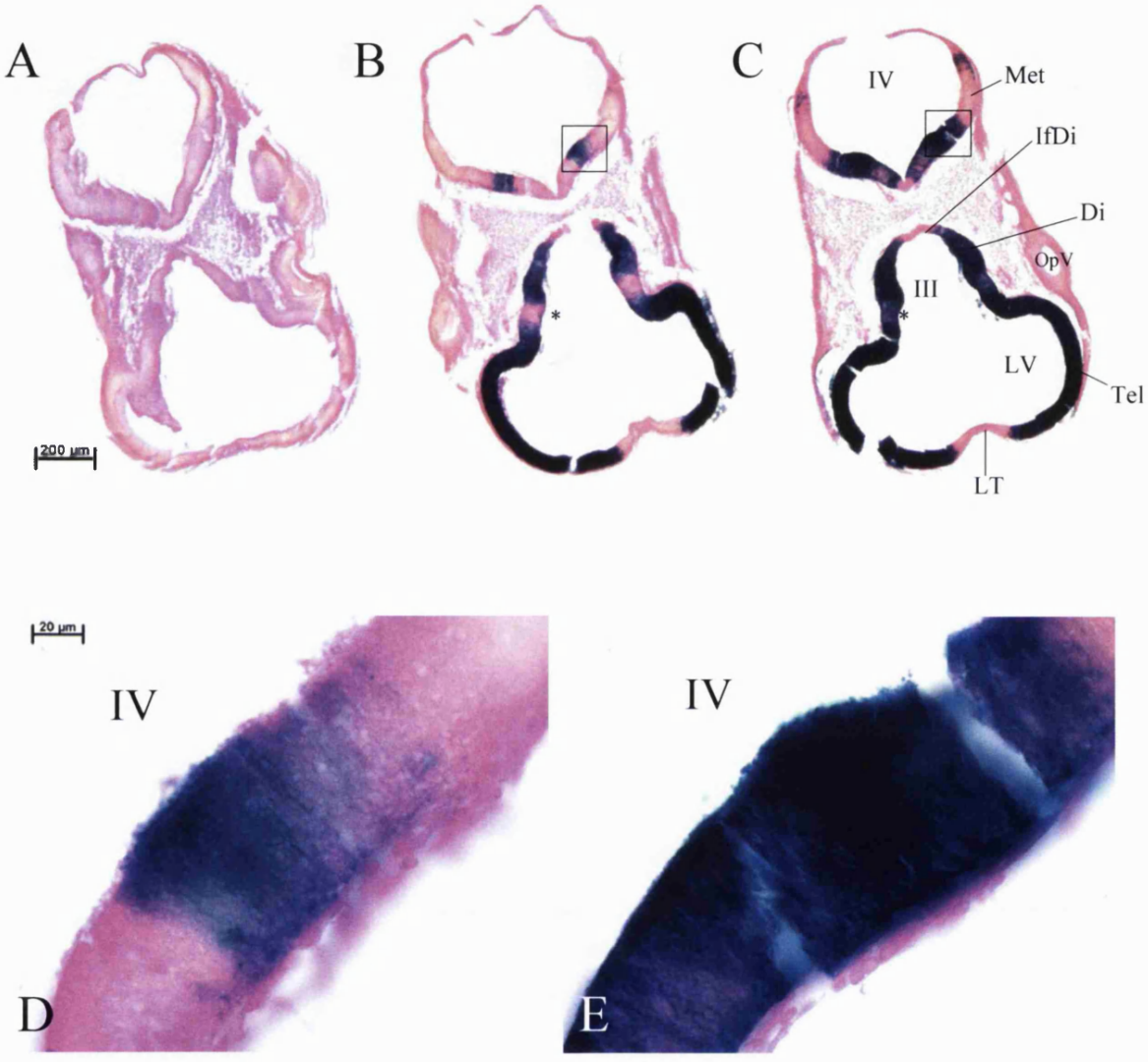

Figure 3.12 Id4/lacZ fusion protein expression differs between $Id4^{+/-}$ and $Id4^{-/-}$ 10.5 dpc mouse embryos. A-C are equivalent transverse sections of $Id4^{+/+}$, $Id4^{+/-}$ and $Id4^{-/-}$ embryos respectively, showing there are no gross morphological abnormalities in the Id4 mutant embryos. D and E represent the boxed regions in B and C respectively. The domains expressing the Id4/lacZ fusion protein are more restricted in the $Id4^{+/-}$ than in the $Id4^{-/-}$. Di, diencephalon; IfDi, infundibular recess of the diencephalon; III, third ventricle; IV, fourth ventricle; LT, lamina terminalis; LV, lateral ventricle; Met, metencephalon; OpV, optic vesicle; Tel, telencephalon.

$Id4^{+/-}$ is approximately one third of that evident in the $Id4^{-/-}$. Similarly, the domain of Id4/lacZ protein expression evident in the dorsal part of the metencephalon is considerably wider in the $Id4^{-/-}$ than in the $Id4^{+/-}$ (figures 3.12B and C). This scenario was also evident in the developing forebrain. The domain between the telencephalon and diencephalon did not exhibit X-gal staining in the $Id4^{+/-}$ embryo, but X-gal staining was clearly evident in this region in the $Id4^{-/-}$ embryo (figures 3.12B and C, asterisk). Notably, the X-gal staining in this region was not as strong as that observed in other regions of the $Id4^{-/-}$ developing forebrain.

At this stage of embryogenesis, the walls of the developing brain are mostly mitotically active cells of the VZ, with a few post-mitotic cells at the periphery beginning to form the intermediate and preplate zones. X-gal staining in the $Id4^{+/-}$ and $Id4^{-/-}$ 10.5 dpc embryos appears to be throughout the wall of the developing brain, indicating that Id4 is expressed during proliferation and early development of neural cells.

3.4.2.3 Id4/lacZ Fusion Protein Expression in the Developing Cerebral Cortex Differs between $Id4^{+/-}$ and $Id4^{-/-}$ Mouse Embryos

Comparison of equivalent sections showed no obvious morphological abnormalities between 14.5 dpc $Id4^{+/+}$, $Id4^{+/-}$ and $Id4^{-/-}$ embryos (figures 3.13A-C and data not shown). As shown in figure 3.13, the Id4/lacZ fusion protein was expressed in the walls of the developing cerebral cortex at 14.5 dpc. Comparison of $Id4^{+/-}$ and $Id4^{-/-}$ cortices revealed that the expression pattern of the Id4/lacZ fusion protein was different between these embryos (figures 3.13B-G). In the $Id4^{+/-}$, X-gal staining was evident in scattered cells in the ventricular zone, and throughout the intermediate

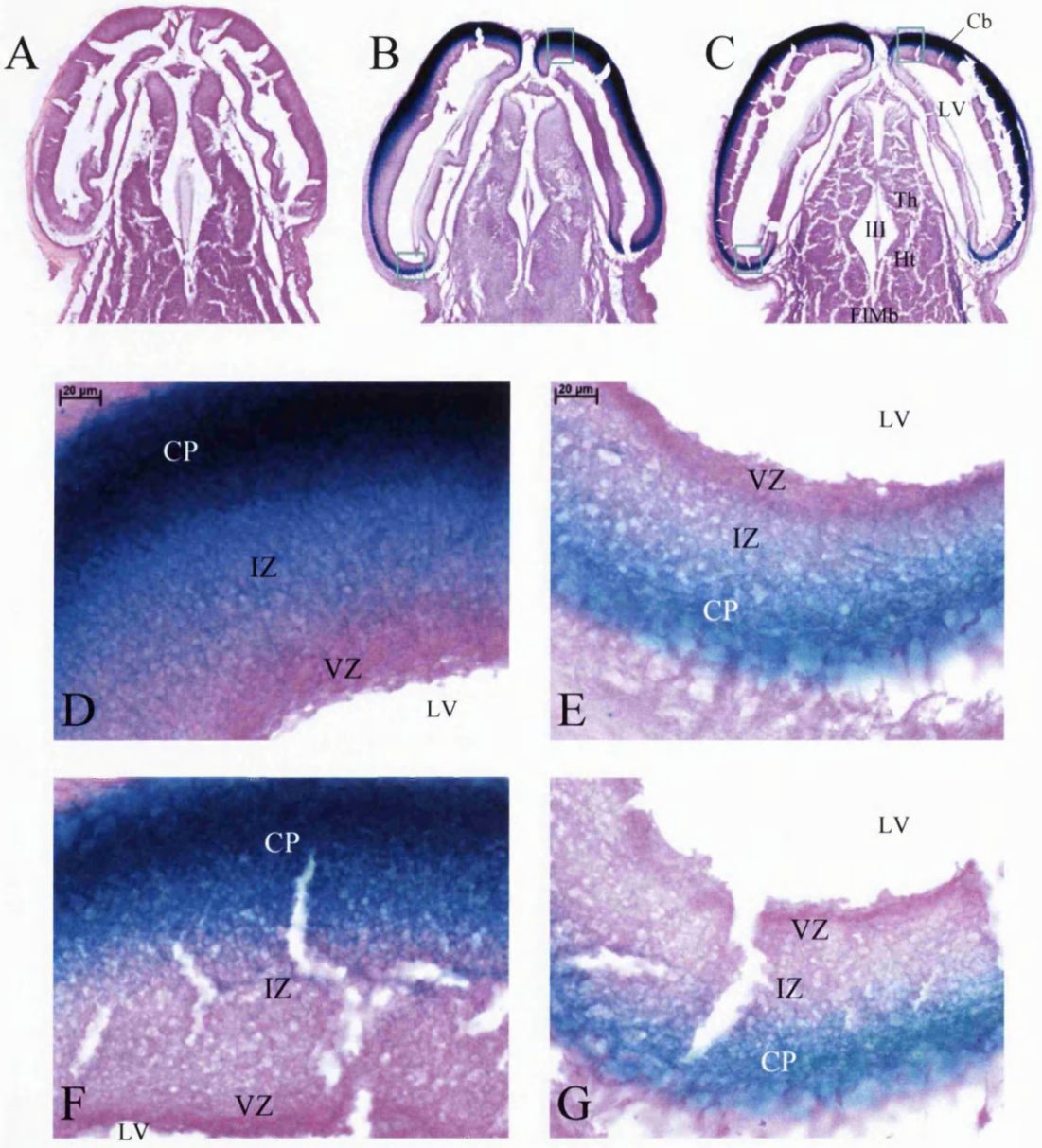

Figure 3.13 Id4/lacZ fusion protein expression in the developing cerebral cortex differs between $Id4^{+/-}$ and $Id4^{-/-}$ mouse embryos. A-C are equivalent transverse sections of 14.5 dpc $Id4^{+/+}$, $Id4^{+/-}$ and $Id4^{-/-}$ embryos respectively, showing there are no gross morphological abnormalities in the Id4 mutant embryos. D and E represent the boxed regions in B, and F and G represent the boxed regions in C. D-G show that cells expressing the Id4/lacZ fusion protein are in more mature regions of the developing cerebral cortex in the $Id4^{-/-}$ compared to in the $Id4^{+/-}$. Cb, cerebral cortex; CP, cortical plate; Ht, hypothalamus; III, third ventricle; IZ, intermediate zone; LV, lateral ventricle; Th, thalamus; FlMb, floor of the midbrain; VZ, ventricular zone.

zone and cortical plate (figures 3.13D and E). X-gal staining became gradually more intense through the intermediate zone into the cortical plate. In the $Id4^{-/-}$, X-gal staining was not observed in the ventricular zone, and was only evident in a few cells of the adjacent intermediate zone (figures 3.13F and G). X-gal staining was evident in cells of the intermediate zone near to the cortical plate and throughout the cortical plate, where the majority of the staining was observed in the $Id4^{-/-}$. This indicates that cells expressing the Id4/lacZ fusion protein are in more mature regions of the developing cerebral cortex in the $Id4^{-/-}$ compared to in the $Id4^{+/-}$ embryo.

3.5 Defects in the Id4 Knockout Adult Mouse Brain

In the experiments documented in this section, $Id4^{+/+}$ and $Id4^{-/-}$ adult brains were from mouse littermates, and seven sets of wild-type and homozygous Id4 mutant brains have been analysed during the preparation of this work. $Id4^{+/-}$ adult mouse brains were not included in the analyses. The brains were sectioned in sagital, coronal and horizontal orientations, and analysis was carried out on $Id4^{+/+}$ and $Id4^{-/-}$ sections that represented approximately equivalent positions in the brain.

3.5.1 Id4/lacZ Fusion Protein is Differentially Expressed Within the Adult Mouse Brain

Id4 mRNA is highly expressed in the brain of adult mice (Riechmann *et al.*, 1994). To establish the pattern of expression of Id4 protein in the adult brain, the expression pattern of the Id4/lacZ fusion protein in Id4 knockout brain was analysed, similar to the expression studies during embryogenesis. Coronal and sagital cryosections of $Id4^{+/+}$ and $Id4^{-/-}$ adult mouse brains were X-gal stained and then eosin Y counterstained. The wild-type cryosections served as a negative control for the X-gal

We note that without quantitative data reflecting the body and brain sizes of wild-type and Id4 knockout mice, it is possible that the decreased size of the Id4 knockout adult mouse brain reflects the reduced size of the Id4 knockout mouse compared to wild-type (figure 3.2).

staining (data not shown). The Id4/lacZ fusion protein was differentially expressed within the adult brain (figure 3.14 and data not shown). Figure 3.14A is a sagital brain section showing the areas where the Id4/lacZ fusion protein was expressed and the relative extent of expression in each area. The Id4/lacZ fusion protein was highly expressed in the caudate putamen, colliculus, septum, thalamus and hypothalamus (figure 3.14B and data not shown). Id4/lacZ protein expression was evident in a few, scattered cells in the cortex, cerebellum and hippocampus (figures 3.14C and D, and data not shown). In the cerebellum, the Id4/lacZ fusion protein was expressed specifically in Purkinje cells (figure 3.14D). To further analyse the expression of the Id4/lacZ fusion protein in the brain, the cryosections were counterstained with cresyl violet solution instead of eosin Y following X-gal staining. This showed that the Id4/lacZ fusion protein was expressed in a primarily overlapping manner with the cresyl violet stain, indicative of the expression of Id4 in cell bodies (figure 3.14E).

3.5.2 Decreased Size of the Id4 Knockout Adult Mouse Brain

Upon dissection, the Id4 mutant brain was evidently smaller than its wild-type counterpart (data not shown). Figure 3.15 shows equivalent brain sections from $Id4^{+/+}$ and $Id4^{-/-}$ mice made in sagital, coronal and horizontal orientations, which confirm the reduced size of the Id4 knockout brain in comparison to the wild-type brain. The size difference between the $Id4^{+/+}$ and $Id4^{-/-}$ mouse brains was most evident in the horizontal sections (figures 3.15G and H). The horizontal brain sections shown in figure 3.15 were used as a representation of the $Id4^{+/+}$ and $Id4^{-/-}$ brains, and the area of each brain region for $Id4^{+/+}$ and $Id4^{-/-}$ was quantified and compared (table 3.2). To quantify the area of each brain region, the pictures of the

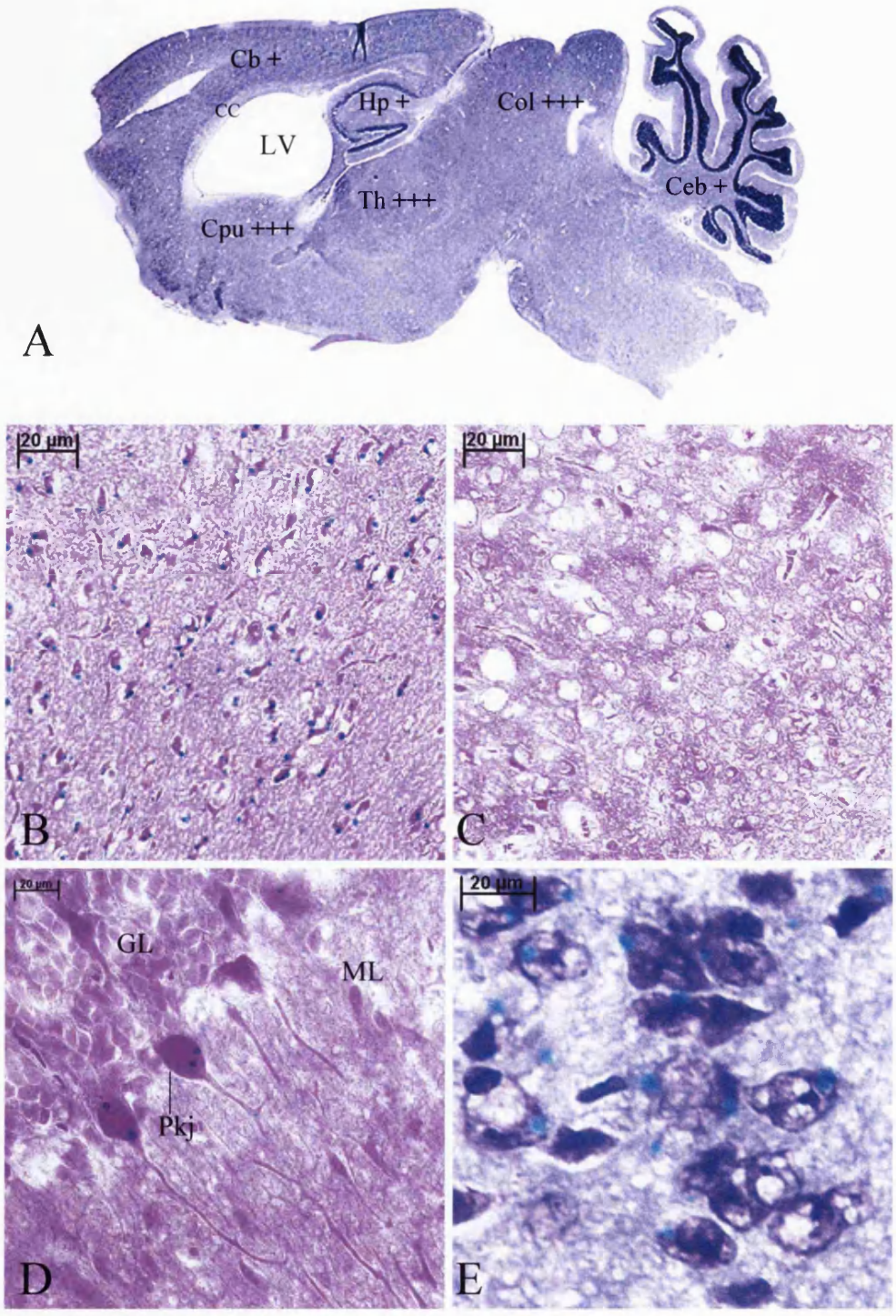

Figure 3.14 The Id4/lacZ fusion protein is differentially expressed within the adult mouse brain. X-gal staining on sagital cryosections of adult Id4$^{-/-}$ brain to show expression of the Id4/lacZ fusion protein. Eosin Y (pink; B-D) or cresyl violet (purple; E) counterstain following X-gal staining (blue). (A) A sagital section showing the regions and relative extent of Id4/lacZ protein expression in the brain. +++ → + represents lots → few cells expressing the Id4/lacZ fusion protein. B-D show Id4/lacZ fusion protein expression in the thalamus, cortex and Purkinje cells of the cerebellum respectively. Id4/lacZ protein expression is primarily overlapping with cell bodies in the brain (E). Cb, cerebral cortex; CC, corpus callosum; Ceb, cerebellum; Col, colliculus; CPu, caudate putamen; GL, granular layer; Hp, hippocampus; ML, molecular layer; Pkj, Purkinje cells; Th, thalamus.

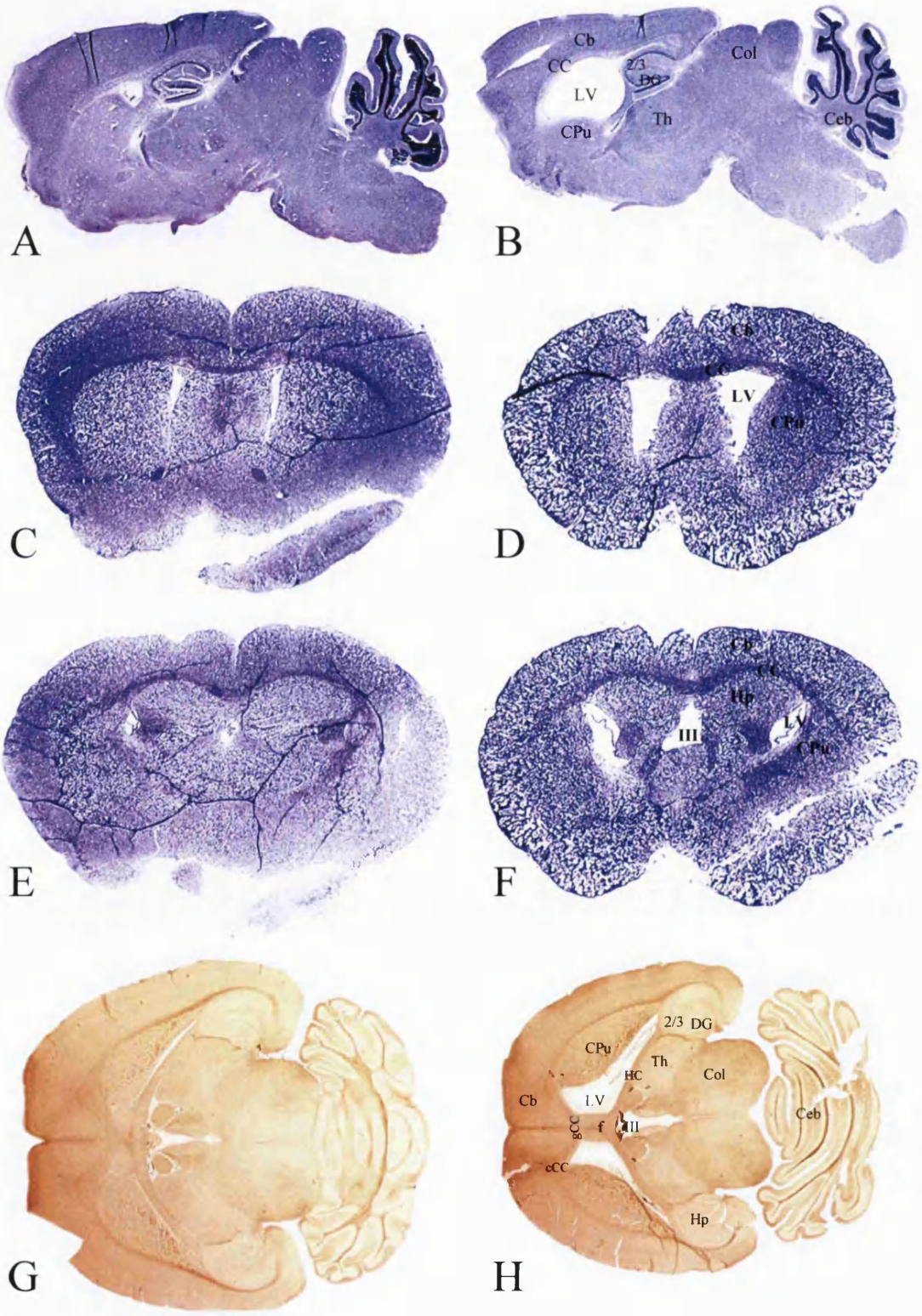

Figure 3.15 Reduced size of the Id4 knockout adult mouse brain. Equivalent sagital (A and B), coronal (C-F) and horizontal (G and H) brain sections from wild-type (A, C, E, G) and Id4 knockout (B, D, F, H) mice. 2/3, CA2/CA3 fields of hippocampus; Cb, cerebral cortex; CC, corpus callosum; cCC, cingulum of corpus callosum; gCC, genu of corpus callosum; Ceb, cerebellum; Col, colliculus; CPu, caudate putamen; DG, dentate gyrus; f, fornix; HC, hippocampal commisure; Hp, hippocampus; III, third ventricle; LV, lateral ventricle; Th, thalamus.

$Id4^{+/+}$ and $Id4^{-/-}$ horizontal brain sections were enlarged, overlaid on a 1 cm^2 grid on a light box and the area calculated.

	$Id4^{+/+}$ area (cm^2)	$Id4^{-/-}$ area (cm^2)	Ratio $Id4^{+/+}$: $Id4^{-/-}$
Cortex	103	72	1 : 0.70
Caudate putamen	30	26	1 : 0.86
Hippocampus	21	18	1 : 0.86
Septum	9	4.5	1 : 0.50
Thalamus	37	20	1 : 0.54
Colliculus	50	38	1 : 0.76

Table 3.2 The Id4 knockout ($Id4^{-/-}$) brain is smaller than the wild-type ($Id4^{+/+}$) brain. The horizontal brain sections shown in figure 3.15 were used to calculate the area of each brain region in the $Id4^{+/+}$ and $Id4^{-/-}$, and the ratio of $Id4^{+/+}$: $Id4^{-/-}$ areas is given.

Table 3.2 indicates that all regions of the brain in the $Id4^{-/-}$ are smaller than in the wild-type. The septum and the thalamus were the most affected regions of the homozygous Id4 mutant brain, which were approximately half the size of the same regions in the wild-type brain. The cortex and the colliculus of the $Id4^{-/-}$ brain were also significantly reduced in size compared to their $Id4^{+/+}$ counterparts. However, the caudate putamen and the hippocampus were only slightly smaller in the Id4 mutant brain than in the wild-type brain. It is noted that the observed area of a region in the brain is affected by the orientation that the section is made in. For example, although the caudate putamen was only slightly reduced in size when comparing horizontal brain sections (figures 3.15G and H, and table 3.2), it appears to be significantly reduced in size when sagital sections of $Id4^{+/+}$ and $Id4^{-/-}$ brains are compared (figures 3.15A and B). Therefore, the horizontal brain sections are used only as an indication of the size differences between $Id4^{+/+}$ and $Id4^{-/-}$ mice.

We note that the anti-N200 and anti-CNPase antibodies do not recognise the cell body of neurons and oligodendrocytes respectively. Therefore, there are limitations when using these antibodies to represent cell number in the brain. Hence, the differences in cell number between wild-type and Id4 knockout mice that are referred to in section 3.5.4 should be taken as tentative conclusions.

3.5.3 Abnormal Morphology of the Id4 Knockout Adult Mouse Brain

Detailed analysis of $Id4^{+/+}$ and $Id4^{-/-}$ brain sections revealed significant differences in morphology between the wild-type and Id4 mutant brains. In addition to the decreased size of the adult Id4 knockout brain, the lateral ventricles were greatly enlarged in the $Id4^{-/-}$ compared to the $Id4^{+/+}$ brain (figure 3.15). The 3rd and 4th ventricles were also larger in the Id4 mutant brain (figures 3.15E-H and data not shown).

3.5.4 Cellular Composition of the Id4 Knockout Adult Mouse Brain

Following the histochemical analysis, the cellular composition of the $Id4^{+/+}$ and $Id4^{-/-}$ brains was examined. The reduced size of the Id4 mutant brain indicates there is a reduction in the overall number of neurons, astrocytes and oligodendrocytes in the Id4 mutant brain compared to the wild-type. To analyse the brain at a cellular level, neurons, astrocytes and oligodendrocytes were specifically stained using mouse monoclonal antibodies for neurofilament 200 (N200), glial fibrillary acidic protein (GFAP) and 2',3'-cyclic nucleotide 3'-phosphodiesterase (CNPase) respectively. A fluorophore-labeled anti-mouse antibody was used for secondary detection, which was visualised as red fluorescence using fluorescence microscopy. In each experiment, a 'no primary' and a 'no secondary' antibody control was carried out, and the results of these are shown in each figure. Antibody staining was performed on serial horizontal brain sections following the horizontal $Id4^{+/+}$ and $Id4^{-/-}$ sections shown in figure 3.15. Therefore, neurons and glia are compared in the same region of the brain. Figure 3.15H illustrates the regions in the brain that are referred to in this section. The brightness/contrast of the $Id4^{-/-}$ pictures from N200 and CNPase staining

(figures 3.16 and 3.18) has been altered to account for photobleaching, which resulted from using high magnification and was worsened by the prolonged time required to find an equivalent region of the $Id4^{-/-}$ brain for comparison to the $Id4^{+/+}$. In consideration of this, the intensity of N200 and CNPase staining cannot be compared between $Id4^{+/+}$ and $Id4^{-/-}$.

3.5.4.1 Reduction in the Number of Neurons in the $Id4^{-/-}$ Brain is Proportional to the Reduction in Size of the Brain compared to the $Id4^{+/+}$

Figures 3.16A and B show N200 staining in the corpus callosum of wild-type and Id4 knockout brain respectively. As expected, the corpus callosum was smaller in the $Id4^{-/-}$ brain than in the $Id4^{+/+}$ brain, indicating a reduction in the overall number of neurons in the $Id4^{-/-}$ corpus callosum. N200 staining showed that the density of neurons in the $Id4^{+/+}$ and $Id4^{-/-}$ corpus callosum was the same, and therefore the reduction in neurons in the $Id4^{-/-}$ was in proportion to the reduction in size of the corpus callosum compared to the wild-type. Apart from in the corpus callosum (figures 3.16A and B), the size difference between the Id4 mutant and wild-type brains was not evident at the magnification required to analyse N200 staining. Figures 3.16C-L demonstrate that the density of $N200^{+}$ neurons throughout the brain was the same in the $Id4^{-/-}$ as in the $Id4^{+/+}$. Therefore, the reduction in neuronal cell number in the $Id4^{-/-}$ brain was simply in proportion to the reduction in size of the Id4 mutant brain compared to the wild-type.

N200 Staining of Neurons in the Adult Mouse Brain

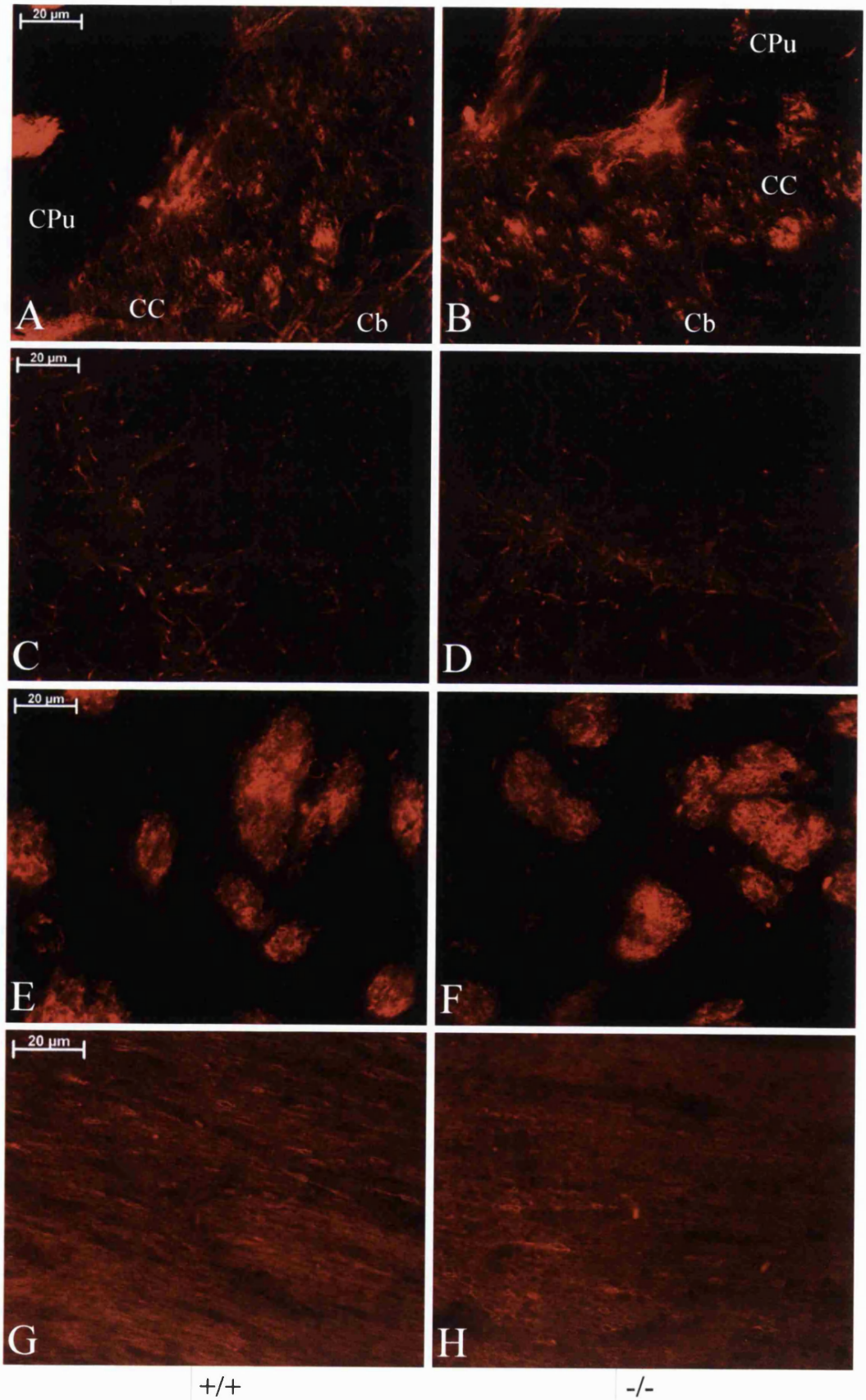

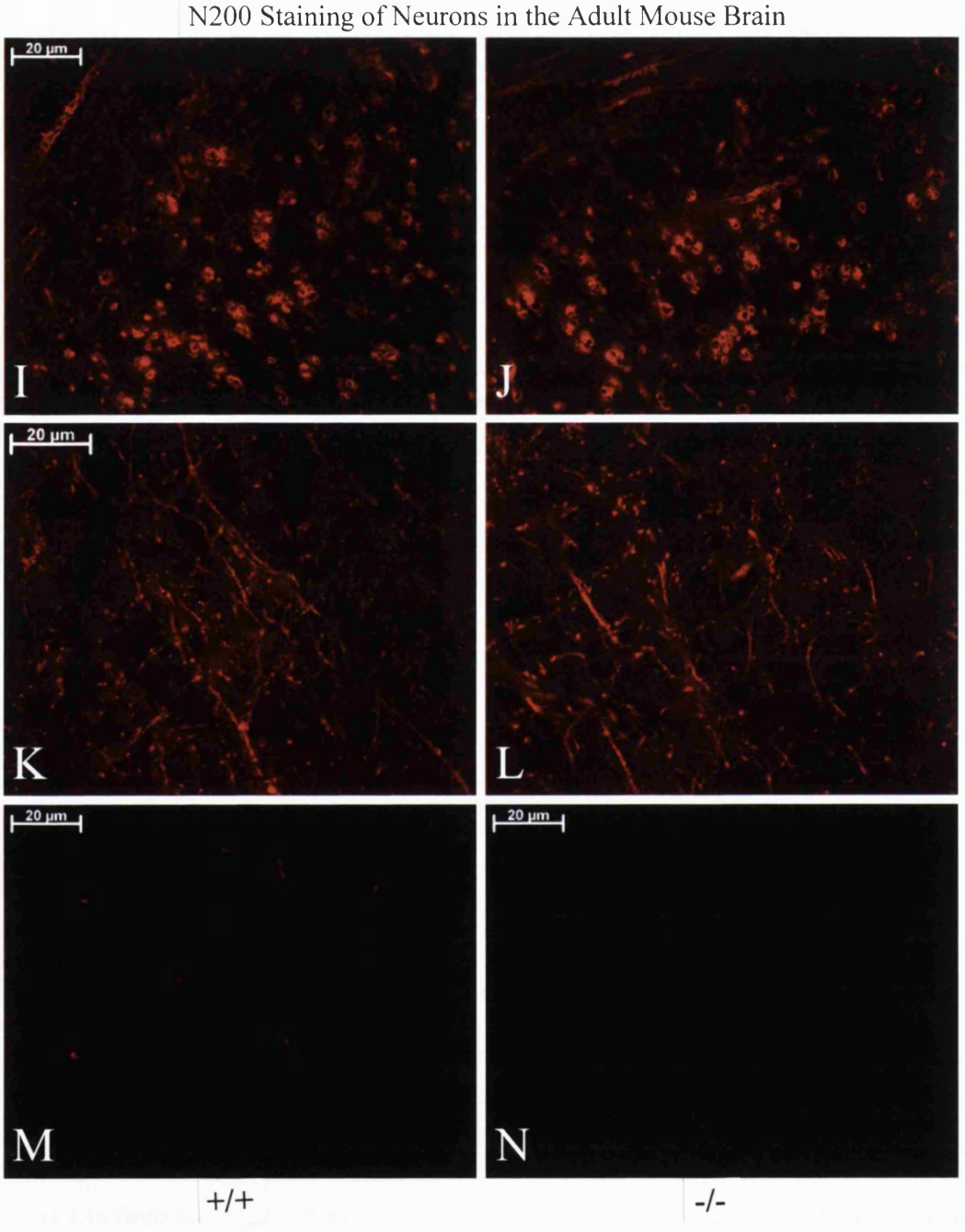

Figure 3.16 Reduction in the number of neurons in the $Id4^{-/-}$ brain is proportional to the reduction in size of the brain compared to the $Id4^{+/+}$. N200 staining of neurons in the corpus callosum (A and B), CA2 and CA3 fields of the hippocampus (C and D), caudate putamen (E and F), hippocampal commisure (G and H), colliculus (I and J) and cortex (K and L) of $Id4^{+/+}$ (A, C, E, G, I, K) and $Id4^{-/-}$ (B, D, F, H, J, L) brains. (M) and (N) show the 'no primary' and 'no secondary' antibody controls respectively. Note that the density of neurons is the same in the $Id4^{-/-}$ and $Id4^{+/+}$ brains. Cb, cerebral cortex; CC, corpus callosum; CPu, caudate putamen.

3.5.4.2 Reduction in the Number of Glia in the $Id4^{-/-}$ Brain is Disproportional to the Reduction in Size of the Brain compared to the $Id4^{+/+}$

GFAP and CNPase staining revealed that the reduction in glial cell number in the $Id4^{-/-}$ compared to $Id4^{+/+}$ brain was not in proportion to the reduction in size of the Id4 mutant brain (figures 3.17 and 3.18).

3.5.4.2.1 Astrocyte Cell Number is Disproportionally Reduced in the Id4 Knockout Brain

Figure 3.17 shows GFAP staining in comparative regions of the $Id4^{+/+}$ and $Id4^{-/-}$ brains, indicating the disproportional loss of astrocytes in the mutant brain. A clear reduction in $GFAP^{+}$ astrocytes was evident in the subgranular zone of the dentate gyrus, which was similar in size in the $Id4^{+/+}$ and $Id4^{-/-}$ brains (figures 3.17G and H). In addition, the CA2 and CA3 fields of the hippocampus (figures 3.17E and F), the genu and cingulum of the corpus callosum (figures 3.17A-D), the hippocampal commisure (figures 3.17I and J), the thalamus (figures 3.17K and L) and the colliulus (figures 3.17M and N) exhibited a reduction in astrocytes that was greater than the reduction in size of that region of the brain in the $Id4^{-/-}$ compared to the $Id4^{+/+}$. Notably, the intensity of GFAP staining appeared to be reduced in some astrocytes in the $Id4^{-/-}$ compared to $Id4^{+/+}$, as seen in the dentate gyrus (figures 3.17G and H). However, most astrocytes were brightly stained (figures 3.17E, F, I and J, insets) indicating that loss of Id4 resulted in a reduction in the number of astrocytes rather than a reduction in GFAP expression.

GFAP Staining of Astrocytes in the Adult Mouse Brain

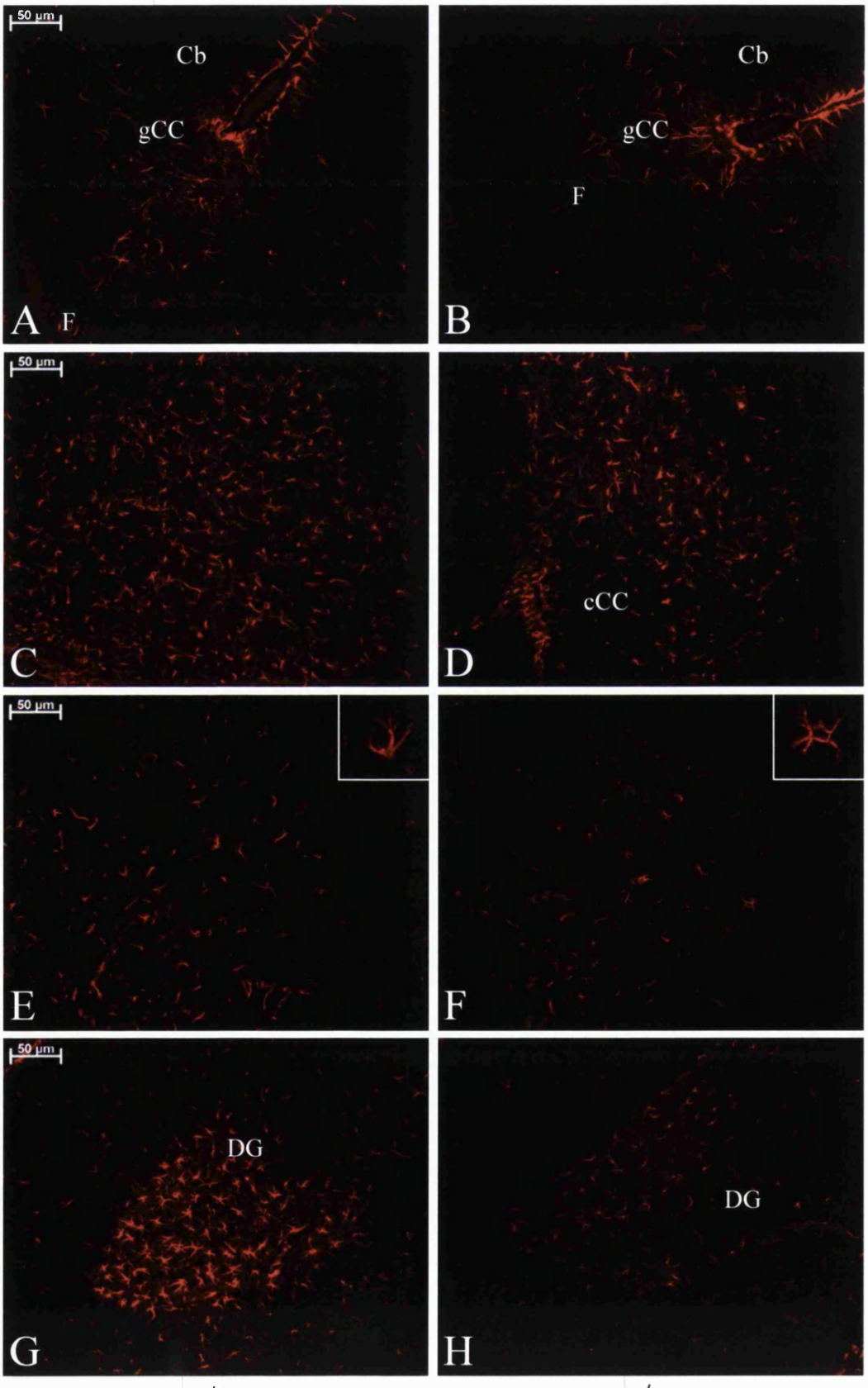

GFAP Staining of Astrocytes in the Adult Mouse Brain

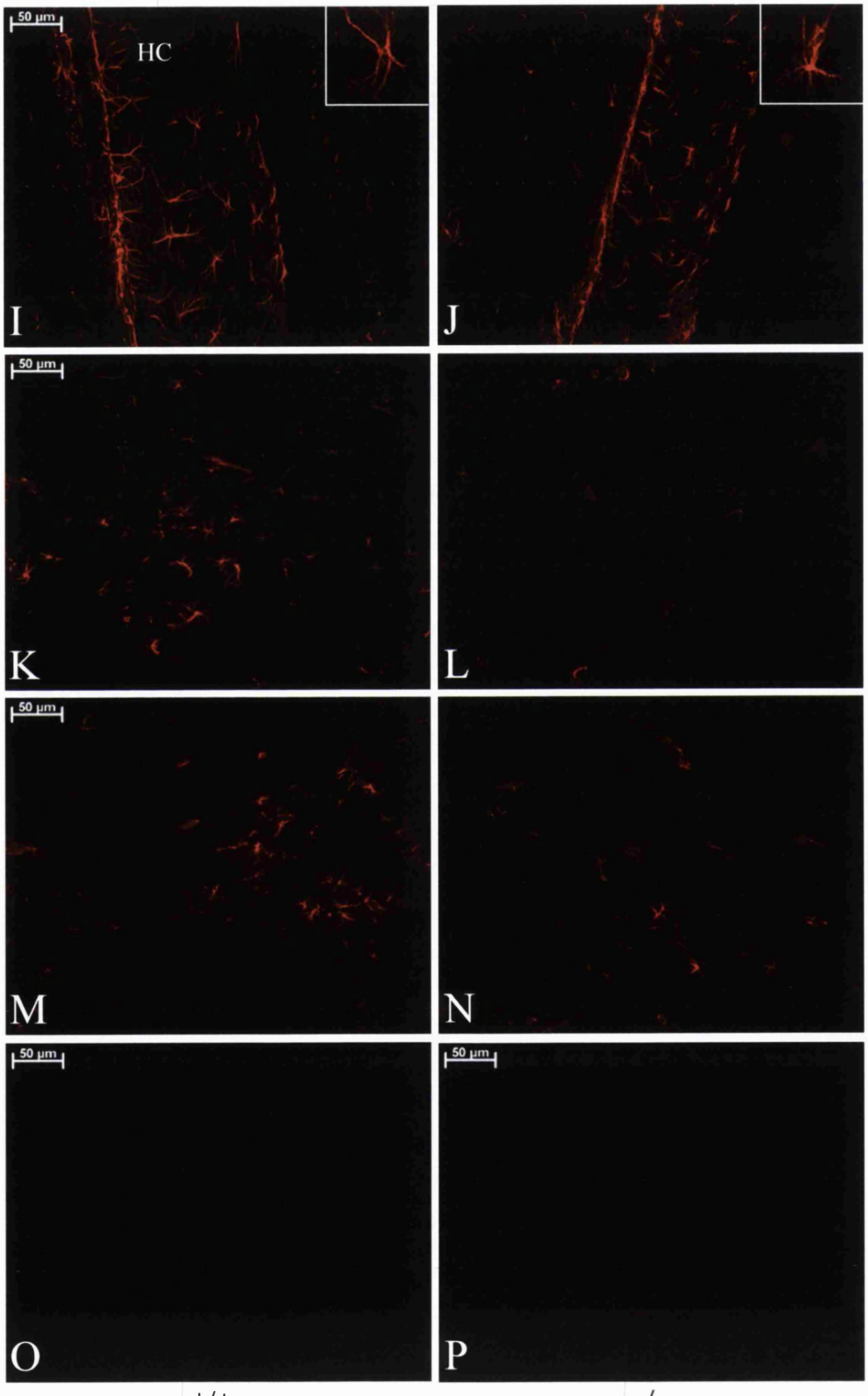

Figure 3.17 Reduction in the number of astrocytes in the $Id4^{-/-}$ brain is disproportional to the reduction in size of the brain compared to the $Id4^{+/+}$. GFAP staining of astrocytes in the genu of corpus callosum (A and B), cingulum of corpus callosum (C and D), CA2 and CA3 fields of the hippocampus (E and F), dentate gyrus (G and H), hippocampal commisure (I and J), thalamus (K and L) and colliculus (M and N) of $Id4^{+/+}$ (A, C, E, G, I, K, M) and $Id4^{-/-}$ (B, D, F, H, J, L, N) brains. (O) and (P) show the 'no primary' and 'no secondary' antibody controls respectively. Note that in addition to the reduction in astrocytes in the $Id4^{-/-}$ due to the reduction in brain size, the density of astrocytes in a given area is reduced in the $Id4^{-/-}$ compared to the $Id4^{+/+}$. Cb, cerebral cortex; cCC, cingulum of corpus callosum; CC, corpus callosum; DG, dentate gyrus; F, fornix; gCC, genu of corpus callosum; HC, hippocampal commisure.

3.5.4.2.2 Oligodendrocyte Cell Number is Disproportionally Reduced in the Id4 Knockout Brain

Figure 3.18 shows CNPase staining in the brain of $Id4^{+/+}$ and $Id4^{-/-}$ mice. In the corpus callosum for example, there is a reduction in the overall number of oligodendrocytes in the $Id4^{-/-}$ compared to $Id4^{+/+}$ due to the difference in size (figures 3.18C and D). CNPase staining showed there was also a significant reduction in the density of oligodendrocytes in the $Id4^{-/-}$ corpus callosum compared to the $Id4^{+/+}$ (figures 3.18A-D). Therefore, the number of oligodendrocytes was greatly reduced in the $Id4^{-/-}$ corpus callosum compared to the wild-type. A disproportional reduction in the number of oligodendrocytes was also evident in the hippocampus, caudate putamen, septum, thalamus, colliculus and cortex of the $Id4^{-/-}$ brain (figures 3.18E-L and data not shown). Even the $Id4^{-/-}$ caudate putamen, which was only marginally smaller than its $Id4^{+/+}$ counterpart, exhibited a drastic reduction in oligodendrocytes, again demonstrating the disproportional reduction of oligodendrocytes in the Id4 mutant brain (figures 3.18G and H).

3.5.5 No Differences in Apoptosis between Id4 Knockout and Wild-type Adult Mouse Brains

Immunohistochemical analysis indicated a reduction in the density of astrocytes and oligodendrocytes in the $Id4^{-/-}$ brain compared to the $Id4^{+/+}$. To determine if these observations could be explained by increased apoptosis in the brain of Id4 knockout mice, sections of $Id4^{+/+}$ and $Id4^{-/-}$ brains were examined for evidence of apoptotic cells. In the apoptosis assay, fragmented DNA is labelled with fluorescein-12-dUTP using the principal of TUNEL, and is evident as localised green fluorescence using direct fluorescence microscopy. Propidium iodide is then used to stain all cells (apoptotic and non-apoptotic) in the section, and is visualised as red fluorescence by

CNPase Staining of Oligodendrocytes in the Adult Mouse Brain

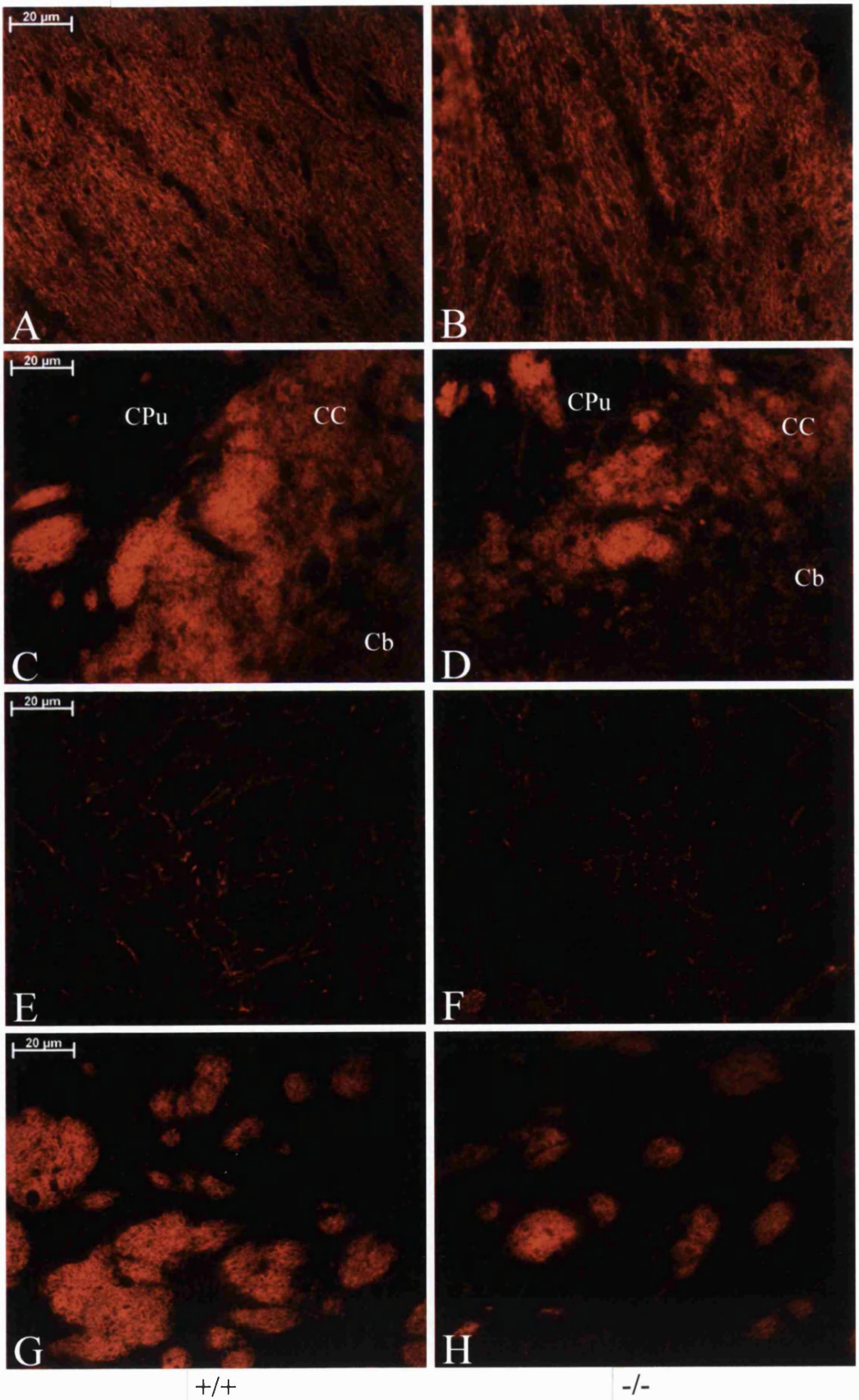

CNPase Staining of Oligodendrocytes in the Adult Mouse Brain

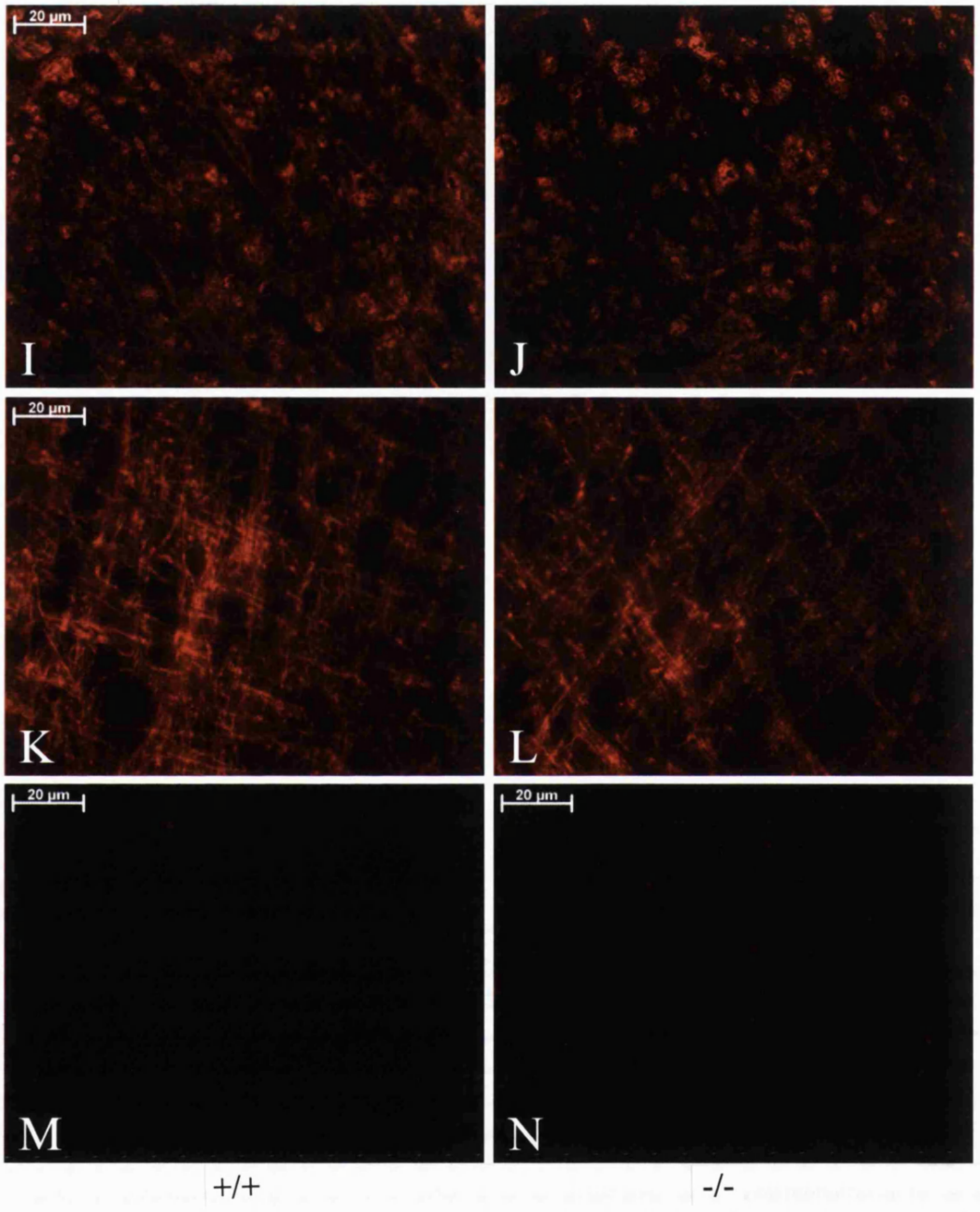

Figure 3.18 Reduction in the number of oligodendrocytes in the $Id4^{-/-}$ brain is disproportional to the reduction in size of the brain compared to the $Id4^{+/+}$. CNPase staining of oligodendrocytes in the corpus callosum (A-D), CA2/CA3 fields of the hippocampus (E and F), caudate putamen (G and H), colliculus (I and J) and cortex (K and L) of $Id4^{+/+}$ (A, C, E, G, I, K) and $Id4^{-/-}$ (B, D, F, H, J, L) brains. (M) and (N) show the 'no primary' and 'no secondary' antibody controls respectively. Note that in addition to the reduction in oligodendrocytes in the $Id4^{-/-}$ due to the reduction in brain size, the density of oligodendrocytes in a given area is reduced in the $Id4^{-/-}$ compared to the $Id4^{+/+}$. Cb, cerebral cortex; CC, corpus callosum; CPu, caudate putamen.

direct fluorescence microscopy. Therefore, co-localisation of these two fluorochromes results in a yellow colour that is indicative of apoptotic cells. A positive and a negative control for this assay were included (figures 3.19A and B). As can be seen in figures 3.19A and B respectively, no apoptosis was evident in the negative control, which had no TdT enzyme in the TUNEL reaction, and extensive apoptosis was observed in the positive control, which was treated with DNaseI prior to the TUNEL reaction. Apoptosis in the wild-type adult brain was minimal, and there was no evidence of increased apoptosis in any region of the brain in the $Id4^{-/-}$ compared to the $Id4^{+/+}$ (figures 3.19C-H and data not shown). For example, figures 3.19C and D, E and F, and G and H, show the results for the $Id4^{+/+}$ and $Id4^{-/-}$ cortex, caudate putamen and colliculus respectively.

3.6 Id4 Knockout Neural Stem Cells

The results described in this section were prepared in collaboration with Dr Toru Kondo at The Department of Cell Fate Modulation, Kumamoto University, Japan. The reduction in size of the $Id4^{-/-}$ brain suggested that the proliferation capacity of $Id4^{-/-}$ NSCs might be reduced, resulting in a reduction in both neurons and glia. The disproportional reduction in glial cell number in the $Id4^{-/-}$ brain suggests that glial precursors lacking Id4 also have reduced proliferation capacity. To address these points, NSCs from the ventricular and subventricular zone of $Id4^{+/+}$ and $Id4^{-/-}$ adult brains were isolated and analysed in culture.

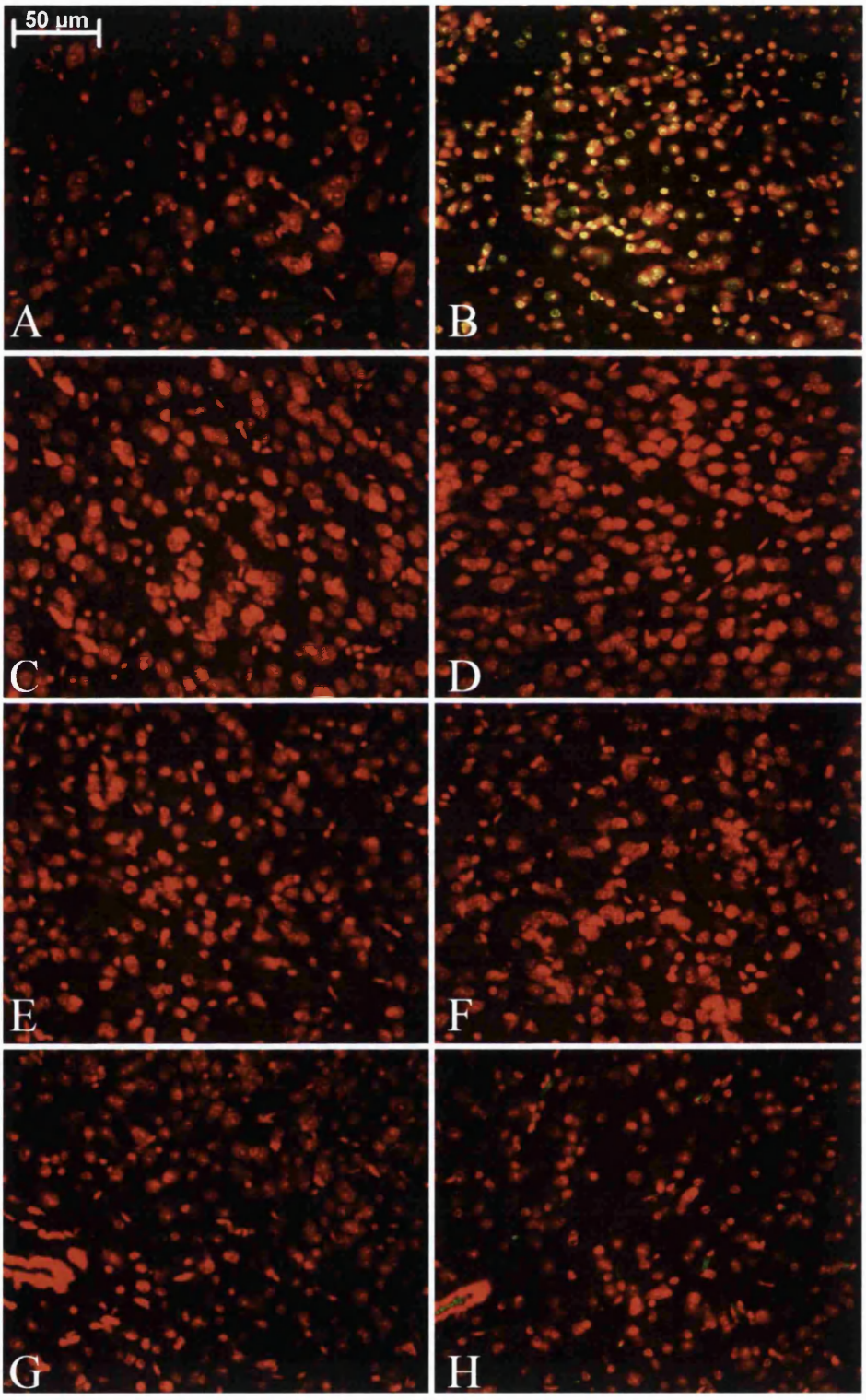

Figure 3.19 No differences in apoptosis between $Id4^{+/+}$ and $Id4^{-/-}$ adult brains. $Id4^{+/+}$ and $Id4^{-/-}$ brain sections were assayed for apoptosis using the Apoptosis Detection System, Fluorescein (Promega). Fragmented nuclear DNA was labelled with fluorescein-12-dUTP by TUNEL and visualised as green using direct fluorescence microscopy. All nuclei were counterstained red with propidium iodide. Images were overlaid and apoptotic cells indicated by yellow. Results for the cortex (C and D), caudate putamen (E and F) and colliculus (G and H) of $Id4^{+/+}$ (C, E, G) and $Id4^{-/-}$ (D, F, H) brains are shown. (A) and (B) show negative and positive controls respectively.

3.6.1 Reduced Proliferation Capacity of Id4 Knockout Neural Stem Cells

Wild-type and $Id4^{-/-}$ NSCs expressed both nestin and microtubule associated protein 2 (MAP2; figure 3.20), which are markers for early neural precursor cells (Lendahl *et al.*, 1990). NSCs were cultured in the presence of bFGF and EGF to examine their proliferation capacity. In contrast to wild-type NSCs, which proliferated well and produced big spheres, Id4 knockout NSCs grew poorly. Even in the presence of conditional medium including cystatin C, which is secreted by NSCs and accelerates their growth, $Id4^{-/-}$ NSCs did not grow well (data not shown). To quantify the reduced proliferation capacity of $Id4^{-/-}$ compared to $Id4^{+/+}$ NSCs, NSCs were pulsed with bromodeoxyuridine (BrdU) for 6 hours and then stained with anti-BrdU antibody. Only 25 % of $Id4^{-/-}$ NSCs incorporated BrdU compared to 54 % of wild-type NSCs (figure 3.21). To confirm that the proliferation defect was due to the lack of Id4, $Id4^{-/-}$ NSCs were infected with a retroviral vector expressing Id4 (Id4 v), and then BrdU incorporation was measured. As shown in figure 3.21, ectopic expression of Id4 in $Id4^{-/-}$ NSCs reverted their proliferation capacity to that of wild-type NSCs, indicating that Id4 is a key regulator of NSC proliferation.

3.6.2 Id4 is a Crucial Factor in Glial Cell Development

NSCs are multipotent and have the potential to generate neurons, astrocytes and oligodendrocytes. $Id4^{-/-}$ NSCs were examined for their ability to differentiate into neurons and glia compared to $Id4^{+/+}$ NSCs. NSCs differentiate into neurons in response to platlet-derived growth factor (PDGF), and anti-middle molecular weight neurofilament protein (anti-NFM) antibody stains neurons in culture. 47 % of $Id4^{+/+}$ and 43 % of $Id4^{-/-}$ NSCs differentiated into NFM^{+} neurons when cultured in medium

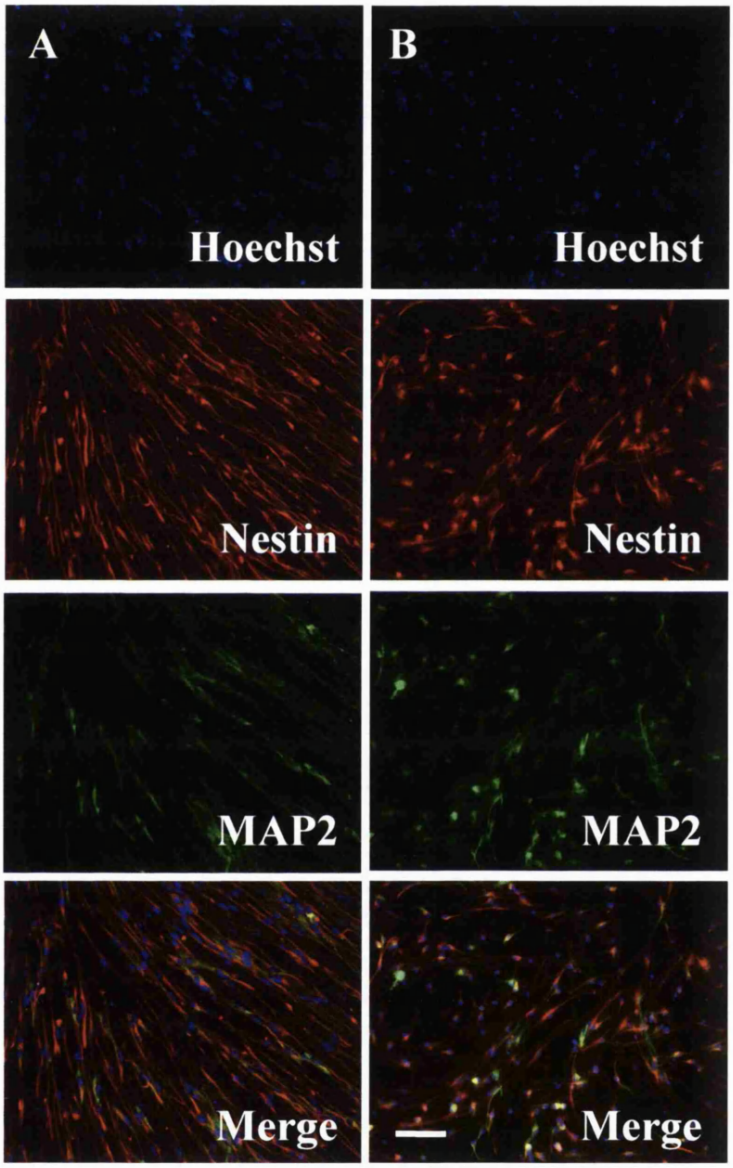

Figure 3.20 Wild-type (Wild; A) and Id4 knockout (Id4-/-; B) NSCs in culture express both nestin and MAP2, which are markers of early neural precursor cells. Cell nuclei were stained with Hoechst dye. The merged images for wild-type and Id4 knockout are shown at the bottom of each panel. Scale bar 25 μm. Figure kindly provided by Dr Toru Kondo.

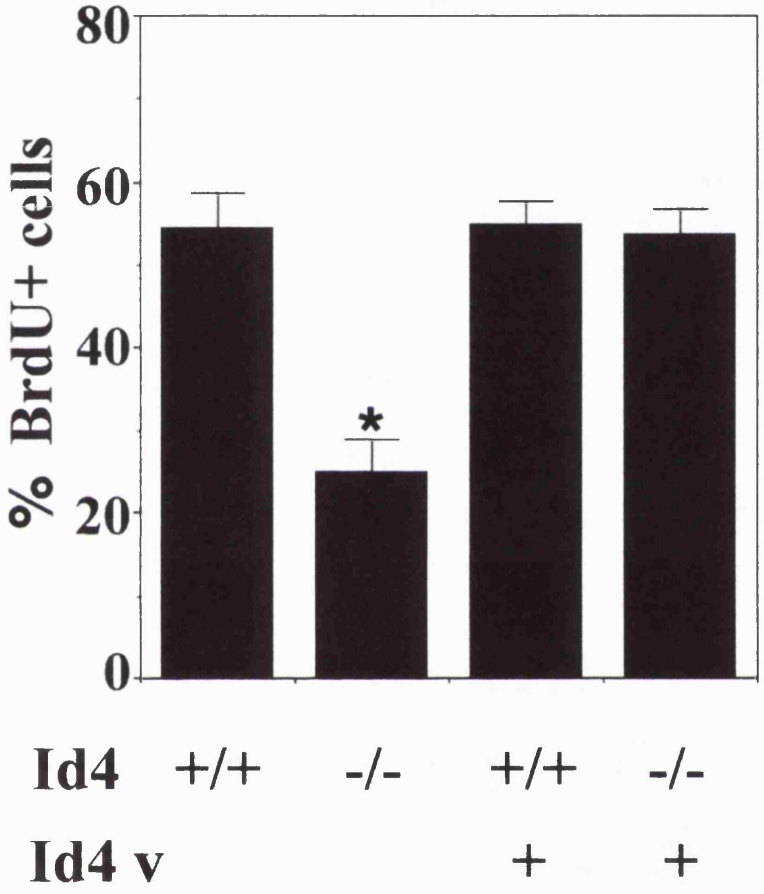

Figure 3.21 Id4 is a key intracellular regulator of NSC proliferation. The proliferation capacity of wild-type (+/+) and Id4 knockout (-/-) NSCs was quantified by analysing BrdU incorporation. Id4 v indicates the presence (+) of a retroviral vector expressing Id4 in wild-type and Id4 knockout NSCs. * indicates $p < 0.01$. Figure kindly provided by Dr Toru Kondo.

including PDGF (data not shown). Therefore, the ability of NSCs to differentiate into neurons is unaffected by the absence of Id4, indicating that Id4 is not involved in the regulation of neuronal development. To analyse oligodendrocyte differentiation, wild-type and Id4 knockout NSCs were cultured in the presence of TH and Shh, which promote oligodendrocyte development by NSCs. The cultures were then stained with anti-galactocerebroside (anti-GC) antibody, which is a marker of mature oligodendrocytes. After 2 days, 0 % and 31.5 % of $Id4^{+/+}$ and $Id4^{-/-}$ NSCs respectively had differentiated into GC^{+} oligodendrocytes (figures 3.22 and 3.23A). At 4 days, 9 % of $Id4^{+/+}$ and 41 % of $Id4^{-/-}$ NSCs had differentiated into GC^{+} cells (data not shown). This data indicates that $Id4^{-/-}$ NSCs prematurely differentiate into GC^{+} oligodendrocytes. To examine the ability of Id4 mutant NSCs to differentiate into astrocytes, wild-type and mutant NSCs were cultured in the presence of either BMP2/4 or CNTF, which promote astrocyte differentiation. In the presence of BMP2/4, 72 % of $Id4^{-/-}$ NSCs had differentiated into $GFAP^{+}$ astrocytes within 2 days, compared to 3 % of wild-type NSCs (figure 3.23B). Accelerated astrocyte differentiation by $Id4^{-/-}$ NSCs was already apparent after 24 hours in the presence of BMP2 (figure 3.24). At 4 days, 89 % and 74 % of $Id4^{-/-}$ and $Id4^{+/+}$ NSCs respectively had differentiated into $GFAP^{+}$ astrocytes (data not shown). Premature astrocyte differentiation by $Id4^{-/-}$ NSCs was not observed in the presence of CNTF (figure 3.23B). These findings suggest that Id4 negatively regulates the BMP signalling pathway, but not the signalling pathway activated by CNTF. Taken together, the *in vitro* data suggests that Id4 is not only an important regulator of NSC proliferation, but is also a crucial factor for normal glial cell development.

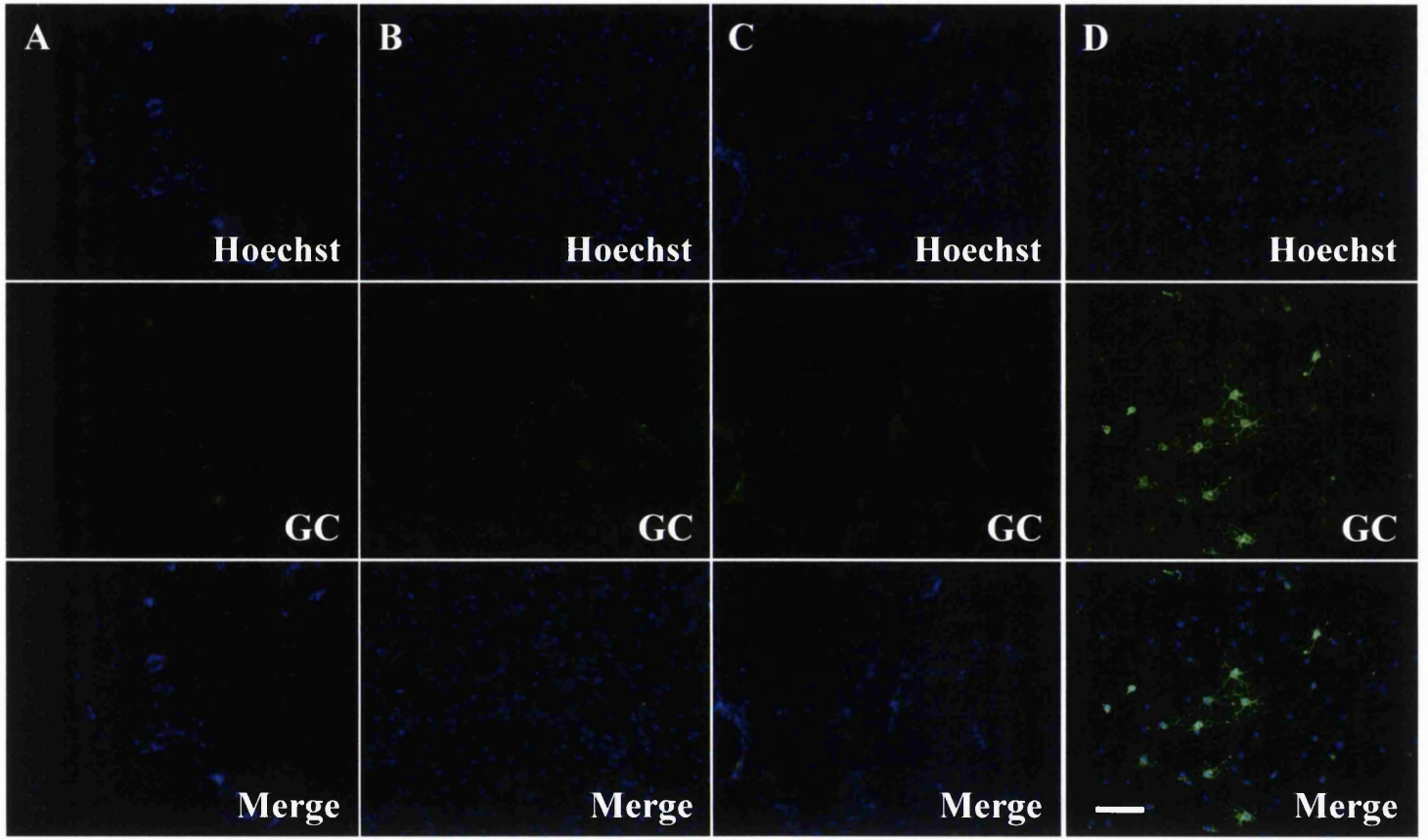

Figure 3.22 Id4 knockout NSCs prematurely differentiate into oligodendrocytes compared to wild-type NSCs. Wild-type (Wild; A and B) and Id4 knockout (Id4-/-; C and D) cultures were stained with anti-GC antibody at 0 hours (A and C) and 48 hours (B and D) after addition of TH and Shh, which promote oligodendrocyte differentiation. Hoechst dye was used to stain all nuclei and the merged images are shown at the bottom of each panel. Scale bar 25 μm. Figure kindly provided by Dr Toru Kondo.

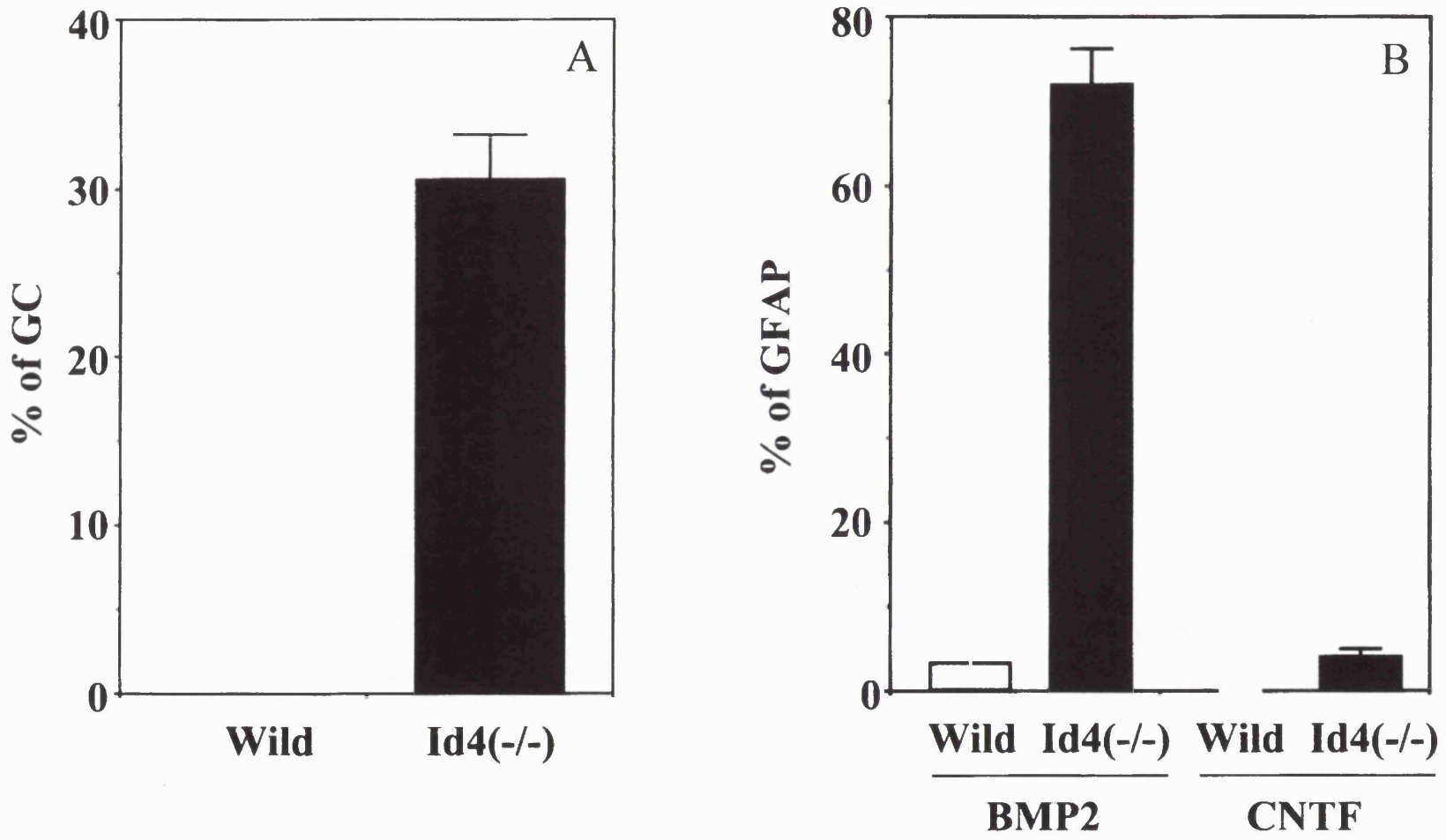

Figure 3.23 Id4 is an important regulator of glial cell development. (A) % wild-type (Wild) and Id4 knockout (Id4-/-) NSCs that differentiated into GC^+ oligodendrocytes after 48 hours in the presence of TH and Shh. (B) % wild-type (Wild) and Id4 knockout (Id4-/-) NSCs that differentiated into $GFAP^+$ astrocytes after 48 hours in the presence of BMP2 or CNTF. Figure kindly provided by Dr Toru Kondo.

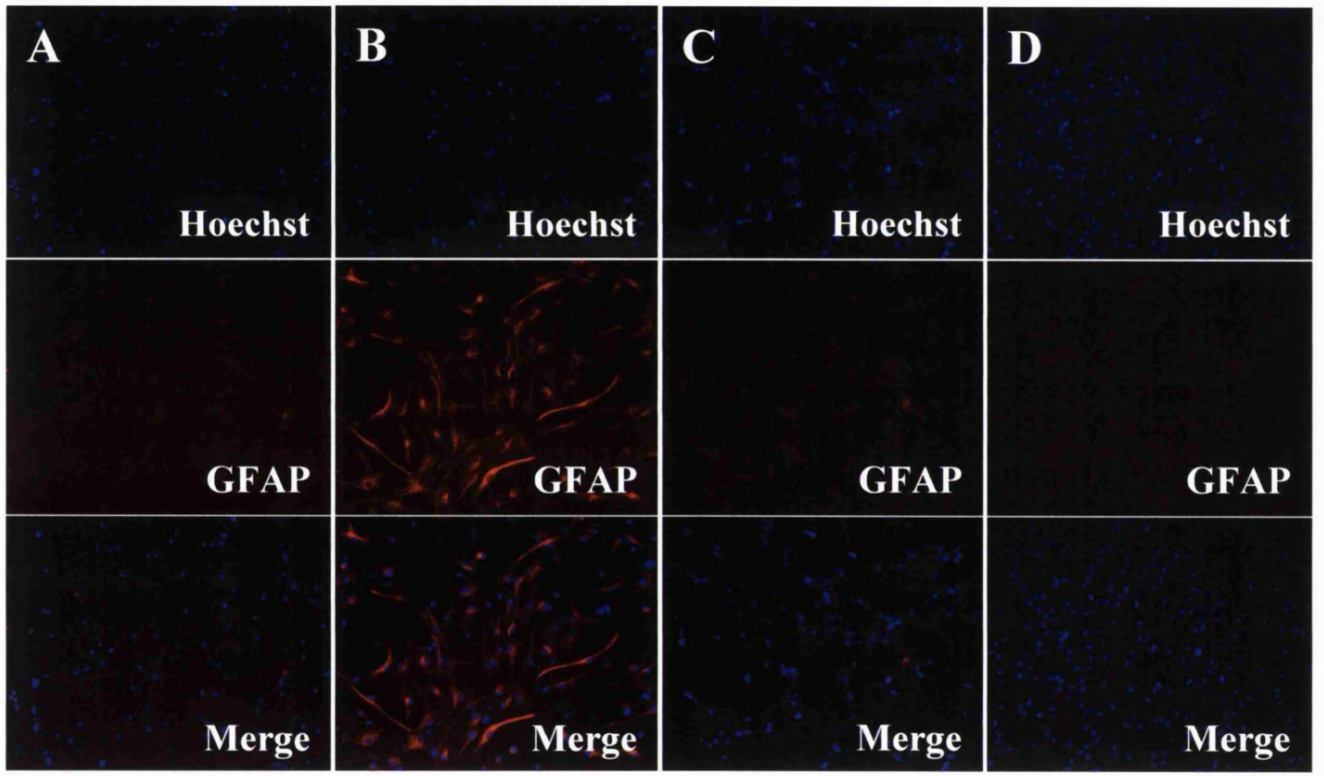

Figure 3.24 Id4 knockout NSCs prematurely differentiate into astrocytes compared to wild-type NSCs. Wild-type (Wild; C and D) and Id4 knockout (Id4-/-; A and B) cultures were stained with anti-GFAP antibody at 0 hours (A and C) and 24 hours (B and D) after addition of BMP2, which induces astrocyte differentiation. Hoechst dye was used to stain all nuclei and the merged images are shown at the bottom of each panel. Scale bar 25 μm.
Figure kindly provided by Dr Toru Kondo.

Chapter 4

Discussion

Id4 is a Key Intracellular Regulator of Neural Stem Cell Proliferation and Glial Cell Development

4.1 Id4 is Necessary for the Normal Development of Mice

Here we have shown that Id4 is necessary for the normal development of mice (chapter 3). Approximately 50 % of Id4 knockout mice died either in utero or during the early postnatal period before weaning. In general, there were no obvious differences between wild-type, heterozygous and homozygous Id4 mutant embryos up to 14.5 dpc, which was the last time point analysed, suggesting that Id4 null mice die sometime during late foetal and early postnatal life. In addition, Id4 knockout mice died during their development following weaning and in adulthood. These mice exhibited a similar significant weight loss over approximately three weeks before death. The reason for death of Id4 knockout mice remains to be determined. The growth of homozygous Id4 mutant mice was retarded compared to wild-type and heterozygous Id4 mutant mice, and the adult Id4 knockout mice were evidently smaller. Id2 knockout mice also show retarded growth, and are smaller than their adult wild-type counterparts (Yokota *et al.*, 1999), suggesting that functions of Id2 and Id4 are important for the normal development of mice. Id1- and Id3-deficient mice exhibit normal growth (Yan *et al.*, 1997a; Pan *et al.*, 1999). Id4 knockout mice surviving to adulthood appeared to be healthy and showed normal activity, but

exhibited abnormal brain morphology with an overall reduction in both neurons and glia. Neural stem cells (NSCs) lacking Id4 had a reduced proliferation capacity *in vitro*, which may explain the fewer numbers of both neuronal and glial cells in the adult $Id4^{-/-}$ brain, and consequently the smaller brain size and abnormal brain morphology. The reduction in the number of glia in the adult $Id4^{-/-}$ brain was disproportional to the reduction in size of the brain compared to the wild-type, but neurons were reduced proportionally, suggesting that glial cell development was affected by the absence of Id4. Furthermore, $Id4^{-/-}$ NSCs prematurely differentiated into astrocytes and oligodendrocytes, whereas neuronal differentiation was unaffected. Together, the results indicate that Id4 is an important intracellular factor regulating NSC proliferation and glial cell development.

4.2 Id4/lacZ Fusion Protein Expression Reflects that of the Id4 mRNA During Mouse Embryogenesis

The patterns of mRNA expression of all of the Id genes during mouse embryogenesis have been well documented (Duncan *et al.*, 1992; Wang *et al.*, 1992; Evans and O'Brien, 1993; Neuman *et al.*, 1993; Nagata and Todokoro, 1994; Riechmann *et al.*, 1994; Riechmann and Sablitzky, 1995; Jen *et al.*, 1996, 1997). Although this provides an indication of the developmental functions of the dnHLH proteins, the expression of mRNA may not be indicative of the presence of functional protein. In this work, we characterised the expression pattern of the Id4 protein during embryonic development by analysing the expression of the Id4/lacZ fusion protein in Id4 mutant mice. In general, the spatiotemporal pattern of Id4/lacZ protein expression reflected the previously reported Id4 mRNA expression data. Expression of the Id4/lacZ fusion protein was upregulated during embryogenesis and was mainly

restricted to specific areas of the developing central and peripheral nervous system. In previous studies, Id4 mRNA expression was first detectable at 9.5 dpc (Riechmann *et al.*, 1994; Jen *et al.*, 1996, 1997). However, Id4/lacZ protein expression was evident at low levels at day 8.5, indicating that Id4 is upregulated in the embryo from around 8.5 dpc. Taken together, the results suggest that, in general, the expression of Id4 mRNA is indicative of the presence of Id4/lacZ protein.

4.2.1 Id4/lacZ Fusion Protein Expression in the Developing Nervous System and Sensory Organs

Two papers have described the pattern of Id4 mRNA expression in the developing nervous system of the mouse, using *in situ* hybridisation on serial sections of mouse embryos (Riechmann and Sablitzky, 1995; Jen *et al.*, 1997), and the expression of the Id4/lacZ fusion protein exhibited a similar pattern to that described for the Id4 mRNA transcript. For example, in the developing telencephalon, Id4 mRNA expression is first detectable at low levels at 9.5 dpc. Expression of Id4 mRNA is dramatically upregulated from day 9.5, and transcripts are highly expressed in the telencephalon between 10 and 14.5 dpc. In a similar pattern, Id4/lacZ fusion protein expression was first detectable at low levels in the telencephalon at 9.5 dpc (figure 3.3). Expression was significantly upregulated between 9.5 and 10.5 dpc (figures 3.3 and 3.4), and the Id4/lacZ protein was highly expressed between 10.5 and 14.5 dpc (figures 3.4, 3.6 and 3.8), which was the last time point in the fusion protein expression analysis. Notably, sections of stained 10.5 and 14.5 dpc Id4 mutant embryos revealed that the area of the telencephalon expressing the Id4/lacZ fusion protein was the same as that which expressed Id4 mRNA (figures 3.12 and 3.13; Riechmann and Sablitzky, 1995; Jen *et al.*, 1997). Jen *et al.* (1997) described a similar change from ventral to dorsal expression for Id4 mRNA to that which was

evident for the Id4/lacZ fusion protein between 10.5 and 14.5 dpc of spinal cord development (figures 3.4, 3.6 and 3.8), except Id4 mRNA expression was still detectable in the motor neuron column at 14.5 dpc, whereas fusion protein expression appeared to be restricted to the dorsal, future substantia gelatinosa. Although the expression pattern of the Id4/lacZ protein reflects that of the Id4 mRNA in the majority of the developing CNS, the temporal expression of the fusion protein and Id4 mRNA in the diencephalon do not correlate throughout brain development. The *in situ* hybridisation analyses showed Id4 mRNA expression in the diencephalon at 11.5 and 12.5 dpc, and then in the thalamus at 14.5 and 16.5 dpc (Riechmann and Sablitzky, 1995; Jen *et al.*, 1997). The Id4/lacZ fusion protein was highly expressed in the diencephalon at 10.5 dpc (figures 3.4 and 3.12), but the expression of the fusion protein in this region was decreased at 12.5 dpc (figure 3.6), and no expression of the Id4/lacZ protein was detectable in the thalamus at 14.5 dpc (figure 3.13). This suggests that Id4 expression may be regulated at the post-transcriptional level in this region of the brain. Differences between the Id4 mRNA and Id4/lacZ fusion protein expression data may also be due to differences in the sensitivity of the detection techniques.

In the developing PNS, Id4/lacZ protein expression was found in cells of the V, VII, VIII, IX and X sensory cranial ganglia (figures 3.4-3.10), and in the dorsal root ganglia (figures 3.6-3.10), which is supported by expression of Id4 mRNA in these parts of the PNS (Riechmann and Sablitzky, 1995; Jen *et al.*, 1997). The Id4/lacZ fusion protein was also expressed in dorsal root sensory nerves and spinal nerves (figures 3.6 and 3.8-3.10), which has not previously been reported. The sensory cranial ganglia that express Id4 are derived from neural crest cells and cells of the epibranchial placodes, and the origin of the cells expressing Id4 is not known at the

present time. Since the remaining craniofacial ganglia are derived from only neural crest, it is tempting to speculate that these cells are placodal in origin.

The Id4/lacZ fusion protein was clearly expressed in the developing eye at 12.5 and 14.5 dpc (figures 3.6-3.9). This expression is probably in the neural layer of the optic cup, which has been shown to exhibit Id4 mRNA expression at these stages of development (Jen *et al.*, 1997). Expression of the fusion protein was also detected in the optic (II) nerve (figures 3.9E). In the developing nose, the Id4/lacZ fusion protein was highly expressed in the sensory olfactory (I) nerves (figure 3.9D), and embryo sections showed that the Id4/lacZ protein was also expressed in the post-mitotic olfactory neuroepithelium at 14.5 dpc (figure 3.10D), reflecting the pattern that was described for the Id4 mRNA by Jen *et al.* (1997).

4.2.2 Id4/lacZ Fusion Protein Expression in Other Regions of the Developing Embryo

Id4/lacZ fusion protein expression was found in several other tissue types in addition to the nervous system during embryogenesis, including the dorsal aorta, heart, stomach, vibrissae and skin (figures 3.3-3.10). Id4 mRNA expression has been described in the vibrissae, although this was first evident at 16.5 dpc (Jen *et al.*, 1996), whereas expression of the Id4/lacZ protein was evident in the vibrissae from 12.5 dpc. Id4/lacZ fusion protein expression was detected in the ventral part of the developing stomach, similar to that described for the Id4 mRNA (Jen *et al.*, 1996), but the Id4/lacZ protein was also expressed in the dorsal region of the developing stomach. To date, Id4 mRNA expression in the dorsal aorta, heart and skin has not been described. Therefore, Id4/lacZ fusion protein expression in these regions of the

developing embryo suggests novel regions where Id4 may also be expressed during embryogenesis.

4.3 Id4/lacZ Fusion Protein is Differentially Expressed Within the Adult Mouse Brain

Although studies have shown that Id1-Id4 mRNAs are expressed in the adult mouse brain (Riechmann *et al.*, 1994), their patterns of expression within the brain have not been fully documented. Id2 is expressed in Purkinje cells of the adult cerebellum, and in layers II/III and V of the cerebral cortex (Tzeng and de Vellis, 1998). Here we describe the expression pattern of the Id4/lacZ fusion protein in the adult Id4 knockout mouse brain as an indication of the pattern of Id4 protein expression within the brain (figure 3.14 and data not shown). Id4/lacZ protein expression was high in the caudate putamen, colliculus, septum, thalamus and hypothalamus of the adult brain. The Id4/lacZ fusion protein was also expressed at low levels in the cortex and hippocampus, and was in the Purkinje cells of the cerebellum.

4.4 Id4 has a Key Role in Nervous System Development

The fact that Id4 expression is largely restricted to the nervous system during embryogenesis, whereas that of Id1-Id3 is in multiple tissues, suggests that Id4 is an important factor regulating proliferation and differentiation of the nervous system. Id4 is also expressed in the adult brain. In light of the expression data, and the studies on Ids in neural cells in culture (section 1.2.3.2), the analysis of Id4 knockout mice focused on the brain.

4.4.1 Defects in the Brain of Adult Id4 Knockout Mice

Id4 knockout mice that reached adulthood exhibited a drastic alteration in brain morphology. A reduction in brain size compared to wild-type was accompanied by significantly larger ventricles (figure 3.15). Although a reduction in the overall number of neurons and glia was associated with the reduced size of the Id4 null brain, the reduction in the number of astrocytes and oligodendrocytes appeared to be disproportional to the reduction in size of the $Id4^{-/-}$ brain (figures 3.16-3.18). Analysis of adult NSCs *in vitro* revealed that NSCs lacking Id4 proliferated more slowly than $Id4^{+/+}$ NSCs (figure 3.21). This supported the reduced size of the Id4 knockout brain because there would be a reduction in the overall number of neurons and glia generated in the brain of these mice. The reduced proliferation capacity of $Id4^{-/-}$ NSCs, and the fact that ectopic expression of Id4 could rescue the proliferation defect (figure 3.21), indicate that Id4 is a key regulator of NSC proliferation. The proportional reduction in the number of neurons in the $Id4^{-/-}$ brain (figure 3.16) was supported by the observation that neuronal differentiation by NSCs in culture was unaffected by the absence of Id4 (data not shown). Hence, Id4 appears to be dispensable for neuronal development. The disproportional reduction in the number of glia in the $Id4^{-/-}$ brain (figures 3.17 and 3.18) suggested that glial cell development was affected in Id4 knockout mice. No difference between wild-type and Id4 null brains was found when apoptosis was analysed (figure 3.19). However, analysis of the differentiation capacity of NSCs revealed that NSCs lacking Id4 prematurely differentiated into astrocytes and oligodendrocytes compared to $Id4^{+/+}$ NSCs (figures 3.22-3.24), which also suggests that glial cell development is affected by the absence of Id4. Together, the results indicate that Id4 is involved in the regulation of NSC proliferation and glial cell development.

4.4.2 Reduced Proliferation Capacity of Neural Stem Cells Lacking Id4

The results indicate that Id4 is a crucial regulator of NSC proliferation. Although the mechanism of Id4 function in cell cycle control is unknown, there is considerable evidence that Id proteins are important in the control of cell proliferation (section 1.1.1.2). For example, Id2 binds to each of the three pocket proteins of the pRb family in a cell cycle-regulated fashion, inhibiting their anti-proliferative function (Iavarone *et al.*, 1994; Lasorella *et al.*, 1996, 2000). *In vitro* binding studies have shown that Id4, like Id2, but not Id1 or Id3, interacts with pRb (J. Newton, R. Deed, J. Norton and F. Sablitzky, unpublished). Therefore, it is tempting to speculate that Id4, like Id2, interferes with the checkpoint control mechanism provided by pRb and the related pocket proteins.

4.4.3 Neuronal Development is Unaffected in Mice Lacking Id4

The data from adult brains suggests that Id4 is not involved in the regulation of neuronal development. The reduction in the overall number of neurons in the adult Id4 knockout brain appears to be simply a reflection of the reduced proliferation capacity of Id4 knockout NSCs compared to wild-type. Previous studies and the Id4/lacZ expression data presented here show Id4 expression during neurogenesis, which suggests that Id4 has a role in neuronal development. However, it could be that Id4 is dispensable in this lineage of the nervous system. The Id4/lacZ expression data from the developing cerebral cortex of $Id4^{+/-}$ and $Id4^{-/-}$ embryos suggests that neuronal differentiation may be accelerated in Id4 knockout mice (figure 3.13). Cells expressing the Id4/lacZ fusion protein were in more mature layers of the developing cortex in the $Id4^{-/-}$ than in the $Id4^{+/-}$, indicating that neural cells lacking both copies of

the Id4 gene were ahead in their development. However, it is possible that accelerated neuronal development reflects premature generation of neuronal progenitors *in vivo*, which then differentiate normally. Premature neuronal development was not observed *in vitro*, but it is possible that adult and embryonic NSCs behave differently or that factors present *in vivo* are influencing neuronal development.

4.4.4 Glial Cell Development is Affected in Mice Lacking Id4

4.4.4.1 Premature Oligodendrocyte Differentiation in Id4 Knockout Mice

A recent study by Kondo and Raff (2000) supports a role for Id4 in the development of oligodendrocyte lineage cells. The authors demonstrated in rat optic nerve OPCs *in vitro* that Id4 was an important factor in the intracellular mechanism that times when OPCs withdraw from the cell cycle and differentiate. It was proposed that Id4 normally functions to promote cell cycle progression and negatively regulate differentiation of OPCs, and that the progressive decrease in its expression in proliferating OPCs was likely to be part of the timing of oligodendrocyte differentiation (Kondo and Raff, 2000). We have now shown that oligodendrocyte development is affected in the absence of Id4. There were fewer oligodendrocytes in the adult $Id4^{-/-}$ brain than if oligodendrocyte development was normal, and *in vitro*, $Id4^{-/-}$ NSCs prematurely differentiated into GC^{+} oligodendrocytes compared to $Id4^{+/+}$ NSCs. In consideration with the previous study, we suggest that $Id4^{-/-}$ OPCs both proliferate more slowly and differentiate prematurely, resulting in fewer oligodendrocytes than in wild-type mice. Taken together, the data indicates that Id4 is an important factor for normal oligodendrocyte development, and it likely

functions by enhancing the rate of cell proliferation and slowing the rate of differentiation of the OPC population.

Although Id4 is evidently important for oligodendrocyte development, oligodendrocytes are generated in the brain of $Id4^{-/-}$ mice. Since Id2 has been shown to behave similarly to Id4 in OPCs *in vitro* (Kondo and Raff, 2000; Wang *et al.*, 2001), it is possible that Id4 and Id2 have redundant functions in these cells, and that Id2 compensates, at least in part, for Id4 in $Id4^{-/-}$ mice, preventing a more severe phenotype. Unlike Id4, Id2 levels do not decrease over time as OPCs proliferate, but Id2 translocates out of the nucleus prior to the onset of differentiation (Wang *et al.*, 2001). Id1 and Id3 are also expressed in OPCs (Kondo and Raff, 2000; Wang *et al.*, 2001), but there was little effect of Id1 or Id3 overexpression in OPCs, suggesting that not all the Id proteins have overlapping functions.

4.4.4.2 Premature Astrocyte Differentiation in Id4 Knockout Mice

The findings in $Id4^{-/-}$ mice suggest that Id4 is also necessary for normal astrocyte development. Id4 knockout mice have fewer astrocytes in the brain than expected if astrocyte development was normal, and adult NSCs from these mice prematurely differentiated into $GFAP^{+}$ astrocytes compared to wild-type NSCs *in vitro*. *In vitro* studies by Andres-Barquin *et al.* (1997, 1999) support a role for Id4 in the modulation of astrocyte development. They found that only Id4 of the Id gene family was downregulated during astrocyte differentiation, and overexpression of Id4 induced apoptosis. It is proposed here that Id4 has a similar function during astrocyte development to that during oligodendrocyte development, where Id4 promotes proliferation and inhibits differentiation of OPCs, and is progressively downregulated as part of the mechanism timing oligodendrocyte differentiation. In

the astrocyte cell lineage, Id4 may be expressed during early astrocyte development in proliferating astrocyte precursor cells (APCs), and then decrease over time as part of the timing of astrocyte differentiation. Hence, in the absence of Id4, APCs would proliferate less and differentiate earlier in development, resulting in fewer astrocytes in the $Id4^{-/-}$ brain.

4.5 Neural Development in the Brains of Mice Lacking Id4

The data suggests that Id4 plays an important role in the timing of glial, but not neuronal, differentiation during mouse development. It is most likely that Id4 functions to prevent premature glial differentiation by promoting cell cycle progression and slowing the rate of differentiation of glial precursor cells. The function of Id4 in the glial lineage is similar to that of Id1 and Id3 in the neuronal lineage (Lyden *et al.*, 1999). Lyden *et al.* (1999) showed that Id1 or Id3 was necessary to prevent premature neuronal differentiation in the mouse embryo. Therefore, the Id proteins may have similar functions in distinct lineages of the mouse nervous system. Currently, we have no evidence *in vivo* for premature glial differentiation in Id4 knockout mice. However, the fact that approximately 50 % of Id4 knockout mice die during late foetal and early postnatal life, which is the main period of gliogenesis, supports a role for Id4 during this time of development.

The lack of a more severe phenotype in Id4 knockout mice may be due to compensation by other members of the Id family. For example, during the period of neurogenesis, Id4 expression in the VZ, apart from in the developing telencephalon, is overlapping with that of Id1-Id3 (Jen *et al.*, 1997). This suggests that the functions of these proteins could be, at least partly, redundant, and that Id1-Id3 may

compensate for Id4 in Id4 knockout mice. During early telencephalic development (10-11.5 dpc), Id4 is uniquely expressed in the VZ from which the cerebral cortex is derived. At later stages (12.5-14.5 dpc), when neurogenesis is maximal, Id2 expression is overlapping with that of Id4. Therefore, Id2 may compensate for the loss of Id4 in the developing telencephalon. The expression patterns of the Id genes in the brain, including that of Id4, during the time of gliogenesis have not been fully documented. It is thought that Id1 and Id3 expression is downregulated following neurogenesis, and the importance of these genes in neurogenesis has been shown in Id1/Id3 double-knockout mice (Lyden *et al.*, 1999). Id2 and Id4 expression in the nervous system persists in presumptive maturing neurons, but expression data after 16.5 dpc is very limited. Id4 is expressed in the VZ of the telencephalon at 16.5 dpc (Jen *et al.*, 1997), suggesting that it may be involved in early gliogenesis. Since the expression data on the Id genes during the period of gliogenesis is minimal, it is difficult to suggest any compensatory mechanisms that may occur. However, Id2 and Id4 expression is overlapping in OPCs in the rodent optic nerve (Kondo and Raff, 2000; Wang *et al.*, 2001), supporting redundant functions for these genes in oligodendrocyte development. We also have evidence that Id2 may compensate for Id4 during mouse development. We have intercrossed $Id2^{+/-}Id4^{+/-}$ mice to generate mice lacking combinations of Id2 and Id4 alleles, which were genotyped at weaning. In a total of 87 mice from 3 different intercrosses, no Id2/Id4 double-mutant mice were found, indicating that these mice were inviable (table 4.1).

Genotype		Expected Number	Actual Number
Id2	Id4		
+/+	+/+	1 in16	1 in 15.3
-/-	+/+	1 in 16	1 in 23
+/+	-/-	1 in 16	1 in 13.1
-/-	-/-	1 in 16	0
+/-	+/+	1 in 8	1 in 7.7
+/+	+/-	1 in 8	1 in 4
-/-	+/-	1 in 8	1 in 13.1
+/-	-/-	1 in 8	1 in 11.5
+/-	+/-	1 in 4	1 in 3.7

Table 4.1 $Id2^{-/-}Id4^{-/-}$ mice are inviable. The expected and actual number of each genotype from $Id2^{+/-}$ $Id4^{+/-}$ intercrosses.

The differences between the expected and actual number of each genotype obtained from the $Id2^{+/-}Id4^{+/-}$ intercrosses requires further analysis. There was no significant difference between the number of mice born and the number genotyped at weaning, which indicates that Id2/Id4 double-knockout mice die in utero. Further studies will establish when $Id2^{-/-}Id4^{-/-}$ die.

The discussion has focused on the role of Id4 in nervous system development, but Id4 may also have a function(s) in the mature nervous system. Id4 was differentially expressed within the adult brain, which suggests that Id4 has a role in specific regions of the mature brain. The function(s) of Id4 in the adult brain remain to be determined.

4.6 How is Id4 Integrated into the Pathways Regulating Neural Differentiation?

The results show that Id4 is an important factor in glial cell development. Several signals are known to promote gliogenesis, such as CNTF, BMPs and Notch activation, and it may be that Id4 is involved in and/or downstream of these signalling pathways. CNTF and BMPs are known to promote astrocyte differentiation by NSCs. CNTF signalling involves the STAT proteins and that of BMPs involves the Smad proteins (section 1.2.2.2.1). Synergy between CNTF and BMPs has been described (Nakashima *et al.*, 1999). In our analysis of astrocyte differentiation *in vitro*, we found that NSCs lacking Id4 prematurely differentiated into astrocytes in response to BMP2/4, but not CNTF, indicating that Id4 is involved in BMP2/4-, but not CNTF-mediated astrocyte differentiation. A mechanism by which Id4 could function to suppress premature astrocyte differentiation in response to BMP2/4 is by direct inhibition of the BMP2/4 signalling pathway. In view of the apparent molecular promiscuity of Id protein interactions, it is possible that Id4 interacts with the Smad proteins. An alternative mechanism could also explain premature astrocyte differentiation in the absence of Id4. We have suggested that Id4 may function in the astrocyte lineage to promote cell cycle progression and slow the rate of differentiation of APCs, analogous to its function in OPCs (Kondo and Raff, 2000). Although we have no data about the expression of Id4 in APCs, BMP2/4 signalling may be involved in stimulating the expression of Id4, which then functions in the APCs to prevent premature astrocyte differentiation. Hence, precocious astrocyte differentiation would occur when Id4 was absent. BMPs exert their functions via the Smad transcription factors and a Smad-binding motif is present in the Id4 promoter. Recently, BMP2 was shown to stimulate the expression of Id1, Id3

and Hes5 in a Smad-dependent manner in telencephalic neural progenitor cells *in vitro* (Nakashima *et al.*, 2001). This was part of the mechanism by which BMP2 inhibited neurogenesis whilst mediating a switch from neurogenesis to astrocytogenesis. The regulation of Id2 and Id4 expression by BMP2 has not been examined.

If the function of Id4 is as described above, in the APC population, you would expect any astrocyte-promoting signal to result in premature astrocyte differentiation in the absence of Id4, since astrocyte development is understood to proceed through the APCs. However, astrocyte differentiation in response to CNTF was unaffected by the absence of Id4. A possible explanation for this observation could be that more than one type of APC exists, and the different APCs are involved in different signalling pathways. Id4 may only be a part of the mechanism timing differentiation in specific APCs, such as those involved in BMP2/4-mediated astrocyte differentiation. Astrocyte differentiation promoted by CNTF may then be independent of Id4.

Notch signalling is known to inhibit neurogenesis and promote gliogenesis (section 1.2.2.2.1). Notch acts instructively to inhibit neurogenesis via upregulating Hes bHLH repressors, which inhibit the expression and function of neurogenic bHLH factors. It is possible that Notch activation may also upregulate the expression of Id4, either via the Notch/RBP-J transcription factor complex, which upregulates Hes expression, or via the Hes proteins themselves, although the Hes proteins usually act as transcriptional repressors. Id4 may then function to maintain the timing of glial differentiation as described above. However, although Notch activation was not

analysed in this work, Wang and Barres (unpublished) indicate that Notch signalling upregulates only Id1 and Id3, and not Id2 and Id4 (Wang *et al.*, 2001).

4.7 What is the Mechanism by which Id4 Prevents Premature Glial Differentiation?

Since Id proteins function primarily as dominant negative regulators of bHLH proteins, it is likely that Id4 has a role in preventing the precocious functioning of positively acting bHLH proteins that are involved in glial development. Although numerous bHLH proteins have been identified that are involved in the neurogenesis, few bHLH proteins have been identified that are involved in the formation of glia from multipotent progenitors. In fact, only two class B bHLH proteins have been identified to date, Olig1 and Olig2, which are linked to oligodendrocyte development in the vertebrate CNS and are induced by Shh (Lu *et al.*, 2000; Takebayashi *et al.*, 2000; Zhou *et al.*, 2000). The Olig genes are potential candidates for regulation by Id4, and this is supported by our *in vitro* data showing premature oligodendrocyte differentiation by $Id4^{-/-}$ NSCs in response to TH and Shh. The expression patterns of the Olig genes during CNS development have been described in several papers (Lu *et al.*, 2000; Takebayashi *et al.*, 2000; Zhou *et al.*, 2000). Although the expression pattern of Id4 during spinal cord development is not fully overlapping with that of the Olig genes, Id4 is expressed in the ventral portion of the spinal cord at 10.5 dpc, where it may overlap with the region of Olig gene expression. Since the study by Lu *et al.* (2000) suggested that there were no significant differences between Olig1 and Olig2 expression domains in the embryonic brain, and that by Takebayashi *et al.* (2000) suggested that Olig1 expression was more widespread than that of Olig2, it is difficult to say of Id4 is overlapping with the Olig genes in the embryonic brain.

Studies are needed to determine whether Id4 expression is overlapping with that of the Olig genes, and also whether Id4 can antagonise the functions of these genes. bHLH proteins associated with astrocytogenesis have yet to be identified. Alternatively, we have suggested that Id4 may interact with and inhibit the Smad proteins, such as Smad4, to prevent premature astrocyte differentiation promoted by BMP signalling.

4.8 Summary: Ids in Nervous System Development

Figure 4.1 is a summary of our current knowledge of the functions of Id proteins in nervous system development. A picture is emerging that Id proteins play an important role in NSC proliferation as well as in proliferation and differentiation of lineage-restricted precursor cells. Although development of the neuronal lineage was unaffected in Id1 and Id3 single knockout mice (Yan *et al.*, 1997a; Pan *et al.*, 1999), premature neuronal differentiation was evident in Id1/Id3 double-knockout mice (Lyden *et al.*, 1999). Id1/Id3 double-knockout neuroblasts prematurely withdrew from the cell cycle and differentiated into neurons. It seems that Id1 and Id3 proteins are negative regulators of neuronal cell differentiation, and both genes are downregulated upon neuronal differentiation. In contrast to Id1 and Id3, Id2 and Id4 function seems to be important in gliogenesis. However, the function of Id2 and Id4 in the glial lineage is similar to that of Id1 and Id3 in neurogenesis. Id2 and Id4 proteins appear to play an important role in timing when glial-restricted progenitors withdraw from the cell cycle and differentiation (this work; Kondo and Raff, 2000; Wang *et al.*, 2001). Id2 function in OPCs is inhibited by translocation of the Id2 protein out of the nucleus, whereas that of Id4 is inhibited by downregulation of Id4 gene expression upon differentiation of OPCs into oligodendrocytes (Kondo and

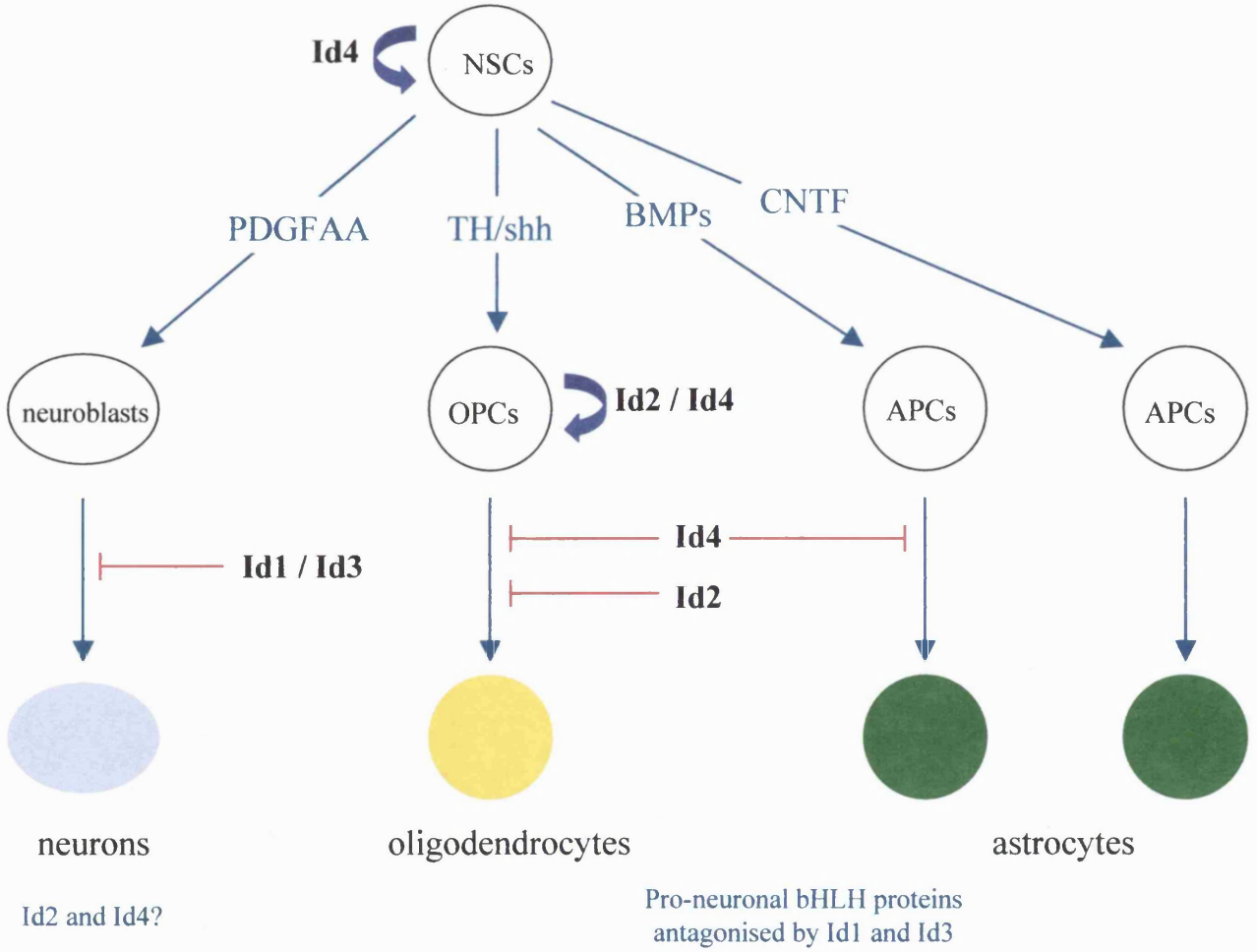

Figure 4.1 Summary of the functions of Id proteins in nervous system development. Neural stem cell (NSC) proliferation is positively regulated by Id4. The function of Id1 and Id3 in the neuronal lineage, and Id2 and Id4 in the glial lineage, is to maintain the timing of differentiation of lineage-restricted precursor cells, where Id proteins function to promote cell cycle progression and negatively regulate differentiation. In astrocyte differentiation, Id4 inhibits BMP-induced astrocyte differentiation, but not that induced by CNTF. Id1 and Id3 may be involved in the neuronal versus glial fate decision by antagonising pro-neuronal bHLH transcription factors. The function(s) of Id2 and Id4 in the neuronal lineage remain elusive.

Raff, 2000; Wang *et al.*, 2001). The mechanism by which Id4 function is inhibited in the astrocyte lineage is unknown at the present time. The role for Id4 in oligodendrocyte development demonstrated by this work supports the previous data from Kondo and Raff (2000), but we indicate a novel role for Id4 in BMP2/4-mediated astrocyte differentiation. Interestingly, Id1 and Id3 are transiently upregulated as part of the switch from neurogenesis to astrocytogenesis induced by BMP2, and function to antagonise pro-neuronal bHLH transcription factors (Nakashima *et al.*, 2001). Also, Id1 and Id3 are expressed in OPCs, and their expression is not significantly altered upon differentiation to oligodendrocytes (Kondo and Raff, 2000; Wang *et al.*, 2001). Therefore, these studies suggest that Id1 and Id3 may be involved in the neuronal versus glial fate decision, antagonising the functions of pro-neuronal bHLH proteins in glial cells. Although Id2 and Id4 are expressed in the neuronal lineage, neuronal cell differentiation seems to be normal in the absence of Id2 or Id4 (this work; Yokota, 2001). Hence, their function in the neuronal lineage remains elusive. Whether the absence of both Id2 and Id4 will have an effect on neuronal differentiation remains to be determined

4.9 Future Work

Several ideas for future work have been mentioned through the discussion. An important focus will be to obtain evidence of premature glial differentiation *in vivo* in the Id4 knockout embryo. This will involve analysis of embryo sections for a series of neural markers, initially focusing on the developing cerebral cortex. For the detection of astrocytes, anti-S100β and anti-GFAP antibodies will be used, which detect immature and mature astrocytes respectively. If premature astrocyte differentiation occurs in the absence of Id4, we would expect to detect expression of

S100β and/or GFAP at earlier embryonic stages in the Id4 knockout compared to the wild-type. To analyse oligodendrocyte development *in vivo* there are two possibilities. In a similar way to that which has just been described for the analysis of astrocytes, oligodendrocyte-specific markers could be examined to obtain evidence of premature oligodendrocyte differentiation in the absence of Id4. Alternatively, we could analyse oligodendrocyte development in the optic nerve, which is composed mainly of glia, and in which the pattern of oligodendrocyte development has been well characterised. NG2, O4 and APC are oligodendrocyte marker proteins for early oligodendrocyte precursors, mature oligodendrocyte precursors/immature oligodendrocytes and mature oligodendrocytes respectively. To support the functions of Id4 in OPCs, OPCs could be purified from the Id4 knockout brain and analysed in a manner analogous to that which was done by Wang *et al.* (2001) with OPCs purified from Id2 knockout mice. *In vivo* evidence for the decreased proliferation capacity of Id4 knockout NSCs could be obtained by analysing embryos for expression Ki-67, which is a nuclear antigen expressed in all proliferating cells except those in G_0/early G_1, or for BrdU incorporation following administration of the thymidine analogue BrdU to the mother.

Another important focus for future work will involve further analysis of X-gal stained embryos. X-gal staining of embryos at 0.5 day intervals between the time points that were analysed in this work, and then comparison of the X-gal staining pattern between $Id4^{+/-}$ and $Id4^{-/-}$ embryos, may show if the pattern in the $Id4^{-/-}$ is similar to that of a later stage in the $Id4^{+/-}$, i.e. if the $Id4^{-/-}$ is ahead in development. This may help to explain the differences in the size of the Id4/lacZ expression domains at 10.5 dpc (figure 3.12) and in the pattern of expression at 14.5 dpc (figure 3.13) between $Id4^{+/-}$ and $Id4^{-/-}$ embryos. Also, X-gal staining of embryos in later

stages of embryogenesis and of mice in early postnatal development will establish the expression pattern for Id4 during the period of gliogenesis, which has yet to be reported.

Chapter 5

Results

Reduced Fertility and Defective Spermatogenesis in Male Mice Lacking Helix-Loop-Helix Protein Id2

Sablitzky *et al.* (1998) described a unique stage- and subcellular-specific expression pattern for each Id protein in spermatogenesis. Id2 was expressed in germ and Sertoli cells of the testis, raising the possibility that, without a functional Id2 gene, male reproduction would be compromised. To investigate the functional roles of Id2 in spermatogenesis, the testes of Id2 knockout mice were analysed.

5.1 Generation of Id2 Knockout Mice

The Id2 knockout mice were generated by Yoshifumi Yokota at Kyoto University in Japan (Yokota *et al.*, 1999). Yoshifumi Yokota kindly sent two pairs of heterozygous Id2 mutant mice from Japan to enable us to establish a colony of Id2 knockout mice in our animal facility. The Id2 mutant mice were of 129/Sv genetic background. Yokota *et al.* confirmed inactivation of the Id2 gene by Northern blot analysis of RNA from neonatal livers, showing no Id2 mRNA expression in homozygous Id2 mutant mice. Female homozygous Id2 mutant mice could not be used for breeding because of a lactation defect, reported by Yokota *et al.* in 2000.

5.2 Male Id2 Knockout Mice have Reduced Fertility

During the course of colony expansion, we noticed that very few of the male homozygous Id2 mutant mice were able to produce offspring, suggesting that Id2 may play a role in the fertility of male as well as female mice. Heterozygous mutant males were able to produce offspring reliably. Therefore, heterozygous intercrosses were used to maintain the Id2 knockout colony.

In the results documented in this chapter, the wild-type ($Id2^{+/+}$), heterozygous Id2 mutant ($Id2^{+/-}$) and homozygous Id2 mutant ($Id2^{-/-}$) testes were from mouse littermates unless otherwise stated. The mice were approximately four months old when they were sacrificed and their testes isolated. Transverse sections of each testis were made for analysis.

5.3 Testis Weight is not Affected in Id2 Knockout Mice

As shown in figure 5.1, there was no significant difference in the mean testis weight between $Id2^{+/+}$, $Id2^{+/-}$ and $Id2^{-/-}$ mice. This was confirmed by Student's *t*-tests ($P < 0.05$). Testes for each group were dissected out and the average weight of the two testes from each male was used for statistical analysis. Mice used in this analysis were not littermates, but were matched for age. The total number of mice in each group is small, but this result is supported by several observations. There is no difference in the average testis weight between wild-type mice and mice lacking bone morphogenetic protein 8A (Bmp8a) or high mobility group 2 protein (Hmgb2), although both $Bmp8a^{-/-}$ and $Hmgb2^{-/-}$ mice exhibit reduced fertility (Zhao *et al.*, 1998; Ronfani *et al.*, 2001).

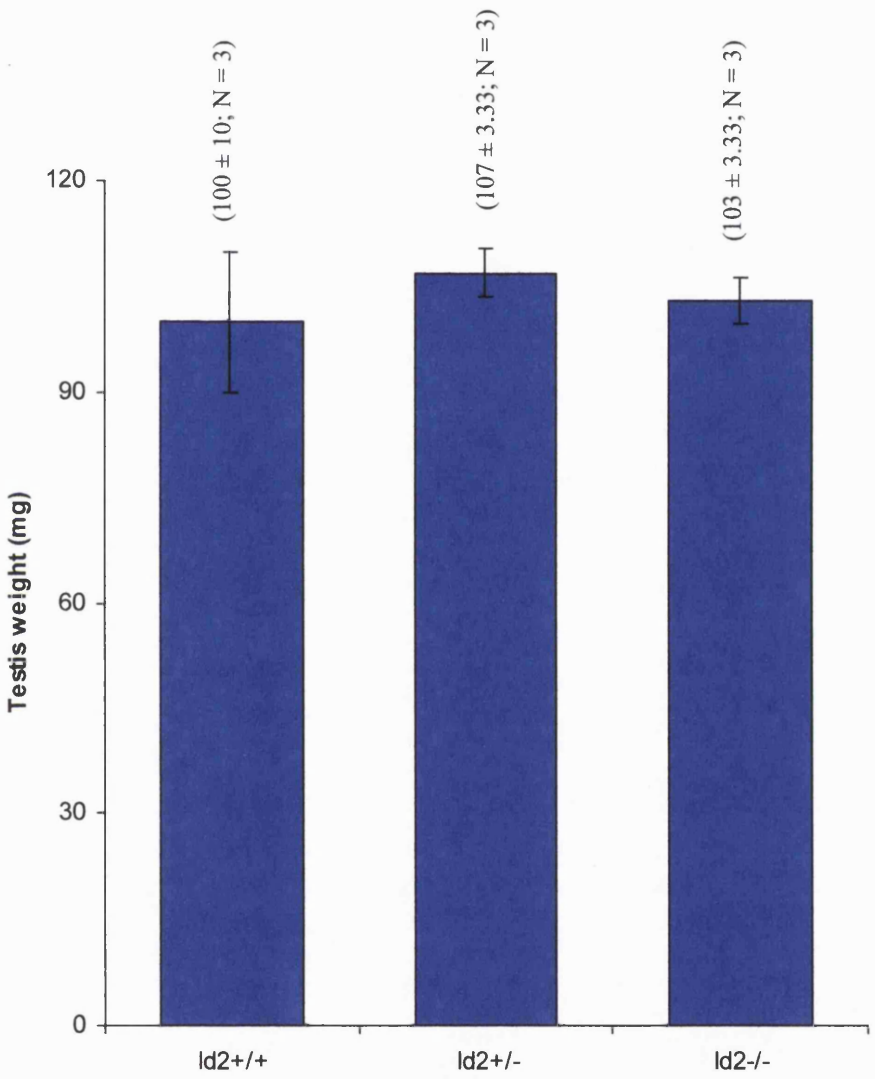

Figure 5.1 Testis weight is not significantly different between wild-type (Id2+/+), heterozygous (Id2+/-) and homozygous (Id2-/-) Id2 mutant mice. Testes for each group were dissected out and the average weight of the two testes from each male was used for statistical analysis. Mean ± s.d. is indicated in brackets, N represents the total number of mice in each group.

5.4 Male Id2 Knockout Mice have Defective Spermatogenesis

To analyse the morphology of the testes, wild-type, heterozygous Id2 mutant and homozygous Id2 mutant testis sections were stained with haematoxylin and eosin. $Id2^{+/-}$ seminiferous tubules showed normal spermatogenesis and were indistinguishable from $Id2^{+/+}$ tubules, supporting the normal reproductive performance of $Id2^{+/-}$ males (figures 5.2A-D and data not shown). In the $Id2^{-/-}$ testis, many of the seminiferous tubules showed morphological abnormalities that reflected defective spermatogenesis (figures 5.2A, B, E, F, 5.3 and 5.4). Therefore, further results in this chapter compare wild-type and homozygous Id2 mutant testes. Quantitative analysis using testis sections revealed that 52 % (58 of 111 tubules) of $Id2^{-/-}$ seminiferous tubules showed varied degrees of morphological abnormalities compared to 18 % (15 of 83 tubules) of $Id2^{+/+}$ tubules. Since apoptosis occurs during normal spermatogenesis, apoptosis was not included in the criteria for morphologically abnormal tubules. Apoptosis in $Id2^{+/+}$ and $Id2^{-/-}$ seminiferous tubules is described in section 5.5. Figures 5.3 and 5.4 show examples of the morphological abnormalities observed in the $Id2^{-/-}$ seminiferous tubules. The following descriptions compare the abnormal tubules of the Id2 knockout testis to the tubules showing normal spermatogenesis in the wild-type. Comparison of $Id2^{+/+}$ and $Id2^{-/-}$ seminiferous tubules in similar stages of spermatogenesis showed that the numbers of elongating and condensing spermatids, and spermatozoa were reduced in the $Id2^{-/-}$ tubules (figures 5.3 and 5.4). The spermatogonia and spermatocyte populations appeared to be relatively normal in the Id2 knockout tubules. In many $Id2^{-/-}$ seminiferous tubules, normal spermatogenesis was observed in a portion of the seminiferous epithelium and perturbed spermatogenesis in the remainder of the tubule (figures 5.3J, K and L). The organisation of developing germ cells within the

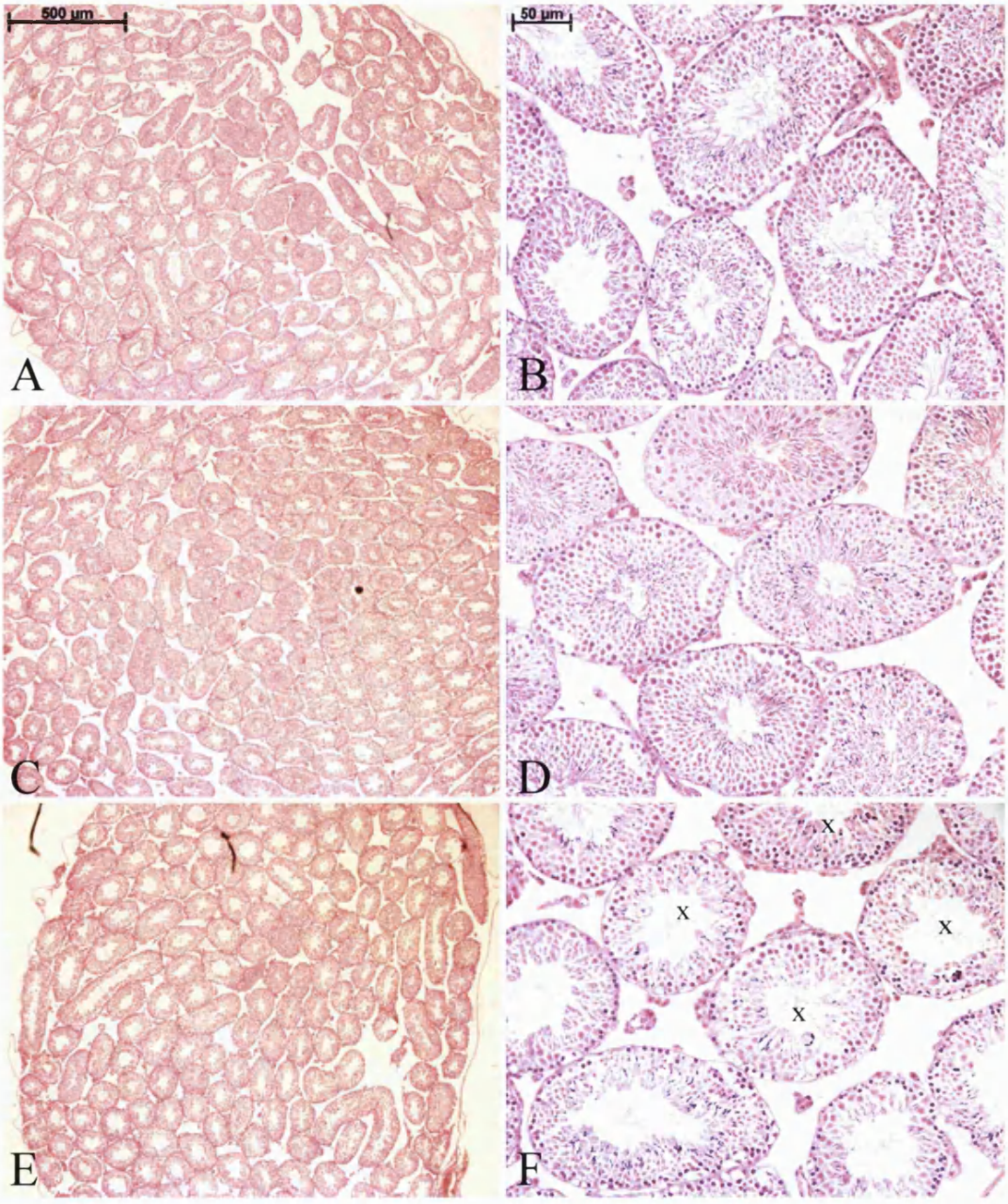

Figure 5.2 Morphological comparison of testes from adult $Id2^{+/+}$ (A, B), $Id2^{+/-}$ (C, D) and $Id2^{-/-}$ (E, F) mice. A representative area for each genotype is shown (B, D, F). $Id2^{+/-}$ seminiferous tubules were indistinguishable from wild-type tubules, showing normal spermatogenesis. Numerous $Id2^{-/-}$ seminiferous tubules showed morphological abnormalities (F, x) exemplified by reduced numbers of sperm, large cytoplasmic bodies in the lumen and disorganised seminiferous epithelium.

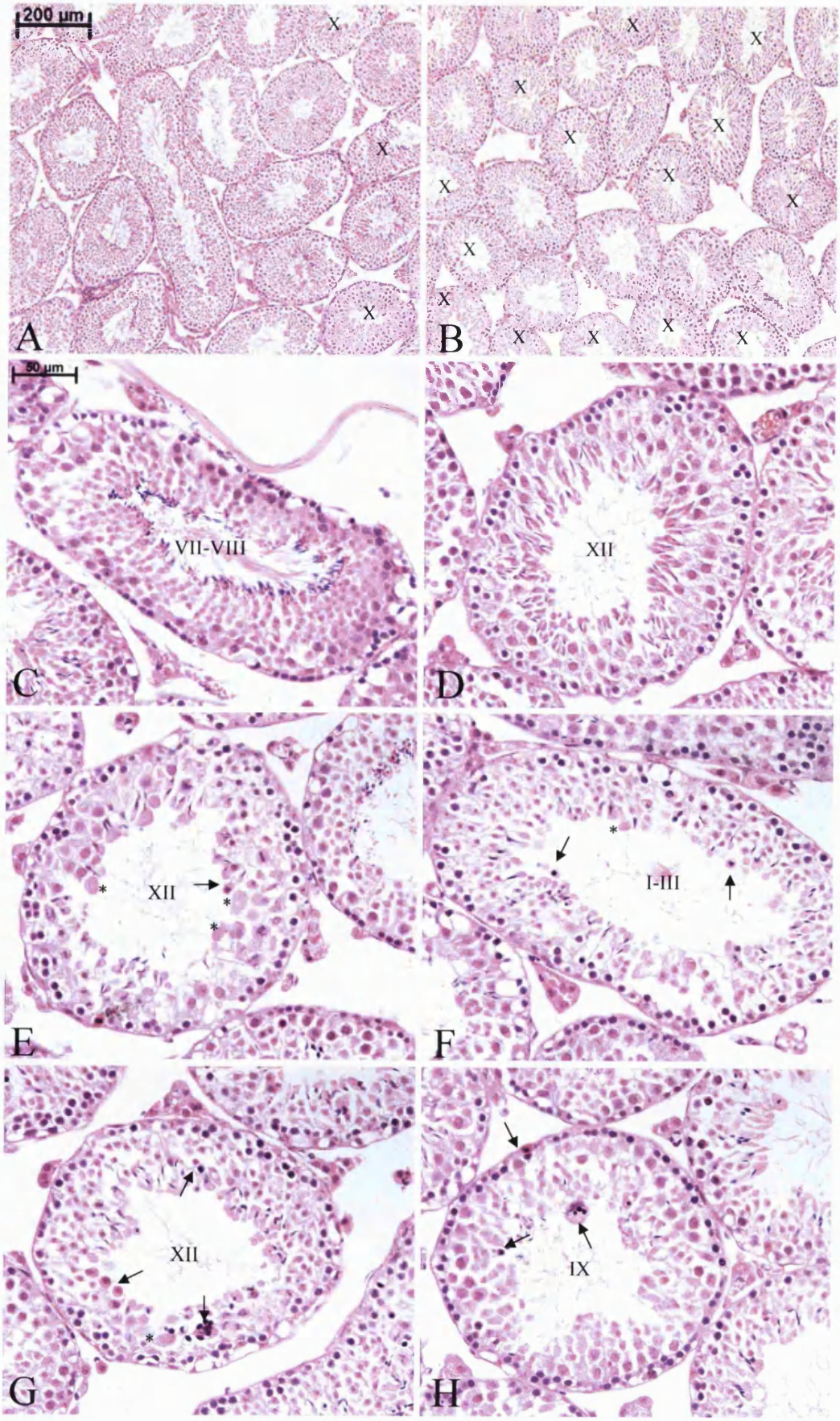
200 µm
X
A
B
50 µm
VII-VIII
C
XII
D
XII
E
I-III
F
XII
G
IX
H

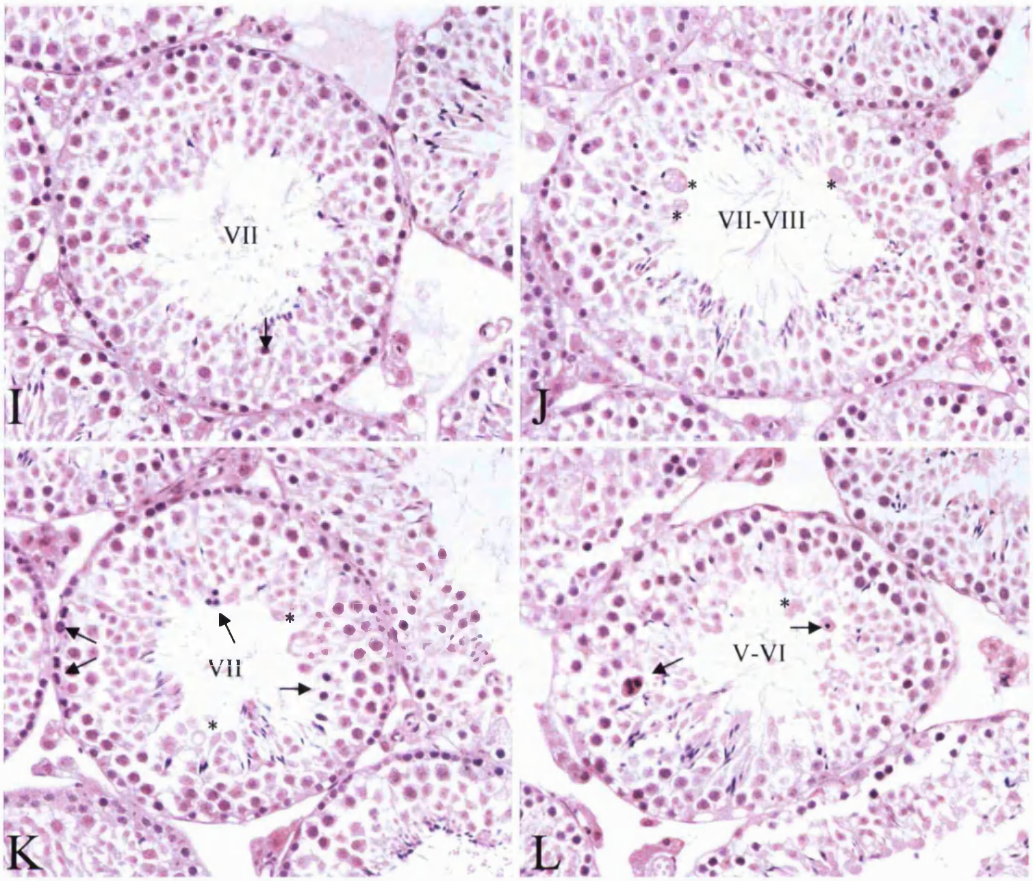

Figure 5.3 Morphological comparison of $Id2^{+/+}$ and $Id2^{-/-}$ testes showing the disrupted spermatogenesis in $Id2^{-/-}$ seminiferous tubules. (A, B) Low-power magnification indicating morphologically abnormal seminiferous tubules in $Id2^{+/+}$ and $Id2^{-/-}$ testis sections (x). Numerous tubules are abnormal in the homozygous mutant testis. (C, D) Wild-type seminiferous tubules showing normal spermatogenesis. (E-L) Examples of morphologically abnormal tubules observed in the $Id2^{-/-}$ testis, similar to those indicated in B. The stage (cell association) of each tubule is indicated by Roman Numerals (Russell *et al.*, 1990). The numbers of elongating and condensing spermatids, and spermatozoa are reduced in the $Id2^{-/-}$ tubules, indicating defective spermatogenesis. Also, the tubule lumina contain large cytoplasmic bodies (*), and apoptotic cells (arrows) are prevalent.

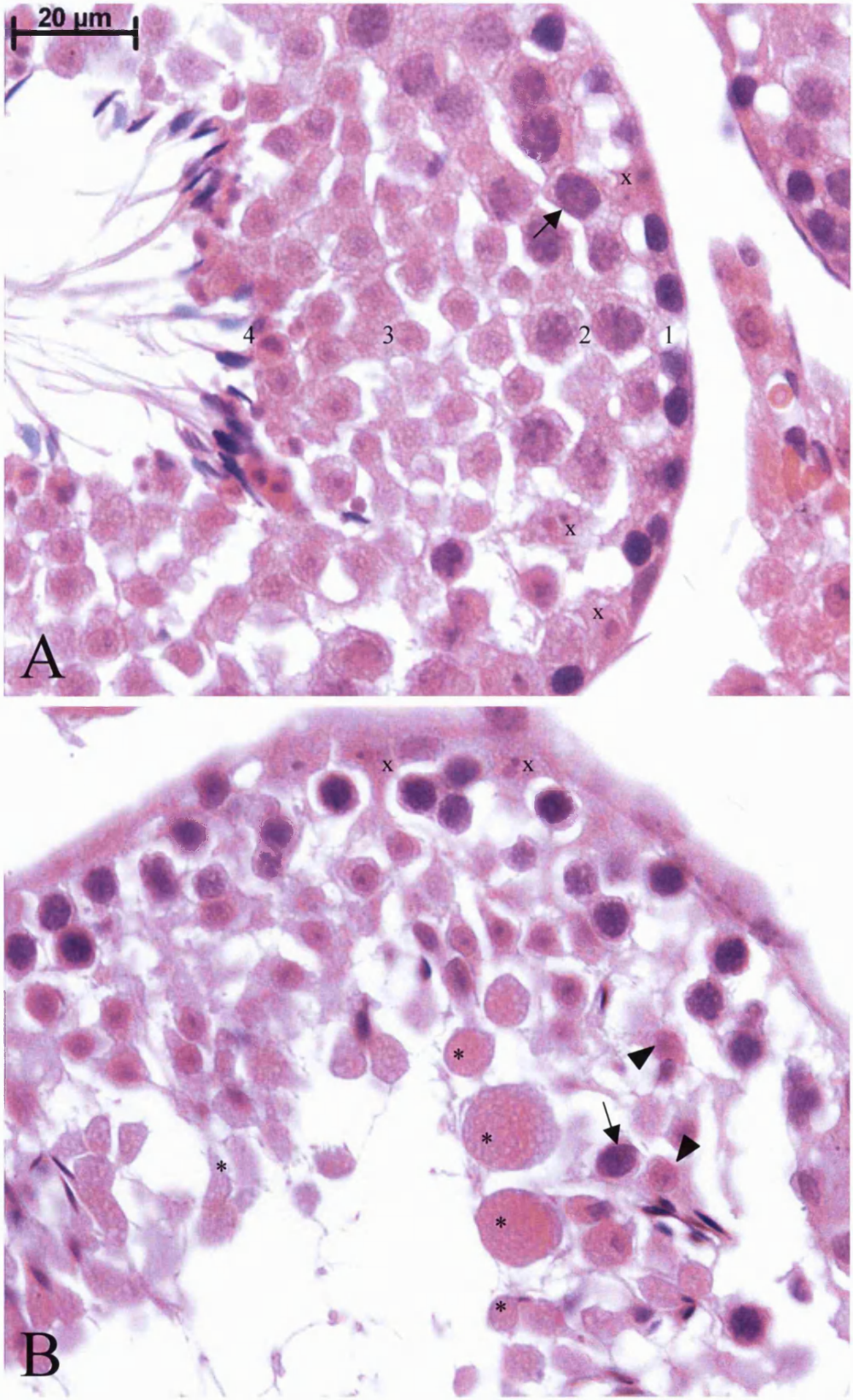

Figure 5.4 Morphological comparison of a portion of seminiferous tubule wall from wild-type ($Id2^{+/+}$, A) and Id2 null ($Id2^{-/-}$, B) testes. In the $Id2^{+/+}$, germ cells are organised, with spermatogonia (1), spermatocytes (2), round spermatids (3) and spermatozoa (4) in successive layers towards the tubule lumen, and Sertoli cells (x) among developing germ cells. In the $Id2^{-/-}$, germ cells are not tightly organised within the tubule epithelium. For example, a spermatocyte (arrow) is among developing spermatids (arrowheads). Also, the $Id2^{-/-}$ tubule lumen contains reduced numbers of maturing sperm and large cytoplasmic bodies (*).

tubule epithelium was often perturbed in $Id2^{-/-}$ seminiferous tubules. In wild-type tubules, germ cells are arranged in a regular periphery-to-lumen succession of spermatogonia, spermatocytes, spermatids and spermatozoa, as shown in figure 5.4A. In $Id2^{-/-}$ seminiferous tubules, the germ cells were often not as tightly organised in successive layers towards the tubule lumen (figure 5.4B). Figure 5.4B shows a spermatocyte (arrow) adjacent to the tubule lumen, among developing spermatids (arrowheads). Numerous $Id2^{-/-}$ seminiferous tubules contained large cytoplasmic bodies in the lumen (figures 5.3E, F, J, K, L and 5.4B, asterisks), which were observed in only a few wild-type tubules (data not shown).

The phenotypes observed in the Id2 knockout seminiferous tubules are typical of mice with reduced fertility, like those lacking bone morphogenetic protein 8A (Bmp8a) (Zhao *et al.*, 1998) or high mobility group 2 protein (Hmgb2) (Ronfani *et al.*, 2001), or the triple knockout for Tyro3, Ax1 and Mer receptors (Lu *et al.*, 1999). Similar to the $Id2^{-/-}$ testis, only a fraction of the seminiferous tubules in the testes of these mice exhibit defective spermatogenesis.

5.5 Increased Apoptosis in the Id2 Knockout Testis

Apoptosis in wild-type and Id2 knockout testes was analysed by two independent assays. The testis sections that had been stained with haematoxylin and eosin (section 5.4) were analysed for apoptotic cells, and $Id2^{+/+}$ and $Id2^{-/-}$ testis sections were analysed for apoptosis using TUNEL (Terminal Deoxynucleotidyl Transferase-mediated dUTP Nick-End Labelling). Apoptosis is a normal part of spermatogenesis, therefore apoptotic cells are found in wild-type seminiferous tubules.

In sections stained with haematoxylin and eosin, apoptotic germ cells are characterised by condensed and darkly stained nuclei or chromatin and strongly eosinophilic cytoplasm, and are often large multinucleate structures (figures 5.3E, F, G, H, I, K and L, arrows). During morphological analysis of the testes, the number of seminiferous tubules containing apoptotic cells was quantified for wild-type and homozygous Id2 mutant testes (table 5.1B). As shown in table 5.1B (all tubules), apoptosis was increased approximately 2-fold in the Id2 knockout testis. Apoptosis in morphologically normal and abnormal seminiferous tubules of the $Id2^{+/+}$ and $Id2^{-/-}$ testes was also quantified (table 5.1B). The apoptosis in morphologically abnormal tubules was similar in wild-type and homozygous Id2 mutant testes, and was increased approximately 3-fold compared to the apoptosis observed in morphologically normal tubules of the wild-type testis, which can be taken as an indication of apoptosis that occurs as a part of normal spermatogenesis. This suggests that increased apoptosis correlates with morphologically abnormal seminiferous tubules. However, comparison of apoptosis in morphologically normal tubules between $Id2^{+/+}$ and $Id2^{-/-}$ testes indicates that apoptosis is increased approximately 2-fold in the normal seminiferous tubules of the homozygous Id2 mutant testis, suggesting that spermatogenesis is disrupted in a larger fraction of the $Id2^{-/-}$ tubules than observed by the morphological analysis. This observation would increase the fraction of tubules undergoing defective spermatogenesis to approximately 60 %. Apoptotic cells were observed at various positions within the $Id2^{-/-}$ seminiferous epithelium, which may be an indication of the type of cell undergoing apoptosis. For example, figures 5.3H and K show apoptotic cells around the periphery of the seminiferous tubule, suggesting that spermatogonia or maybe Sertoli cells are undergoing apoptosis.

Analysis (method)		$Id2^{+/+}$	$Id2^{-/-}$	Increase: $Id2^{-/-}$ compared to $Id2^{+/+}$
A. Morphological (haematoxylin and eosin staining)		18 % of tubules morphologically abnormal	52 % of tubules morphologically abnormal	2.9-fold
B. Apoptosis (haematoxylin and eosin staining)	All tubules Morphologically normal tubules Morphologically abnormal tubules	12 % (10 of 83 tubules) 9 % (6 of 68 tubules) 27 % (4 of 15 tubules)	25 % (28 of 111 tubules) 17 % (9 of 53 tubules) 33 % (19 of 58 tubules)	2.1-fold
C. Apoptosis (TUNEL)		9.3 tubules contained apoptotic cells (figure 5.6)	21.3 tubules contained apoptotic cells (figure 5.6)	2.3-fold

Table 5.1 Summary of the quantitative data from the morphological and apoptosis analyses.

Wild-type and homozygous mutant testis sections were also analysed for apoptotic cells using the Apoptosis Detection System, Fluorescein (Promega). In this assay, fragmented nuclear DNA is labelled with fluorescein-12-dUTP using the principle of TUNEL, and is evident as localised green fluorescence using direct fluorescence microscopy. Propidium iodide is used to stain all nuclei in the section and is visualised as red fluorescence. Any co-localisation of these two fluorochromes results in a yellow colour, which indicates apoptotic cells. In wild-type and homozygous Id2 mutant seminiferous tubules, bright yellow was evident in condensed nuclei, which were often in multinucleate structures (figure 5.5B, arrows and inset, and data not shown). This apoptosis reflects that observed in the haematoxylin and eosin stained testis sections. Another type of bright yellow was observed in both wild-type and homozygous mutant tubules, this was within bright green nuclei (figure 5.5B, asterisk). This may reflect germ cells in meiosis, and not cells undergoing apoptosis. Breaks in DNA during crossing over in meiosis may be labelled by TUNEL in this assay. In the $Id2^{-/-}$ testis, some seminiferous tubules contained germ cells near to the periphery that were yellow/orange (figure 5.5B, arrowheads), suggesting that these cells were undergoing apoptosis. The position of these cells within the epithelium implies that they are spermatocytes. This apoptosis was not observed in any tubules of the wild-type testis, and therefore could be a result of defective spermatogenesis in the Id2 knockout testis. To compare the level of apoptosis between wild-type and homozygous Id2 mutant testes, the number of tubules containing bright yellow apoptotic nuclei was quantified for similar sized $Id2^{+/+}$ and $Id2^{-/-}$ testis sections in three independent experiments. Apoptosis in morphologically normal and abnormal seminiferous tubules could not be analysed independently in this apoptosis assay. As shown in figure 5.6, the mean number of tubules containing apoptotic cells increased 2.3-fold in the Id2 knockout testis

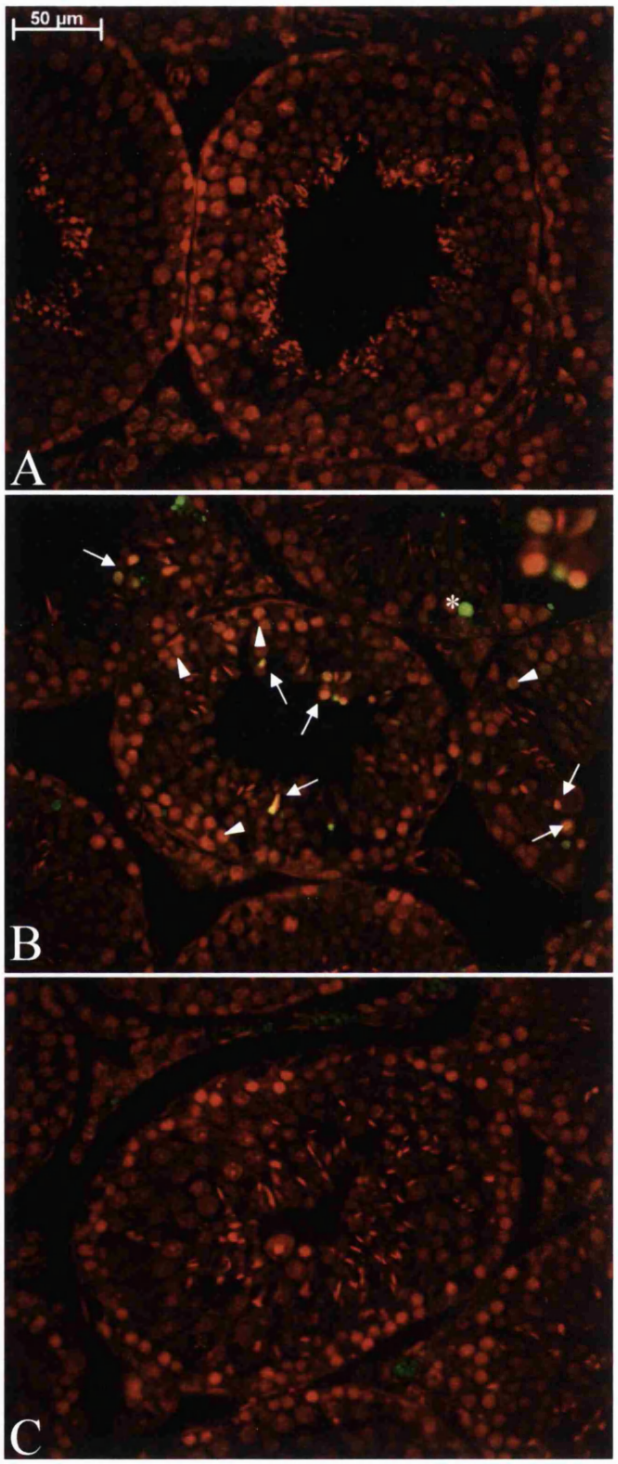

Figure 5.5 Increased apoptosis in the Id2 null testis. Testis sections were assayed for apoptosis using the Apoptosis Detection System, Fluorescein (Promega). Fragmented nuclear DNA was labelled with fluorescein-12-dUTP by TUNEL and visualised as green using direct fluorescence microscopy. All nuclei were counterstained red with propidium iodide. Images were overlaid and apoptotic cells indicated by yellow. Representative seminiferous tubules from $Id2^{+/+}$ (A) and $Id2^{-/-}$ (B) testes are shown. (C) shows a $Id2^{-/-}$ negative control, where no TdT was present in the TUNEL assay. Apoptosis is indicated by bright yellow (arrows and inset), which is in condensed, often multinucleate structures, and yellow/orange (arrowheads), which is in germ cells near to the periphery of tubules. (*) indicates germ cells in meiosis.

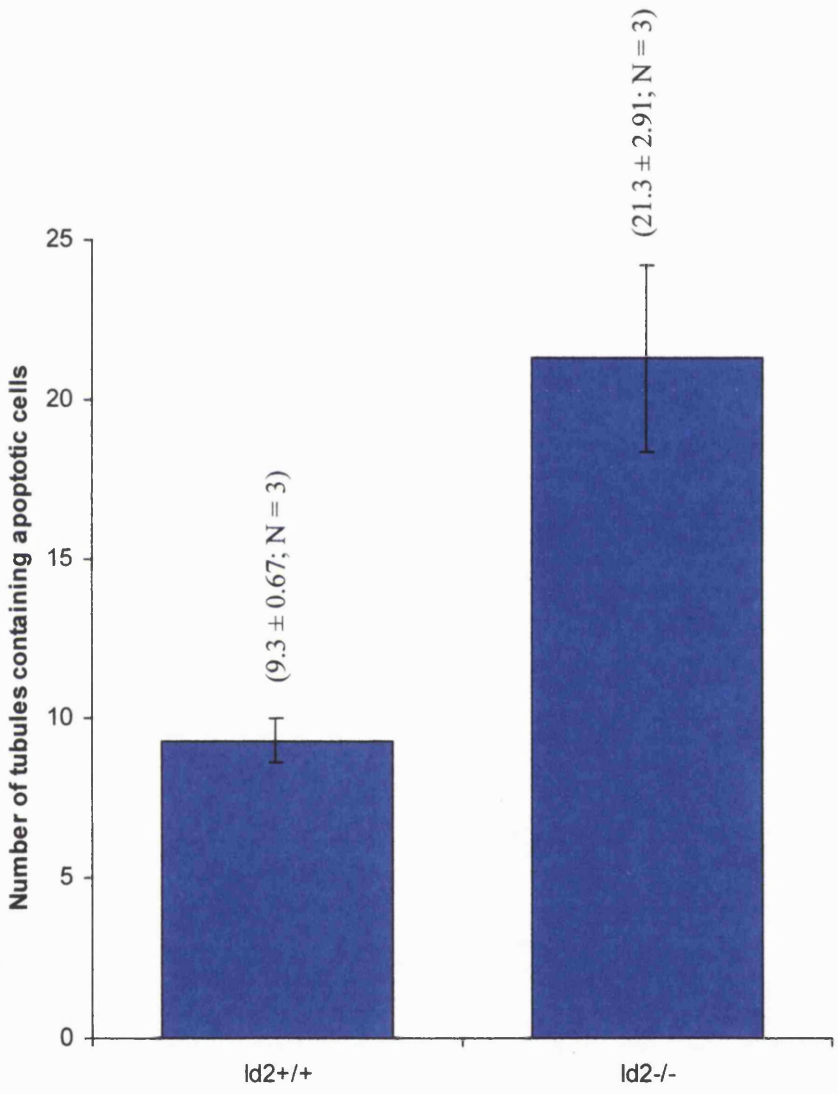

Figure 5.6 Increased apoptosis in the Id2 knockout testis. Mean ± s.d. is indicated in brackets, N represents the number of times the experiment was repeated.

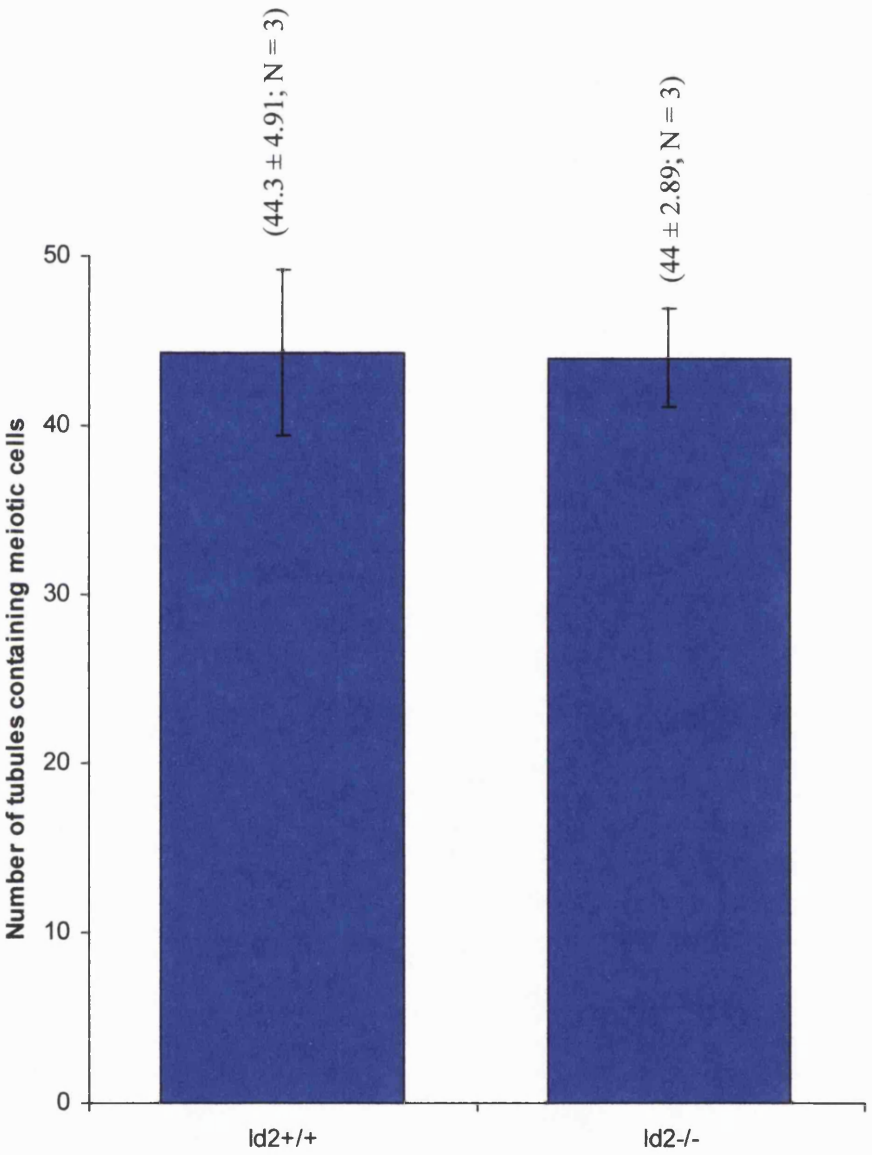

Figure 5.7 The number of seminiferous tubules containing cells in meiosis was not significantly different between wild-type (Id2+/+) and homozygous Id2 mutant (Id2-/-) testes. Mean ± s.d. is indicated in brackets, N represents the number of times the experiment was repeated.

compared to the wild-type. This difference was statistically significant by Student's *t*-test ($P < 0.05$). There was no significant difference in the mean number of tubules containing cells in meiosis between wild-type and homozygous Id2 mutant testis (figure 5.7). This was confirmed by Student's *t*-test ($P < 0.05$).

Table 5.1 is a summary of the quantitative data from the morphological and apoptosis analyses, indicating that apoptosis is increased in the Id2 knockout testis. Interestingly, apoptosis was increased in seminiferous tubules of the $Id2^{-/-}$ testis that appeared to be morphologically normal (table 5.1B), suggesting there that is an increased number of tubules undergoing defective spermatogenesis in the homozygous Id2 mutant testis than was evident by only the morphological criteria.

5.6 Sertoli Cell Numbers are not Affected in the Id2 Knockout Testis

Since Id2 protein is abundant in Sertoli cell nuclei (Sablitzky *et al.*, 1998), lack of Id2 protein may affect Sertoli cell development and/or function. The testis sections stained with haematoxylin and eosin showed large cytoplasmic bodies in the lumen of many $Id2^{-/-}$ seminiferous tubules (figures 5.3E, F, J, K, L and 5.4B, asterisks), which may be residual bodies. Residual bodies are normally phagocytosed by Sertoli cells, therefore this suggests a Sertoli cell defect in the $Id2^{-/-}$ mice. Sertoli cells in wild-type and homozygous mutant testis sections were examined using immunohistochemistry with anti-GATA-1 antibodies. GATA-1 is only expressed in the Sertoli cell lineage of the mouse testis, and is expressed only in stages VII, VIII and IX of spermatogenesis in the adult mouse (Yomogida *et al*, 1994). To compare the number of Sertoli cells in seminiferous tubules between wild-type and

homozygous Id2 mutant testes, the number of GATA-1 positive (GATA-1^+) Sertoli cells was quantified in tubules that were approximately the same size in wild-type and homozygous mutant testis sections. In light of the fact that not all seminiferous tubules in the homozygous mutant testis have defective spermatogenesis, the morphologically normal and abnormal tubules were considered separately. Ten seminiferous tubules were analysed in each case, and figure 5.8 shows examples of tubules used in this statistical analysis. As shown in figure 5.9, there was no significant difference in the mean number of Sertoli cells between $Id2^{+/+}$ tubules and morphologically normal $Id2^{-/-}$ tubules. Although the mean number of Sertoli cells appeared to be reduced in abnormal $Id2^{-/-}$ tubules compared to $Id2^{+/+}$, this difference was not statistically significant by Student's *t*-test ($P < 0.05$).

Since GATA-1 is expressed only in stages VII, VIII and IX of spermatogenesis, seminiferous tubules in these stages could be easily identified and compared between wild-type and homozygous Id2 mutant testes. Figures 5.8A and B show wild-type tubules in stage VII-VIII, which is associated with the presence of lots of mature sperm in the lumen of the seminiferous tubule. Figures 5.8C-F are $Id2^{-/-}$ seminiferous tubules in stage VII-VIII of spermatogenesis, showing reduced numbers of mature sperm in the tubule lumen compared to the wild-type. This comparison further supports the disrupted spermatogenesis of $Id2^{-/-}$ seminiferous tubules.

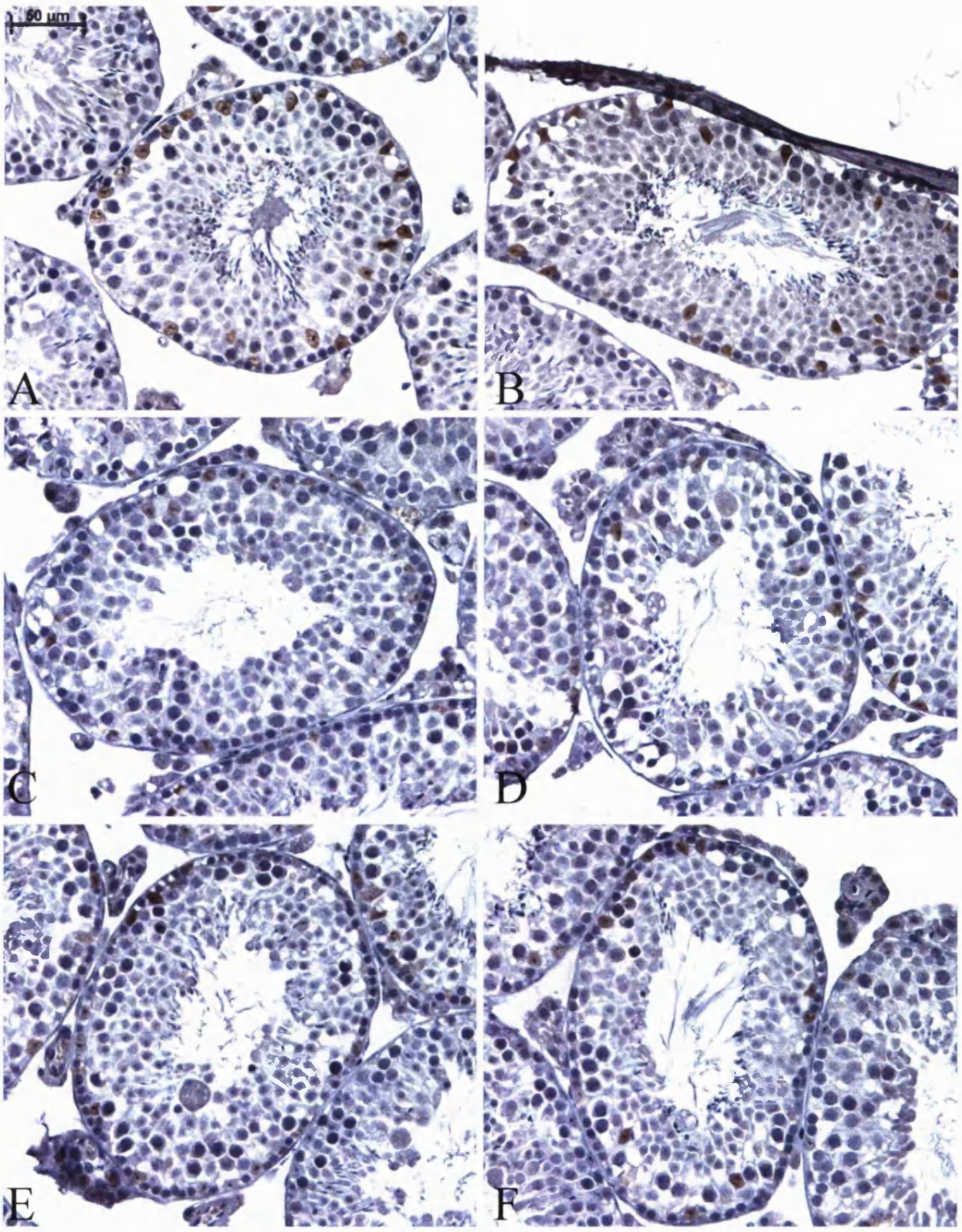

Figure 5.8 Comparison of seminiferous tubules in stage VII-VIII of spermatogenesis between wild-type (A, B) and Id2 null (C-F) testes. GATA-1 is expressed only in Sertoli cells of the testis, and a GATA-1-specific antibody was used to label Sertoli cells (brown) in $Id2^{+/+}$ and $Id2^{-/-}$ testis sections. GATA-1 is only expressed in stages VII, VIII and IX of spermatogenesis, and A-F show tubules from $Id2^{+/+}$ (A, B) and $Id2^{-/-}$ (C-F) testis sections in stage VII-VIII. Notably, the $Id2^{-/-}$ seminiferous tubules have reduced numbers of mature sperm. The stage of spermatogenesis of each tubule was confirmed using Russell *et al.* (1990).

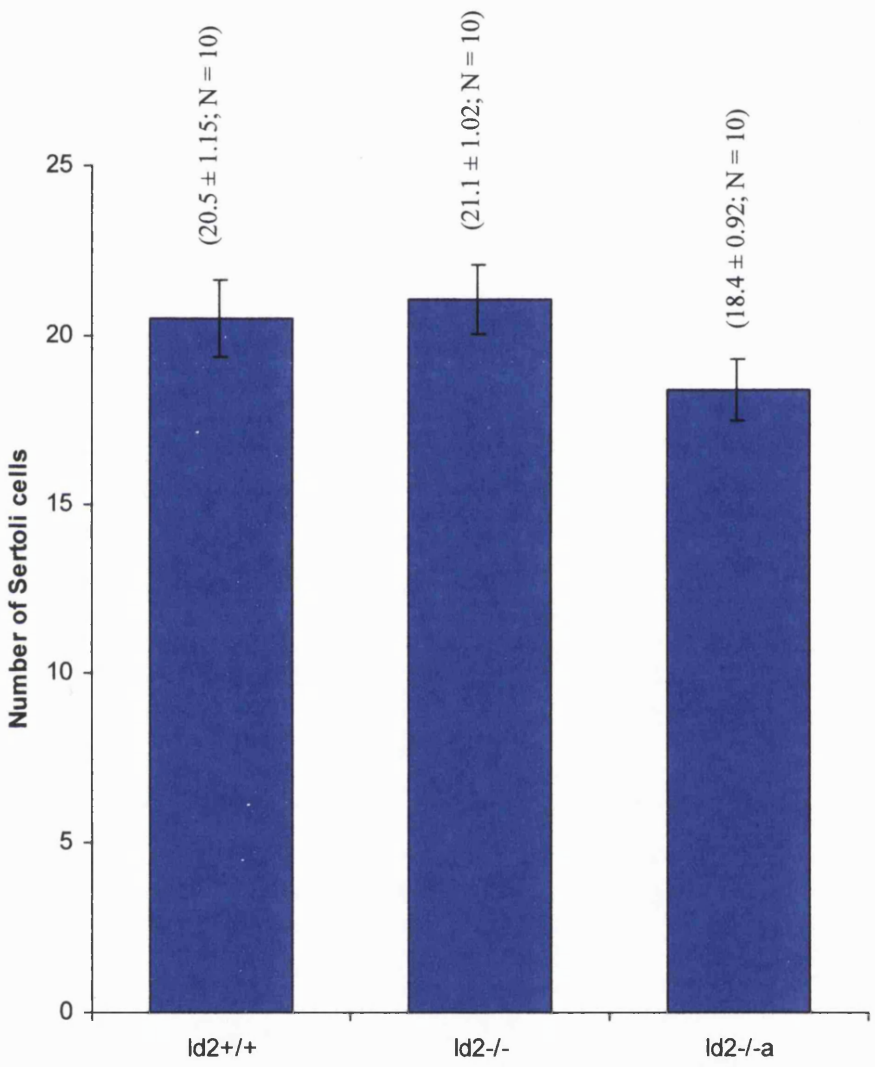

Figure 5.9 The number of Sertoli cells was not significantly different between wild-type (Id2+/+) and homozygous Id2 mutant (Id2-/-, Id2-/-a) seminiferous tubules. Id2-/- and Id2-/-a represent morphologically normal and abnormal tubules in the homozygous mutant testis, respectively. Mean ± s.d. is indicated in brackets, N represents the total number of seminiferous tubules analysed.

Chapter 6

Discussion

Id2 Function is Crucial for Normal Spermatogenesis

6.1 Male Id2 Knockout Mice Exhibit Reduced Fertility and Spermatogenesis Defects

Id2 protein was expressed in germ and Sertoli cells of the adult mouse testis, suggesting that Id2 plays a role in male fertility (Sablitzky *et al.*, 1998). This is now supported by the findings that adult $Id2^{-/-}$ male mice exhibit reduced fertility and spermatogenesis defects (chapter 5). We noticed that many of the male homozygous Id2 mutant mice were unable to produce offspring, indicating that Id2 is involved in male fertility. Although there was no significant difference in testis weight between $Id2^{+/+}$, $Id2^{+/-}$ and $Id2^{-/-}$ mice, 52 % of the seminiferous tubules in the $Id2^{-/-}$ testis showed morphological abnormalities, which reflected defective spermatogenesis, compared to 18 % of tubules in the wild-type testis. Defective spermatogenesis was exemplified by lack of maturing sperm within the tubule lumen, loss of the periphery-to-lumen development of sperm, and large cytoplasmic bodies in the lumen of tubules. The defects, and their severity, were variable between seminiferous tubules and were often only in a portion of the tubule epithelium. Apoptosis was also significantly increased in the Id2 knockout testis. Interestingly, apoptosis was increased approximately 2-fold (17 % in the $Id2^{-/-}$ compared to 9 % in the $Id2^{+/+}$) in morphologically normal seminiferous tubules in the $Id2^{-/-}$ testis, which suggests that in fact approximately 60 % of the seminiferous tubules in the homozygous Id2

mutant testis were undergoing defective spermatogenesis. Together, the results show that Id2 knockout males have reduced fertility, which correlates with germ cell loss and disorganised spermatogenesis.

Several recent reports have described mice with reduced fertility, which show impaired spermatogenesis in only a fraction of the seminiferous tubules of the testis, such as Bmp8a (Zhao *et al.*, 1998) and Hmgb2 (Ronfani *et al.*, 2001) mutant mice. These mice have a similar testis size to wild-type mice, but exhibit varied anomalies in the histological organisation of their seminiferous tubules, such as loss of periphery-to-lumen succession of germ cell development and increased apoptosis, reflecting impaired spermatogenesis. Therefore, the phenotypes observed in the Id2 mutant mice seem typical of mice with reduced fertility, supporting a role for Id2 in male fertility.

Since Id2 is expressed in germ and Sertoli cells of the testis, the defective spermatogenesis in $Id2^{-/-}$ mice could be due to failure of supporting Sertoli cells and/or cell-intrinsic defects in germ cells. Sablitzky *et al.* (1998) showed that only Id2 and Id3 proteins were expressed in mature, non-dividing Sertoli cells. Furthermore, Id2 was expressed in the nuclei of Sertoli cells, whereas Id3 was restricted to Sertoli cell cytoplasm. Although the expression of Id2 has only been investigated in the adult testis, it was tempting to speculate that lack of Id2 protein would disrupt Sertoli cell development as well as function. Since spermatogenesis is strictly dependent on the support of Sertoli cells, the defects in germ cell development as well as the increased apoptosis could be the result of insufficient support from Sertoli cells.

6.2 The Sertoli Cell

6.2.1 Id2 is not involved in Sertoli Cell Proliferation

The number of Sertoli cells in the adult Id2 knockout testis was not significantly different from the number in the wild-type testis (figure 5.9), suggesting that Id2 is not involved in the proliferation of Sertoli cells during perinatal development, and that defective spermatogenesis in $Id2^{-/-}$ mice is not the result of insufficient numbers of Sertoli cells in the testis to support germ cell development. Currently, it is not known if Id2 is expressed in Sertoli cells during foetal and neonatal life. Therefore, Id2 may not play a role in Sertoli cell proliferation because it is not expressed during the perinatal period when Sertoli cell proliferation occurs.

6.2.2 Id2 may be involved in Sertoli Cell Differentiated Functions

Although the Sertoli cell complement is not affected in the $Id2^{-/-}$ testis, the ability of $Id2^{-/-}$ Sertoli cells to support spermatogenesis may be impaired. We know that Id2 is expressed in the nuclei of post-mitotic Sertoli cells in the adult testis (Sablitzky *et al.*, 1998), therefore, Id2 could be involved in the regulation of Sertoli cell differentiated functions, which maintain spermatogenesis in the adult testis. Hence, the defective spermatogenesis in the $Id2^{-/-}$ testis may be the result of insufficient support from the Sertoli cells due to defects in their function. Although $Id2^{-/-}$ Sertoli cell functions have not yet been examined directly, several observations suggest that Sertoli cell function is impaired in $Id2^{-/-}$ mice, and thereby support a role for Id2 in the function of the post-mitotic Sertoli cell. The haematoxylin and eosin stained testis sections showed cytoplasmic bodies within the lumen of seminiferous tubules, which are probably residual bodies (figures 5.3 and 5.4). Sertoli cells normally rapidly phagocytose residual bodies following spermiation. Hence, few residual bodies were

evident in the wild-type testis. However, residual bodies were observed in numerous seminiferous tubules of the $Id2^{-/-}$ testis, suggesting a defect in Sertoli cell function in the absence of Id2.

A recent paper highlighted the importance of Sertoli cell function for Sertoli cells to support normal spermatogenesis (Wreford *et al.*, 2001). Wreford *et al.* (2001) showed that the ability of Sertoli cells to nurture germ cells was compromised in mice with diminished FSH action, exemplified by a decrease in the round spermatid to Sertoli cell ratio in the testis. Since FSH regulates Sertoli cell differentiated functions, this study demonstrates that the functions of the Sertoli cell are important in its ability to support spermatogenesis.

A paper by Chaudhary *et al.* (2001), which was published during the preparation of this work, strongly supports a role for Id2 in Sertoli cell differentiated functions. This study focused on the expression and function of Id proteins in the post-mitotic rat Sertoli cell *in vitro*. FSH was used to stimulate cultured Sertoli cell differentiated functions. Chaudhary *et al.* (2001) found that Id2 was expressed in FSH-stimulated Sertoli cells. Furthermore, using transient transfection assays, the authors showed that the presence of Id2 antisense oligonucleotide in Sertoli cells downregulated transferrin promoter activity in response to FSH, and that ectopic expression of Id2 increased transferrin promoter activation. Taken together, this data strongly supports a role for Id2 in the regulation of post-mitotic Sertoli cell differentiated functions, such as transferrin expression. Although Chaudhary *et al.* (2001) showed that Id3 and Id4 mRNAs were also expressed in FSH-stimulated post-mitotic Sertoli cells *in vitro*, the immunohisological analysis by Sablitzky *et al.* (1998) indicated that only Id2 and Id3 proteins were expressed in the post-mitotic Sertoli cell *in vivo*. Id2 and

Id3 protein expression in the post-mitotic Sertoli cell suggests that both these factors have a role in maintaining Sertoli cell function. Moreover, the expression of Id2 in the nucleus and Id3 in the cytoplasm of Sertoli cells indicates that they may have distinct functions within this cell type.

The long-standing view is that Id levels are high in proliferative, undifferentiated cells, and are downregulated upon induction of differentiation, indicating their functions as negative regulators of cell differentiation and positive regulators of cell growth (section 1.1.1). Indeed, Chaudhary *et al.* (2001) showed that Id1 expression was downregulated by FSH in post-mitotic Sertoli cells *in vitro*. This group have also shown that overexpression of Id1 in Sertoli cells inhibits the ability of FSH to stimulate transferrin promoter activity, and furthermore, when Id1 mRNA levels are decreased using an antisense oligonucleotide, FSH-mediated transferrin promoter activation is increased (Chaudhary *et al.*, 1997, 2001). Together, these observations indicate, as anticipated, that Id1 is a negative regulator of Sertoli cell differentiation. In contrast, Id2 appears to play a role in post-mitotic Sertoli cell differentiated functions. Several recent studies have also indicated that Id proteins may function as positive regulators of differentiation in particular cell types (Chen *et al.*, 1999; Janatpour *et al.*, 2000; Liu *et al.*, 2000). Liu *et al.* (2000) found that Id2 expression was increased with terminal differentiation of alveolar epithelial cells (AECs), suggesting that Id2 can act as a positive regulator of differentiation in this cell type. The authors speculated that, since Id2 induces differentiation and inhibits proliferation in adult AECs, Id2 is required for determination and maintenance of the differentiated state of AECs. In another study, expression of Id4 was upregulated during adipose cell differentiation *in vitro*, and was found in mouse and human

adipose tissue, which suggests that Id4 may be involved in the regulation of adipocyte differentiation and function (Chen *et al.*, 1999).

6.2.2.1 How might Id2 Regulate Sertoli Cell Functions?

The mechanism by which Id2 regulates Sertoli cell function is a focus for subsequent research. Id proteins modulate the transcriptional activity of bHLH proteins by sequestering these proteins in non-functional heterodimers, and therefore act as dominant negative regulators of bHLH protein function. Considerable research has demonstrated that bHLH transcription factors may be involved in Sertoli cell differentiation. Therefore, a speculation is that Id2 may inhibit a specific bHLH transcription complex(s) that normally represses Sertoli cell differentiated functions.

FSH and PmodS modulate the differentiated functions of Sertoli cells, including stimulation of transferrin gene expression (Skinner and Griswold, 1980; Skinner and Fitz, 1985; Norton and Skinner 1989; Skinner *et al.*, 1988, 1989). Investigation of the transcriptional regulation of transferrin gene expression has provided insight into the control of Sertoli cell differentiation. Chaudhary and Skinner (1999) demonstrated that the activity of the mouse transferrin gene is regulated by at least two different pathways in Sertoli cells. One involves cAMP response element binding protein (CREB) binding to a cAMP response element (CRE)-like PRII region in the transferrin promoter, and the other involves bHLH proteins binding to an E box response element (figure 6.1). The authors showed that optimal activation of the transferrin promoter by FSH required both E box and PRII elements of the promoter, where the PRII region regulated the PKA-mediated activation of the promoter. For PmodS-induced stimulation of the transferrin promoter, only the E box was required. PmodS activity does not act through the cAMP-PKA pathway (Norton and Skinner

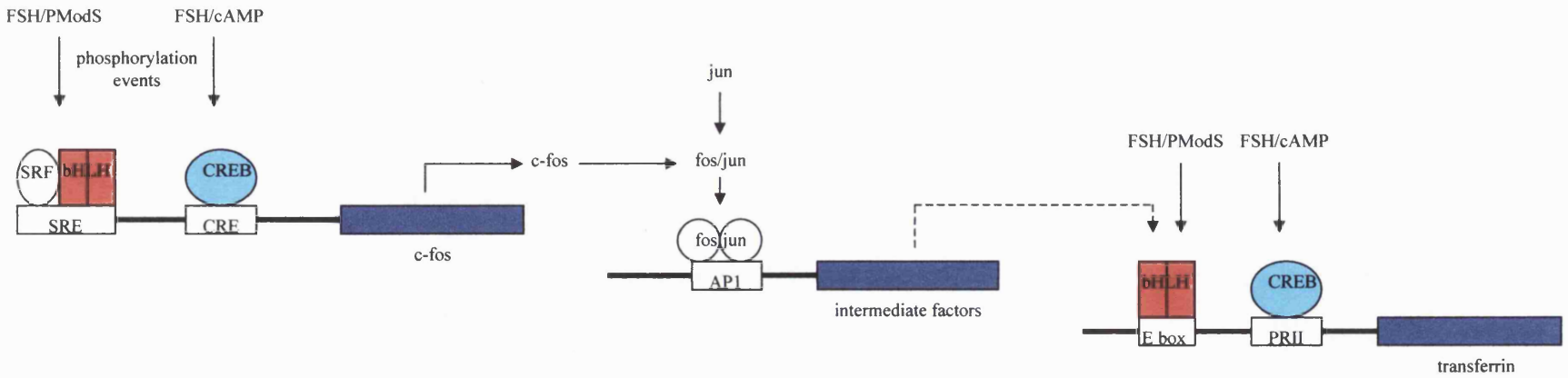

Figure 6.1 A representation of the proposed cascade of events involved in Sertoli cell differentiated gene expression. Refer to section 6.2.2.1 for details

1989; Chaudhary and Skinner 1999). Potential E box, PRII and CRE response elements have been identified in the promoters of a number of Sertoli cell genes, suggesting this could be a general phenomenon for regulation of Sertoli cell gene transcription (Chaudhary *et al.*, 1997; Chaudhary and Skinner, 1999).

The immediate-early gene c-*fos* is involved in the regulation of Sertoli cell differentiated functions by FSH and PmodS (figure 6.1; Norton and Skinner, 1992; Whaley *et al.*, 1995; Chaudhary *et al.*, 1996; Chaudhary and Skinner, 1999b). FSH and PmodS activate the c-*fos* promoter primarily at the level of the *cis*-acting serum response element (SRE), which binds serum response factor (SRF; Whaley *et al.*, 1995; Chaudhary *et al.*, 1996). However, a consensus CRE site is also present in the c-*fos* promoter, which can be activated by FSH (Chaudhary *et al.*, 1996). c-*fos* forms a dimer with c-*jun* and binds to the AP-1 site to activate transcription (Angel and Karin, 1991). Since the transferrin promoter does not contain an AP-1 binding site, intermediate transcription factor(s) under the control of c-*fos* may regulate the activity of downstream Sertoli cell differentiated genes, such as transferrin expression (Whaley *et al.*, 1995; Chaudhary and Skinner, 1999b). Chaudhary and Skinner (1999b) demonstrated that in Sertoli cells, hormone-induced c-*fos* promoter activation is influenced by bHLH proteins, which act at an E box within the SRE of the promoter (Chaudhary and Skinner, 1999b). They also indicate that formation of a multiprotein complex between SRF and E12/E47/bHLH dimer at the SRE may be required for efficient transcription of the c-*fos* gene. Together, the studies suggest that bHLH proteins may be involved in regulating differentiated gene expression in Sertoli cells, at the level of immediate-early event genes (e.g. c-*fos*) and downstream Sertoli cell differentiated genes (e.g. transferrin). The role of Id2 in the differentiated Sertoli cell may be to inhibit a specific bHLH transcription factor complex(s) that

normally represses transcription of c-*fos* and/or transferrin. Sertoli cells have been shown to express the ubiquitous class A bHLH protein E47 (Chaudhary and Skinner, 1999a). Since Id proteins associate avidly with class A bHLH proteins, Id2 may influence bHLH complexes in Sertoli cells by sequestering E47. However, E47 is also involved in bHLH transcription factor complexes that activate differentiated gene expression in Sertoli cells (Chaudhary and Skinner, 1999, 1999b). Therefore, there must be more specificity in the action of Id2. The possibility exists that E47 forms heterodimers with different, as yet unknown, cell-specific bHLH factors within the Sertoli cell, and that these heterodimers may differentially regulate the activity of genes involved in Sertoli cell differentiation. In light of this, Id2 may inhibit only specific bHLH heterodimer complexes, which function to repress Sertoli cell differentiated function. Although Id2 probably functions by sequestering bHLH transcription factors, it is possible that the activity of Id2 involves other HLH-mediated interactions or is independent of the HLH domain. The ability of Id2 to promote apoptosis resides in its N-terminal region (Florio *et al.*, 1998). The paper presented by Chaudhary *et al.* (2001) has shown that Id2 may be involved in the regulation of transferrin promoter activation. The role of Id2 in the transcriptional activation of the c-*fos* promoter in Sertoli cells is currently unknown.

Liu *et al.* (2000) recently showed that in A549 lung epithelial cells, Id2 inhibits the activity of the cyclin A promoter, which functions throughout S phase and is required for DNA replication (Knudsen *et al.*, 1998), and thereby promotes differentiation. The speculation presented was that Id2 negatively regulates a bHLH transcription factor complex that is involved in activation of the cyclin A promoter. This suggests that Id2 may affect cell cycle regulatory genes, through which Id2 could influence cellular proliferation and differentiation.

6.3 The Germ Cell

Although considerable evidence supports a role for Id2 in the Sertoli cell of the testis, the stage- and subcellular-specific expression of Id2 protein in germ cells during spermatogenesis (Sablitzky *et al.*, 1998) implies Id2 has an important functional role(s) during meiotic and post-meiotic development in spermatogenesis. Hence, the defective spermatogenesis in $Id2^{-/-}$ mice could also be a result of cell-autonomous defects in germ cells during their development. Id2 protein was not expressed in spermatogonia or germ cells entering meiotic prophase. Zygotene spermatocytes expressed low levels of Id2 in the cytoplasm, which was upregulated in pachytene and diplotene spermatocytes. Id2 did not appear to be associated with any subcellular organelles or structures in the cytoplasm. Also, Id2 was expressed in a punctate pattern within the nucleus of pachytene and diplotene spermatocytes, but did not coincide with the nucleolus. Cells undergoing meiotic division did not express Id2 protein. Low levels of Id2 were expressed in the cytoplasm of early round spermatids, which continued and increased during spermatid maturation as the cytoplasmic volume decreased. In addition, a focus of high Id2 expression overlaid the acrosomal granule within the acrosomal vesicle of developing spermatids. The dynamics of Id2 protein expression indicate that Id2 could play a role in the regulation of gene expression during late pachytene and diplotene stages of meiosis. In spermatid maturation, Id2 may be involved in acrosomal granule development as well as cytoplasmic regulatory mechanisms. Taken together, it is plausible to say that particular stages of spermatogenesis may be affected in the $Id2^{-/-}$ testis, contributing, at least in part, to the defective spermatogenesis observed in the male Id2 knockout mice.

Although the results show that spermatogenesis is affected in the $Id2^{-/-}$ testis, they do not clearly indicate a stage in development at which spermatogenesis becomes impaired by the absence of Id2. The defects in spermatogenesis, and their severity, varied between seminiferous tubules in the $Id2^{-/-}$ testis. Considering the expression pattern of Id2 protein in spermatogenesis (Sablitzky *et al.*, 1998), Id2 is first expressed during meiosis, where its expression is stage- and subcellular-specific. Therefore, we can suggest that meiosis will be affected in the $Id2^{-/-}$ testis. In haematoxylin and eosin stained testis sections, the $Id2^{-/-}$ spermatocyte population appeared to be relatively normal (figures 5.2 and 5.3), but the TUNEL assay suggested that spermatocytes in the $Id2^{-/-}$ seminiferous tubules were undergoing apoptosis (figure 5.5). However, there was no significant difference in the number of tubules in meiosis between Id2 knockout and wild-type testes (figure 5.7). Round spermatids show classic morphological apoptotic features and often degenerate en mass, as multinucleated symplasts, reflecting the incomplete cytokinesis of spermatogenesis (Russell *et al.*, 1990). In the Id2 knockout testis, many apoptotic structures are multinucleated (figures 5.3 and 5.5), suggesting that round spermatids lacking Id2 may undergo apoptosis more frequently. Since Id2 protein is expressed in the acrosomal region and cytoplasm of round spermatids (Sablitzky *et al.*, 1998), it is plausible that round spermatid development is affected in the absence of Id2, resulting in increased apoptosis. Taken together, these observations would support the decreased numbers of elongating and condensing spermatids, and spermatozoa observed in $Id2^{-/-}$ seminiferous tubules. It is significant to note that impaired Sertoli cell function in the $Id2^{-/-}$ testis could affect all stages of germ cell development, including those where Id2 is not expressed, resulting in defective spermatogenesis.

In most stages of spermatogenesis, the expression of Id proteins is not overlapping (Sablitzky *et al.*, 1998). This suggests that the Id proteins have distinct functions during spermatogenesis and that another Id protein cannot compensate for Id2 in $Id2^{-/-}$ spermatogenesis. For example, during meiosis, Id2 is expressed in the cytoplasm of zygotene, pachytene and diplotene primary spermatocytes, and in the nucleus of late pachytene and diplotene spermatocytes in a punctate pattern that does not coincide with the nucleolus. Id1 is also expressed at low levels in the cytoplasm of primary spermatocytes, but unlike Id2, Id1 is often associated with cytoplasmic organelles or structures. Since Id4 protein expression is localised to a juxta- or peri-nucleolar region within the nucleus of late pachytene and diplotene spermatocytes, the function of Id2 during meiosis is unlikely to be compensated for by either Id1 or Id4, and Id3 protein is not expressed in developing germ cells. An exception to this may occur during spermatid maturation, where Id1 and Id2 expression may be overlapping in the cytoplasm of elongating and condensing spermatids, suggesting that they could have redundant functions during this stage of development and that Id1 could compensate for Id2. The molecular mechanism(s) by which Id2 regulates particular stages of germ cell development remains elusive. Potential bHLH protein candidates with which Id2 could interact have yet to be identified. Id2 is also known to bind and negatively regulate the function of other proteins, such as the retinoblastoma protein (pRb).

6.4 Summary: Id2 Function is Crucial for Normal Spermatogenesis

In summary, the Id2 knockout mice have reduced fertility and spermatogenesis defects. Id2 may be involved in Sertoli cell differentiation during puberty and the

maintenance of Sertoli cell differentiated functions in the adult testis. Also, Id2 could play a role in meiotic and post-meiotic development of sperm during spermatogenesis. To understand the role(s) of Id2 in the testis, Sertoli cell function and germ cell development in the absence of Id2 must be investigated without the influence of each other. Although questions remain on where and how Id2 exerts its function in the testis, the results clearly demonstrate that Id2 function, be it in the Sertoli cell and/or germ cell development, is crucial for normal spermatogenesis.

6.5 Future Work

Future work to elucidate the role(s) of Id2 in the seminiferous epithelium will include the technique of testicular germ cell transplantation. This technique was pioneered in the laboratory of Ralph Brinster (University of Pennsylvania, Philadelphia. PA, USA). Germ cell transplantation involves microinjection of a mixed population of germ cells from a donor testis into the seminiferous tubules, rete testis or efferent ductules of a recipient mouse testis (Brinster and Zimmermann, 1994; Ogawa *et al.*, 1997). In this technique, mice that have no endogenous spermatogenesis, such as the W/W^V mutant (c-kit receptor mutant), are used as germ cell recipients, or recipient mice are made infertile by treatment with chemotherapeutic busulfan at a dose that eliminates most germ cells from the testis. The testicular somatic cell environment is unaffected in these recipients. Using this technique with the Id2 mutant mice will enable us to identify the testicular cell type(s) where Id2 is important in the testis. If $Id2^{-/-}$ germ cells are injected into W/W^V or busulfan-treated wild-type recipients, the resulting spermatogenesis will indicate if Id2 function is important for germ cell development, as there would be normal Sertoli cell support in these testes. In a similar approach, transplantation of wild-type germ cells into busulfan-treated $Id2^{-/-}$

males will provide insight into the ability of $Id2^{-/-}$ Sertoli cells to support normal spermatogenesis. Therefore, germ cell transplantation will allow the influence on somatic and germ cell function in Id2 mutant mice to be differentiated experimentally. This will indicate whether the reduced fertility in these mice results from defects in somatic and/or germ cell function in the testis. These experiments would also provide testes models in which we could further study $Id2^{-/-}$ Sertoli cell function and spermatogenesis independently.

In haematoxylin and eosin stained testis sections, it was often difficult to identify the germ cell types. Therefore, the use of more specialised histochemical stains will be more advantageous in the future. Periodic Acid Schiff (PAS) is a stain that targets carbohydrate moieties, which specifically stains the acrosome of the spermatid. The characteristics of the developing acrosomal system can be used to identify steps of spermiogenesis, which were classified based on changes in the acrosome and nuclear shape of spermatids. Not only will this stain be more useful to identify cell types within the seminiferous tubule and therefore stages of spermatogenesis, but it will highlight the acrosomal region, which is anticipated to be affected in the $Id2^{-/-}$ mice. Further histological analyses of the testes will include markers for particular cell types in the seminiferous tubule, such as spermatogonia, so that the stage(s) that is affected in the mutant testis may be more easily identified. For example, proliferating spermatogonia can be identified by expression of EE2 (Koshimizu *et al.*, 1995). In addition, electron microscopy of testis sections may reveal anomalies that are not evident by light microscopy. To quantify the reduction in spermatozoa in the Id2 mutant testis, seminal fluid will be extracted from the epididymis and analysed. Extracted spermatozoa can also be examined for motility and fertility in *in vitro* assays.

To begin investigating the effect of Id2 deficiency in Sertoli cells, Sertoli cell RNA from $Id2^{+/+}$ and $Id2^{-/-}$ mice is to be analysed with a panel of Sertoli cell-specific genes, such as c-*fos*, transferrin, SF-1 and FSH receptor. The results of this will reflect the differentiated state of the Sertoli cell, and indicate pathways and factors with which Id2 may be involved in the Sertoli cell. In another approach, $Id2^{-/-}$ Sertoli cells could be isolated and analysed in culture. For example, in transient transfection assays, we would expect activity of the transferrin promoter in response to FSH to be lower in $Id2^{-/-}$ than $Id2^{+/+}$ Sertoli cells, and introduction of Id2 into $Id2^{-/-}$ Sertoli cells to restore the activity to wild-type levels. Therefore, manipulation of Sertoli cells *in vitro* will support and provide insight into Id2 function in the Sertoli cell.

This work has focused on spermatogenesis in the testes of adult mice. Therefore, it will be both interesting and important to extend this research to include the affect on initiation of spermatogenesis (juvenile mice) as well as on spermatogenesis with advancing age. Defective spermatogenesis often becomes progressively more severe as males age, such as in Hmgb2 deficient mice (Ronfani *et al.*, 2001) or triple knockout mice for Tryo3, Axl and Mer receptors (Lu *et al.*, 1999).

References

Anderson, D. J. (2001). Stem cells and pattern formation in the nervous system: the possible versus the actual. Neuron 30, 19-35.

Andres-Barquin, P. J., Hernandez, M. C., Hayes, T. E., McKay, R. D., and Israel, M. A. (1997). Id genes encoding inhibitors of transcription are expressed during *in vitro* astrocyte differentiation and in cell lines derived from astrocytic tumors. Cancer Res. 57, 215-220.

Andres-Barquin, P. J., Hernandez, M. C., and Israel, M. A. (1999). Id4 expression induces apoptosis in astrocytic cultures and is down-regulated by activation of cAMP-dependent signal transduction pathway. Exp. Cell. Res. 247, 347-355.

Andres-Barquin, P. J., Hernandez, M. C., and Israel, M. A. (2000). Id genes in nervous system development. Histol. Histopathol. 15, 603-618.

Angel, P., and Karin, M. (1991). The role of jun, fos and the AP-1 complex in cell proliferation and transformation. Biochim. Biophys. Acta. 1072, 129-157.

Artavanis-Tsakonas, S., Rand, M. D., and Lake, R. J. (1999). Notch signalling: cell fate control and signal integration in development. Science 284, 770-776.

Askew, D. S., Ashmun, R. A., Simmons, B. C., and Cleveland, J. L. (1991). Constitutive c-myc expression in an IL-3-dependent cell line suppresses cell cycle arrest and accelerates apoptosis. Oncogene 6, 1915-1922.

Atherton, G., Travers, H., Deed, R., and Norton, J. D. (1996). Regulation of cell differentiation in C2C12 myoblasts by the Id3 helix-loop-helix protein. Cell Growth Diff. 7, 1059-1066.

Baker, P. J., and O'Shaughnessy, P. J. (2001). Role of gonadotrophins in regulating numbers of leydig and Sertoli cells during fetal and postnatal development of mice. Reproduction 122, 227-234.

Bao, Z. Z., and Cepko, C. L. (1997). The expression and function of Notch pathway genes in the developing rat eye. J. Neurosci. 17, 1425-1434.

Barone, M. V., Pepperkok, R., Peverali, F. A., and Philipson, L. (1994). Id proteins control cell growth induction in mammalian cells. Proc. Natl. Acad. Sci. USA 91, 4985-4988.

Barres, B. A., Lazar, M. A., and Raff, M. C. (1994). A novel role for thyroid hormone, glucocorticoids and retinoic acid in the timing of oligodendrocyte development. Development 120, 1097-1108.

Barres, B. A., and Raff, M. C. (1994). Control of oligodendrocyte number in the developing rat optic nerve. Neuron 12, 935-942.

Bayer, S. A., and Altman, J. (1991). In: Neocortical Development (Second Edition). New York: Raven Press.

Benezra, R., Davis, R., Lockshon, D., Turner, D., and Weintraub, H. (1990). The protein Id – a negative regulator of helix-loop-helix DNA binding proteins. Cell 61, 49-59.

Biggs, J., Murphy, E. V., and Israel, M. A. (1992). A human Id-like helix-loop-helix protein expressed during early development. Proc. Natl. Acad. Sci. USA 89, 1512-1516.

Bloch, B., Popovivi, T., Levin, M. J., Tuil, D., and Kahn, A. (1985). Transferrin gene expression visualised in oligodendrocytes of the rat brain by using *in situ* hybridisation and immunohistochemistry. Proc. Natl. Acad. Sci. USA 82, 6706-6710.

Bonni, A., Sun, Y., Nadal-Vicens, M., Bhatt, A., Frank, D. A., Rozovsky, I., Stahl, N., Yancopoulos, G. D., and Greenberg, M. E. (1997). Regulation of gliogenesis in the central nervous system by the JAK-STAT signalling pathway. Science 278, 477-483.

Bortolussi, M., Zanchetta, R., Belvedere, P., and Colombo, L. (1990). Sertoli and leydig cell numbers and gonadotrophin receptors in rat testis from birth to puberty. Cell and Tissue Research 260, 185-191.

Brinster, R. L., and Zimmermann, J. W. (1994). Spermatogenesis following male germ cell transplantation. Proc. Natl. Acad. Sci. USA 91, 11298-11302.

Briscoe, J., Pierani, A., Jessell, T. M., and Ericson, J. (2000). A homeodomain protein code specifies progenitor cell identity and neuronal fate in the ventral neural tube. Cell 101, 435-445.

Briscoe, J., and Ericson, J. (2001). Specification of neuronal fates in the ventral neural tube. Curr. Opin. Neurobiol. 11, 43-49.

Cahill, M. A., Janknecht, R., and Nordheim, A. (1996). Signalling pathways: jack of all cascades. Curr. Biol. 6, 16-19.

Cai, J., Xu, X., Yin, H., Wu, R., Modderman, G., Chen, Y., Jensen, J., Hui, C. C., and Qiu, M. (2000). Evidence for the differential regulation of Nkx-6.1 expression in the ventral spinal cord and foregut by Shh-dependent and -independent mechanisms. Genesis 27, 6-11.

Cai, L., Morrow, E. M., and Cepko, C. L. (2000a). Misexpression of basic helix-loop-helix genes in the murine cerebral cortex affects cell fate choices and neuronal survival. Development 127, 3021-3030.

Casarosa, S., Fode, C., and Guillemot, F. (1999). Mash1 regulates neurogenesis in the ventral telencephalon. Development 127, 3021-3030.

Cau, E., Gradwohl, G., Fode, C., and Guillemot, F. (1997). Mash1 activates a cascade of bHLH regulators in olfactory neuron progenitors. Development 124, 1611-1621.

Chalpin, D. D., and Fu, Y. (1998). Cytokine regulation of secondary lymphoid organ development. Curr. Opin. Immunol. 10, 289-297.

Chaudhary, J., Whaley, P. D., Cupp, A., Skinner, M. K. (1996). Transcriptional regulation of Sertoli cell differentiation by follicle stimulating hormone at the level of the c-fos and transferrin promoters. Biol. Reproduction 54, 692-699.

Chaudhary, J., Cupp, A. S., and Skinner, M. K. (1997). Role of basic-helix-loop-helix factors in Sertoli cell differentiation: Identification of an E-box response element in the transferrin promoter. Endocrinology 138, 667-675.

Chaudhary, J., Kim, G., and Skinner, M. K. (1999). Expression of the basic helix-loop-helix protein REBα in rat testicular Sertoli cells. Biol. Reprod. 60, 1244-1250.

Chaudhary, J., and Skinner, M. K. (1999). E box and cyclic adenosine monophosphate response elements are both required for follicle stimulating hormone-induced transferrin promoter activation in Sertoli cells. Endocrinology 140, 1262-1271.

Chaudhary, J., and Skinner, M. K. (1999a). The basic helix-loop-helix E2A gene product E47, not E12, is present in differentiating Sertoli cells. Mol. Reprod. Dev. 52, 1-8.

Chaudhary, J., and Skinner, M. K. (1999b). Basic helix-loop-helix proteins can act at the E box within the serum response element of the c-fos promoter to influence hormone-induced promoter activation in Sertoli cells. Mol. Endocrinology 13, 774-786.

Chaudhary, J., Johnson, J., Kim, G., and Skinner, M. K. (2001). Hormonal regulation and differential actions of the helix-loop-helix transcriptional inhibitors of differentiation (Id1, Id2, Id3 and Id4) in Sertoli cells. Endocrinology 142, 1727-1736.

Chen, H., Thiagalingam, A., Chopra, H., Borges, M. W., Feder, J. N., Nelkin, B. D., Baylin, S. B., and Ball, D. W. (1997). Conservation of the Drosophila lateral inhibition pathway in human lung cancer: a hairy-related protein (HES-1) directly represses achaete-scute homolog-1 expression. Proc. Natl. Acad. Sci. USA 94, 5355-5360.

Chen, H., Weng, Y. C., Schatteman, G. C., Sanders, L., Christy, R. J., and Christy, B. A. (1999). Expression of the dominant negative regulator Id4 is induced during adipocyte differentiation. Biochem. Biophys. Res. Commun. 256, 614-619.

Choi, B. H., and Lapham, L. W. (1978). Radial glia in the human fetal cerebrum: a combined Golgi, immunofluorescent and electron microscopic study. Brain Res. 148, 295-311.

Christy, B. A., Sanders, L. K., Lau, L. F., Coupland, N. G., Jenkins, N. A., and Nathans, D. (1991). An Id-related helix-loop-helix protein encoded by a growth factor inducible gene. Proc. Natl. Acad. Sci. USA 88, 1815-1819.

Clermont, Y., and Harvey, S. G. (1965). Duration of the cycle of the seminiferous epithelium of normal hypophysectomised and hypophysectomised-hormone treated albino rats. Endocrinology 76, 80-89.

Cook, P. S., Hess, R. A., Procelli, J., and Meisami, E. (1991). Increased sperm production in adult rats after transient neonatal hypothyroidism. Endocrinology 129, 244-248.

Cooper, C. L., and Newburger, P. E. (1998). Differential expression of Id genes in multipotent myeloid progenitor cells: Id1 is induced by early and late-acting cytokines while Id2 is selectively induced by cytokines that drive terminal granulocytic differentiation. J. Cell. Biochem. 71, 277-285.

Couchie, D., Fages, C., Bridoux, A. M., Rolland, B., Tardy, M., and Nunez, J. (1985). Microtubule-associated proteins and *in vitro* astrocyte differentiation. J. Cell. Biol. 101, 2095-2103.

Cunningham, G. R., and Huckins, C. (1979). Persistence of complete spermatogenesis in the presence of low intra-testicular concentration of testosterone. Endocrinology 105, 177-186.

Daggett, M. A., Rice, D. A., Heckert, L. L. (2000). Expression of steroidogenic factor 1 in the testis requires an E box and CCAAT box in its promoter proximal region. Biol. Reprod. 62, 670-679.

Davis, A., and Temple, S. (1994). A self-renewing multipotent stem cell in embryonic rat cerebral cortex. Nature 372, 263-266.

De Togni, P., Goellner, J., Ruddle, N. H., Streeter, P. R., Fick, A., Mariathasan, S., Smith, S. C., Carlson, R., Shornick, L. P., Strauss-Schoenberger, J., *et al.* (1994). Abnormal development of peripheral lymphoid organs in mice deficient in lymphotoxin. Science 264, 703-707.

Deed, R. W., Bianchi, S. M., Atherton, G. T., Johnston, D., Santibanez-Koref, M., Murphy, J. J., and Norton, J. D. (1993). An immediate early human gene encodes an Id-like helix-loop-helix protein and is regulated by protein kinase C activation in diverse cell types. Oncogene 8, 599-607.

Deed, R. W., Hirose, T., Mitchell, E. L. D., Santibanez-Koref, M. F., and Norton, J. D. (1994). Structural organisation and chromosomal mapping of the human Id3 gene. Gene 151, 309-314.

Deed, R. W., Hara, E., Atherton, G. T., Peters, G., and Norton, J. D. (1997). Regulation of Id3 cell cycle function by Cdk2-dependent phosphorylation. Mol. Cell. Biol. 17, 6815-6821.

Desprez, P-Y., Hara, E., Bissell, M. J., and Campisi, J. (1995). Suppression of mammary epithelial cell differentiation by the helix-loop-helix protein Id1. Mol. Cell. Biol. 15, 3398-3404.

Dorshkind, K. (1994). Transcriptional control points during lymphopoiesis. Cell 79, 751-753.

Dorsky, R. I., Rapaport, D. H., and Harris, W. A. (1995). Xotch inhibits cell differentiation in the Xenopus retina. Neuron 14, 487-496.

Duncan, M. K., DiCicco Bloom, E. M., Xiang, X., Benezra, R., and Chada, K. K. (1992). The gene for the helix-loop-helix proteins, Id, is specifically expressed in neural precursors. Dev. Biol. 154, 1-10.

Duncan, M. K., Bordas, L., DiCicco Bloom, E. M., and Chada, K. K. (1997). Expression of the helix-loop-helix genes Id-1 and NSCL-1 during cerebellar development. Dev. Dyn. 208, 107-114.

Durand, B., Fero, M. L., Roberts, J. M., and Raff, M. C. (1997). P27Kip1 alters the response of cells to mitogen and is part of a cell-intrinsic timer that arrests the cell cycle and initiates differentiation. EMBO J. 16, 306-317.

Durand, B., and Raff, M. C. (2000). A cell-intrinsic timer that operates during oligodendrocyte development. Bioessays 22, 64-71.

Dym, M., and Fawcett, D. W. (1970). The blood-testis barrier in the rat and the physiological compartmentation of the seminiferous epithelium. Biol. Reprod. 3, 308-326.

Dym, M. (1977). The role of the Sertoli cell in spermatogenesis. In: Male Reproductive System (R. Yates and M. Gorden, eds). New York: Raven Press, 155-169.

Dym, M., and Caviccia, J. C. (1977). Further observations on the blood-testis barrier in monkeys. Biol. Reprod. 117, 390-403.

Einarson, M. B., and Chao, M. V. (1995). Regulation of Id1 and its association with basic helix-loop-helix proteins during nerve growth factor-induced differentiation of PC12 cells. Mol. Cell. Biol. 15, 4175-4183.

Ellis, H. M., Spann, D. R., and Posakony, J. W. (1990). Extramacrochaetae, a negative regulator of sensory organ development in Drosophila, defines a new class of helix-loop-helix proteins. Cell 61, 27-37.

Ellmeier, W., Aguzzi, A., Kleiner, E., Kurzbauer, R., and Weith, A. (1992). Mutually exclusive expression of a helix-loop-helix gene and N-myc in human neuroblastomas and in normal development. EMBO J. 11, 2563-2571.

Ericson, J., Rashbass, P., Schedl, A., Brenner-Morton, S., Kawakami, A., van Heyningen, V., Jessell, T. M., and Briscoe, J. (1997). Pax6 controls progenitor cell identity and neuronal fate in response to graded Shh signaling. Cell 90, 169-180.

Evan, G. I., Whyllie, A. H., Gilbert, C. S., Littlewood, D. T., Land, H., Brooks, M., Waters, C. M., Penn, L. Z., and Hancock, D. C. (1992). Induction of apoptosis in fibroblasts by c-myc protein. Cell 69, 119-128.

Evans, S. M., and O'Brien, T. X. (1993). Expression of the helix-loop-helix factor Id during mouse embryonic development. Dev. Biol. 159, 485-499.

Fakunding, J. L., Tindall, D. J., Dedman, J. R., Mena, C. R., and Means, A. R. (1976). Biochemical actions of follicle-stimulating hormone in Sertoli cells of the rat testis. Endocrinology 98, 392-402.

Fawcett, D. W., Ito, S., and Slautterback, D. L. (1959). The occurrence and intracellular bridges in groups of cells exhibiting synchronous differentiation. J. Biophys. Biochem. Cytol. 5, 453-460.

Fawcett, D. W., and Phillips, D. M. (1969). Observations on the release of spermatozoa and on the changes in the head during passage through the epididymis. J. Reprod. Fertil. (suppl. 6), 405-418.

Fawcett, D. W. (1975). The ultrastructure and functions of the Sertoli cell. In: Handbook of Physiology (D. W. Hamilton and R. O. Greep, eds). Volume 5, Male Reproductive System. American Physiology Society, Washington D. C., 143-172.

Florio, M., Hernandez, M. C., Yang, H., Shu, H. K., Cleveland, J. L., and Israel, M. A. (1998). Id2 promotes apoptosis by a novel mechanism independent of dimerisation with basic helix-loop-helix factors. Mol. Cell. Biol. 18, 2371-2381.

Fode, C., Gradwohl, G., Morin, X., Dierich, A., LeMeur, M., Goridis, C., and Guillemot, F. (1998). The bHLH protein neurogenin 2 is a determination factor for epibranchial placode-derived sensory neurons. Neuron 20, 483-494.

Fode, C., Ma, Q., Casarosa, S., Ang, S. L., Anderson, D. J., and Cepko, C. L. (2000). A role for neural determination genes in specifying the dorsoventral identity of telencephalic neurons. Genes Dev. 14, 67-80.

Fuchs, E., and Segre, J. A. (2000). Stem cells: a new lease on life. Cell 100, 143-155.

Furukawa, T., Mukherjee, S., Bao, Z. Z., Morrow, E. M., and Cepko, C. L. (2000). rax, Hes1, and notch1 promote the formation of Muller glia by postnatal retinal progenitor cells. Neuron 26, 383-394.

Futterer, A., Mink, K., Luz, A., Kosco-Vilbois, M. H., and Pfeffer, K. (1998). The lymphotoxin beta receptor controls organogenesis and affinity maturation in peripheral lymphoid tissues. Immunity 9, 59-70.

Gage, F. (2000). Mammalian neural stem cells. Science 287, 1433-1438.

Gaiano, N., Nye, J. S., and Fishell, G. (2000). Radial glial identity is promoted by Notch1 signalling in the murine forebrain. Neuron 26, 395-404.

Gao, F. B., Apply, J., and Raff, M. C. (1998). Cell-intrinsic timer and thyroid hormone regulate the probability of cell cycle withdrawal and differentiation of oligodendrocyte precursor cells. Dev. Biol. 197, 54-66.

Garrell, J., and Modolel, J. (1990). The Drosophila extramacrochaetae locus, an antagonist of pro-neural genes that like these genes encodes a helix-loop-helix protein. Cell 61, 39-48.

Ghosh, A., and Greenberg, M. E. (1995). Distinct roles of bFGF and TH-3 in the regulation of cortical neurogenesis. Neuron 15, 89-103.

Ginsburg, M., Snow, M., McLaren, A. (1990). Primordial germ cells in the mouse embryo during gastrulation. Development 110, 521-528.

Goetz, T. L., Lloyd, T. L., and Griswold, M. D. (1996). Role of E box and initiator region in the expression of the rat follicle-stimulating hormone receptor. J. Biol. Chem. 271, 33317-33324.

Gomperts, M., Wylie, C., and Heasman, J. (1994). Primordial germ cell migration. Ciba Found. Symp. 182, 121-134.

Gradwohl, G., Fode, C., and Guillemot, F. (1996). Restricted expression of a novel murine atonal-related bHLH protein in undifferentiated neural precursors. Dev. Biol. 180, 227-241.

Griswold, M. D. (1988). Protein secretions of Sertoli cells. Int. Rev. Cytol. 110, 133-156.

Griswold, M. D., Morales, C., and Sylvester, S. R. (1988). Molecular biology of the Sertoli cell. Oxf. Rev. Reprod. Biol. 10, 124-161.

Griswold, M. D. (1998). The central role of Sertoli cells in spermatogenesis [see Comments]. Semin. Cell. Dev. Biol. 9, 411-416.

Gritti, A., Parati, E. A., Cova, L., Frolichsthal, P., Galli, R., Wanke, E., Faravelli, L., Morassutti, D. J., Roisen, F., Nickel, D. D., and Vescovi, A. L. (1996). Multipotential stem cells from the adult mouse brain proliferate and self-renew in response to basic fibroblast growth factor. J. Neurosci. 16, 1091-1100.

Gromoll, J., Simoni, M., and Nieschlag, E. (1996). An activating mutation of the follicle-stimulating hormone receptor autonomously sustains spermatogenesis in a hypophysectomised man. J. Clin. Endocrinol. Metab. 81, 1367-1370.

Gross, R. E., Mehler, M. F., Mabie, P. C., Zang, Z., Santschi, L., and Kessler, J. A. (1996). Bone morphogenetic proteins promote astroglial lineage commitment by mammalian subventricular zone progenitor cells. Neuron 17, 595-606.

Guillemot, F., Lo, L-C., Johnson, J. E., Auerbach, A., Anderson, D. J., and Joyner, A. L. (1993). Mammalian achaete-scute homologue 1 is required for the early development of olfactory and autonomic neurons. Cell 75, 463-476.

Guillemot, F. (1999). Vertebrate bHLH genes and the determination of neuronal fates. Exp. Cell Res. 253, 357-364.

Hagedorn, L., Suter, U., and Sommer, L. (1999). P0 and PMP22 mark a multipotent neural crest-derived cell type that displays community effects in response to TGF-β family members. Development 126, 3781-3794.

Hara, E., Yamaguchi, T., Nojima, H., Ide, T., Campisi, J., Okayama, H., and Oda, K. (1994). Id-related genes encoding helix-loop-helix proteins are required for G1 progression and are repressed in senescent human fibroblasts. J. Biol. Chem. 269, 2139-2145.

Hara, E., Hall, M., and Peters, G. (1997). Cdk2-dependent phosphorylation of Id2 modulates activity of E2A-related transcription factors. EMBO J. 16, 101-110.

Hernandez, M. C., Andres-Barquin, P. J., and Israel, M. A. (1996). Molecular cloning of the cDNA encoding a helix-loop-helix protein, mouse ID1B: tissue-specific expression of ID1A and ID1B genes. Biochim. Biophys. Acta. 1308, 28-30.

Hiebert, S. W., Packham, G., Strom, D. K., Haffner, R., Oren, M., Zambetti, G., and Cleveland, J. L. (1995). E2F-1:DP-1 induces p53 and overrides survival factors to trigger apoptosis. Mol. Cell. Biol. 15, 6864-6874.

Hochereau-de Reviers, M. T., Perreau, C., Pisslet, C., Locatelli, A., and Bosc, M. (1995). Ontogenesis of somatic and germ cells in sheep fetal testis. J. Reprod. Fertil. 103, 41-46.

Hosoya, T., Takizawa, K., Nitta, K., Hotta, Y. (1995). glial cells missing: a binary switch between neuronal and glial determination in Drosophila. Cell 82, 1025-1036.

Huckins, C. (1971). The spermatogonial stem cell population in adult rats. Their morphology, proliferation, and maturation. Anat. Rec. 169, 533-558.

Huckins, C. (1978). Spermatogonial intracellular bridges in whole-mounted seminiferous tubules from normal and irradiated rodent testes. Am. J. Anat. 153, 97-122.

Huneycutt, B. S., and Benveniste, E. N. (1995). Regulation of astrocyte cell biology by the cAMP/protein kinase A signaling pathway. Adv. Neuroimmunol. 5, 261-269.

Iavarone, A., Garg, O., Lasorella, A., Hsu, J., and Israel, M. A. (1994). The helix-loop-helix protein Id2 enhances cell proliferation and binds to the Retinoblastoma protein. Genes Dev. 8, 1270-1284.

Inoue, T., Shoji, W., and Obinata, M. (1999). MIDA1, an ID-associated protein, has two distinct DNA binding activities that are converted by the association with Id1: a novel function of Id protein. Biochem. Biophys. Res. Commun. 266, 147-151.

Inoue, T., Shoji, W., and Obinata, M. (2000). MIDA1 is a sequence specific DNA binding protein with novel DNA binding properties. Genes Cells 5, 699-709.

Ishibashi, M., Ang, S. L., Shiota, K., Nakanishi, S., Kageyama, R., and Guillemot, F. (1995). Targeted disruption of mammalian hairy and enhancer of split homolog-1 (HES-1) leads to up-regulation of neural helix-loop-helix factors, premature neurogenesis, and severe neural tube defects. Genes Dev. 9, 3136-3148.

Ishiguro, A., Konstantin, S., Spirin, M. S., Tobler, A., Gombart, A., Israel, M., Norton, J. D., and Keoffler, H. P. (1996). Id2 expression increases with differentiation of human myeloid cells. Blood 87, 5225-5231.

Jacobson, M. (1991). Developmental Neurobiology. New York: Plenum Press.

Jan, Y. N., and Jan, L. Y. (1993). HLH proteins, fly neurogenesis, and vertebrate myogenesis. Cell 75, 827-830.

Janatpour, M. J., McMaster, M. T., Genbacev, O., Zhou, Y., Dong, J., Cross, J. C., Israel, M. A., and Fisher, S. J. (2000). Id-2 regulates critical aspects of human cytotrophoblast differentiation, invasion and migration. Development 127, 549-558.

Jegou, B. (1992). The Sertoli cell *in vivo* and *in vitro*. Cell Biol. Toxicol. 8, 49-54.

Jen, Y., Weintraub, H., and Benezra, R. (1992). Overexpression of Id protein inhibits the muscle differentiation program: *in vivo* association of Id with E2A proteins. Genes Dev. 6, 1466-1479.

Jen, Y., Manova, K., and Benezra, R. (1996). Expression patterns of Id1, Id2 and Id3 are highly related but distinct from that of Id4 during mouse embryogenesis. Dev. Dyn. 207, 235-252.

Jen, Y., Manova, K., and Benezra, R. (1997). Each member of the Id gene family exhibits a unique expression pattern in mouse gastrulation and neurogenesis. Dev. Dyn. 208, 92-106.

Jessell, T. M. (2000). Neuronal specification in the spinal cord: inductive signals and transcriptional codes. Nat. Rev. Genet. 1, 20-29.

Jia, M. C., Ravindranath, N., Papadopoulos, V., and Dym, M. (1996). Regulation of c-fos mRNA expression in Sertoli cells by cyclic AMP, calcium and protein kinase C mediated pathways. Mol. Cell. Biochem. 156, 43-49.

Johe, K. K., Hazel, T. G., Muller, T., Dugich-Djordjevic, M. M., and McKay, R. D. G. (1996). Single factors direct the differentiation of stem cells from the fetal and adult central nervous system. Genes Dev. 10, 3129-3140.

Johnson, L., Zane, R. S., Petty, C. S., and Neaves, W. B. (1984). Quantification of the human Sertoli cell population – its distribution, relation to germ-cell numbers and age-related decline. Biol. Reprod. 31, 785-795.

Johnson, J. E., Birren, S. J., and Anderson, D. J. (1990). Two rat homologues of Drosophila achaete-scute specifically expressed in neuronal precursors. Nature 377, 355-358.

Johnson, J. E., Birren, S. J., Saito, T., and Anderson, D. J. (1992). DNA binding and transcriptional regulatory activity of mammalian achaete-scute homologous (MASH) proteins revealed by interaction with a muscle-specific enhancer. Proc. Natl. Acad. Sci. USA 89, 3596-3600.

Kageyama, R., Ishibashi, M., Takebayashi, K., and Tomita, K. (1997). bHLH transcription factors and mammalian neuronal differentiation. Int. J. Biochem. Cell. Biol. 29, 1389-1399.

Kageyama, R., and Ohtsuka, T. (1999). The Notch-Hes pathway in mammalian neural development. Cell Res. 9, 179-188.

Karl, J., and Capel, B. (1998). Sertoli cells of the mouse testis originate from the coelomic epithelium. Dev. Biol. 203, 323-333.

Kerr, J. B., and de Kretser, D. M. (1974). The role of the Sertoli cell in phagocytosis of the residual bodies of spermatids. J. Reprod. Fertil. 36, 439-440.

Kilpatrick, T. J., and Bartlett, P. F. (1993). Cloning and growth of multipotential neural precursors-requirements for proliferation and differentiation. Neuron 10, 255-265.

Kilpatrick, T. J., and Bartlett, P. F. (1995). Cloned multipotential precursors from the mouse cerebrum require FGF-2, whereas glial restricted precursors are stimulated with either FGF-1 or EGF. J. Neurosci. 15, 3653-3661.

Kim, J., Jones, B. W., Zock, C., Chen, Z., Wang, H., Goodman, C. S., and Anderson, D. J. (1998). Isolation and characterization of mammalian homologs of the Drosophila gene glial cells missing. Proc. Natl. Acad. Sci. USA 95, 12364-12369.

Kim, D., Peng, X. C., and Sun, X. H. (1999). Massive apoptosis of thymocytes in T cell deficient Id1 transgenic mice. Mol. Cell. Biol. 19, 8240-8253.

Klaes, A., Menne, T., Stollewerk, A., Scholz, H., and Klambt, C. (1994). The ETS transcription factors encoded by the Drosophila gene *pointed* direct glial cell differentiation in the embryonic CNS. Cell 78, 149-160.

Kluin, P. M., Kramer, M. F., and de Rooji, D. G. (1984). Proliferation of spermatogonia and Sertoli cells in maturing mice. Anatomy and Embryoloy 169, 73-78.

Knudsen, E. S., Buckmaster, C., Chen, T. T., Feramisco, J. R., and Wang, J. Y. (1998). Inhibition of DNA synthesis by RB: effects on G1/S transition and S-phase progression. Genes Dev. 12, 2278-2292.

Kondo, T., and Raff, M. (2000). The Id4 HLH protein and the timing of oligodendrocyte differentiation. EMBO J. 19, 1998-2007.

Kondo, T., and Raff, M. (2000a). Basic helix-loop-helix proteins and the timing of oligodendrocyte differentiation. Development 127, 2989-2998.

Koni, P. A., Sacca, R., Lawton, P., Browning, J. L., Ruddle, N. H., and Flavell, R. A. (1997). Distinct roles in lymphoid organogenesis for lymphotoxins alpha and beta revealed in lymphotoxin beta-deficient mice. Immunity 6, 491-500.

Koshimizu, U., Nishioka, H., Watanabe, D., Dohmae, K., and Nishimune, Y. (1995). Characterization of a novel spermatogenic cell antigen specific for early stages of germ cells in mouse testis. Mol. Reprod. Dev. 40, 221.

Kreider, B. L., Benezra, R., Rovera, G., and Kadesch, T. (1992). Inhibition of myeloid differentiation by the helix-loop-helix protein Id. Science 255, 1700-1702.

Lasorella, A., Iavarone, A., and Israel, M. (1996). Id2 specifically alters regulation of the cell cycle by tumour suppressor proteins. Mol. Cell. Biol. 16, 2570-2578.

Lasorella, A., Noseda, M., Beyna, M., Yokota, Y., and Iavarone, A. (2000). Id2 is a retinoblastoma protein target and mediates signalling by Myc oncoproteins. Nature 407, 592-598.

Le Blond, C. P., and Clermont, Y. (1952). Definition of the stages of the cycle of the seminiferous epithelium in the rat. Ann. N. Y. Acad. Sci. 55, 548-573.

Le Prince, G., Fages, C., Rolland, B., Nunez, J., and Tardy, M. (1991). DBcAMP effect on the expression of GFAP and of its encoding mRNA in astroglial primary cultures. Glia 4, 322-326.

Lee, J. E., Hollenberg, S. M., Snider, L., Turner, D. L., Lipnick, N., Weintraub, H. (1995). Conversion of Xenopus ectoderm into neurons by NeuroD, a basic helix-loop-helix protein. Science 268, 836-844.

Lee, J. E. (1997). Basic helix-loop-helix genes in neural development. Curr. Opin. Neurobiol. 7, 13-20.

Lendahl, U., Zimmerman, L. B., and McKay, R. D. (1990). CNS stem cells express a new class of intermediate filament protein. Cell 60, 585-595.

Levitt, P., Cooper, M. L., and Rakic, P. (1983). Early divergence and changing proportions of neuronal and glial precursor cells in the primate cerebral ventricular zone. Dev. Biol. 96, 472-484.

Li, W., Cogswell, C. A., and LoTurco, J. J. (1998). Neuronal differentiation of precursors in the neocortical ventricular zone is trigger by BMP. J. Neurosci. 18, 8853-8862.

Lincoln, D. W., McNeilly, R. M., and Sharpe, R. M. (1989). In: Recent advances in endocrinology and metabolism (C. R. W. Edwards, D. W. Lincoln, eds). Churchill Livingstone, Edinburgh, 77-107.

Lindsell, C. E., Boulter, J., diSibio, G., Gossler, A., and Weinmaster, G. (1996). Expression patterns of Jagged, Delta1, Notch1, Notch2, and Notch3 genes identify ligand-receptor pairs that may function in neural development. Mol. Cell. Neurosci. 8, 14-27.

Lister, J., Forrester, W. C., and Baron, M. H. (1995). Inhibition of an erythroid differentiation switch by helix-loop-helix protein Id1. J. Biol. Chem. 270, 17939-17946.

Liu, J., Shi, W., and Warburton, D. (2000). A cysteine residue in the helix-loop-helix domain of Id2 is critical for homodimerisation and function. Biochem. Biophys. Res. Commun. 273, 1042-1047.

Lo, L., Sommer, L., and Anderson, D. J. (1997). MASH1 maintains competence for BMP2-induced neuronal differentiation in post-migratory neural crest cells. Curr. Biol. 7, 440-450.

Lu, Q., Gore, M., Zhang, Q., Camenisch, T., Boast, S., Casagranda, F., Lai, C., Skinner, M. K., Klein, R., Matsushima, G. K., Shelton Earp, H., Goff, S. P., and

Lemke, G. (1999). Tyro-3 family receptors are essential regulators of mammalian spermatogenesis. Nature 389, 723-728.

Lu, Q. R., Yuk, D., Alberta, J. A., Zhu, Z., Pawlitzky, I., Chan, J., McMahon, A. P., Stiles, C. D., and Rowitch, D. H. (2000). Sonic hedgehog-regulated oligodendrocyte lineage specific genes encoding bHLH proteins in the mammalian central nervous system. Neuron 25, 317-329.

Lyden, D., Young, A. Z., Zagzag, D., Yan, W., Gerald, W., O'Reilly, R., Bader, B. L., Hynes, R. O., Zhuang, Y., Manova, K., and Benezra, R. (1999). Id1 and Id3 are required for neurogenesis, angiogenesis and vascularisation of tumour xenografts. Nature 401, 670-677.

Ma, Q., Sommer, L., Cserjesi, P., and Anderson, D. J. (1996). Identification of neurogenin, a vertebrate neuronal determination gene. Cell 87, 43-52.

Ma, Q., Fode, C., Guillemot, F., and Anderson, D. J. (1999). Neurogenin1 and neurogenin2 control two distinct waves of neurogenesis in developing dorsal root ganglia. Genes Dev. 13, 1717-1728.

Mantani, A., Hernandez, M. C., Kuo, W. L., and Israel, M. A. (1998). The mouse Id2 and Id4 genes: structural organisation and chromosomal localisation. Gene 222, 229-235.

Martinsen, B. J., and Bonner-Fraser, M. (1998). Neural crest specification regulated by the helix-loop-helix repressor, ID2. Science 281, 988-991.

Massari, M. E., and Murre, C. (2000). Helix-loop-helix proteins: regulators of transcription in eukaryotic organisms. Mol. Cell. Biol. 20, 429-440.

Matsumoto, A. M., Karpas, A. E., Paulsen, C. A., Bremner, W. J. (1983). Reinitiation of sperm production in gonadotrophin-suppressed normal men by administration of follicle-stimulating hormone. J. Clin. Invest. 72, 1005-1015.

McLachlan, R. I., Wreford, N. G., Tsonis, C., de Krester, D. M., and Robertson, D. M. (1994). Testosterone effects on spermatogenesis in the gonadotrophin-releasing hormone-immunised rat. Biol. Reprod. 50, 271-280.

McLachlan, R. I., Wreford, N. G., de Krester, D. M., and Robertson, D. M. (1994a). The effects of testosterone on spermatogenic cell populations in the adult rat. Biol. Reprod. 51, 945-955.

Meachem, S. H., McLachlan, R. I., Stanton, P. G., Robertson, D. M., and Wreford, N. G. (1999). FSH immunoneutralisation acutely impairs spermatogonial development in normal adult rats. J. Androl. 20, 756-762.

Melnikova, I. N., and Christy, B. A. (1996). Muscle cell differentiation is inhibited by the helix-loop-helix protein Id3. Cell Growth Differ. 7, 1067-1079.

Melnikova, I. N., Bounpheng, M., Schatteman, G. C., Gilliam, D., and Christy, B. A. (1999). Differential biological activities of mammalian Id proteins in muscle cells. Exp. Cell Res. 247, 94-104.

Miller, R. H., David, S., Patel, R., Abeny, E. R., and Raff, M. C. (1985). A quantitative immunohistochemical study of macroglial cell development in the rat optic nerve. *In vivo* evidence for two distinct astrocyte lineages. Dev. Biol. 111, 35-41.

Mizuguchi, R., Sugimori, M., Takebayashi, H., Kosako, H., Nagao, M., Yoshida, S., Nabeshima, Y., Shimamura, K., and Nakafuku, M. (2001). Combinatorial roles of olig2 and neurogenin2 in the coordinated induction of pan-neuronal and subtype-specific properties of motoneurons. Neuron 31, 757-771.

Moldes, M., Lasnier, F., Feve, B., Pairault, J., and Djian, P. (1997). Id3 prevents differentiation of preadipose cells. Mol. Cell. Biol. 16, 5792-5800.

Moldes, M., Boizard, M., leLiepvre, X., Feve, B., Dugail, I., and Pairault, J. (1999). Functional antagonism between inhibitor of DNA binding (Id) and adipocyte

determination and differentiation factor 1/sterol regulator element-binding protein-1c (ADD1/SREBP-1c) trans-factors for the regulation of fatty acid synthase promoter in adipocytes. Biochem. J. 344, 873-880.

Mori, S., Nishikawa, S. I., and Yokota, Y. (2000) Lactation defect in mice lacking helix-loop-helix inhibitor Id2. EMBO J. 19, 5772-5781.

Morrison, S. J., Shah, N. M., and Anderson, D. J. (1997). Regulatory mechanisms in stem cell biology. Cell 88, 287-298.

Morrison, S. J., White, P. M., Zock, C., and Anderson, D. J. (1999). Prospective identification, isolation by flow cytometry, and *in vivo* self-renewal of multipotent mammalian neural crest stem cells. Cell 96, 737-749.

Morrison, S. J., Perez, S. E., Zhou, Q., Verdi, J. M., Hicks, C., Weinmaster, G., and Anderson, D. J. (2000). Transient Notch activation causes an irreversible switch from neurogenesis to gliogenesis by neural crest stem cells. Cell 101, 499-510.

Muhr, J., Andersson, E., Persson, M., Jessell, T. M., and Ericson, J. (2001). Groucho-mediated transcriptional repression establishes progenitor cell pattern and neuronal fate in the ventral neural tube. Cell 104, 861-873.

Murre, C., McCaw, P. S., Vaessin, H., Caudy, M., Jan, L. Y., Jan, Y. N., Cabrera, C.V., Buskin, J. N., Hauschka, S. D., Lassar, A. B. *et al.* (1989). Interaction between heterologous helix-loop-helix proteins generates complexes that bind specifically to a common DNA sequence. Cell 58, 537-544.

Nagata, Y., and Todokoro, K. (1994). Activation of helix-loop-helix proteins Id1, Id2 and Id3 during neural differentiation. Biochem. Biophys. Res. Commun. 199, 1355-1362.

Nakashima, K., Yanagisawa, M., Arakawa, H., Kimura, N., Hisatsune, T., Kawabata, M., Miyazono, K., and Taga, T. (1999). Synergistic signalling in the fetal brain by STAT3-Smad1 complex bridged by p300. Science 284, 479-482.

Nakashima, K., Takizawa, T., Ochiai, W., Yanagisawa, M., Hisatsune, T., Nakafuku, M., Miyazono, K., Kishimoto, T., Kageyama, R., and Taga, T. (2001). BMP2-mediated alteration in the developmental pathway of fetal mouse brain cells from neurogenesis to astrocytogenesis. Proc. Natl. Acad. Sci. USA 98, 5868-5873.

Neuman, T., Keen, A., Zuber, M. X., Kristjansson, G. I., Gruss, P., and Nornes, H. O. (1993). Neuronal expression of regulatory helix-loop-helix factor Id2 gene in mouse. Dev. Biol. 160, 186-195.

Nieto, M., Schuurmans, C., Britz, O., and Guillemot, F. (2001). Neural bHLH genes control the neuronal versus glial fate decision in cortical progenitors. Neuron 29, 401-413.

Noctor, S. C., Flint, A. C., Wiessman, T. A., Dammerman, R. S., and Kriegstein, A. R. (2001). Neurons derived from radial glial cells establish radial glial units in the neocortex. Nature 409, 714-720.

Norton, J. N., and Skinner, M. K. (1989). Regulation of Sertoli cell function and differentiation through the actions of a testicular paracrine factor PModS. Endocrinology 124, 2771-2719.

Norton, J. N., and Skinner, M. K. (1992). Regulation of Sertoli cell differentiation by the testicular paracrine factor PmodS: potential role of immediate-early genes. Mol. Endocrinol. 6, 2018-2026.

Norton, J. N., Vigne, J-L., and Skinner, M. K. (1994). Regulation of Sertoli cell differentiation by the testicular paracrine factor PmodS: analysis of common signal transduction pathways. Endocrinology 134, 149-157.

Norton, J. D., and Atherton, G. T. (1998). Coupling of cell growth and apoptosis functions of Id proteins. Mol. Cell. Biol. 18, 2371-2381.

Norton, J. D., Craggs, G., Deed, R. W., and Sablitzky, F. (1998). Id helix-loop-helix proteins in cell growth and differentiation. Trends Cell Biol. 8, 58-65.

Norton, J. D. (2000). ID helix-loop-helix proteins in cell growth, differentiation and tumorigenesis. J. Cell Sci. 113, 3897-3905.

Novitch, B. G., Chen, A. I., and Jessell, T. M. (2001). Coordinate regulation of motor neuron subtype identity and pan-neuronal properties by the bHLH repressor Olig2. Neuron 31, 772-789.

Nye, J. S., Kopan, R., and Axel, R. (1994). An activated Notch suppresses neurogenesis and myogenesis but not gliogenesis in mammalian cells. Development 120, 2421-2430.

Oakberg, E. F. (1956). Duration of spermatogenesis in the mouse and timing of stages of the cycle of the seminiferous epithelium. Am. J. Anat. 99, 507-516.

Ogawa, T., Arechaga, J. M., Avarbock, M. R., and Brinster, R. L. (1997). Transplantation of testis germinal cells into mouse seminiferous tubules. Int. J. Dev. Biol. 41, 111-122.

Ohsako, S., Hyer, J., Panganiban, G., Oliver, I., and Caudy, M. (1994). Hairy functions as a DNA-binding helix-loop-helix repressor of Drosophila sensory organ formation. Genes Dev. 8, 2743-2755.

Orentas, D. M., Hayes, J. E., Dyer, K. L., and Miller, R. H. (1999). Sonic hedgehog signalling is required during the appearance of spinal cord oligodendrocyte precursors. Development 126, 2419-2429.

Orth, J. M. (1982). Proliferation of Sertoli cells in fetal and post-natal rats: a quantitative autoradiographic study. Anatomical Records 203, 485-492.

Orth, J. M. (1984). The role of follicle-stimulating hormone in controlling Sertoli cell proliferation in testes of fetal rats. Endocrinology 115, 1248-1255.

Orth, J. M., Gunsalus, G. L., and Lamperti, A. A. (1988). Evidence from Sertoli cell-depleted rats indicates that spermatid number in adults depends on numbers of Sertoli cell produced during perinatal development. Endocrinology 122, 787-794.

O'Shaughnessy, P. J., and Sheffield, J. W. (1990). Effect of testosterone on testicular steroidogenesis in the hypogonadal (hpg) mouse. J. Steroid Biochem. 35, 729-734.

O'Shaughnessy, P. J., Baker, P., Sohnius, U., Havisto, A-M., Charlton, H. M., Huhtaniemi, I. (1998). Fetal development of leydig activity in the mouse is independent of pituitary gonadotroph function. Endocrinology 139, 1141-1146.

Palmer, T. D., Ray, J., and Gage, F. H. (1995). FGF-2-responsive neuronal progenitors reside in the proliferative and quiescent regions of the adult rodent brain. Mol. Cell. Neurosci. 6, 474-486.

Pan, L., Sato, S., Frederick, J. P., Sun, X. H., and Zhuang, Y. (1999). Impaired immune response and B cell proliferation in mice lacking the Id3 gene. Mol. Cell. Biol. 19, 5969-5980.

Park, J. K., Williams, B. P., Alberta, J. A., and Stiles, C. D. (1999). Bipotent cortical progenitor cells process conflicting cues for neurons and glia in a hierarchical manner. J. Neurosci. 19, 10383-10389.

Persengiev, S. P., and Kilpatrick, D. L. (1997). The DNA methyltransferase inhibitor 5-azacytidine specifically alters the expression of helix-loop-helix proteins Id1, Id2 and Id3 during neuronal differentiation. Neuroreport 8, 2091-2095.

Pollenz, R. S., and McCarthy, K. D. (1986). Analysis of cyclic AMP-dependent changes in intermediate filament protein phosphorylation and cell morphology in cultured astroglia. J. Neurochem. 47, 9-17.

Poncet, C., Soula, C., Trousse, F., Kan, P., Hirsinger, E., Pourquie, O., Duprat, A. M., and Cochard, P. (1996). Induction of oligodendrocyte progenitors in the trunk

neural tube by ventralizing signals: effects of notochord and floor plate grafts, and of sonic hedgehog. Mech. Dev. 60, 3-13.

Prabhu, S., Ignatova, A., Park, S. T., and Sun, X. H. (1997). Regulation of expression of the cyclin dependent kinase inhibitor p21 by E2A and Id proteins. Mol. Cell. Biol. 17, 5888-5896.

Pringle, N. P., Yu, W. P., Guthrie, S., Roelink, H., Lumsden, A., Peterson, A. C., and Richardson, W. D. (1996). Determination of neuroepithelial cell fate: induction of the oligodendrocyte lineage by ventral midline cells and sonic hedgehog. Dev. Biol. 177, 30-42.

Qian, X., Goderie, S. K., Shen, Q., Stern, J. H., and Temple, S. (1998). Intrinsic programs of patterned cell lineages in isolated vertebrate CNS ventricular zone cells. Development 125, 3143-3152.

Qian, X., Shen, Q., Goderie, S. K., He, W., Capela, A., Davis, A. A., and Temple, S. (2000). Timing of CNS cell generation: a programmed sequence of neuron and glial cell production from isolated murine cortical stem cells. Neuron 28, 69-80.

Qin, X. Q., Livingston, D. M., Kaelin, W. G., and Adams, P. D. (1994). Deregulated transcription factor E2F-1 expression leads to S-phase entry and p53-mediated apoptosis. Proc. Natl. Acad. Sci. USA 91, 10918-10922.

Raff, M. C., Abeny, E. R., and Fok-Seang, J. (1985). Reconstitution of a developmental clock *in vitro*: a critical role for astrocytes in the timing of oligodendrocyte differentiation. Cell 42, 61-69.

Raff, M. C., Lillien, L., Richardson, W., Burne, J. F., and Noble, M. (1988). Platlet-derived growth factor from astrocytes drives the clock that times oligodendrocyte development in culture. Nature 333, 562-565.

Rajan, P., and McKay, R. D. (1998). Multiple routes to astrocytic differentiation in the CNS. J. Neurosci. 18, 3620-3629.

Rea, M. A., Marshall, G. R., Weinbauer, G. F., and Nieschlag, E. (1996). Testosterone maintains pituitary and serum FSH and spermatogenesis in gonadotrophin-releasing hormone antagonist-suppressed rats. J. Endocrinol. 108, 101-103.

Rennert, P. D., James, D., Mackay, F., Browning, J. L., and Hochman, P. S. (1998). Lymph node genesis is induced by signalling through the lymphotoxin beta receptor. Immunity 9, 71-79.

Richardson, W. D., Smith, H. K., Sun, T., Pringle, N. P., Hall, A., and Woodruff, R. (2000). Oligodendrocyte lineage and the motor neuron connection. Glia 29, 136-142.

Riechmann, V., van Crüchten, I., and Sablitzky, F. (1994). The expression pattern of Id4, a novel dominant negative helix-loop-helix protein, is distinct from that of Id1, Id2 and Id3. Nucleic Acids Res. 22, 749-755.

Riechmann, V., and Sablitzky, F. (1995). Mutually exclusive expression of two dominant-negative helix-loop-helix genes, Id4 and Id3, in the developing brain of the mouse suggests distinct regulatory roles of these dnHLH proteins during cellular proliferation and differentiation of the nervous system. Cell Growth Differ. 6, 837-843.

Rogister, B., Ben-Hur, T., and Dubois-Dalcq, M. (1999). From neural stem cells to myelinating oligodendrocytes. Mol. Cell. Neurosci. 14, 287-300.

Ronfani, I., Ferraguti, M., Croci, L., Ovitt, C. E., Scholer, H. R., Consalez, G. G., and Bianchi, M. E. (2001). Reduced fertility and spermatogenesis defects in mice lacking chromosomal protein Hmgb2. Development 128, 1265-1273.

Russell, L. D. (1977). Movement of spermatocytes from the basal to adluminal compartments of the rat testis. Am. J. Anat. 148, 313-328.

Russell, L. D., and Clermont, Y. (1977). Degeneration of germ cells in normal hypophysectomised and hormone-treated hypophysectomised rats. Anat. Rec. 187, 347-366.

Russell, L. D. (1978). The blood-testis barrier and its formation relative to spermatocyte maturation in the adult rat: An lanthanum tracer study. Anat. Rec. 190, 99-112.

Russell, L. D. (1980). Sertoli-germ cell interrelations: A review. Gamete Res. 3, 179-202.

Russell, L. D. (1984). Spermiation – the sperm release process: Ultrastructural observations and unresolved problems. In: Electron Microscopy in Biology and Medicine (J. Van Blerkom and P. M. Motta, eds). Chapter 5, Ultrastructure of Reproduction. New York: Plenum Press, 46-65.

Russell, L. D., and Peterson, R. N. (1985). Sertoli cell junctions: Morphological and functional correlates. Int. Rev. Cytol. 94, 177-211.

Russell, L. D., Ettlin, R. A., Sinha Hikim, A. P., and Clegg, E. D. (1990). Histological and histopathological evaluation of the testis. Cache River Press.

Sablitzky, F., Moore, A., Bromley, M., Deed, R. W., and Norton, J. D. (1998). Stage- and subcellular-specific expression of Id proteins in male germ cells and Sertoli cells implicates distinct regulatory roles for Id proteins during meiosis, spermatogenesis and Sertoli cell function. Cell Growth Diff. 9, 1015-1024.

Saito, T., Lo, L., Anderson, D. J., and Mikoshiba, K. (1996). Identification of novel paired homeodomain protein related to C. elegans unc-4 as a potential downsteam target of MASH1. Dev. Biol. 180, 143-155.

Santulli, R., Sprando, R. L., Awoniyi, C. A., Ewing, L. L., and Zirkin, R. B. (1990). To what extent can spermatogenesis be maintained in the hypophysectomized adult rat testis with exogenously administered testosterone? Endocrinology 126, 95-102.

Sasai, Y., Kageyama, R., Tagawa, Y., Shigemoto, R., and Nakanishi, S. (1992). Two mammalian helix-loop-helix factors structurally related to Drosophila hairy and enhancer of split. Genes Dev. 6, 2620-2634.

Schroeter, E. H., Kisslinger, J. A., and Kopan, R. (1998). Notch-1 signalling requires ligand-induced proteolytic release of the intracellular domain. Nature 393, 382-386.

Sdrulla, A., Wang, S., and Barres, B. A. (1999). Overexpression of the Id2 protein inhibits oligodendrocyte differentiation *in vitro*. Society for Hemosueme [see Abstracts], 2039.

Setchell, B. P., and Waites, G. M. H. (1975). The blood-testis barrier. In: Handbook of Physiology (D. W. Hamilton and R. O. Greep, eds). Volume 5, Male Reproductive System. American Physiology Society, Washington D. C., 143-172.

Shah, N. M., Marchionni, M. A., Isaacs, I., Stroobant, P. W., and Anderson, D. J. (1994). Glial growth factor restricts mammalian neural crest stem cells to glial fate. Cell 77, 349-360.

Shah, N. M., Groves, A., and Anderson, D. J., (1996). Alternative neural crest cell fates are instructively promoted by TGFβ superfamily members. Cell 85, 331-343.

Shan, B., and Lee, W. H. (1994) Deregulated expression of E2F-1 induces S-phase entry and leads to apoptosis. Mol. Cell. Biol. 14, 8166-8173.

Sharpe, R. M. (1994). Regulation of spermatogenesis. In: The Physiology of Reproduction (E. Knobil and J. D. Neill, eds). New York: Raven Press, 1363-1434.

Shenker, A., Laue, L., Kosugi, S., Merendino, L., Minegishi, T., and Cutler, G. N. (1993). A constitutively activating mutation of the luteinising hormone receptor in familial precocious puberty. Nature 365, 652-654.

Shoji, W., Yamamoto, T., and Obinata, M. (1994). The helix-loop-helix protein Id inhibits differentiation of murine erythroleukemia cells. J. Biol. Chem. 269, 5078-5084.

Shoji, W., Inoue, T., Yamamoto, T., and Obinata, M. (1995). MIDA1, a protein associated with Id regulates cell growth. J. Biol. Chem. 270, 24818-24825.

Simorangkir, D., Wreford, N. G., and de Krester, D. M. (1995). Increased numbers of Sertoli cells and germ cells in adult rat testis induced by synergistic action of transient neonatal hypothyroidism and neonatal hemicastration. J. Reprod. Fertil. 104, 207-213.

Singh, J., O'Neill, C., and Handelsmann, D. J. (1995). Induction of spermatogenesis by androgen in gonadotrophin deficient (hpg) mice. Endocrinology 136, 5311-5321.

Singh, J., and Handelsman, D. J. (1996). Neonatal administration of FSH increases Sertoli cell numbers and spermatogenesis in gonadotrophin-deficient (hpg) mice. J. Endocrinol. 151, 37-48.

Skinner, M. K., and Griswold, M. D. (1980). Sertoli cells synthesize and secrete transferrin-like protein. J. Biol. Chem. 255, 9523-9525.

Skinner, M. K., and Griswold, M. D. (1982). Secretion of testicular transferrin by cultured Sertoli cells is regulated by hormones and retinoids. Biol. Reprod. 27, 211-221.

Skinner, M. K., and Fritz, I. B. (1985). Testicular cells secrete a protein under androgen control that modulates Sertoli cell function. Proc. Natl. Acad. Sci. USA 82, 114-118.

Skinner, M. K., Fetterolf, P. M., and Anthony, C. T. (1988). Purification of testicular paracrine factor PmodS produced by testicular peritubular cells that modulates Sertoli cell function. J. Biol. Chem. 263, 2884-2890.

Skinner, M. K., Schlitz, S. M., and Anthony, C. T. (1989). Regulation of Sertoli cell differentiated function: testicular transferrin and androgen-binding protein expression. Endocrinology 124, 3015-3024.

Sommer, L., Shah, N., Rao, M., and Anderson, D. J. (1995). The cellular function of Mash1 in autonomic neurogenesis. Neuron 15, 1245-1258.

Stahl, N., and Yancopoulos, G. D. (1994). The tripartite CNTF receptor complex: activation and signalling involves components shared with other cytokines. J. Neurobiol. 25, 1454-1466.

Steinberger, A., and Steinberger, E. (1971). Replication pattern of Sertoli cells in maturing rat testis *in vivo* and in organ culture. Biol. Reprod. 4, 84-87.

Stemple, D. L., and Anderson, D. J. (1992). Isolation of a stem cell for neurons and glia from the mammalian neural crest. Cell 71, 973-985.

Struhl, G., and Greenwald, I. (1999). Presenilin is required for activity and nuclear access of Notch in Drosophila. Nature 398, 522-525.

Sun, X. H., Copeland, N. G., Jenkins, N., and Baltimore, D. (1991). Id proteins, Id1 and Id2 selectively inhibit DNA binding by one class of helix-loop-helix proteins. Mol. Cell. Biol. 11, 5603-5611.

Sun, X. H. (1994). Constitutive expression of the Id1 gene impairs mouse B cell development. Cell 79, 893-900.

Sun, T., Pringle, N. P., Hardy, A. P., Richardson, W. D., and Smith, H. K. (1998). Pax6 influences the time and site of origin of glial precursors in the ventral neural tube. Mol. Cell. Neurosci. 12, 228-239.

Sun, Y., Nadal-Vicens, M., Misono, S., Lin, M. Z., Zubiaga, A., Hua, X., Fan, G., and Greenberg, M. E. (2001). Neurogenin promotes neurogenesis and inhibits glial differentiation by independent mechanisms. Cell 104, 365-376.

Takebayashi, H., Yoshida, S., Sugimori, M., Kosako, H., Kominami, R., Nakafuku, M., and Nabeshima, Y. (2000). Dynamic expression of basic helix-loop-helix Olig family members: implication of Olig2 in neuron and oligodendrocyte differentiation and identification of a new member, Olig3. Mech. Dev. 99, 143-148.

Tamura, K., Taniguchi, Y., Minoguchi, S., Sakai, T., Tun, T., Furukawa, T., and Honjo, T. (1995). Physical interaction between a novel domain of the receptor Notch and the transcription factor RBP-J kappa/Su(H). Curr. Biol. 5, 1416-1423.

Tanigaki, K., Nogaki, F., Takahashi, J., Tashiro, K., Kurooka, H., and Honjo, T. (2001). Notch1 and Notch3 instructively restrict bFGF-responsive multipotent neural progenitor cells to an astroglial fate. Neuron 29, 45-55.

Taupin, P., Ray, J., Fischer, W. H., Suhr, S. T., Hakansson, K., Grubb, A., and Gage, F. H. (2000). FGF-2-responsive neural stem cell proliferation requires CCg, a novel autocrine/paracrine cofactor. Neuron 29, 45-55.

Temple, S., and Raff, M. C. (1986). Clonal analysis of oligodendrocyte development in culture: evidence for a developmental clock that counts cell division. Cell 44, 773-779.

Thomas, G. B., McNeilly, A. S., Gibson, F., and Brooks, A. N. (1994). Effects of pituitary-gonadal suppression with a gonadotrophin-releasing hormone agonist on fetal gonadotrophin secretion, fetal gonadal development and maternal steroid secretion in the sheep. J. Endocrinol. 141, 317-324.

Tietze, K., Oellers, N., and Knust, E. (1992). Enhancer of splitD, a dominant mutation of Drosophila, and its use in the study of functional domains of a helix-loop-helix protein. Proc. Natl. Acad. Sci. USA 89, 6152-6156.

Tomita, K., Moriyoshi, K., Nakanishi, S., Guillemot, F., and Kageyama, R. (2000). Mammalian achaete-scute and atonal homologs regulate neuronal versus glial fate determination in the central nervous system. EMBO J. 19, 5460-5472.

Tournay, O., and Benezra, R. (1996). Transcription of the dominant negative helix-loop-helix protein Id1 is regulated by a protein complex containing the immediate early response gene, Egr-1. Mol. Cell. Biol. 16, 2418-2430.

Tzeng, S. F., and de Vellis, J. (1998). Id1, Id2, and Id3 gene expression in neural cells during development. Glia 24, 372-381.

Vallstedt, A., Muhr, J., Pattyn, A., Pierani, A., Mendelsohn, M., Sander, M., Jessell, T. M., and Ericson, J. (2001). Different levels of repressor activity assign redundant and specific roles to Nkx6 genes in motor neuron and interneuron specification. Neuron 31, 743-755.

van Crüchten, I. (1997). PhD thesis at the University of Cologne, Germany.

van Crüchten, I., Cinato, E., Fox, M., King, E. R., Newton, J. S., Riechmann, V., and Sablitzky, F. (1998). Structure, chromosomal localisation and expression of the murine dominant negative helix-loop-helix Id4 gene. Biochim. Biophys. Acta 1443, 55-64.

Van Doren, M., Bailey, A. M., Esnayra, J., Ede, K., and Posakony, J. W. (1994). Negative regulation of proneural gene activity: hairy is a direct transcriptional repressor of achaete. Genes Dev. 8, 2729-2742.

Vaskivuo, T., Aittomaki, K., Huhtaniemi, I. T., and Tapanainen, J. S. (1998). Follicle-stimulating hormone receptor mutation and fertility. In: Testicular function: from gene expression to genetic manipulation. Berlin: Springer, 295-306.

Verdi, J. M., Bashirullah, A., Goldhawk, D. E., Kubu, C. J., Jamali, M., Meakin, S. O., and Libshitz, H. D. (1999). Distinct human NUMB isoforms regulate differentiation versus proliferation in the neuronal lineage. Proc. Natl. Acad. Sci. USA 96, 10472-10476.

Verhoeven, G., and Caillaeu, J. (1988). Testicular peritubular cells secrete a protein under androgen control that inhibits induction of aromatase activity in Sertoli cells. Endocrinology 122, 1541-1550.

Verhoeven, G. (1992). Androgens and the testis. Verh Koninkl Acad Geneesk Belgie LIV 4, 299-327.

Wakamatsu, Y., Maynard, T. M., Jones, S. U., and Weston, J. A. (1999). NUMB localises in the basal cortex of mitotic avian neuroepithelial cells and modulates neuronal differentiation by binding Notch-1. Neuron 23, 71-81.

Walker, W. H., Fucci, L., and Habener, J. F. (1995). Expression of the gene encoding transcription factor cAMP response element-binding protein (CREB): regulation by follicle-stimulating hormone-induced cAMP signalling in primary rat Sertoli cells. Endocrinology 136, 3534-3545.

Wang, Y., Benezra, R., and Sassoon, D. A. (1992). Id expression during mouse development: a role in morphogenesis. Dev. Dyn. 194, 222-230.

Wang, S., Sdrulla, A. D., diSibio, G., Bush, G., Nofziger, D., Hicks, C., Weinmaster, G., and Barres, B. A. (1998). Notch receptor activation inhibits oligodendrocyte differentiation. Neuron 21, 63-75.

Wang, M., and Sternberg, P. W. (1999). Competence and commitment of Caenorhabditis elegans vulval precursor cells. Dev. Biol. 212, 12-24.

Wang, S., Sdrulla, A., Johnson, J. E., Yokota, Y., and Barres, B. A. (2001). A role for the helix-loop-helix protein Id2 in the control of oligodendrocyte development. Neuron 29, 603-614.

Webb, J. F., and Noden, D. M. (1993). Ectodermal placodes: contributions to the development of the vertebrate head. Am. Zool. 33, 434-447.

Weber, J. E., and Russell, L. D. (1987). A study of intracellular bridges during spermatogenesis in the rat. Am. J. Anat. 180, 1-24.

Weber, J. E., Turner, T. T., Tung, K. S. K., and Russell, L. D. (1988). Effect of cytochalasin D on the integrity of the Sertoli cell (blood-testis) barrier. Am. J. Anat. 182, 130-147.

Weinbauer, G. F., and Neischlag, E. (1998). The role of testosterone in spermatogenesis. In: Testosterone (E. Nieschlag, H. M. Behre, eds). Action-deficiency-substitution. Berlin: Springer, 143-168.

Whaley, P. D., Chaudhary, J., Cupp, A., and Skinner, M. K. (1995). Role of the specific response elements of the c-fos promoter and involvement of intermediate transcription factor(s) in the induction of Sertoli cell differentiation (transferrin promoter activation) by the testicular paracrine factor PmodS. Endocrinology 136, 3046-3054.

Williams, B. P., Park, J. K., Alberta, J. A., Muhlebach, S. G., Hwang, G. Y., Roberts, T. M., and Stiles, C. D. (1997). A PDGF-regulated immediate early gene response initiates neuronal differentiation in ventricular zone progenitor cells. Neuron 18, 553-562.

Willis, S. A., and Nissen, P. D. (1995). Inhibition of lipopolysaccharide-induced IL-1β transcription by cyclic adenosine monophosphate in human astrocytic cells. J. Immunol. 154, 1399-1406.

Wilson, R., and Mohun, T. (1995). Xidx, a dominant negative regulator of bHLH function in early Xenopus embryos. Mech. Dev. 49, 211-222.

Wreford, N. G., Rajendra Kumar, T., Matzuk, M. M., and de Krester, D. M. (2001). Analysis of the testicular phenotype of the follicle-stimulating hormone β-subunit knockout and the activin type II receptor knockout mice by stereological analysis. Endocrinology 142, 2916-2920.

Xu, X., Cai, J., Fu, H., Wu, R., Qi, Y., Modderman, G., Liu, R., and Qiu, M. (2000). Selective expression of Nkx-2.2 transcription factor in chicken oligodendrocyte progenitors and implications for the embryonic origin of oligodendrocytes. Mol. Cell. Neurosci. 16, 740-753.

Yan, W., West, A., Toppari, J., and Lahdetie, J. (1997). Stage-specific expression and phosphorylation of retinoblastoma protein in the rat seminiferous epithelium. Mol. Cell. Biol. 132, 137-148.

Yan, W., Young, A. Z., Soares, V. C., Kelley, R., Benezra, R., and Zhuang, Y. (1997a). High incidence of T cell tumours in E2A-null mice and E2A/Id1 double knockout mice. Mol. Cell. Biol. 17, 7317-7327.

Yates, P. R., Atherton, G. T., Deed, R. W., Norton, J. D., and Sharrocks, A. D. (1999). ID helix-loop-helix proteins inhibit nucleoprotein complex formation by the TCF-ETS domain transcription factors. EMBO J. 18, 968-976.

Ye, Y., Lukinova, H., and Fortini, M. E. (1999). Neurogenic phenotypes and altered Notch processing in Drosophila Presenilin mutants. Nature 398, 525-529.

Yokota, Y., Mansouri, A., Mori, S., Sugawara, S., Adachi, S., Nishikawa, S. I., and Gruss, P. (1999). Development of peripheral lymphoid organs and natural killer cells depends on the helix-loop-helix inhibitor, Id2. Nature 397, 702-706.

Yokota, Y., Mori, S., Narumi, O., and Kitajima, K. (2001). *In vivo* function of a differentiation inhibitor, Id2. IUBMB Life 51, 207-14.

Yokota, Y., and Mori, S. (2002). Role of Id family proteins in growth control. J. Cell. Physiol. 190, 21-28.

Yomogida, K., Ohtani, H., Harigae, H., Ito, E., Nishimune, Y., Engel, J. D., and Yamamoto, M. (1994). Developmental stage- and spermatogenic cycle-specific expression of transcription factor GATA-1 in mouse Sertoli cells. Development 120, 1759-1766.

Zhang, H., Reynaud, S., Kloc, M., Etkin, L. D., and Spohr, G. (1995). Id gene activity during Xenopus embryogenesis. Mech. Dev. 50, 119-130.

Zhang, D., Mehler, M. F., Song, Q., and Kessler, J. A. (1998). Development of bone morphogenetic protein receptors in the nervous system and possible roles in regulating trkC expression. J. Neurosci. 18, 3314-3326.

Zhao, G-Q., Liaw, L., and Hogan, B. L. M. (1998). Bone morphogenetic protein 8A plays a role in the maintenance of spermatogenesis and the integrity of the epididymis. Development 125, 1103-1112.

Zhong, W., Jiang, M. M., Weinmaster, G., Jan, L. Y., and Jan, Y. N. (1997). Differential expression of mammalian Numb, Numblike and Notch1 suggests distinct roles during mouse cortical neurogenesis. Development 124, 1887-1897.

Zhou, Q., Wang, S., and Anderson, D. J. (2000). Identification of a novel family of oligodendrocyte lineage-specific basic helix-loop-helix transcription factors. Neuron 25, 331-343.

Zhou, Q., Choi, G., and Anderson, D. J. (2001). The bHLH transcription factor Olig2 promotes oligodendrocyte differentiation in collaboration with Nkx2.2. Neuron 31, 791-807.

Zigmond, M. J., Bloom, F. E., Landis, S. C., Roberts, J. L., and Larry, R. S. (1999). Fundamental Neuroscience. Academic Press.

References added in addendum:

Hogan, B., Beddington, R., Costantini, F., and Lacy, E. (1994). Manipulating the mouse embryo: A laboratory manual, second edition. Cold Spring Harbor Laboratory Press, Cold Spring Harbor, New York, U. S. A.

Joyner, A. L. (2000). Gene targeting: A practical approach, second edition. Oxford University Press.

Maniatis, T., Fritsch, E., and Sambroof, J. (1982). Molecular cloning: A laboratory manual, first edition. Cold Spring Harbor Laboratory Press, Cold Spring Harbor, New York, U. S. A..

Morgenstern, J. P., and Land, H. (1990). Advanced mammalian gene transfer: high titre retroviral vectors with multiple drug selection markers and a complementary helper-free packaging cell line. Nucleic Acids Res. 18, 3587-3596.

Roberts, E. C., Deed, R. W., Inoue, T., Norton, J. D., and Sharrocks, A. D. (2001). Id helix-loop-helix proteins antagonise pax transcription factor activity by inhibiting DNA binding. Mol. Cell. Biol. 21, 524-533.

Wood, S. A., Allen, N. D., Rossant, K., Auerbach, A., and Nagy, A. (1993). Non-injection methods for the production of embryonic stem cell-embryo chimeras. Nature 365, 87-89.